

Fall 2007

# The coordination chemistry of a chelating tricyclic bisamidine and a new synthetic route to a C(2)-symmetric tricyclic bisamidine

Jingwei Li

*University of New Hampshire, Durham*

Follow this and additional works at: <https://scholars.unh.edu/thesis>

---

## Recommended Citation

Li, Jingwei, "The coordination chemistry of a chelating tricyclic bisamidine and a new synthetic route to a C(2)-symmetric tricyclic bisamidine" (2007). *Master's Theses and Capstones*. 303.  
<https://scholars.unh.edu/thesis/303>

This Thesis is brought to you for free and open access by the Student Scholarship at University of New Hampshire Scholars' Repository. It has been accepted for inclusion in Master's Theses and Capstones by an authorized administrator of University of New Hampshire Scholars' Repository. For more information, please contact [nicole.hentz@unh.edu](mailto:nicole.hentz@unh.edu).

THE COORDINATION CHEMISTRY OF A CHELATING TRICYCLIC BISAMIDINE  
AND A NEW SYNTHETIC ROUTE TO A  $C_2$ -SYMMETRIC TRICYCLIC  
BISAMIDINE

BY

JINGWEI LI

B.S., Lanzhou University, 2001

M.S., Chinese Academy of Sciences, 2004

THESIS

Submitted to the University of New Hampshire

in Partial Fulfillment of

the Requirements for the Degree of

Master of Science

in

Chemistry

September, 2007

UMI Number: 1447894

### INFORMATION TO USERS

The quality of this reproduction is dependent upon the quality of the copy submitted. Broken or indistinct print, colored or poor quality illustrations and photographs, print bleed-through, substandard margins, and improper alignment can adversely affect reproduction.

In the unlikely event that the author did not send a complete manuscript and there are missing pages, these will be noted. Also, if unauthorized copyright material had to be removed, a note will indicate the deletion.

**UMI**<sup>®</sup>

---

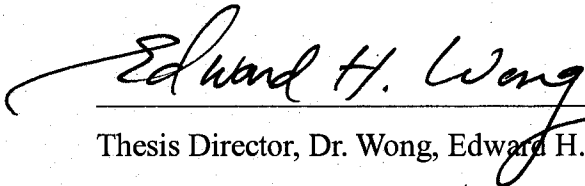
UMI Microform 1447894

Copyright 2007 by ProQuest Information and Learning Company.

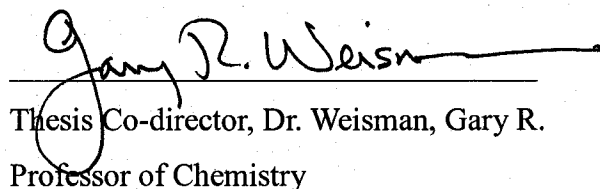
All rights reserved. This microform edition is protected against unauthorized copying under Title 17, United States Code.

ProQuest Information and Learning Company  
300 North Zeeb Road  
P.O. Box 1346  
Ann Arbor, MI 48106-1346

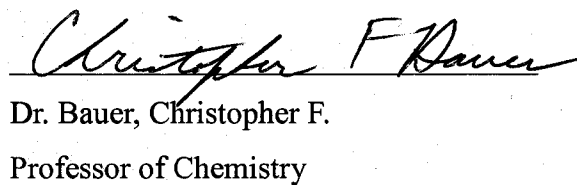
This thesis has been examined and approved.

  
\_\_\_\_\_

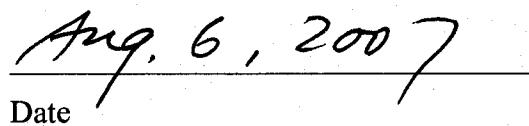
Thesis Director, Dr. Wong, Edward H.  
Professor of Chemistry

  
\_\_\_\_\_

Thesis Co-director, Dr. Weisman, Gary R.  
Professor of Chemistry

  
\_\_\_\_\_

Dr. Bauer, Christopher F.  
Professor of Chemistry

  
\_\_\_\_\_

Date

## DEDICATION

To my parents, brother and sister-in-law for all of the love and support.

## ACKNOWLEDGMENTS

I would first like to thank my advisor, Dr. Edward H. Wong for his guidance, help and patience throughout the last three years. He was always there to listen and to give advice. He always made me feel comfortable in lab and give me freedom in doing research. More importantly, he let me know more about inorganic chemistry. I would also like to thank Dr. Gary R. Weisman for his guidance in synthesis of BisAm ligands and my committee member Dr. Christopher Bauer for his time and help. I would like to thank all the professors who taught me at UNH. I would like to thank Ms. Cathy Gallagher for her assistance in my NMR experiments.

I would like to thank all the students in W-W group for their technical assistance, discussion and friendship. They are: Wei-Chih, Evan, Orjana, Elizabeth, Pete, Antoinette, Dan, Matt and Dave. I am also indebted to several non W-W group members, especially Qinglin, Hui, Weimin, Allison etc.

Last but not least, I would like to acknowledge the following UNH staff members: Ms. Amy Lindsay; Ms. Cindy Rohwer, Ms. Peggy Torch from the chemistry department; Mr. Bob Constantine from the UNH chemical library.

## TABLE OF CONTENTS

DEDICATION .....	iii
ACKNOWLEDGMENTS .....	iv
TABLE OF CONTENTS.....	v
LIST OF SCHEMES.....	ix
LIST OF TABLES.....	xi
LIST OF FIGURES .....	xii
ABSTRACT.....	xv
CHAPTER 1. INTRODUCTION .....	1
1.1 Introduction to tricyclic bisamidines (BisAm) .....	1
1.2 Coordination chemistry of 2,2,2-BisAm.....	5
CHAPTER 2. SYNTHESIS AND COORDINATION CHEMISTRY OF 3,2,3-BISAM ...	
.....	10
2.1 Introduction.....	10
2.2 Synthesis and characterization of 3,2,3-BisAm.....	11
2.3 Transition metal coordination of 3,2,3-BisAm.....	14
A. Palladium(II) .....	14
B. Tungsten(0) .....	18
C. Zinc(II) .....	19
D. Cadmium(II) .....	30
E. Mercury(II) .....	32

F. Silver(I) .....	38
G. Copper(II) .....	49
H. Europium(III) .....	58
2.4 Attempted aza-Diels-Alder reaction of BisAm's.....	63
2.5 Conclusion and future work.....	64
CHAPTER 3. SYNTHESIS OF CHIRAL BISAMS.....	65
3.1 Introduction.....	65
3.2 Synthesis of $C_2$ symmetric chiral 2,2,2-BisAm <b>71</b> .....	72
3.3 Attempted synthesis of $C_2$ symmetric chiral 3,2,3-BisAm <b>74</b> .....	78
3.4 Preliminary study of Cu(II)-BisAm catalyzed aziridination.....	84
3.5 Conclusion and future work.....	85
CHAPTER 4. EXPERIMENTAL SECTION.....	86
A. General experimental .....	86
B. Preparation of 3,2,3-BisAm and its transition metal complexes.....	86
Preparation of 3,2,3-BisAm ( <b>9</b> ) .....	88
Preparation of [Pd(3,2,3-BisAm)(CH <sub>3</sub> CN) <sub>2</sub> ](BF <sub>4</sub> ) <sub>2</sub> ( <b>23</b> ).....	89
Preparation of [Pd(3,2,3-BisAm) <sub>2</sub> ](BF <sub>4</sub> ) <sub>2</sub> ( <b>24</b> ) .....	90
Preparation of [Pd(3,2,3-BisAm) <sub>2</sub> ]Cl <sub>2</sub> ( <b>26</b> ) .....	91
Preparation of W(3,2,3-BisAm)(CO) <sub>4</sub> ( <b>27</b> ) .....	91
Preparation of [Zn(3,2,3-BisAm) <sub>2</sub> ](ClO <sub>4</sub> ) <sub>2</sub> ( <b>28</b> ) .....	92
Preparation of [Zn(3,2,3-BisAm) <sub>3</sub> ]Cl <sub>2</sub> ( <b>29</b> ).....	92
Preparation of [Zn(3,2,3-BisAm) <sub>3</sub> ](ClO <sub>4</sub> ) <sub>2</sub> ( <b>30</b> ) .....	93



Preparation of [Cd(3,2,3-BisAm) <sub>3</sub> ](ClO <sub>4</sub> ) <sub>2</sub> (32) .....	93
Preparation of [Hg(3,2,3-BisAm) <sub>2</sub> ](HgCl <sub>4</sub> ) (33) .....	94
Preparation of [Hg(3,2,3-BisAm) <sub>3</sub> ](BPh <sub>4</sub> ) <sub>2</sub> (34) .....	94
Preparation of [Ag(3,2,3-BisAm) <sub>2</sub> ](BF <sub>4</sub> ) (35) .....	95
Preparation of [Ag(3,2,3-BisAm) <sub>2</sub> ](BPh <sub>4</sub> ) (36) .....	95
Preparation of [Ag <sub>2</sub> (2,2,2-BisAm) <sub>4</sub> ](BF <sub>4</sub> ) <sub>2</sub> (37) .....	96
Preparation of [Ag <sub>2</sub> (2,2,2-BisAm) <sub>3</sub> ](BPh <sub>4</sub> ) <sub>2</sub> (38) .....	96
Preparation of [Cu(3,2,3-BisAm) <sub>3</sub> ](ClO <sub>4</sub> ) <sub>2</sub> (40) .....	97
Preparation of [Cu(3,2,3-BisAm) <sub>2</sub> ](ClO <sub>4</sub> ) <sub>2</sub> (41) .....	97
Preparation of [Cu(3,2,3-BisAm) <sub>2</sub> ](BF <sub>4</sub> ) <sub>2</sub> (44) .....	98
Preparation of [Eu(3,2,3-BisAm) <sub>4</sub> ](ClO <sub>4</sub> ) <sub>3</sub> (45) .....	98
C. Preparation of chiral BisAm's .....	99
Reagents .....	99
(S)-(+)-N-( <i>tert</i> -butoxycarbonyl)valine (66) .....	100
( <i>tert</i> -Butoxycarbonyl)-L-valylsuccinimide (67) .....	101
{1-[2-(2- <i>tert</i> -butoxycarbonylamino-3-methyl-butyrylamino)-ethylcarbamoyl]-2-methy- propyl}-carbamic acid <i>tert</i> -butyl ester (68) .....	102
( <i>S,S</i> )-2-Amino-N-[2-(amino-3-methyl-butyrylamino)-ethyl]-3-methylbutyramide ditrifluoroacetate salt (69) .....	102
( <i>S,S</i> )-2-Amino-N-[2-(amino-3-methyl-butyrylamino)-ethyl]-3-methyl-butane-1,2- diamine (70) .....	103
2,9-Diisopropyl-2,3,5,6,8,9-hexahydro-diimidazo[1,2- <i>a</i> ;2',1'- <i>c</i> ]pyrazine (71) .....	104
(±)-3-Amino-3-phenylpropanoic Acid (80) .....	105

(±)-Methyl 3-Amino-3-phenylpropanoate ( <b>81</b> ) .....	105
(3 <i>S</i> )-Methyl 3-Amino-3-phenylpropanoate ( <b>82a</b> ).....	106
(3 <i>S</i> )-Methyl-3- <i>tert</i> -Butoxycarbonylamino-3-phenylpropanoate ( <b>83</b> ).....	107
(3 <i>S</i> )-3- <i>tert</i> -Butoxycarbonylamino-3-phenylpropanoic acid ( <b>84</b> ).....	107
Preliminary aziridination reaction of styrene catalyzed by Cu(II)-3,2,3-BisAm.....	108
LIST OF REFERENCES .....	109
APPENDICES .....	114
APPENDIX A. SELECTED SPECTRA .....	115
APPENDIX B. COMPOUND INDEX.....	197

## LIST OF SCHEMES

<b>Scheme 1.1:</b> Synthesis of 2,2,2-BisAm and cyclen.....	3
<b>Scheme 1.2:</b> Polarization of a coordinated amidine.....	3
<b>Scheme 1.3:</b> Coordination modes of BisAm ligands.....	4
<b>Scheme 1.4:</b> Synthesis of cyclens.....	4
<b>Scheme 1.5:</b> Variants of 2,2,2-BisAm.....	8
<b>Scheme 1.6:</b> Preparation of TM-2,2,2-BisAm.....	8
<b>Scheme 2.1:</b> Synthesis of 3,2,3-BisAm.....	11
<b>Scheme 2.2:</b> Synthesis of $[\text{Pd}(3,2,3\text{-BisAm})(\text{CH}_3\text{CN})_2](\text{BF}_4)_2$ .....	14
<b>Scheme 2.3:</b> Synthesis of $[\text{Pd}(3,2,3\text{-BisAm})_2](\text{BF}_4)_2$ .....	16
<b>Scheme 2.4:</b> Synthesis of $\text{W}(3,2,3\text{-BisAm})(\text{CO})_4$ .....	18
<b>Scheme 2.5:</b> Synthesis of $[\text{Zn}(3,2,3\text{-BisAm})_2](\text{ClO}_4)_2$ .....	19
<b>Scheme 2.6:</b> Synthesis of $[\text{Zn}(3,2,3\text{-BisAm})_3]\text{Cl}_2$ .....	20
<b>Scheme 2.7:</b> Enantiomerization of $[\text{Zn}(3,2,3\text{-BisAm})_3]^{2+}$ .....	21
<b>Scheme 2.8:</b> Equilibrium between octahedral and tetrahedral isomers in solution.....	26
<b>Scheme 2.9:</b> Synthesis of $\text{Cd}(3,2,3\text{-BisAm})_3(\text{ClO}_4)_2$ .....	30
<b>Scheme 2.10:</b> Synthesis of “ $\text{Hg}(3,2,3\text{-BisAm})\text{Cl}_2$ ”.....	32
<b>Scheme 2.11:</b> Berry pseudorotation of $[\text{Hg}(3,2,3\text{-BisAm})_2]^{2+}$ .....	35
<b>Scheme 2.12:</b> Synthesis of $\text{Hg}(3,2,3\text{-BisAm})_3(\text{BPh}_4)_2$ .....	38
<b>Scheme 2.13:</b> Synthesis of $[\text{Ag}(3,2,3\text{-BisAm})_2](\text{BF}_4)$ .....	39
<b>Scheme 2.14:</b> Synthesis of $[\text{Ag}(3,2,3\text{-BisAm})_2](\text{BPh}_4)$ .....	40
<b>Scheme 2.15:</b> Synthesis of “[ $\text{Ag}(2,2,2\text{-BisAm})_2$ ]( $\text{BF}_4$ )”.....	42
<b>Scheme 2.16:</b> Synthesis of $[\text{Ag}_2(2,2,2\text{-BisAm})_3](\text{BPh}_4)_2$ .....	44

<b>Scheme 2.17:</b>	Synthesis of $[\text{Cu}(3,2,3\text{-BisAm})_3](\text{ClO}_4)_2$ .....	50
<b>Scheme 2.18:</b>	Synthesis of $[\text{Cu}(3,2,3\text{-BisAm})_2](\text{ClO}_4)_2$ .....	52
<b>Scheme 2.19:</b>	Attempted synthesis of $[\text{Cu}^{\text{I}}(3,2,3\text{-BisAm})_2](\text{BF}_4)$ .....	56
<b>Scheme 2.20:</b>	Synthesis of $[\text{Eu}(3,2,3\text{-BisAm})_4](\text{ClO}_4)_3$ .....	59
<b>Scheme 2.21:</b>	Attempted aza-Diels-Alder reaction of BisAms.....	63
<b>Scheme 3.1:</b>	Iwasawa's bisamidine ligands and the catalyzed coupling reaction.....	68
<b>Scheme 3.2:</b>	Oxazolines as chiral building blocks for N-heterocyclic carbene ligands.... .....	68
<b>Scheme 3.3:</b>	Casey's synthetic route to $C_2$ symmetric chiral 2,b,2-BisAm.....	70
<b>Scheme 3.4:</b>	Retrosynthetic analysis of ligand 71.....	71
<b>Scheme 3.5:</b>	Synthesis of ligand 73.....	71
<b>Scheme 3.6:</b>	Synthesis of ligand 71.....	73
<b>Scheme 3.7:</b>	Pd-catalyzed asymmetric allylic alkylation reaction.....	79
<b>Scheme 3.8:</b>	The asymmetric allylic alkylation reaction.....	81
<b>Scheme 3.9:</b>	Retrosynthetic analysis of ligand 74.....	82
<b>Scheme 3.10:</b>	Synthesis of racemic 3-amino-3-phenylpropanoic acid & derivative ....	83
<b>Scheme 3.11:</b>	Resolution of racemic methyl 3-amino-3-phenylpropanoate.....	83
<b>Scheme 3.12:</b>	Synthesis of Boc-protected ( <i>S</i> )-3-amino-3-phenylpropanoic acid.....	84
<b>Scheme 3.13:</b>	Preliminary study of $\text{Cu}^{\text{II}}$ -BisAm catalyzed aziridination.....	85

## LIST OF TABLES

<b>Table 2.1.</b>	Selected bond lengths(Å) and angles(°) for [Zn(3,2,3-BisAm) <sub>3</sub> ](ClO <sub>4</sub> ) <sub>2</sub> .....	24
<b>Table 2.2:</b>	Selected bond lengths(Å) and angles(°) for [Hg(3,2,3-BisAm) <sub>2</sub> ](HgCl <sub>4</sub> ) ...	34
<b>Table 2.3:</b>	Selected bond lengths(Å) and angles(°) for [Ag(3,2,3-BisAm) <sub>2</sub> ](BPh <sub>4</sub> ) .....	41
<b>Table 2.4:</b>	Selected bond lengths(Å) and angles(°) for [Ag <sub>2</sub> (3,2,3-BisAm) <sub>3</sub> ](BPh <sub>4</sub> ) <sub>2</sub> ...	47
<b>Table 2.5:</b>	Selected bond lengths(Å) and angles(°) for [Cu(3,2,3-BisAm) <sub>3</sub> ](ClO <sub>4</sub> ) <sub>2</sub> ....	51
<b>Table 2.6:</b>	Selected bond lengths(Å) and angles(°) for Cu(3,2,3-BisAm) <sub>2</sub> (ClO <sub>4</sub> ) <sub>2</sub> .....	54
<b>Table 2.7:</b>	Selected bond lengths(Å) and angles(°) for [Cu(3,2,3-BisAm) <sub>2</sub> ](BF <sub>4</sub> ) <sub>2</sub> .....	57
<b>Table 2.8:</b>	Selected bond lengths(Å) and angles(°) for [Eu(3,2,3-BisAm) <sub>4</sub> ](ClO <sub>4</sub> ) <sub>3</sub> .....	61
<b>Table 3.1:</b>	<sup>1</sup> H-NMR data for synthetic intermediate <b>70</b> .....	75
<b>Table 3.2:</b>	<sup>1</sup> H-NMR data for C <sub>2</sub> symmetric chiral 2,2,2-BisAm <b>71</b> .....	77

## LIST OF FIGURES

<b>Figure 1.1:</b> Related ligands .....	1
<b>Figure 1.2:</b> Abbreviations of tricyclic bisamidines .....	2
<b>Figure 1.3:</b> Ortep views of the X-ray structures of $[\text{Cu}_2\text{L}_3](\text{BF}_4)_2$ , $[\text{MnL}_3](\text{ClO}_4)_2$ , $[\text{ZnL}_3](\text{NO}_3)_2$ , and $[\text{FeL}_3](\text{BPh}_4)_2$ .....	6
<b>Figure 1.4:</b> Ortep views of the X-ray structures of $[\text{GdL}_4](\text{ClO}_4)_3$ and $[\text{LaL}_4(\text{H}_2\text{O})](\text{ClO}_4)_3$ .....	7
<b>Figure 2.1:</b> Ideal bite angles and coordination distances .....	10
<b>Figure 2.2:</b> Ortep view of the X-ray structure of TM-2,2,2-BisAm's with dithiooxamide .....	13
<b>Figure 2.3:</b> Comparison of the proposed structure of the palladium complex of 3,2,3-BisAm and the structure of the palladium complex of 2,2,2-BisAm .....	17
<b>Figure 2.4:</b> Ortep view of the X-ray structure of $\text{Pd}_2(2,2,2\text{-BisAm})_4\text{Br}_4$ .....	17
<b>Figure 2.5:</b> Ortep view of the X-ray structure of $[\text{Zn}(3,2,3\text{-BisAm})_3](\text{ClO}_4)_2$ .....	23
<b>Figure 2.6:</b> Ortep view of the X-ray structure of $[\text{Zn}(2,2,2\text{-BisAm})_3]^{2+}$ .....	25
<b>Figure 2.7:</b> Structure of tetramethyl-2,2'-biimidazole and zinc tris(tetramethyl-2,2'- biimidazole) complex .....	25
<b>Figure 2.8:</b> VT $^1\text{H-NMR}$ (400 MHz) of $\text{Zn}(3,2,3\text{-BisAm})_3(\text{ClO}_4)_2$ in $\text{CD}_3\text{CN}$ .....	28
<b>Figure 2.9:</b> VT $^1\text{H-NMR}$ (400 MHz) of $\text{Zn}(3,2,3\text{-BisAm})_3\text{Cl}_2$ in $d_6\text{-DMSO}$ .....	28
<b>Figure 2.10:</b> VT $^1\text{H-NMR}$ (400 MHz) of $\text{Zn}(3,2,3\text{-BisAm})_3(\text{ClO}_4)_2$ in $\text{CD}_3\text{CN}$ .....	29
<b>Figure 2.11:</b> Rationalization of the $^1\text{H-NMR}$ spectrum of the zinc complex .....	29
<b>Figure 2.12:</b> Ortep view of the X-ray structure of $[\text{Hg}(3,2,3\text{-BisAm})_2](\text{HgCl}_4)$ .....	33
<b>Figure 2.13:</b> Views of the two coordinated 3,2,3-BisAms .....	34

<b>Figure 2.14:</b> NMR spectra after addition of excess 3,2,3-BisAm to Hg <sub>2</sub> (3,2,3-BisAm) <sub>2</sub> Cl <sub>4</sub> .....	36
<b>Figure 2.15:</b> Ortep view of the X-ray structure of [Hg <sub>2</sub> (2,2,2-BisAm) <sub>2</sub> ]Cl <sub>4</sub> .....	37
<b>Figure 2.16:</b> Ortep view of the X-ray structure of [Ag(3,2,3-BisAm) <sub>2</sub> ](BPh <sub>4</sub> ) .....	41
<b>Figure 2.17:</b> Partial X-ray structure of [Ag <sub>2</sub> (2,2,2-BisAm) <sub>4</sub> ](BF <sub>4</sub> ) <sub>2</sub> .....	43
<b>Figure 2.18:</b> Ortep view of the X-ray structure of [Ag <sub>2</sub> (3,2,3-BisAm) <sub>3</sub> ](BPh <sub>4</sub> ) <sub>2</sub> .....	46
<b>Figure 2.19:</b> X-ray structure of the cation [Ag <sub>2</sub> (tBu <sub>3</sub> tpy) <sub>2</sub> (NO <sub>3</sub> ) <sup>+</sup> .....	48
<b>Figure 2.20:</b> Ortep view of the X-ray structure of [Cu(2,2,2-BisAm) <sub>3</sub> ] <sup>2+</sup> .....	49
<b>Figure 2.21:</b> Ortep view of the X-ray structure of [Cu(3,2,3-BisAm) <sub>3</sub> ](ClO <sub>4</sub> ) <sub>2</sub> .....	50
<b>Figure 2.22:</b> Ortep view of the X-ray structure of [Cu(3,2,3-BisAm) <sub>2</sub> (ClO <sub>4</sub> )]ClO <sub>4</sub> .....	53
<b>Figure 2.23:</b> Ortep view of the X-ray structure of [Cu <sub>2</sub> (2,2,2-BisAm) <sub>4</sub> (ClO <sub>4</sub> ) <sub>2</sub> ](ClO <sub>4</sub> ) <sub>2</sub> .. .....	55
<b>Figure 2.24:</b> Structures of [Cu <sub>2</sub> (2,2,2-BisAm) <sub>4</sub> ] <sup>4+</sup> and [Cu <sup>I</sup> <sub>2</sub> (2,2,2-BisAm) <sub>3</sub> ](BF <sub>4</sub> ) <sub>2</sub> ....	55
<b>Figure 2.25:</b> Ortep view of the X-ray structure of [Cu(3,2,3-BisAm) <sub>2</sub> ](BF <sub>4</sub> ) <sub>2</sub> .....	57
<b>Figure 2.26:</b> Ortep view of the X-ray structure of [Eu(2,2,2-BisAm) <sub>4</sub> (H <sub>2</sub> O)](ClO <sub>4</sub> ) <sub>3</sub> ..	59
<b>Figure 2.27:</b> Ortep view of the X-ray structure of [Eu(3,2,3-BisAm) <sub>4</sub> ](ClO <sub>4</sub> ) <sub>3</sub> .....	60
<b>Figure 2.28:</b> Paramagnetic effects on an NMR spectrum .....	62
<b>Figure 2.29:</b> Rationalization of the <sup>13</sup> C{ <sup>1</sup> H}-NMR spectrum of Europium complex...	62
<b>Figure 3.1:</b> Structures of privileged ligands.....	66
<b>Figure 3.2:</b> Structures of bis(oxazolines) .....	67
<b>Figure 3.3:</b> C <sub>2</sub> symmetric chiral 2,b,2-BisAm .....	69
<b>Figure 3.4:</b> Target molecules in this work .....	72
<b>Figure 3.5:</b> <i>Syn</i> - and <i>anti</i> -rotamer of Boc-protected ( <i>S</i> )-valine .....	73

<b>Figure 3.6:</b>	Structure of $C_2$ symmetric chiral tetraamine <b>70</b> .....	75
<b>Figure 3.7:</b>	Structure of $C_2$ symmetric chiral 2,2,2-BisAm <b>71</b> .....	77
<b>Figure 3.8:</b>	DEPT spectra of $C_2$ symmetric chiral 2,2,2-BisAm <b>71</b> .....	78
<b>Figure 3.9:</b>	Structural comparison of chiral 2,2,2-BisAm and 3,2,3-BisAm .....	80
<b>Figure 3.10:</b>	Steric interactions during alkylation.....	81



## ABSTRACT

# THE COORDINATION CHEMISTRY OF A CHELATING TRICYCLIC BISAMIDINE AND A NEW SYNTHETIC ROUTE TO A $C_2$ -SYMMETRIC TRICYCLIC BISAMIDINE

by

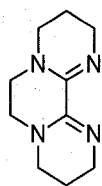
Jingwei Li

University of New Hampshire, September, 2007

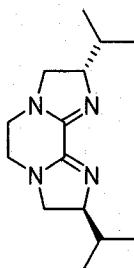
This thesis presents the synthesis of a novel tricyclic bisamidine, 3,2,3-BisAm **9** (2,3,4,6,7,9,10,11-octahydro-pyrazino[1,2-a:4,3-a'] dipyrimidine) and its coordination chemistry with transition metals. By comparison with its analogue 2,2,2-BisAm, which has diverse coordination modes including both symmetrical and unsymmetrical chelating as well as metal-bridging coordination modes, 3,2,3-BisAm, with a substantially larger ideal bite angle, only exhibits the chelating mode. The preparation and characterization of its complexes with W(0), Cu(II), Pd(II), Zn(II), Cd(II), Hg(II), Ag(I), and Eu(III) will be discussed in detail.

This thesis also describes the completion of a novel multi-step synthesis from *S*-valine of a  $C_2$  symmetric chiral 2,2,2-BisAm **71** (2,9-diisopropyl-2,3,5,6,8,9-hexahydro-diimidazo [1,2-a;2',1'-c] pyrazine, which can potentially serve as a chiral ligand in asymmetric catalysis. In addition, the synthesis of a  $C_2$  symmetric chiral 3,2,3-BisAm **74**

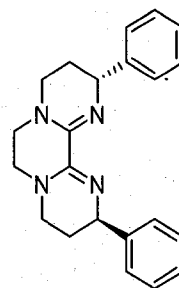
was initiated by adopting the same synthetic strategy. On the basis of these studies, a general synthetic route can be developed to prepare  $C_2$ -symmetric tricyclic bisamidines from chiral amino acids.



9



71



74

## CHAPTER 1

### INTRODUCTION

#### 1.1 Introduction to tricyclic bisamidines (BisAm)

Development of ligands has been the subject of intense interest for years due to their important roles in coordination and organometallic chemistry. Diimine ligands, especially bicyclic  $\alpha$ -diimines like 2,2'-bipyridine (BIPY), 2,2'-bimidazole (BIIM), 2,2'-bioxazoline (BOX) and tricyclic  $\alpha$ -diimines such as 1,10-phenanthroline (PHEN), have been widely studied. The coordination, biomimetic, supramolecular, material, and catalytic chemistry as well as photophysics and photochemistry of their complexes have been investigated.<sup>1-6</sup> However, there were no literature reports of the coordination chemistry of the novel  $\alpha$ -diimine ligand, tricyclic bisamidine **8**, before Weisman and

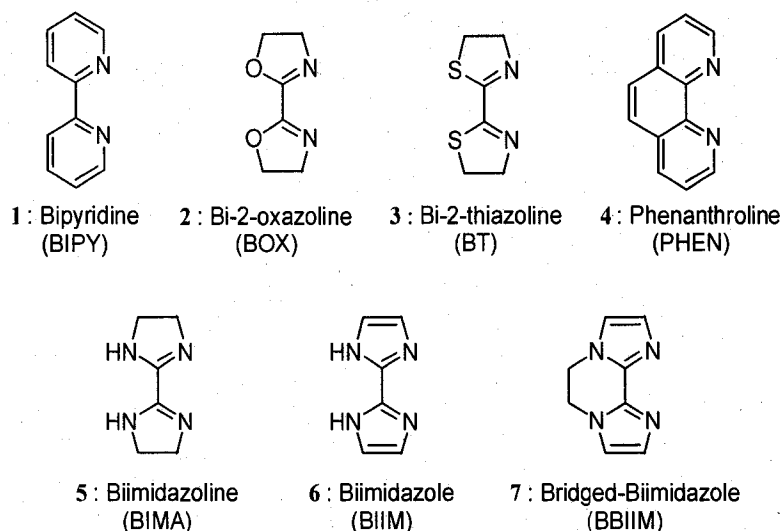
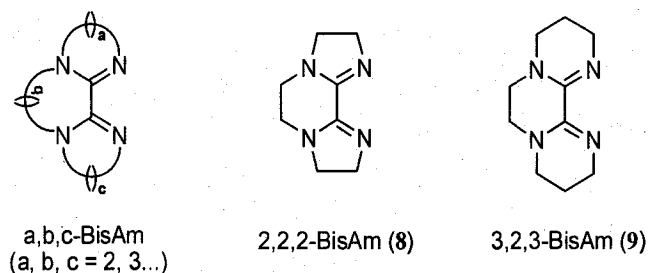


Figure 1.1 Related ligands

Wong's report in 2000.<sup>7,8</sup> Amongst these ligands, the known bridged biimidazole (BBIIM, 7) is the closest in structure to tricyclic bisamidine, though the additional unsaturation in the five-membered rings makes BBIIM more rigid and aromatic.<sup>9</sup> (Figure 1.1) Herein we report the synthesis and coordination chemistry of related tricyclic bisamidines including 9.

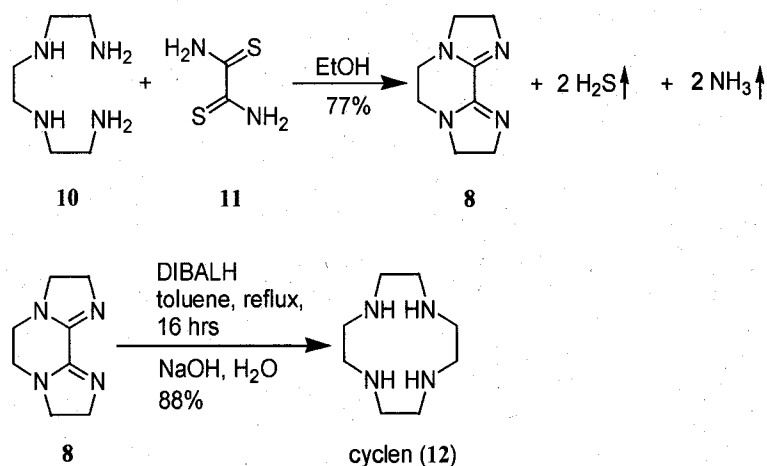
For convenience, a,b,c-BisAm will be employed as abbreviations of tricyclic bisamidines in this thesis. As shown in Figure 1.2, a, b and c stand for the number of methylenes, in the three bridges between the four nitrogen atoms.



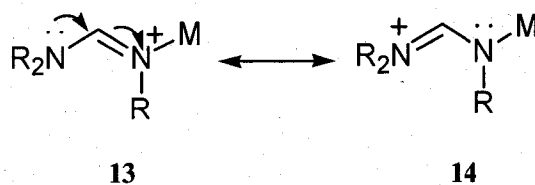
**Figure 1.2 Abbreviations of tricyclic bisamidines**

The first tricyclic bisamidine ligand, 2,3,5,6,8,9-hexahydrodiimidazo[1,2-a:2',1'-c]pyrazine) (8), 2,2,2-BisAm for short, was prepared by Reed and Weisman in 1997.<sup>10</sup> It was synthesized by direct condensation of dithiooxamide and triethylenetetraamine, releasing ammonia and hydrogen sulfide. The toxic hydrogen sulfide was trapped in a basic aqueous solution. At that time, 2,2,2-BisAm was not the final intended target but a synthetic intermediate. Reed and Weisman used it to develop a more efficient path to the popular 1,4,7,10-tetraazamacrocyclic, Cyclen (12), through the ring expansion of 2,2,2-BisAm.<sup>11</sup> (Scheme 1.1)

BisAm itself is an interesting ligand for a wide range of metal ions due to its specific structural features. Firstly, BisAm contains an  $\alpha$ -diimine within two C-linked amidines, so it has some advantages over diimine or bicyclic  $\alpha$ -diimine ligands. The amine lone pairs in the two amidines are in enhanced conjugation with imine  $\pi$ -bonds when a BisAm coordinates with a metal cation (**Scheme 1.2**). This makes BisAm a better electron donor. As a consequence of this conjugation, the formal C=N double bond will be slightly weakened and the formal C-N single bond will be shortened by gaining some double-bond character. Secondly, the prestrained but still somewhat torsionally flexible synperiplanar BisAm moiety can potentially adopt a variety of metal

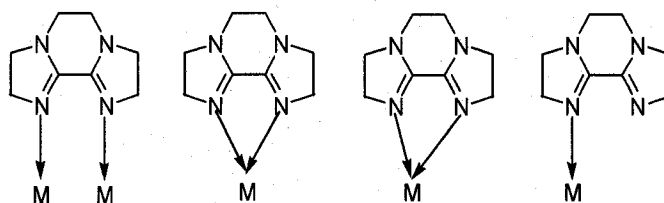


**Scheme 1.1 Synthesis of 2,2,2-BisAm and cyclen**

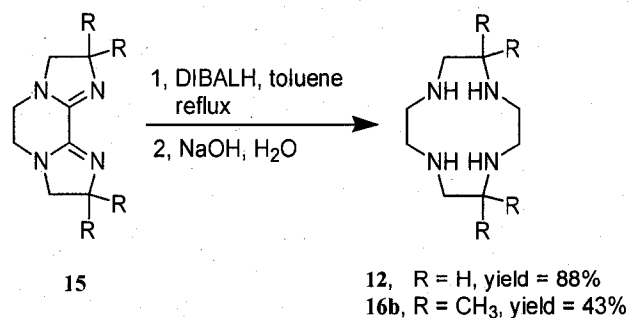


**Scheme 1.2 Polarization of a coordinated amidine**

coordination modes including symmetrical and unsymmetrical chelation, monodentate, as well as bimetallic bridging (**Scheme 1.3**). Molecular modeling of 2,2,2-BisAm suggested that the tricyclic backbone causes the imine lone pairs to splay out towards a near-parallel rather than convergent orientation.<sup>12</sup> A MM2 calculated model of 2,2,2-BisAm in a relaxed conformation showed that it has a small ideal bite angle ( $\sim 35^\circ$ ) and unrealistically long coordination distance (4.4 Å), which allows the possibility of its bridging two metals. Thirdly, many amidine ligands contain a secondary amino group, which may be deprotonated to form amidinate anion, to further complex with metals. The absence of such readily deprotonated amidine NH groups in BisAm eliminates potential complications due to this amidinate formation.



**Scheme 1.3 Coordination modes of BisAm ligands**



**Scheme 1.4 Synthesis of cyclens**

BisAms also have potential applications as precursors in the synthesis of C-substituted azamacrocycles. For example, 2,2,2-BisAm and its substituted analog (**15**) are convenient precursors to the popular tetraazamacrocyclic cyclen and its C-substituted cyclen derivative (**Schemes 1.4**).

## 1.2 Coordination Chemistry of 2,2,2-BisAm

The tricyclic biimidazoline, BisAm, features a prestrained synperiplanar bisamidine N=C-C=N donor set and potentially versatile metal coordination chemistry. Earlier work on BisAm complexation was performed by Widlicka and Fichter of Wong research group. Widlicka investigated the coordination chemistry of 2,2,2-BisAm with Mo(0), W(0), Mn(II), Fe(II), Co(II), Ni(II), Cu(II), Cu(I), Zn(II), Cd(II), Hg(II), Pd(II), as well as La(III) and found that 2,2,2-BisAm exhibits all four coordination modes shown in **Scheme 1.3**.<sup>12</sup> Fichter studied the synthesis and characterization of Ru(II), dimeric Pd(II), La(III), Eu(III), Gd(III), and Lu(III) complexes of 2,2,2-BisAm.<sup>13</sup>

2,2,2-BisAm (L) is chelating when it coordinates with manganese(II) in  $[\text{MnL}_3](\text{ClO}_4)_2$  (~ trigonal prismatic), iron(III) in  $[\text{FeL}_3](\text{BPh}_4)_3$  (~ octahedral), cobalt(II) in  $[\text{CoL}_3](\text{BPh}_4)_2$  (~ octahedral), cadmium(II) in  $[\text{CdL}_3](\text{ClO}_4)_2$  (~ trigonal prismatic), lanthanum(III) in  $[\text{LaL}_4(\text{H}_2\text{O})](\text{ClO}_4)_3$  (~ capped square-antiprism), europium(III) in  $[\text{EuL}_4(\text{H}_2\text{O})](\text{ClO}_4)_3$  (~ capped square-antiprism), gadolinium(III) in  $\text{GdL}_4(\text{ClO}_4)_3$  (~ rhombic-antiprismatic), and lutetium(III) in  $\text{LuL}_4(\text{ClO}_4)_3$  (~ dodecahedron). The 2,2,2-BisAm ligand exhibits a highly unsymmetrical chelation mode in the copper(II) complex  $[\text{CuL}_3](\text{ClO}_4)_2$  and dimeric mercury complex  $[\text{HgCl}_2\text{L}]_2$ . Two of the 2,2,2-BisAm molecules are monodentate while the third ligand chelates zinc(II) in  $[\text{ZnL}_3](\text{NO}_3)_2$ .

Three dimers, the copper(I) complex  $[\text{Cu}_2\text{L}_3](\text{BF}_4)_2$ , copper(II) complex  $[\text{Cu}_2\text{L}_4](\text{ClO}_4)_4$ , and palladium complex  $[\text{Pd}_2\text{L}_4]\text{Br}_4$  feature bridging 2,2,2-BisAms. (**Figure 1.3 and 1.4**)

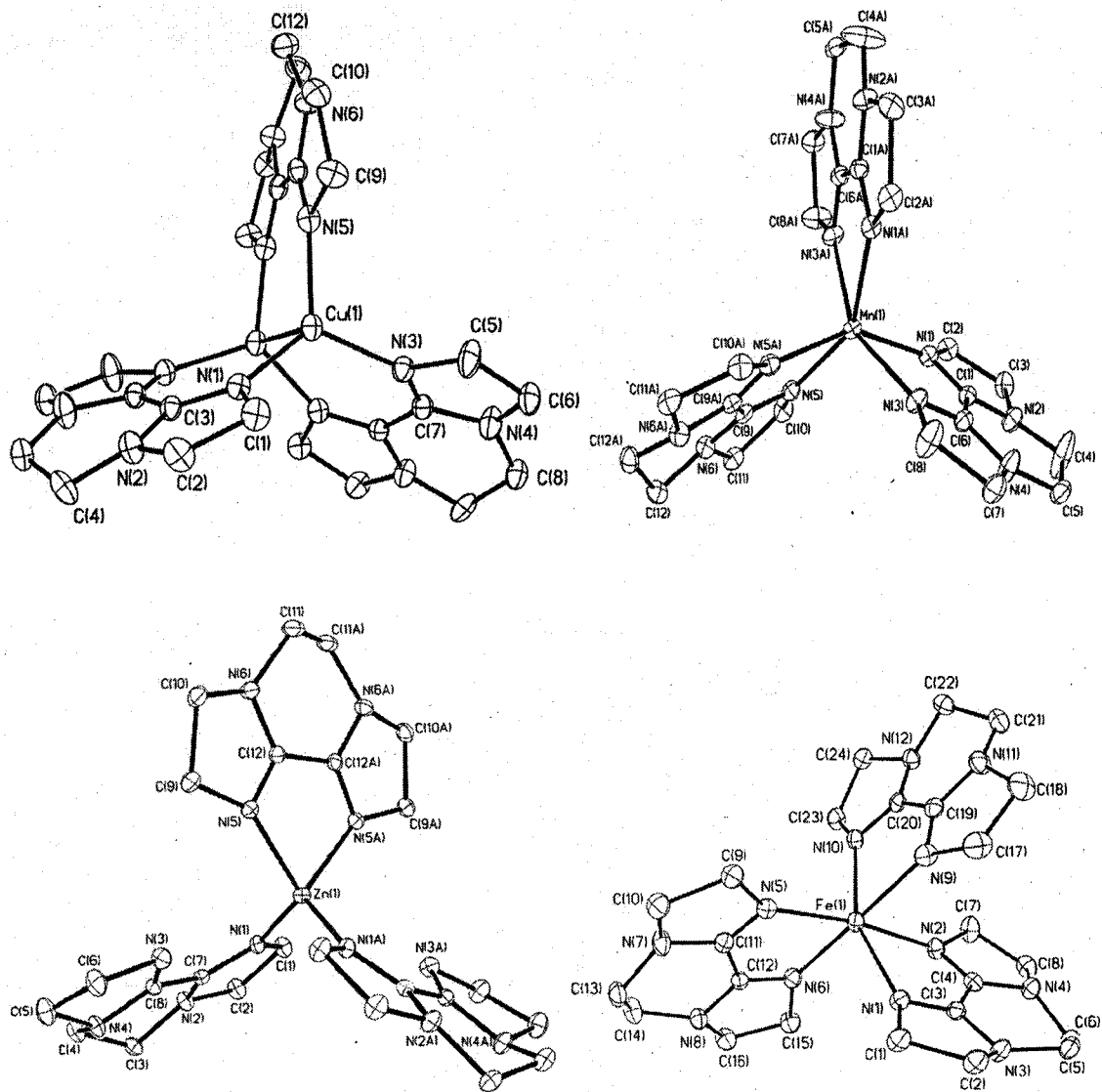


**Figure 1.3 Ortep views of the X-ray structures of  $[\text{Cu}_2\text{L}_3](\text{BF}_4)_2$  (top-left),  $[\text{MnL}_3](\text{ClO}_4)_2$  (top-right),  $[\text{ZnL}_3](\text{NO}_3)_2$  (bottom-left) and  $[\text{FeL}_3](\text{BPh}_4)_2$  (bottom-right) (Anions not shown)**



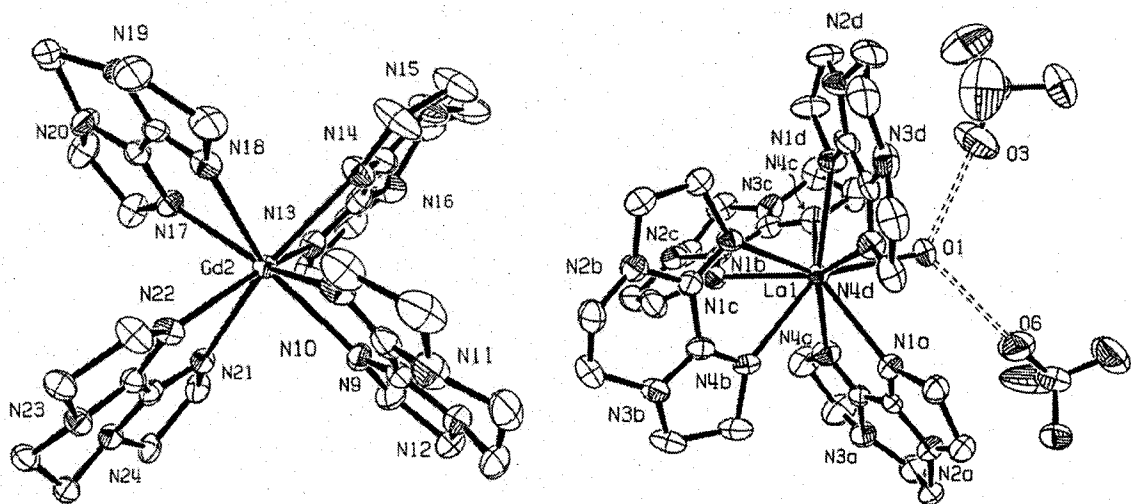
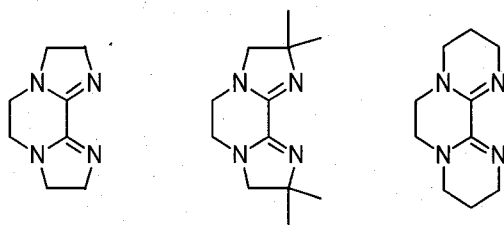


**Figure 1.4** Ortep views of the X-ray structures of  $\text{GdL}_4(\text{ClO}_4)_3$  (left, perchlorates not shown) and  $[\text{LaL}_4(\text{H}_2\text{O})](\text{ClO}_4)_3$  (right, remaining perchlorate not shown)

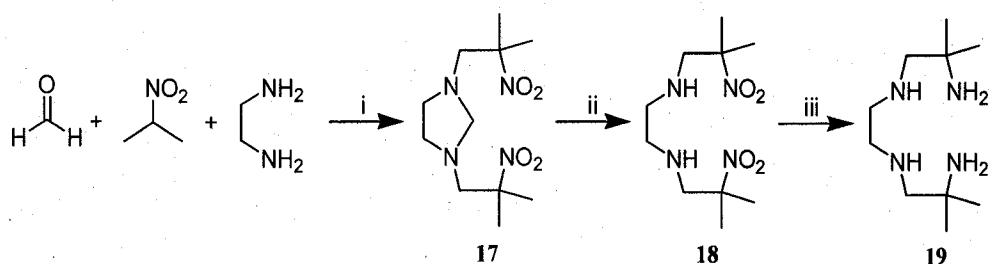
2,2,2-BisAm complexes are intriguing compounds. For example, the Pd(II) dimer can potentially be oxidized to form a Pd(III) dimer, reduced to a Pd(I) dimer, or in between mixed-valent species. The Eu(III) 2,2,2-BisAm complex has been found to be luminescent.<sup>13</sup> In addition, chiral BisAms can be effective ligands for metal-catalyzed asymmetric reactions.<sup>14</sup>

In order to investigate the impact of a structural modification of 2,2,2-BisAm, especially changes of the steric environment on its ability to coordinate, a bulkier ligand variant, Tetramethyl-2,2,2-BisAm **15**, was synthesized by incorporating two methyl groups on each carbon  $\alpha$  to the imine nitrogen (Scheme 1.5). Widlicka utilized a Mannich type reaction and cleavage of aminal **17** by acid hydrolysis to install 2-methyl-2-nitropropyl arms on ethylenediamine. Then the desired tetramethyl triethylenetetraamine **19** was obtained

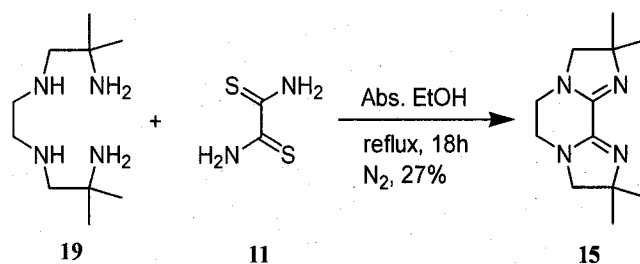


2,2,2-BisAm (8) TM-2,2,2-BisAm (15) 3,2,3-BisAm (9)

### Scheme 1.5 Variants of 2,2,2-BisAm



i) 60°C, H<sub>2</sub>O, 3 h, 81%; ii) conc. HCl, EtOH, 1 h, then 6M NaOH, 80%; iii) conc. HCl Sn (100 mesh), EtOH/H<sub>2</sub>O (4/1), 74%



### Scheme 1.6 Preparation of TM-2,2,2-BisAm

through nitro reduction by granular tin with hydrochloric acid in 80% ethanol. The last step was to condense the tetraamine 19 with dithiooxamide to afford Tetramethyl-2,2,2-BisAm (TM-2,2,2-BisAm) 15 (Scheme 1.6). With the TM-2,2,2-BisAm 15 in hand, Widlicka investigated the coordination chemistry of TM-2,2,2-BisAm with Zn(II), Cd(II) and Hg(II).<sup>8</sup> NMR studies of Cd(TM-2,2,2-BisAm)<sub>3</sub>(ClO<sub>4</sub>)<sub>2</sub> indicated that this ligand does exert a larger steric presence in the coordination sphere of cadmium. For the smaller

zinc(II), however, both 1:2 and 1:3 complexes coexist in solution, and a pure sample of  $\text{Zn(TM-2,2,2-BisAm)}_3^{2+}$  could not be isolated.

## CHAPTER 2

### SYNTHESIS AND COORDINATION CHEMISTRY OF 3,2,3-BISAM

#### 2.1 Introduction

Different ring-sized BisAm's can have different preferred coordination distances and bite angles which can lead to distinctive coordination chemistry. As pointed out in chapter 1, 2,2,2-BisAm has an ideal bite angle of only about  $35^\circ$  with a unreasonably long coordination distance of about  $4.4\text{\AA}$ . These led to its preference for chelating or bridging the bigger metals. While 3,2,3-BisAm prefers to coordinate the smaller metals in a chelating mode as a result of its larger ideal bite angle and shorter coordination distance (Figure 2.1). It will be much less likely to form bridged bimetallic complexes. The data in Figure 2.1 were obtained from MM2(Chem3D)-calculated models of BisAm's in relaxed conformations by Wong. In catalysis, ligand bite angles can significantly influence the steric properties of these ligands, enough to affect both the rates and selectivities of reactions. For example, diphosphine ligands with different ideal bite angles were applied in hydroformylation reactions.<sup>15</sup>

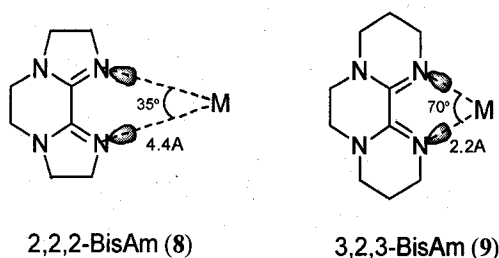
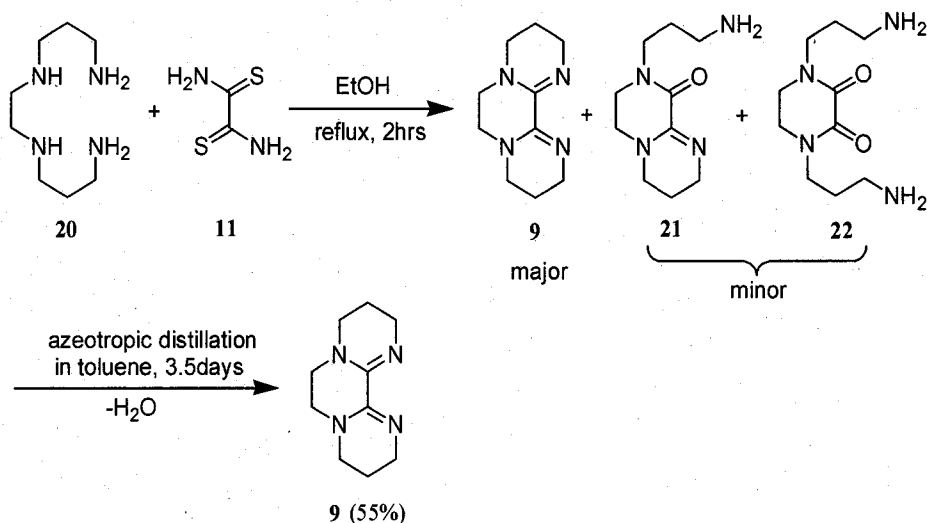


Figure 2.1 Ideal bite angles and coordination distances

We are interested in discovering the experimental consequences of the addition of extra methylene groups in the amidine rings of 2,2,2-BisAm. This modification was easily realized through the replacement of triethylenetetraamine by *N,N'*-bis-(3-aminopropyl)-1,2-ethylenediamine in the condensation reaction with dithioamide.

## 2.2 Synthesis and characterization of 3,2,3-BisAm



**Scheme 2.1** Synthesis of 3,2,3-BisAm

Synthesis of 3,2,3-BisAm was first performed by David Reed using the same condensation reaction as for 2,2,2-BisAm.<sup>16</sup> But a mixture resulted because hydrolysis of 3,2,3-BisAm had occurred (**Scheme 2.1**). Reed carried out an azeotropic distillation for three days to give an oily product of ~90% purity. The overall yield was approximately 25% following the dehydration. Upon repeating this reaction in this work, the reaction time was shortened to 2 hours from 4 hours, which gave the same <sup>1</sup>H-NMR spectrum. This indicated that the reaction was completed in two hours. The period that the residual

gases were purged from the reaction mixture was extended to 24 hours. This extended purge decreased the formation of black oil, which was insoluble in boiling toluene. The time of azeotropic distillation was also extended to 3.5 days. In this way a yellow solid was obtained after evaporating the solution under reduced pressure to give an overall yield of 55%. Occasionally, water removal by azeotropic distillation still did not yield pure 3,2,3-BisAm. In these cases, a kugelrohr distillation at 120°C and 150 millitorr was done to remove tetraamine impurities to give a yellow solid product. This yellow product was characterized by IR, UV-Vis, NMR spectroscopy and elemental analysis. The IR spectrum shows the asymmetric and symmetric  $\alpha$ -diimine stretching bands may merge to give a single strong and broad band at 1601  $\text{cm}^{-1}$ . The UV-Vis spectrum exhibits an intense  $\pi \rightarrow \pi^*$  band at 248 nm ( $\epsilon = 7500 \text{ M}^{-1}\text{cm}^{-1}$ ). Due to the time-averaged  $C_2$  symmetry of 3,2,3-BisAm, the  $^{13}\text{C}\{^1\text{H}\}$ -NMR spectrum ( $\text{CDCl}_3$  solvent) contains four peaks in the upfield region at 48.1 (tentatively  $\text{N}-\underline{\text{CH}_2}-\underline{\text{CH}_2}-\text{N}$ ), 47.7 (tentatively  $\gamma\text{-CH}_2$  to the imine N), 45.0 ( $\alpha\text{-CH}_2$  to the imine N) and 21.5 ( $\beta\text{-CH}_2$  to the imine N), with the amidine carbon observed at 148.0 ppm. Its proton NMR spectrum should contain two apparent triplets, one apparent quintet and one singlet, which is consistent with our experimental results. In the  $^1\text{H}$ -NMR spectrum ( $\text{CDCl}_3$ ), the four sets of resonances appear at 1.85 (quintet,  $\beta\text{-CH}_2$  to the imine N), 3.21 (triplet,  $\alpha\text{-CH}_2$  to the amine N), 3.22 (singlet,  $\text{N}-\underline{\text{CH}_2}-\underline{\text{CH}_2}-\text{N}$ ), 3.54 (triplet,  $\alpha\text{-CH}_2$  to the imine N) with the same integration values. The triplet at 3.21 ppm overlaps partly with the singlet at 3.22 ppm. The NMR spectra in  $\text{CD}_3\text{CN}$  were obtained to compare with the NMR spectra of the 3,2,3-BisAm complexes since most of the complexes dissolve easily in  $\text{CD}_3\text{CN}$ . In the NMR spectra in  $\text{CD}_3\text{CN}$ , it was observed that some 3,2,3-BisAm was hydrolyzed. Upon metal

coordination, all these signals should be shifted downfield. The elemental analysis confirmed that the yellow product has an empirical formula of  $C_{10}H_{16}N_4 \cdot (H_2O)_{0.8}$ .

Pure 3,2,3-BisAm should be expected to be colorless. The observed yellow color may be due to a small amount of dithiooxamide impurity in the sample. In the synthesis of TM-2,2,2-BisAm, Widlicka found not only the formation of TM-2,2,2-BisAm but also the presence of dithiooxamide in an X-ray structure of yellow crystals. In this X-ray structure, one molecule of dithiooxamide is held by hydrogen bonding of the N-H protons to an imine on each of two equivalents of TM-2,2,2-BisAm. Dithiooxamide is disordered over two orientations as shown (**Figure 2.2**). Two methods were attempted to purify the

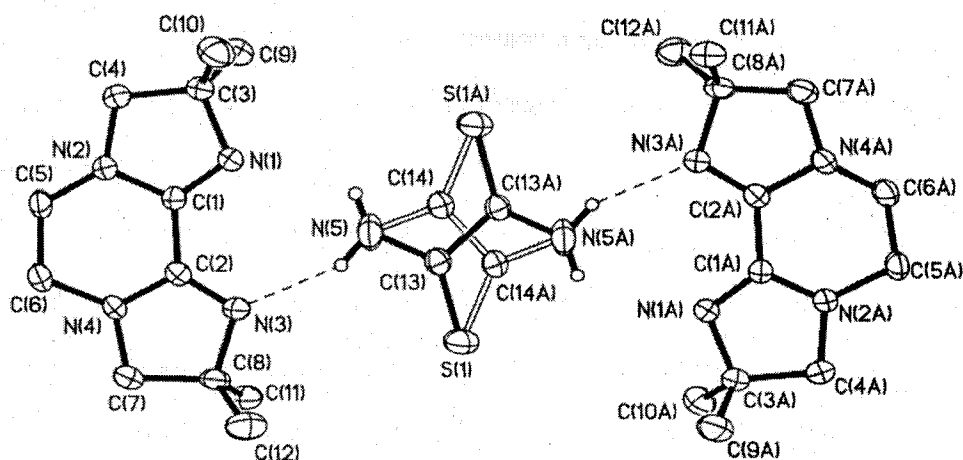


**Figure 2.2 Ortep view of the X-ray structure of TM-2,2,2-BisAm's with Dithiooxamide**

yellow product. One is sublimation at 130 °C and ~20 millitorr, which afforded a lighter yellow product after two sublimations. The other is recrystallization in hexane solution, which finally gave white 3,2,3-BisAm, but some 3,2,3-BisAm was hydrolyzed as

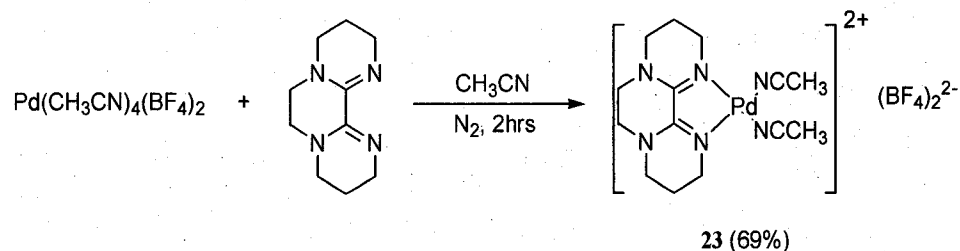
indicated by its NMR spectra. The combination of two methods, sublimation of the white 3,2,3-BisAm from recrystallization, afforded a pure white 3,2,3-BisAm.

## 2.3 Transition Metal Coordination of 3,2,3-BisAm

### A. Palladium (II)

Initial investigation into the coordination chemistry of 3,2,3-BisAm was made with palladium due to square-planar palladium(II) being of great interest for potential catalytic activity. Several attempts were therefore made to synthesize BisAm complexes of palladium.

The reaction between 3,2,3-BisAm and an equivalent of air-sensitive yellow, tetrakis(acetonitrile)palladium(II) tetrafluoroborate in CH<sub>3</sub>CN under N<sub>2</sub> atmosphere



**Scheme 2.2 Synthesis of [Pd(3,2,3-BisAm)(CH<sub>3</sub>CN)<sub>2</sub>](BF<sub>4</sub>)<sub>2</sub>**

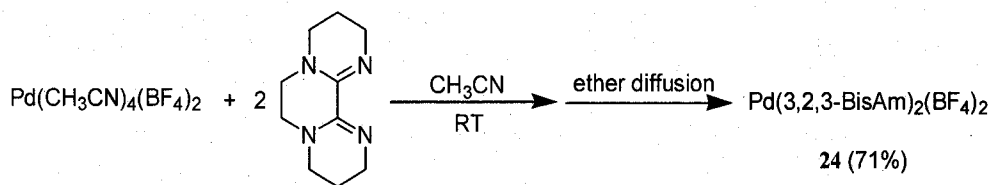
resulted in the formation of a dark-orange solution (**Scheme 2.2**). Yellow crystals were harvested by diffusion of diethyl ether into the CH<sub>3</sub>CN solution. This complex was characterized by IR, NMR spectroscopy and elemental analysis. Elemental analysis of this complex is consistent with the empirical formula of Pd(C<sub>10</sub>H<sub>16</sub>N<sub>4</sub>)(CH<sub>3</sub>CN)<sub>2</sub>(BF<sub>4</sub>)<sub>2</sub>. The <sup>1</sup>H-NMR spectrum of this complex maintains the same pattern for the free 3,2,3-BisAm though the resonances have different downfield shifts. This is due to the



deshielding of the protons of the ligand as the metal withdraws electron density from 3,2,3-BisAm when it coordinates to a metal. The multiplet that corresponds to the protons on the  $\beta$ -carbons overlaps with the residual solvent  $\text{CD}_3\text{CN}$  peak. The singlet at 1.99 ppm accounts for six protons from the two acetonitrile ligands. The  $^{13}\text{C}\{^1\text{H}\}$ -NMR spectrum contains the four expected resonances in the upfield region, with the amidine carbon observed at 156.5 ppm, a downfield shift of 8.5 ppm compared with the amidine carbon in free 3,2,3-BisAm. Besides a sharp  $\alpha$ -diimine stretching band at  $1621\text{ cm}^{-1}$ , the IR spectrum contains  $\text{C}\equiv\text{N}$  stretching bands at  $2259$  and  $2320\text{ cm}^{-1}$  and a broad strong band between  $1000$  and  $1150\text{ cm}^{-1}$ , which are characteristic B-F stretches in  $\text{BF}_4^-$ . It should be noted that the band at  $1621\text{ cm}^{-1}$  may be not a pure  $\text{C}=\text{N}$  stretch but is likely strongly coupled to C-C as well as other vibrational modes.<sup>77</sup> The  $d^8$  electron configuration of palladium(II) strongly favors square-planar coordination, so the structure proposed is that shown in **Scheme 2.2**. The FAB-MS spectrum further confirmed that the complex has a monomeric structure since the base peak is at 467.0978 amu, consistent with the mass of  $[\text{Pd}(3,2,3\text{-BisAm})(\text{CH}_3\text{CN})_2(\text{BF}_4)]^+$ .

When 3,2,3-BisAm was combined with tetrakis(acetonitrile)palladium(II) tetrafluoroborate in a 2:1 ratio in acetonitrile, a yellow solution also formed (**Scheme 2.3**). Diffusion of diethyl ether into the solution resulted in the formation of yellow needles. The complex was characterized by IR, NMR, ESI-MS spectroscopy and elemental analysis. The IR spectrum contains a sharp and strong imine stretching band at  $1612\text{ cm}^{-1}$ . The major change in the  $^{13}\text{C}\{^1\text{H}\}$ -NMR spectrum is that the amidine carbon shifted downfield to 155 ppm. In the  $^1\text{H}$ -NMR spectrum ( $\text{CD}_3\text{CN}$ ), the singlet was observed with a slight downfield shift at 3.45 ppm while the two apparent triplets now overlapped

partially between 3.36-3.43 ppm. Compared with the  $^1\text{H-NMR}$  spectrum of free 3,2,3-BisAm in  $\text{CD}_3\text{CN}$ , all the signals have expected downfield shifts. The ESI-MS spectrum provided further proof of composition since a major peak at 577.1 amu, consistent with the mass of  $[\text{Pd}(3,2,3\text{-BisAm})_2(\text{BF}_4)]^+$ , appeared. The elemental analysis confirmed that the complex is a bis-3,2,3-BisAm complex (**Figure 2.3**) with an empirical formula  $\text{Pd}(\text{C}_{10}\text{H}_{16}\text{N}_4)_2(\text{BF}_4)_2 \cdot (\text{H}_2\text{O})_{1.5}$ . Unfortunately, X-ray quality crystals were not obtained. In order to get X-ray quality crystals of the palladium complex, different palladium salts were tried.  $\text{PdCl}_2 \cdot 2\text{PhCN}$  was prepared by the reaction between  $\text{PdCl}_2$  and excess PhCN at  $80\text{-}100^\circ\text{C}$  for two hours.  $\text{PdCl}_2 \cdot 2\text{PhCN}$  reacted with two equivalents 3,2,3-BisAm in acetonitrile, which also afforded a yellow solution. However, X-ray quality crystals were still not obtained. This product was only characterized by NMR spectroscopy. Very similar  $^1\text{H-NMR}$  and  $^{13}\text{C}\{^1\text{H}\}\text{-NMR}$  spectra to those of  $\text{Pd}(3,2,3\text{-BisAm})_2(\text{BF}_4)_2$  were obtained. This suggested that the same cation  $[\text{Pd}(3,2,3\text{-BisAm})_2]^{2+}$  was obtained and that the chlorides were not coordinated.



**Scheme 2.3** Synthesis of  $[\text{Pd}(3,2,3\text{-BisAm})_2](\text{BF}_4)_2$

By contrast, 2,2,2-BisAm was previously found to adopt a bridging coordination mode when two equivalents of 2,2,2-BisAm was reacted with bis(phenylnitrile)palladium bromide in  $\text{CH}_3\text{CN}$ , and a novel dimeric structure resulted<sup>12</sup>. Two palladium centers are held in close proximity ( $2.747\text{\AA}$ ) by four bridging 2,2,2-BisAm molecules, although the

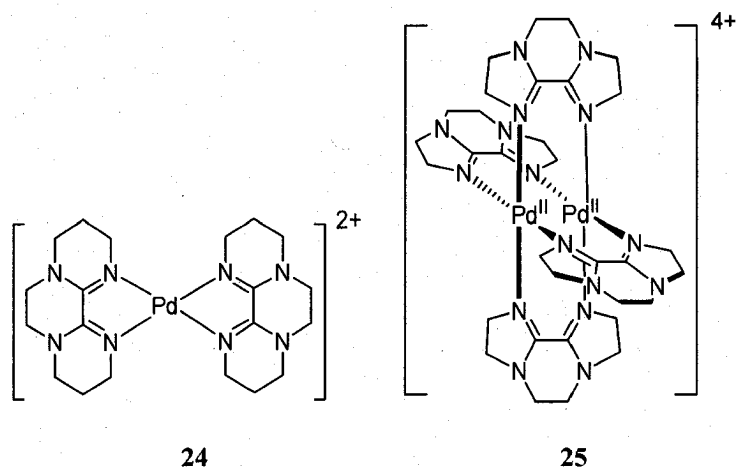


**Figure 2.3 Comparison of the proposed structure of the palladium complex of 3,2,3-BisAm and the structure of the palladium complex of 2,2,2-BisAm**

coordination sphere of the metal is also square planar (Figure 2.3 and Figure 2.4). This is exactly consistent with our prediction that 2,2,2-BisAm can coordinate in a bimetallic bridging mode, while this is unlikely for 3,2,3-BisAm.

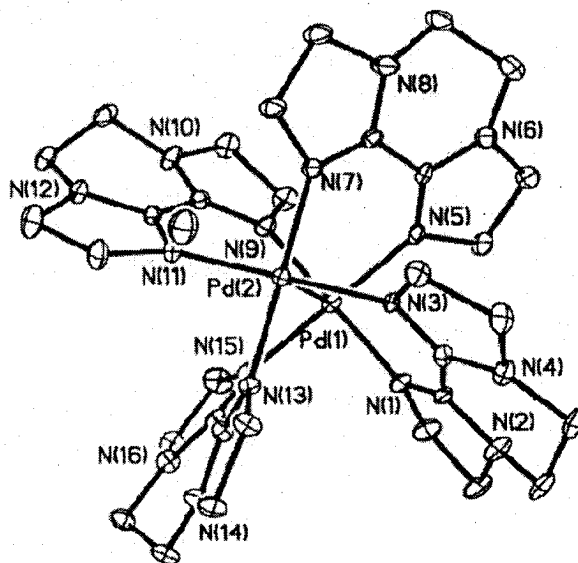
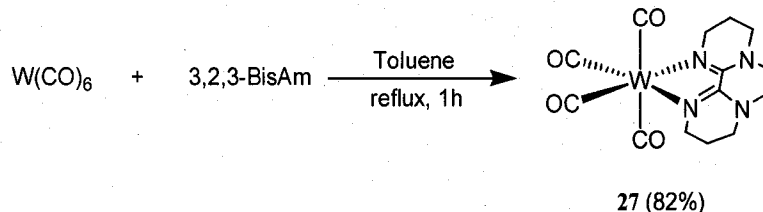


**Figure 2.4 Ortep view of the X-ray structure of  $[\text{Pd}_2(2,2,2\text{-BisAm})_4]\text{Br}_4$  (Bromides not shown for clarity)**

## B. Tungsten (0)

Due to their photophysical characteristics, mixed-ligand Group 6 transition metal carbonyls  $[M(CO)_4L]$  have many interesting applications such as candidates for probes in polymerization processes<sup>17</sup> and in the labeling of biomolecules<sup>18</sup> as well as nonlinear optical materials.<sup>19</sup> When less than one equivalent of 3,2,3-BisAm was added to tungsten hexacarbonyl in toluene with heating, a bright red precipitate formed (**Scheme 2.4**). The excess tungsten hexacarbonyl was sublimed out under vacuum to leave the crude product. This was characterized by NMR and FT-IR spectroscopy.



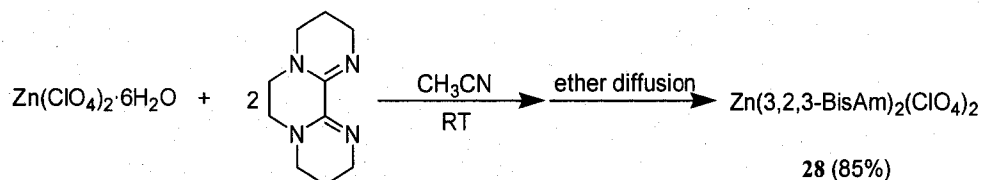
**Scheme 2.4 Synthesis of  $W(3,2,3\text{-BisAm})(CO)_4$**

In its IR spectrum, there are two strong stretching bands for the diimine at 1603  $\text{cm}^{-1}$  and 1625  $\text{cm}^{-1}$ . In addition, the complex has three strong bands at 2000  $\text{cm}^{-1}$ , 1851  $\text{cm}^{-1}$  (broad) and 1787  $\text{cm}^{-1}$ , which are characteristically CO stretches for  $C_{2v}$  tetracarbonyl complexes. Such complexes should have one symmetric stretch at high wavenumber and three asymmetric stretches. It is likely that two asymmetric stretching bands are overlapped in the broad 1851  $\text{cm}^{-1}$  band. NMR experiments were performed in  $d^7$ -DMF and  $CD_3CN$ , respectively. All the resonances in the  $^1H$ -NMR spectrum show downfield shifts relative to the free ligand. The  $^{13}C\{^1H\}$ -NMR spectrum is also informative; it contains two carbonyl resonances at 203 and 217 ppm, which confirmed the presence of CO's in axial and equatorial positions with respect to the diimine. All

data indicated that 3,2,3-BisAm had displaced two cis-carbonyls to form a 1:1 L:M complex with  $W(CO)_4$ . This complex is very unstable in  $CHCl_3$  in which the red color of the complex vanished within minutes due to decomposition.

Several years ago, Widlicka synthesized a tungsten analogue with 2,2,2-BisAm.<sup>12</sup> All the experimental data showed that the 2,2,2-BisAm also chelated tungsten by displacing two cis- carbonyls, forming the complex  $W(CO)_4(2,2,2-BisAm)$ . From the IR spectra, it was revealed that the  $\pi$ -acceptor ability of 2,2,2-BisAm is similar to that of BIIM but greater than that of 3,2,3-BisAm by comparison of symmetric  $A_1$  CO stretches ( $W(CO)_4(2,2,2-BisAm)$  :  $2002.7\text{ cm}^{-1}$ ;  $W(CO)_4(BIIM)$  :  $2003\text{ cm}^{-1}$ ;  $W(CO)_4(3,2,3-BisAm)$  :  $2000\text{ cm}^{-1}$ ) since higher  $\nu_{CO}$  frequencies indicate greater W-L  $\pi$ -back bonding.

### C. Zinc (II)

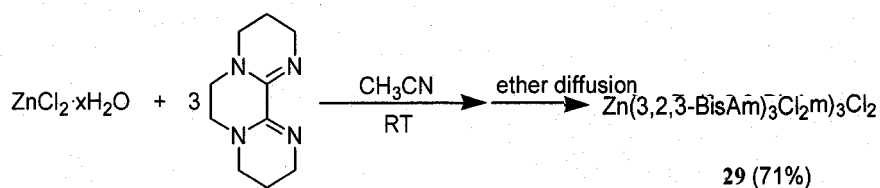


**Scheme 2.5** Synthesis of  $[Zn^{II}(3,2,3-BisAm)_2](ClO_4)_2$

Treatment of zinc perchlorate hexahydrate with two equivalents of 3,2,3-BisAm in acetonitrile gave a colorless solution (Scheme 2.5). Recrystallization of the product from acetonitrile by diethyl ether diffusion yielded colorless crystals. This complex was characterized by elemental analysis, IR and NMR spectroscopy. The elemental analysis confirmed the formation of this zinc bis-(3,2,3-BisAm) complex. It has a simple  $^1H$ -NMR spectrum which maintains the same pattern as the free ligand but with downfield shifts.

Its  $^{13}\text{C}\{^1\text{H}\}$ -NMR spectrum contains the four expected resonances in the upfield region and the amidine carbon signal at 149.8 ppm. In the IR spectrum, a sharp and strong band shows up at  $1614\text{ cm}^{-1}$ , consistent with  $\alpha$ -diimine stretches. The asymmetric and symmetric  $\alpha$ -diimine stretching bands may overlap.

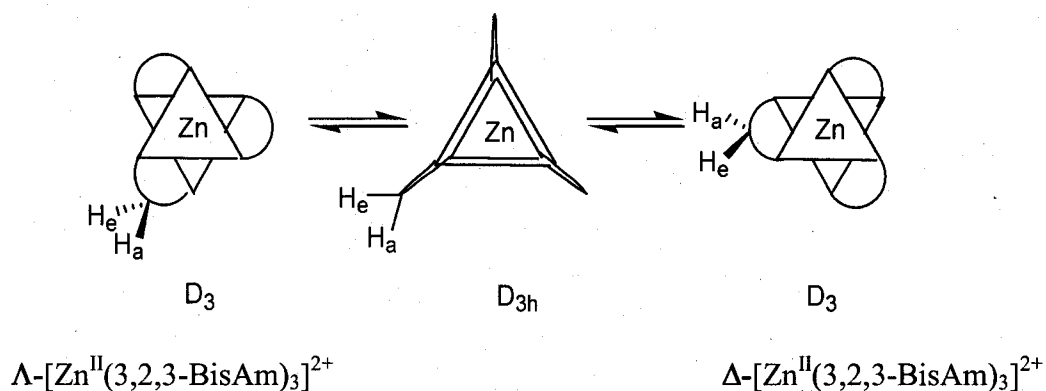
Treatment of  $\text{ZnCl}_2 \cdot x\text{H}_2\text{O}$  with  $\sim$  three equivalents of 3,2,3-BisAm in acetonitrile led to a colorless solution. This solution was transferred to small vials and recrystallized by diethyl ether diffusion to afford a white solid product (**Scheme 2.6**).



### Scheme 2.6 Synthesis of $[\text{Zn(3,2,3-BisAm)}_3]\text{Cl}_2$

This white product was characterized by elemental analysis, IR, and NMR spectroscopy. Elemental analysis of this product confirmed that it is indeed a tris-3,2,3-BisAm complex with an empirical formula  $[\text{Zn(3,2,3-BisAm)}_3]\text{Cl}_2 \cdot (\text{H}_2\text{O})_4$ . In the IR spectrum, there is a broad band between  $1607$  and  $1619\text{ cm}^{-1}$ , which suggests overlapping diimine stretching bands. This may be ascribed to different ligand coordination modes in the solid state. Interestingly, the  $^1\text{H}$ -NMR spectrum ( $\text{CD}_3\text{CN}$  as NMR solvent) provides important information since there are two multiplets in the upfield region at 1.91 ppm and 1.76 ppm and the area ratio of these two multiplets is approximately 7:5. This region can be assigned to the methylene protons  $\beta$  to the imine N. In addition, the downfield region of this spectrum is also more complicated than that of free ligand or the other metal complexes. It is composed of four groups of resonances. The integrated ratio of these four

downfield groups of resonances (3.10 ppm to 3.56 ppm) relative to the two upfield multiplets is 3: 1, as expected for 3,2,3-BisAm. On the basis of the  $^1\text{H}$ -NMR spectrum of free ligand, it can be conjectured that the smaller multiplet at 1.76 ppm is due to the  $\beta$ - $\text{CH}_2$  on uncoordinated imines. In the  $^{13}\text{C}\{^1\text{H}\}$ NMR spectrum, three minor peaks showed up beside three of the four major resonances (46.6, 42.5 and 20.4 ppm). These three signals correspond to carbons  $\gamma$ - $\text{CH}_2$ ,  $\alpha$ - $\text{CH}_2$  and  $\beta$ - $\text{CH}_2$  to the imine N respectively. However, the height ratio of major to minor peaks is only about 8:1. Ascribing the minor signals to two different amidine environments cannot be reconciled with the  $^1\text{H}$  NMR data. Nor were we able to grow X-ray quality crystals of this complex.



**Scheme 2.7 Enantiomerization of  $[\text{Zn}^{\text{II}}(3,2,3\text{-BisAm})_3]^{2+}$**

It was also considered that the severe steric hindrance which results from three ligands around the  $\text{Zn}(\text{II})$  center may slow the enantiomerization of a  $\text{D}_3$ -symmetric  $[\text{Zn}^{\text{II}}(3,2,3\text{-BisAm})_3]^{2+}$  (Scheme 2.7), rendering the methylene protons on the ligands diastereotopic. This may be the reason why its  $^1\text{H}$ -NMR spectrum is more complicated. However, if the upfield methylene protons on  $\beta$ -carbons are indeed diastereotopic, a 1 : 1 ratio of  $\text{H}_{\text{eq}} : \text{H}_{\text{ax}}$  should result instead of the observed 7 : 5 ratio.

The appearance of only a trace proton NMR multiplet around 2.6 ppm confirmed that 3,2,3-BisAm was not significantly hydrolyzed by water, although the  $\text{ZnCl}_2$  used contained waters of hydration. Both mono- and di- hydrolyzed species should produce a triplet resonance around 2.6 ppm corresponding to two hydrogen on the  $\alpha\text{-CH}_2$  to  $\text{NH}_2$ . This confirmed that reagent metal salts with some waters of crystallization will not be detrimental to metal complexation.

In order to grow X-ray quality crystals of this zinc 3,2,3-BisAm complex, the zinc perchlorate salt was used as a starting material. Treatment of zinc perchlorate hexahydrate with three equivalents of 3,2,3-BisAm in acetonitrile also gave a colorless solution. The  $^1\text{H-NMR}$  and  $^{13}\text{C}\{^1\text{H}\}\text{-NMR}$  spectra of this perchlorate complex are identical to those of chloride complex **29**. The  $^{13}\text{C}\{^1\text{H}\}\text{-NMR}$  spectrum revealed that those three minor peaks might indeed be from small amounts of hydrolyzed ligand **21** (see **Scheme 2.1**). This is because, in addition to the three minor signals mentioned above, two resonances at 39.3 and 30.3 ppm also appeared, indicative of some 3,2,3-BisAm hydrolysis. In its  $^1\text{H-NMR}$  spectrum, a small apparent triplet resonance at 2.50 ppm and a small apparent quintet at 1.62 ppm were observed, which provided additional proof of some 3,2,3-BisAm's hydrolysis. Recrystallization of this product from acetonitrile/ether diffusion yielded colorless crystals. The X-ray structure of  $\text{Zn}(\text{3,2,3-BisAm})_3(\text{ClO}_4)_2$  (**30**) was thus determined (**Figure 2.5**). All three ligands are in the chelating coordination mode. This complex has a pseudo- $C_3$  axis passing through the central zinc(II) and an approximate  $C_2$  axis passing through each of the ligands, giving the complex approximate overall  $D_3$  symmetry. Its trigonal twist angle is about  $45^\circ$ , which is closer to idealized octahedral ( $60^\circ$ ) than trigonal prismatic ( $0^\circ$ ). (A trigonal twist



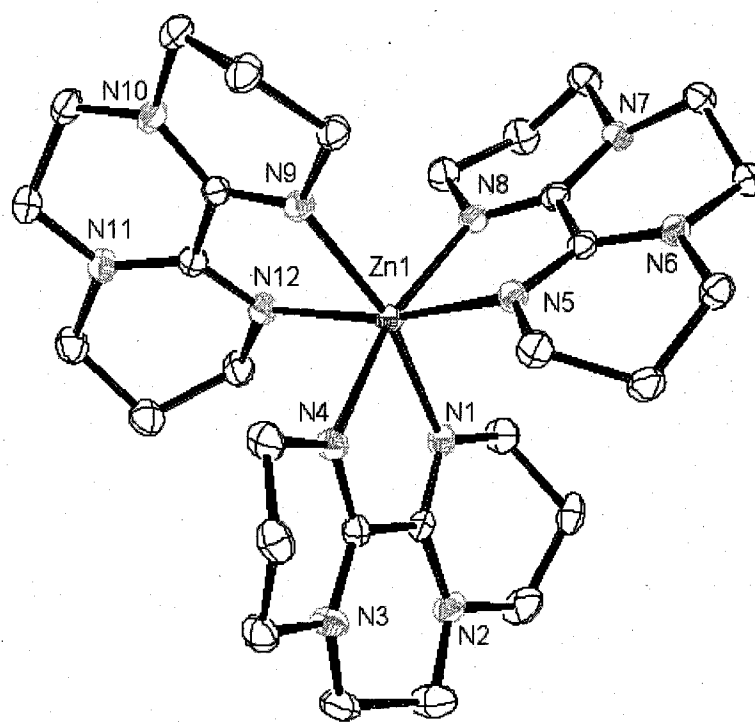


**Figure 2.5** Ortep view of the X-ray structure of  $[\text{Zn}(3,2,3\text{-BisAm})_3](\text{ClO}_4)_2 \cdot 30$   
(Perchlorates not shown)

angle is defined as the N-M-N angle measured on the projection of the two triangular faces of the octahedron projected along its pseudo-threefold axes on the medium plane containing the metal ion and it can be used to account for any deviation in the M-N<sub>6</sub> geometry from a perfect octahedron ( $O_h$ ) to a perfect trigonal prismatic structure ( $D_{3h}$ .)

3,2,3-BisAm ligands are coordinated to zinc with an average Zn-N bond length of 2.15 Å and average bite angle of 75.7° with both values close to the calculated ideal numbers in **Figure 2.1.** (Page 10) With an average diimine torsion angle of 5.8°, the ligand is only slightly distorted from planarity with the sum of amine (C-N-C) bond angles of 357.2°. The average amidine C=N distance is 1.29 Å and the average C-N is 1.35 Å (**Table 2.1**).

**Table 2.1** Selected bond lengths(Å) and angles(°) for [Zn(3,2,3-BisAm)<sub>3</sub>](ClO<sub>4</sub>)<sub>2</sub> **30**

Bond lengths		Bond angles	
Zn(1)-N(1)	2.1370(16)	N(1)-Zn(1)-N(4)	75.54(6)
Zn(1)-N(4)	2.1501(16)	N(5)-Zn(1)-N(8)	76.85(6)
Zn(1)-N(5)	2.1490(16)	N(12)-Zn(1)-N(9)	74.80(6)
Zn(1)-N(8)	2.1059(16)	N(1)-Zn(1)-N(8)	95.50(6)
Zn(1)-N(9)	2.1695(15)	N(8)-Zn(1)-N(9)	94.56(6)
Zn(1)-N(12)	2.1949(16)	N(4)-Zn(1)-N(9)	96.23(6)
C(9)-N(4)	1.290(2)	N(5)-Zn(1)-N(12)	167.29(6)
C(9)-N(3)	1.354(2)	C(10)-N(2)-C(4)	122.78(17)
C(10)-N(2)	1.348(2)	C(10)-N(2)-C(3)	120.32(17)
C(10)-N(1)	1.290(2)	C(4)-N(2)-C(3)	114.14(17)
C(19)-N(7)	1.353(2)	C(9)-N(3)-C(5)	119.30(17)
C(19)-N(8)	1.290(2)	C(9)-N(3)-C(6)	119.35(16)
C(20)-N(5)	1.293(2)	C(5)-N(3)-C(6)	118.59(16)
C(20)-N(6)	1.351(2)		
		Dihedral angles	
		N(4)-C(9)-C(10)-N(1)	-2.93
		N(5)-C(20)-C(19)-N(8)	-8.66

Esd's are in parentheses.

With the X-ray structure of zinc tris(3,2,3-BisAm) complex in hand, it is easy to draw a conclusion that 3,2,3-BisAm is a better chelating ligand than 2,2,2-BisAm. The zinc tris(2,2,2-BisAm) coordination sphere is pseudo-tetrahedral in its X-ray analysis. Two coordination modes were found in the solid state (**Figure 2.6**). Two of the 2,2,2-BisAm molecules are monodentate while the third ligand chelates zinc. By contrast, all three ligands chelate the metal in the zinc 3,2,3-BisAm complex in an approximately octahedral geometry.

A search of the *Cambridge Structural Database* revealed few structures of zinc tris( $\alpha$ -diimine) complexes. The zinc tris(tetramethyl-2,2'-biimidazole) complex was

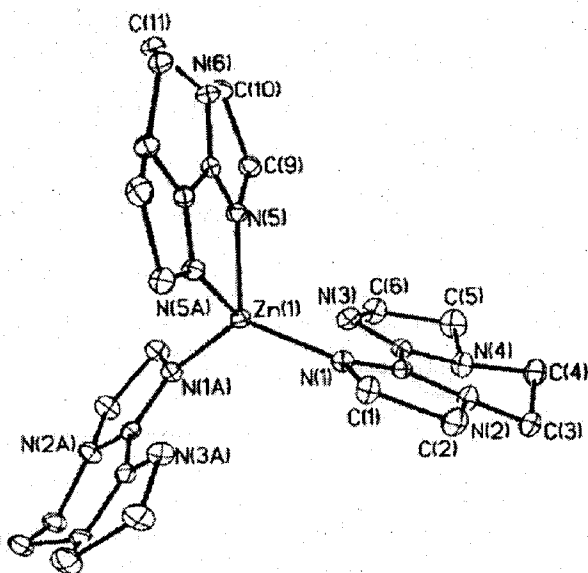


**Figure 2.6** Ortep view of the X-ray structure of  $[\text{Zn}^{\text{II}}(2,2,2\text{-BisAm})_3]^{2+}$

reported to have a distorted octahedral coordination environment and the biimidazole ligands chelated to zinc through their unprotonated N atoms with a Zn-N distance range of 2.149(3)-2.208(2)Å.<sup>20</sup> (**Figure 2.7**) The BIIM ligand chelated zinc with an average bite angle of 78.3°, which is slightly larger than what we observed for bidentate 3,2,3-BisAm in its zinc complex.

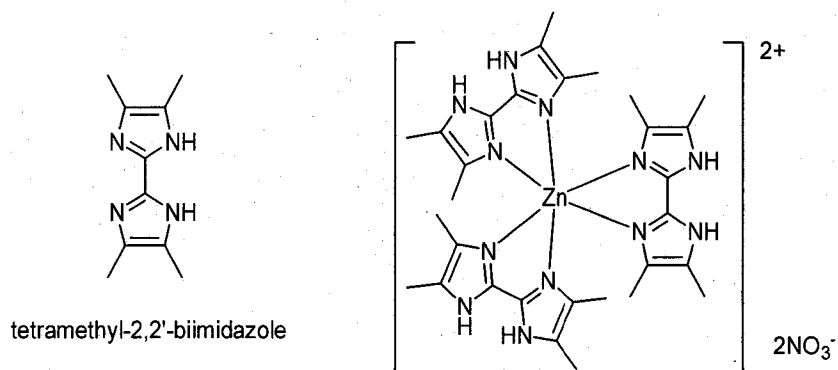
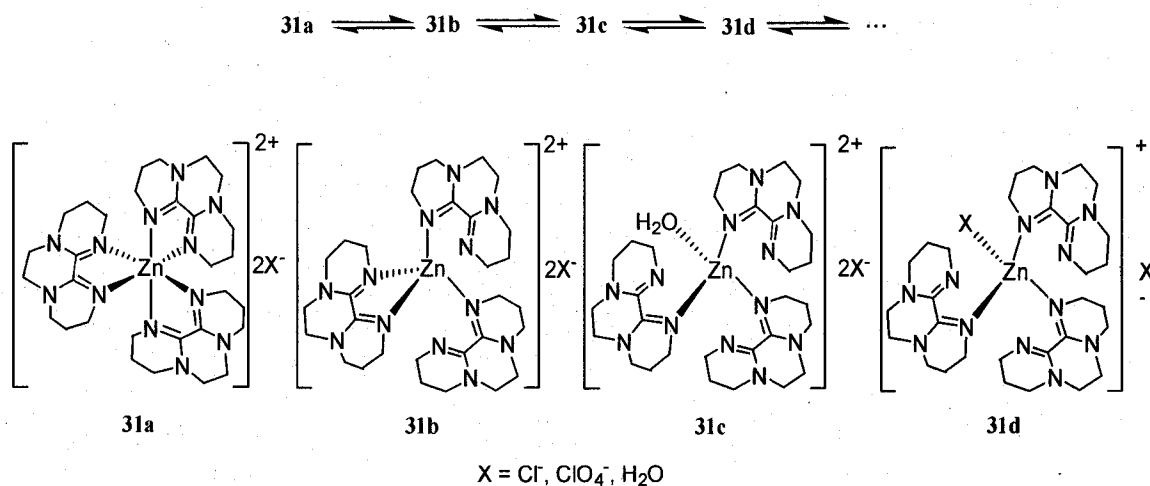


**Figure 2.7** Structure of tetramethyl-2,2'-biimidazole and zinc tris(tetramethyl-2,2'-biimidazole) complex

Studies into the coordination preferences of zinc have been carried out by comparing data in the *Cambridge Structural Database* to *ab initio* molecular orbital calculations on hydrated structures.<sup>21</sup> These revealed that both four- and six-coordinate structures are possible.<sup>21</sup> The flexibility of zinc coordination geometry and number is important in solution as well as in the solid state and can lead to equilibria of species with different coordination numbers. Such equilibria between  $Zn^{2+}$  species with coordination numbers 6 and 5 or 4 are indeed quite common in solution for small ligands. For example, zinc with the relatively simple ligand 1,2-ethylenediamine forms 1:1 and 1:2 metal to ligand complexes in aqueous solution and equilibria can also exist between tetrahedral and octahedral species, with 50% (1:1) and 90% (1:2) existing as tetrahedral, respectively.<sup>22</sup> Based on these facts and our NMR data, it is possible that an equilibrium between octahedral and tetrahedral isomers exists in solution (**Scheme 2.8**). The slow  $\eta^1$ - $\eta^2$  exchange on the NMR time scale can produce the  $^1H$ -NMR spectrum mentioned above.



**Scheme 2.8 Equilibria between octahedral and tetrahedral isomers in solution**

If the two multiplets at 1.90 and 1.75 ppm are due to the  $\beta$ -CH<sub>2</sub> on the coordinated and uncoordinated amidines respectively, the existence of isomer **31b**, **31c**, **31d**, etc. can then

result in the ratio of 7:5 observed in the upfield region. This is because a mixture including only **31a** and **31b** will give a higher ratio of coordinated  $\beta$ -CH<sub>2</sub>'s than 7:5.

A variable-temperature NMR experiment was conducted. When the sample was warmed, the rate of exchange may become faster than the NMR timescale so that an averaged spectrum is observed. At 70°C, the two broad peaks at 1.75 and 1.90 ppm almost coalesced in CD<sub>3</sub>CN solution (**Figure 2.8**). The position of a coalesced resonance at high-temperature is the weighted average of the resonance positions at the lower-temperature<sup>23</sup>. If  $n_1$  nuclei resonates at  $\delta_1$  and  $n_2$  at  $\delta_2$ , then at the higher temperature, the resonance position will be the weighted average  $\delta_{av} \approx (n_1 \cdot \delta_1 + n_2 \cdot \delta_2) / (n_1 + n_2)$ , assuming that the equilibrium doesn't change with temperature. Those variable-temperature NMR spectra further confirmed that the two broad peaks in the upfield region are not entirely due to the two diastereotopic methylene protons on the  $\beta$ -carbons since the coalesced resonance is not in the middle. In the <sup>1</sup>H-NMR spectrum of [Zn(3,2,3-BisAm)<sub>3</sub>]Cl<sub>2</sub> in d<sub>6</sub>-DMSO at 25°C, if we assume that the resonance at 1.65 ppm corresponds to the protons of  $\beta$ -CH<sub>2</sub> on uncoordinated imines, then the resonance at 1.78 ppm is due to the protons of  $\beta$ -CH<sub>2</sub> on coordinated imines (**Figure 2.9**). At 100°C, a coalesced broad peak is found around 1.8 ppm.

These VT-NMR experiments inspired us to consider an alternative possibility that ZnL<sub>3</sub>(ClO<sub>4</sub>)<sub>2</sub> dissociates into ZnL<sub>2</sub>(ClO<sub>4</sub>)<sub>2</sub> and free 3,2,3-BisAm with increasing temperature (**Figure 2.8** and **Figure 2.11**). At a low enough temperature, no dissociation of ZnL<sub>3</sub>(ClO<sub>4</sub>)<sub>2</sub> takes place, so a 6 : 6 ratio of H<sub>eq</sub> : H<sub>ax</sub> on  $\beta$  carbons results due to slow enantiomerization. With the temperature going up, some ZnL<sub>3</sub>(ClO<sub>4</sub>)<sub>2</sub> dissociates. At room temperature, more of ZnL<sub>3</sub>(ClO<sub>4</sub>)<sub>2</sub> dissociates into ZnL<sub>2</sub>(ClO<sub>4</sub>)<sub>2</sub> and free 3,2,3-

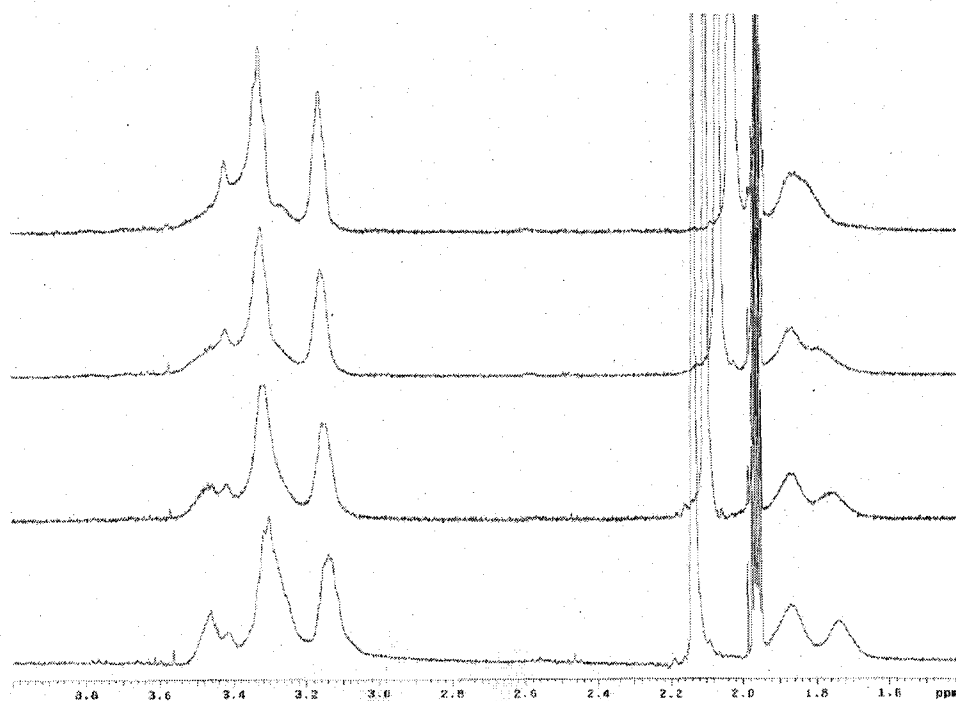


**Figure 2.8** VT  $^1\text{H-NMR}$  (400 MHz) of  $\text{Zn}(\text{3,2,3-BisAm})_3(\text{ClO}_4)_2$  in  $\text{CD}_3\text{CN}$   
 (From top to bottom:  $70^\circ\text{C}$ ,  $60^\circ\text{C}$ ,  $50^\circ\text{C}$ ,  $40^\circ\text{C}$ ;  $\text{CD}_3\text{CN}$  as NMR solvent)

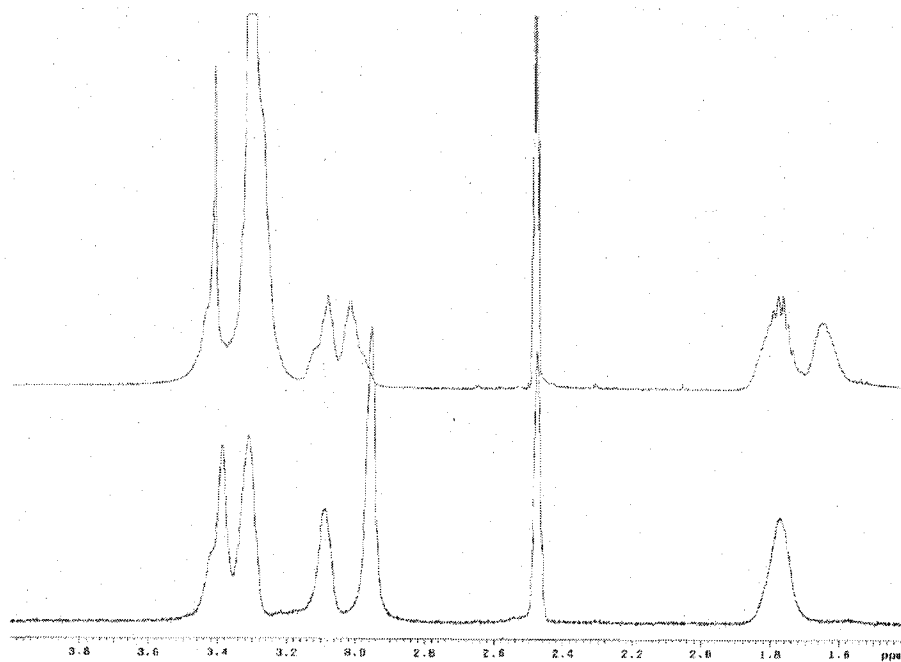


**Figure 2.9** VT  $^1\text{H-NMR}$  (400 MHz) of  $\text{Zn}(\text{3,2,3-BisAm})_3\text{Cl}_2$  in  $\text{d}_6\text{-DMSO}$   
 (Top:  $25^\circ\text{C}$ , bottom:  $100^\circ\text{C}$ ;  $\text{d}_6\text{-DMSO}$  as NMR solvent)

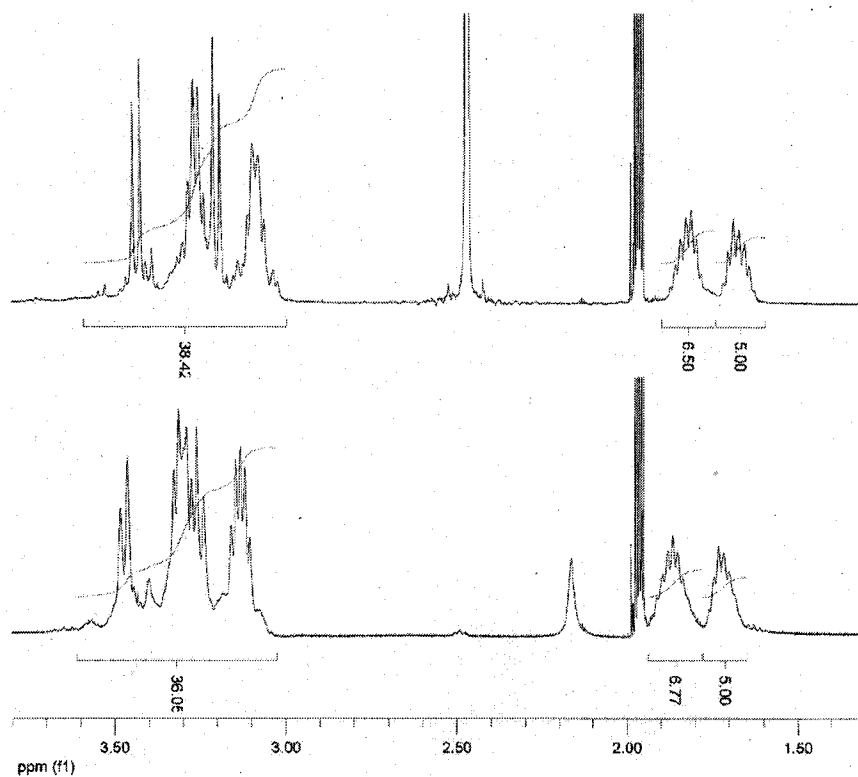


**Figure 2.10** VT  $^1\text{H-NMR}$  (400 MHz) of  $\text{Zn}(3,2,3\text{-BisAm})_3(\text{ClO}_4)_2$  in  $\text{CD}_3\text{CN}$  (Top:  $-40^\circ\text{C}$ , bottom:  $25^\circ\text{C}$ ;  $\text{CD}_3\text{CN}$  as NMR solvent)

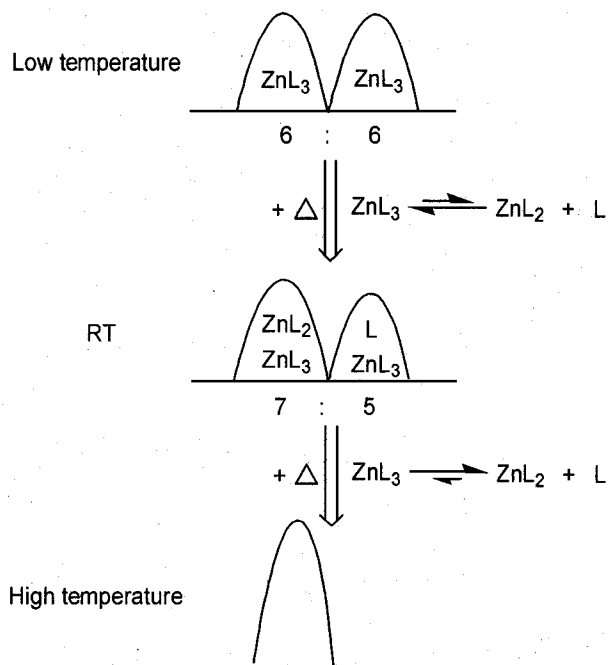
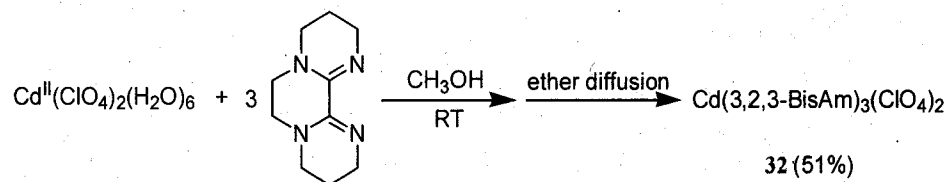


**Figure 2.11** Rationalization of the  $^1\text{H-NMR}$  spectrum of the zinc complex

BisAm. Similar chemical shifts lead to the overlapping resonances generating a 7 : 5 ratio of two broad peaks in the upfield region of the  $^1\text{H}$ -NMR spectrum. The ratio will become larger with increasing temperature, which was confirmed through comparison of low temperature  $^1\text{H}$ -NMR spectrum (at  $-40^\circ\text{C}$ , the ratio is  $\sim 1.3$  or  $6.5 : 5$ , **Figure 2.10**) and room temperature  $^1\text{H}$ -NMR spectrum (the ratio is  $\sim 1.36$  or  $6.8 : 5$ ). When the temperature goes up enough, all the  $\text{ZnL}_3(\text{ClO}_4)_2$  should be converted into  $\text{ZnL}_2(\text{ClO}_4)_2$ . Due to a fast exchange between coordinated ligands and free ligand, only one set of averaged 3,2,3-BisAm peaks was observed (**Figure 2.9**). This is not inconsistent with the observation of one set of major resonances as well as one set of minor ones in the compound's room temperature  $^{13}\text{C}$ -NMR spectrum.

#### D. Cadmium (II)



**Scheme 2.9** Synthesis of  $[\text{Cd}(3,2,3\text{-BisAm})_3](\text{ClO}_4)_2$

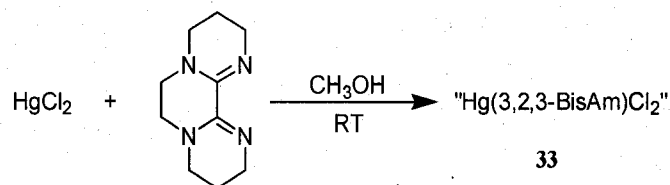
Tris(3,2,3-BisAm)cadmium(II) perchlorate was prepared by mixing a methanol solution of cadmium perchlorate hexahydrate with a solution of slightly over three equivalents of 3,2,3-BisAm in MeOH (**Scheme 2.9**). The solution remained clear after mixing. Diethyl ether diffusion into the methanol solution was performed to crystallize the complex. Clear, colorless needle crystals were harvested from the vial overnight. The complex was characterized by elemental analysis, IR and NMR spectroscopy.



Elemental analysis of this complex confirmed that it is a tris-3,2,3-BisAm complex with the empirical formula  $\text{Cd}(\text{C}_{10}\text{H}_{16}\text{N}_4)_3(\text{ClO}_4)_2$ . Its IR spectrum includes an imine stretching band at  $1606\text{ cm}^{-1}$ . The  $^1\text{H}$ -NMR spectrum of this complex maintains the same symmetry pattern as free 3,2,3-BisAm. However, one of triplets has a slight upfield shift while the other resonances have downfield shifts relative to free ligand. The  $^{13}\text{C}\{^1\text{H}\}$ -NMR spectrum contains all the five expected peaks and the amidine carbon is observed at 148.0 ppm. Absence of any  $J(^{13}\text{C}-^{111}\text{Cd}/^{113}\text{Cd})$  satellites around any carbon resonances supports rapid ligand exchange in the solution.

In 2002, Widlicka synthesized and reported a cadmium tris-2,2,2-BisAm complex. Its X-ray analysis showed that each of the three 2,2,2-BisAm ligands is chelated to cadmium in the solid-state structure and the complex has approximate  $D_3$  symmetry with a pseudo trigonal prismatic geometry.<sup>8</sup> Although no X-ray quality crystals were obtained, we can propose that  $\text{Cd}(3,2,3\text{-BisAm})_3(\text{ClO}_4)_2$  has a similar structure in the solid state. Except for this tris-2,2,2-BisAm cadmium complex, a search of the *Cambridge Structural Database* revealed only three structures of cadmium tris( $\alpha$ -diimine) complexes. Goldberg et al. reported two of three cadmium complexes in one of which three optically pure bis(4-phenyl-1,3-oxazoline) ligands chelate to cadmium in an octahedral geometry.<sup>24,25</sup> Chen et al. published the structure of a cadmium(II) cryptate derived from the condensation of tri(2-aminoethyl)amine with glyoxal, also in a distorted octahedral geometry.<sup>26</sup>

## E. Mercury (II)



**Scheme 2.10** Synthesis of “Hg(3,2,3-BisAm)Cl<sub>2</sub>”

An amount of 3,2,3-BisAm was dissolved in methanol followed by the addition of slightly less than one equivalent of HgCl<sub>2</sub>, which resulted in the precipitation of a white solid (**Scheme 2.10**). After filtration, the product was washed with additional MeOH and dried under reduced pressure to give a white powder. This complex was characterized by solid-state IR, ESI-MS, NMR spectroscopy and X-ray analysis. The IR spectrum contains an imine C=N stretching band at 1608 cm<sup>-1</sup>. The <sup>1</sup>H-NMR spectrum of this complex maintains the same symmetry pattern as the free ligand but with different downfield shifts. In addition, there are no overlapping resonances. There are again five resonances in the <sup>13</sup>C{<sup>1</sup>H}-NMR spectrum and the carbons of the imines appear at 148 ppm.

Clear, cubic crystals of good quality for X-ray analysis were grown by diethyl ether diffusion into a solution of “Hg(3,2,3-BisAm)Cl<sub>2</sub>” in DMF. The structure of the complex is shown in **Figure 2.12**. The compound is actually composed of a [Hg(3,2,3-BisAm)<sub>2</sub>]<sup>2+</sup> cation and HgCl<sub>4</sub><sup>2-</sup> counterion. The complex can be viewed as five-coordinate with the geometry of a distorted trigonal bipyramid ( $\tau = 0.825$ , see page 53). Besides two chelating 3,2,3-BisAm ligands, there is a weak Cl coordination (3.045(5) Å) in one equatorial site. This bis-chelate cation has an approximate C<sub>2</sub> symmetry with a pseudo-C<sub>2</sub> axis passing through the Hg(1)-Cl(1) axis. Selected bond data are presented in **Table 2.2**. The bidentate ligand has an average bite angle of 73.4°. These two small bite

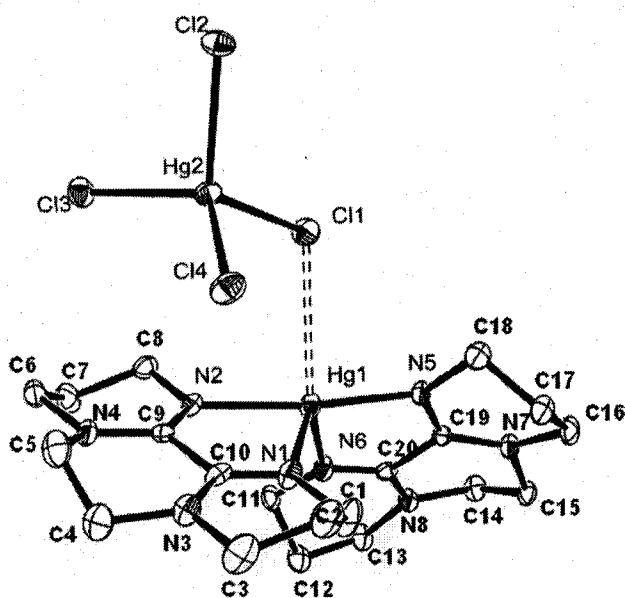


**Figure 2.12** Ortep view of the X-ray structure of  $[\text{Hg}(3,2,3\text{-BisAm})_2](\text{HgCl}_4)$

angles distort the trigonal-bipyramid. In addition, the axial angle N(2)-Hg-N(5) of  $170.3(2)^\circ$  is also somewhat distorted. However, in the equatorial plane, the N(1)-Hg-N(6) angle is  $120.8(2)^\circ$ , close to the ideal value of  $120^\circ$ . The equatorial Hg(1)-N(1 or 6) distance with an average of  $2.358(5) \text{ \AA}$  is significantly longer than the axial Hg(1)-N(2 or 5) distance with an average of  $2.144(4) \text{ \AA}$ , which makes for a slightly unsymmetrical chelating mode. Such N=C-C=N moiety is nearly planar, with an average diimine torsion angle of  $5.6^\circ$  and the average sum of the angles around the amine nitrogen atoms is  $358.3^\circ$ , consistent with the enhanced  $sp^2$  hybridization. Interestingly, the two coordinated ligands have different symmetry: one has a  $C_2$  axis while the other has none (**Figure 2.13**). This indicates that conformational equilibria between chair-like and boat-like conformers exist in solution. On average, the C=N bonds are lengthened to  $1.295$  from a normal  $1.27 \text{ \AA}$  while the C-N(amine) bonds are shortened to  $1.340$  from a normal  $1.36 \text{ \AA}$ , which reflects

the conjugation effect of imine  $\pi$ -bonds and amine N when 3,2,3-BisAm coordinates with a metal cation.

**Table 2.2 Selected bond lengths(Å) and angles(°) for [Hg(3,2,3-BisAm)<sub>2</sub>](HgCl<sub>4</sub>)**

Bond lengths		Bond angles	
Hg(1)-N(5)	2.137(4)	N(2)-Hg(1)-N(5)	170.3(2)
Hg(1)-N(2)	2.151(4)	N(2)-Hg(1)-N(1)	73.5(1)
Hg(1)-N(1)	2.329(5)	N(1)-Hg(1)-N(6)	120.8(2)
Hg(1)-N(6)	2.387(5)	N(5)-Hg(1)-N(6)	73.2(2)
Hg(1)-Cl(1)	3.045(5)	N(5)-Hg(1)-N(1)	115.98(16)
Hg(2)-Cl(1)	2.5349(13)	N(2)-Hg(1)-N(6)	104.35(15)
C(9)-N(2)	1.294(7)	C(9)-N(4)-C(5)	120.6(4)
C(9)-N(4)	1.344(6)	C(9)-N(4)-C(6)	119.5(4)
C(10)-N(1)	1.286(7)	C(6)-N(4)-C(5)	117.1(4)
C(10)-N(3)	1.339(7)	C(10)-N(3)-C(3)	120.7(5)
C(19)-N(5)	1.309(6)	C(10)-N(3)-C(4)	111.6(5)
C(19)-N(7)	1.342(6)	C(3)-N(3)-C(4)	116.9(5)
C(20)-N(6)	1.289(6)		
C(20)-N(8)	1.333(6)	Dihedral angles	
		N(2)-C(9)-C(10)-N(1)	1.16
		N(5)-C(19)-C(20)-N(6)	-12.32

Esd's are in parentheses.

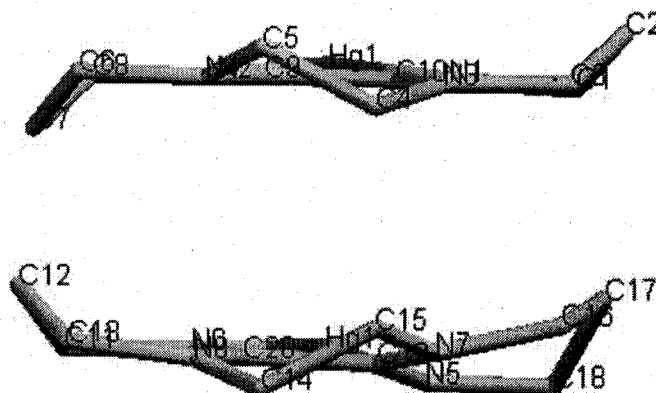
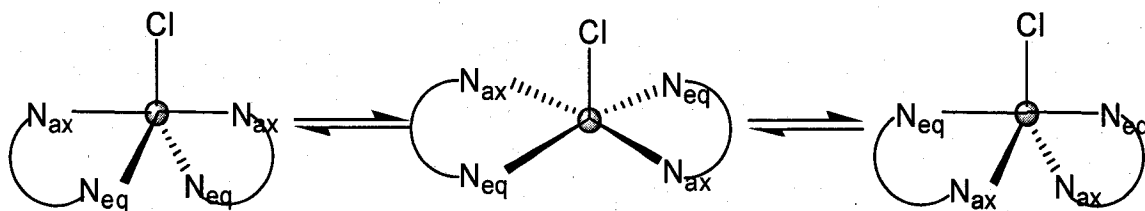


**Figure 2.13 Views of the two coordinated 3,2,3-BisAms**

The coordinated chlorine (Cl(1)) is 3.045(5) Å from the mercury center, out of normal Hg-Cl bonding distance range (2.2~2.8 Å). However, several similarly long Hg-Cl bond lengths can be found in the literature.<sup>27,28</sup> The anion  $\text{HgCl}_4^{2-}$  has an approximate tetrahedral geometry at the Hg(2) center. Not only are the bond lengths of Hg-Cl identical but also Cl-Hg(2)-Cl angles are all between 99.7° and 118.1°, reasonably close to 109.5° in an ideal tetrahedron.

This solid structure is not consistent with the observed solution  $^1\text{H}$  and  $^{13}\text{C}\{^1\text{H}\}$ -NMR data. This may be explained by a facile Berry pseudorotation (**Scheme 2.11**) through a square pyramidal intermediate. If the axial and equatorial positions interchange at a rate that is fast on the NMR timescale, a simplified NMR spectrum results. Another possibility is that the complex undergoes exchange through dissociation of one or two Hg-N bonds since  $J_{\text{C-}^{199}\text{Hg}}$  satellites around the  $^{13}\text{C}$  resonances of the two carbons  $\alpha$  to the imino N were not observed in the  $^{13}\text{C}\{^1\text{H}\}$ -NMR spectrum.



**Scheme 2.11** Berry pseudorotation of  $[\text{Hg}(3,2,3\text{-BisAm})_2]^{2+}$

A ligand exchange experiment involving the addition of free ligand to an NMR sample also supported this possibility. Only one set of 3,2,3-BisAm signals was observed. As the concentration of 3,2,3-BisAm increased, all peaks shifted towards the free 3,2,3-BisAm ligand values (**Figure 2.14**). This indicated that the coordinated ligand is in fast exchange at room temperature with the free ligand in solution on the NMR timescale.

Appropriately, we note that the NMR spectrum **S4** is similar to that of  $\text{Hg}(\text{3,2,3-BisAm})_3(\text{BPh}_4)_2$  in both pattern and chemical shift in the upfield region.

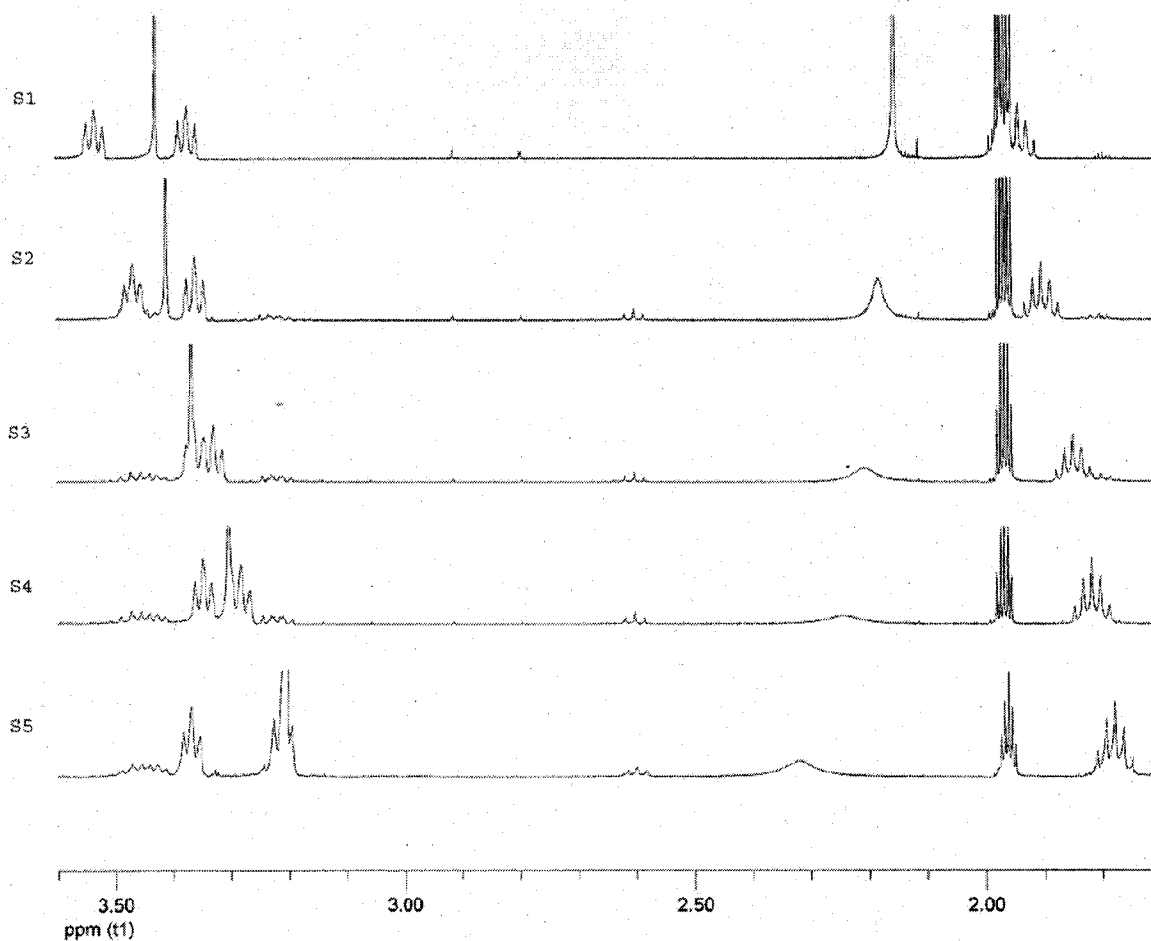


**Figure 2.14** NMR spectra after addition of excess 3,2,3-BisAm to  $\text{Hg}_2(\text{3,2,3-BisAm})_2\text{Cl}_4$

<b>S1:</b>	$[\text{Hg}_2\text{L}_2\text{Cl}_4] = 3.02 \text{ mM};$	$[\text{L}] = 0 \text{ mM};$	Ratio L/Hg = 1
<b>S2:</b>	$[\text{Hg}_2\text{L}_2\text{Cl}_4] = 3.02 \text{ mM};$	$[\text{L}] = 3.64 \text{ mM};$	Ratio L/Hg = 1.60
<b>S3:</b>	$[\text{Hg}_2\text{L}_2\text{Cl}_4] = 3.02 \text{ mM};$	$[\text{L}] = 7.80 \text{ mM};$	Ratio L/Hg = 2.29
<b>S4:</b>	$[\text{Hg}_2\text{L}_2\text{Cl}_4] = 3.02 \text{ mM};$	$[\text{L}] = 14.04 \text{ mM};$	Ratio L/Hg = 3.32
<b>S5:</b>	$[\text{Hg}_2\text{L}_2\text{Cl}_4] = 0 \text{ mM};$	$\text{L} = \text{3,2,3-BisAm ligand}$	

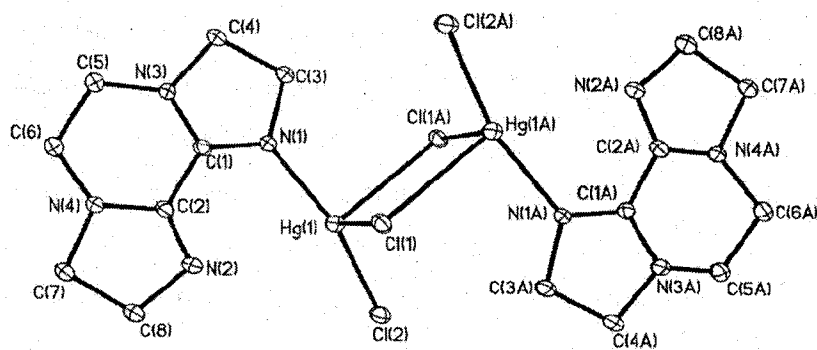
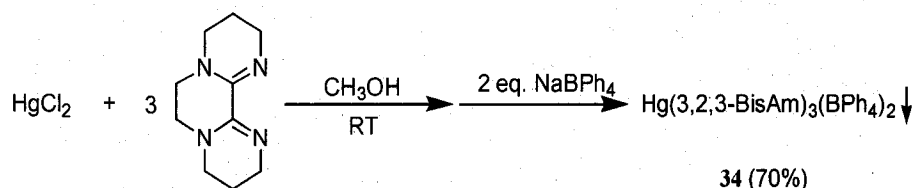


**Figure 2.15** Ortep view of the X-ray Structure of  $\text{Hg}_2(2,2,2\text{-BisAm})_2\text{Cl}_4$

The X-ray structure of the mercury complex of 3,2,3-BisAm and that of 2,2,2-BisAm mercury complex are different. In the 2,2,2-BisAm complex, an interesting dimer formed in which the two metal centers are bridged by two bridging chloride ions (**Figure 2.15**). The structure is  $C_i$  symmetric. Each mercury is five-coordinate filled by two bridging chlorides, one terminal chloride and one unsymmetrically chelating 2,2,2-BisAm. Two significantly different Hg-N coordination distances, 2.13 and 2.95 Å, are observed. The 2.95 Å value has reached the upper limit of Hg-N bond distances through a search of the *Cambridge Structural Database*. In its 3,2,3-BisAm complex, mercury is also five-coordinate, but it has two chelating ligands instead. This is another strong affirmation that it is easier for 3,2,3-BisAm to chelate than for 2,2,2-BisAm.

Tris(3,2,3-BisAm)mercury(II) tetraphenylborate was prepared by adding five equivalents of 3,2,3-BisAm to a solution of mercuric chloride in methanol, then exchanging the chloride anion with the tetraphenylborate anion. Initially, a slightly yellow solution formed. The reaction mixture was stirred at room temperature overnight. Then more than two equivalents of sodium tetraphenylborate were added into the solution to give a white precipitate. After filtration, the product was washed with additional

CH<sub>3</sub>CN and dried under reduced pressure. The complex was characterized by elemental analysis, IR and NMR spectroscopy. Elemental analysis of this complex confirmed an empirical molecular formula of Hg(C<sub>10</sub>H<sub>16</sub>N<sub>4</sub>)<sub>3</sub>(BC<sub>24</sub>H<sub>20</sub>)<sub>2</sub>. The IR spectrum contains one imine stretching band at 1602 cm<sup>-1</sup> (**Scheme 2.12**).



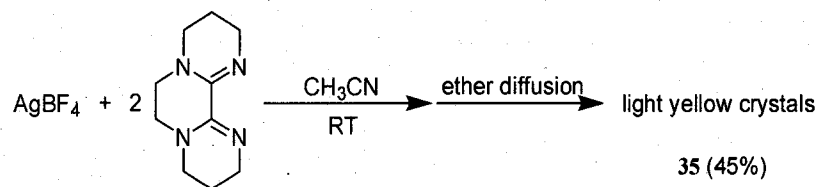
**Scheme 2.12** Synthesis of Hg(3,2,3-BisAm)<sub>3</sub>(BPh<sub>4</sub>)<sub>2</sub>

The <sup>1</sup>H-NMR spectrum of this complex in d<sub>6</sub>-DMSO has signals in the aromatic region and the upfield pattern is the same as for free 3,2,3-BisAm. The integration ratio of the resonances around 3.30 ppm to the quintet at 1.74 ppm is more than three due to overlapping H<sub>2</sub>O peak observed around 3.30 ppm. The <sup>13</sup>C{<sup>1</sup>H}-NMR spectrum reveals the four expected signals in the upfield region, with the amidine carbon observed at 147.1 ppm. The quartet resonance at 164 ppm corresponds to the phenyl carbon bonded to the boron directly. The other aromatic peaks are observed at 136, 125 and 122 ppm. No <sup>13</sup>C-<sup>199</sup>Hg satellites were observed.

## F. Silver (I)

Silver(I) has been shown to have a variety of coordination modes including linear, T-shaped, trigonal, distorted tetrahedral and octahedral. Many factors such as the nature of the ligand, solvent, steric requirements etc. can all modulate the stereochemistry of silver(I) complexes.<sup>29</sup>

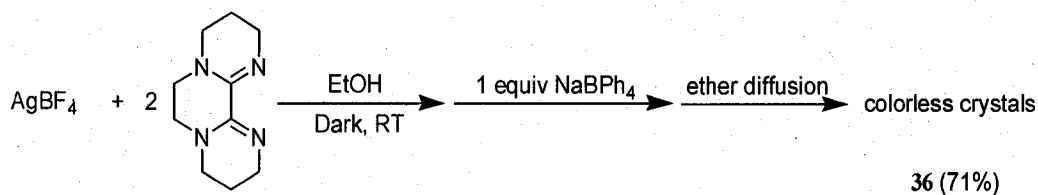




**Scheme 2.13 Synthesis of  $[\text{Ag}^{\text{I}}(\text{3,2,3-BisAm})_2](\text{BF}_4)$**

Bis(3,2,3-BisAm)silver tetrafluoroborate was prepared by adding slightly more than two equivalents of 3,2,3-BisAm to a solution of silver tetrafluoroborate in acetonitrile (**Scheme 2.13**). A light yellow solution formed after the addition of the ligand. Diethylether was diffused into the acetonitrile solution and light-yellow crystals were harvested on the wall of test tubes but were not suitable for X-ray analysis. This complex was characterized by elemental analysis, IR, and NMR spectroscopy. The elemental analysis supports the formation of  $\text{Ag}(\text{C}_{10}\text{H}_{16}\text{N}_4)_2(\text{BF}_4)$ . Two strong overlapping IR bands are observed at 1626 and 1593  $\text{cm}^{-1}$ , which may correspond to the stretching of coordinated C=N compared with the free ligand value of 1601  $\text{cm}^{-1}$ . A broad band between 1000 and 1100  $\text{cm}^{-1}$  is due to B-F bond stretching in the anion  $\text{BF}_4^-$ . The  $^1\text{H}$ -NMR spectrum of this complex has the same peak pattern as for free 3,2,3-BisAm, though with downfield shifts. The  $^{13}\text{C}\{^1\text{H}\}$ -NMR spectrum contains the four signals in the upfield region, with amidine carbon observed at 148.4 ppm.

For the purpose of getting an X-ray quality crystal of the bis(3,2,3-BisAm)silver complex, the counterion  $\text{BF}_4^-$  was exchanged to a bigger anion  $\text{BPh}_4^-$ . Reaction of silver tetrafluoroborate with two equivalents of 3,2,3-BisAm in absolute ethanol gave a light yellow cloudy solution. Then one equivalent of sodium tetraphenylborate was added



**Scheme 2.14** Synthesis of  $[\text{Ag}^{\text{I}}(3,2,3\text{-BisAm})_2](\text{BPh}_4)$

which immediately resulted in a white precipitate (Scheme 2.14). The white precipitate was washed with additional ethanol, then dried under reduced vacuum and stored in the dark. The white product has a poor solubility in acetonitrile and a little better solubility in DMSO and DMF. X-ray quality crystals were grown from a DMF solution by diethyl ether diffusion. Analytical data, however, were not consistent with the expected  $[\text{Ag}(3,2,3\text{-BisAm})_2](\text{BPh}_4)$  complex. An empirical formula  $[\text{Ag}_{1.9}(3,2,3\text{-BisAm})_2](\text{BPh}_4)_{1.9}$  instead was found. This product's IR spectrum contains a C=N stretch at  $1602\text{ cm}^{-1}$ . The  $^1\text{H-NMR}$  spectrum of this complex is very similar to that of  $[\text{Ag}(3,2,3\text{-BisAm})_2](\text{BF}_4)$ . Compared with free 3,2,3-BisAm, its proton signals also have downfield shifts due to metal coordination. More importantly, a similar formula of  $[\text{Ag}_{1.85}(3,2,3\text{-BisAm})_2](\text{BPh}_4)_{1.85}$  was obtained from the ratio of integrations of aromatic protons to ligand's protons in its  $^1\text{H-NMR}$  spectrum. This may be due to  $\text{AgBPh}_4$  crystals forming along with the silver complex during the recrystallization. Its  $^{13}\text{C}\{^1\text{H}\}$ -NMR spectrum was recorded in  $d_6$ -DMSO in order to get a better spectrum, and it contains only three peaks at 20.8, 47.0 and 47.6 ppm in the upfield region, with the amidine carbon observed at 148.3 ppm. The peak at 47.0 ppm is slightly broadened likely due to the overlap of two signals.

In the X-ray structure of  $[\text{Ag}(3,2,3\text{-BisAm})_2](\text{BPh}_4)$  (Figure 2.16), two ligands chelate with one silver in a distorted tetrahedral geometry. The two chelating ligands

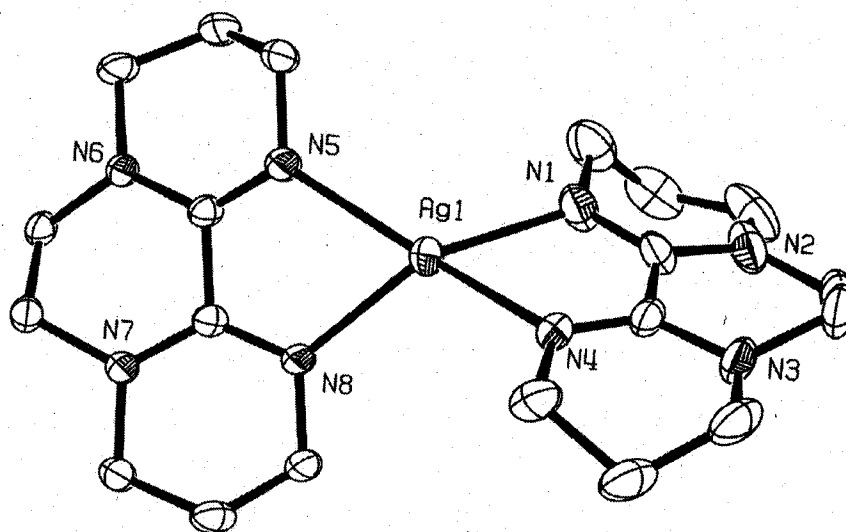


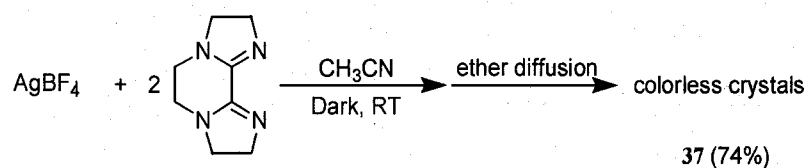
Figure 2.16 Ortep view of the X-ray structure of  $[\text{Ag}(3,2,3\text{-BisAm})_2](\text{BPh}_4)$  (anion not shown)

Table 2.3 Selected bond lengths(Å) and angles(°) for  $[\text{Ag}(3,2,3\text{-BisAm})_2](\text{BPh}_4)$

Bond lengths		Bond angles	
Ag(1)-N(5)	2.274(3)	N(1)-Ag(1)-N(5)	123.56(10)
Ag(1)-N(1)	2.293(3)	N(5)-Ag(1)-N(4)	150.63(10)
Ag(1)-N(4)	2.305(3)	N(1)-Ag(1)-N(4)	71.43(10)
Ag(2)-N(8)	2.321(2)	N(5)-Ag(1)-N(8)	72.50(9)
C(9)-N(1)	1.293(4)	N(1)-Ag(1)-N(8)	104.49(11)
C(9)-N(2)	1.357(4)	N(4)-Ag(1)-N(8)	113.42(9)
C(10)-N(3)	1.367(4)	C(9)-N(2)-C(4)	121.8(4)
C(10)-N(4)	1.287(4)	C(9)-N(2)-C(3)	120.4(3)
		C(4)-N(2)-C(3)	116.3(3)
		Dihedral angles	
		N(1)-C(9)-C(10)-N(4)	8.66(10)
		N(5)-C(20)-C(19)-N(8)	-20.90(10)

Esd's are in parentheses.

have an average N-Ag-N bite angle of  $72.0^\circ$  while the average Ag-N distance is  $2.30 \text{ \AA}$ . Each ligand is nearly planar with an average diimine torsion angle of  $14.8^\circ$ . The sum of the three bond angles around each amine nitrogen atom is  $358^\circ$ , indicative of substantial flattening. Furthermore, the amidine C-N bond shortens to  $1.36 \text{ \AA}$  from the uncoordinated value of  $1.37\text{-}1.38 \text{ \AA}$ , suggesting significant polarization of the N-C=N moiety upon metal coordination. A search of the Cambridge Structural Database revealed only three reports on bis( $\alpha$ -diimine) silver complexes. In one of them, the authors reported self-assembly of different silver salts with two new imidazole-containing Schiff base ligands. More interestingly, they found the ligands exhibited four unusual bridging modes.<sup>30</sup>



**Scheme 2.15** Synthesis of “[Ag<sup>I</sup>(2,2,2-BisAm)<sub>2</sub>](BF<sub>4</sub>)”

In order to compare with the structure of the silver 3.2.3-BisAm complex, a silver 2.2.2-BisAm complex with the same stoichiometry was synthesized. Addition of two equivalents of 2,2,2-BisAm in acetonitrile into silver tetrafluoroborate yielded a colorless solution with a small amount of black precipitate (**Scheme 2.15**). The black residue was removed by filtration. X-ray quality crystals were grown using ether diffusion into the clear acetonitrile solution. Although white crystals were obtained, they gradually became yellow in light. These crystals yielded only a low-quality X-ray structure of a bimetallic complex. Interestingly, a silver-silver interaction ( $3.053 \text{ \AA}$ ) was observed (**Figure 2.17**).

This complex was also characterized by elemental analysis, IR and NMR spectroscopy. Elemental analysis supported  $\text{Ag}(\text{C}_8\text{H}_{12}\text{N}_4)_2\text{BF}_4$  as the empirical formula. The  $^1\text{H}$ -NMR spectrum of this complex has only one set of signals for the ligand shifted downfield from the values of the free 2,2,2-BisAm ligand while the  $^{13}\text{C}\{^1\text{H}\}$ -NMR spectrum has signals shifted slightly upfield. The observation of only one set of signals in these spectra is inconsistent with the solid-state structure. The lack of  $^{13}\text{C}$ - $^{107,109}\text{Ag}$  satellite suggests facile ligand dissociation or exchange in solution.

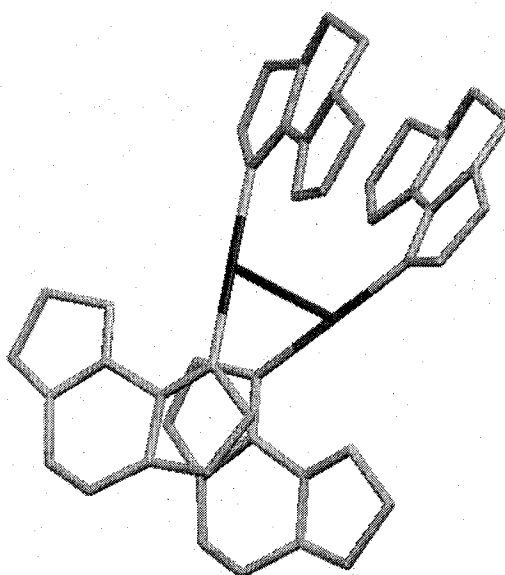
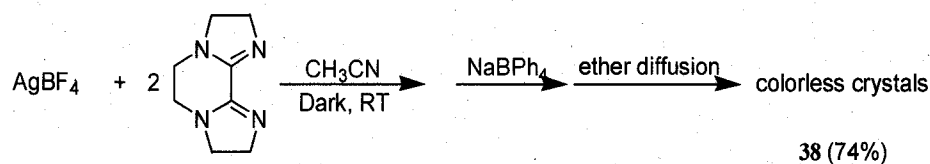


**Figure 2.17 Partial X-ray structure of  $[\text{Ag}_2(2,2,2\text{-BisAm})_4](\text{BF}_4)_2$ , 37**

Metal-metal bonds of orders 1 to 4 are well established in many transition metal compounds. They can be formulated, qualitatively, in terms of overlaps of the metal d orbitals, giving rise to  $\sigma$ ,  $\pi$  and  $\delta$  bonding and antibonding molecular orbitals.<sup>31</sup> As long as there are fewer electrons occupying the antibonding orbitals than the bonding orbitals, metal-metal bonds will be formed. If all the bonding and antibonding orbitals are fully occupied, a bond order of zero may be assigned, for example, in  $d^{10}$ - $d^{10}$  dinuclear

compounds of copper(I) or silver(I). Cotton et al. attributed very short copper(I)-copper(I) distances to a combination of strong Cu-N bonding and very short bite distances for the ligands.<sup>32,33</sup> However, there remains some controversy about the veracity of  $d^{10}$ - $d^{10}$  metal-metal bonding. The discovery of this silver(I)-silver(I) interaction is another addition to the family of dinuclear compounds with a  $d^{10}$ - $d^{10}$  electronic configuration, which may help the study of the interactions between closed-shell transition metals.



**Scheme 2.16** Synthesis of  $[\text{Ag}^{\text{I}}_2(2,2,2\text{-BisAm})_3](\text{BPh}_4)_2$

Bis(2,2,2-BisAm)silver tetraphenylborate was prepared in an attempt to obtain crystals of better X-ray quality. Reaction of silver tetrafluoroborate with two equivalents of 2,2,2-BisAm in acetonitrile gave a colorless solution with some brown precipitate (**Scheme 2.16**). One equivalent of  $\text{NaBPh}_4$  was added which followed by two hours of stirring in the dark. After removal of the insoluble brown solids (by filtration), the filtrate was concentrated and ethanol was added to produce a white precipitate. The white precipitate was collected, washed and dried under vacuum. Clear, colorless X-ray quality crystals were harvested in the dark over several days after diethylether diffusion into an  $\text{CH}_3\text{CN}$  solution of this white solid. However, the data from elemental analysis for this material support an empirical formula of  $[\text{Ag}_2(\text{C}_8\text{H}_{12}\text{N}_4)_3](\text{BPh}_4)_2$ . In the IR spectrum, two strong overlapping C=N stretches at 1621 and 1580  $\text{cm}^{-1}$  are shifted to lower wavenumber compared with the free ligand values of 1642 and 1621  $\text{cm}^{-1}$ . This confirms

that metal coordination has led to a significant polarization of the N-C=N moiety. The  $^1\text{H}$ -NMR spectrum of this complex contains a single set of signals for the ligand shifted downfield from the values of the free 2,2,2-BisAm ligand. The  $^{13}\text{C}\{^1\text{H}\}$ -NMR signals for ligands in the complex show a small upfield shift compared with free ligand. The absence of  $^{13}\text{C}$ - $^{107,109}\text{Ag}$  satellites again suggests facile ligand dissociation or exchange.

The X-ray structure of this [tris(2,2,2-BisAm)disilver(I)] tetrafluoroborate (**Figure 2.18**) revealed the formation of a dimer with a short Ag-Ag distance 2.8749(6) Å, which is close to the distance of 2.89 Å in elemental silver<sup>34,35</sup> and considerably shorter than the sum of Ag-Ag van der Waals radii of 3.44 Å between two silver centers. The structure has a very approximate mirror plane through the two silver atoms splitting the unsymmetrically-chelating ligand. One silver (Ag(1)) is five-coordinate with a distorted square pyramidal coordination sphere while the other silver (Ag(2)) is three-coordinate with a T-shaped geometry. The three 2,2,2-BisAms have three different coordination modes: bridging, unsymmetrically bridging and unsymmetrically chelating. The unsymmetrically bridging mode is a new coordination mode for 2,2,2-BisAm. The unsymmetrically bridging ligand features a short Ag(1)-N(5) bond distance of 2.095(3) Å along with a very long Ag(2)-N(6) distance of 2.820(3) Å. The unsymmetrically-chelating ligand features a short Ag(2)-N(9) bond distance of 2.244(3) Å as well as a long Ag(2)-N(10) distance of 2.551(3) Å. A search of the *Cambridge Crystallographic Database* yielded Ag-N bond distances as long as 3.20 Å.

This crystal structure also supports the polarization of the amidines. In the unsymmetrically bridging ligand, the bond length of the imine on the strongly-coordinated side (1.304(3) Å) is significantly longer than that of the weakly-coordinated

side (1.282(3)Å), while the amine C-N bond length in the amidine is marginally shorter on the strongly coordinated side (1.352(3)Å) than the other side (1.376(3)Å). In addition, the sum of the angles around the amino nitrogen on the strongly coordinated amidine (353.88°) is significantly larger than the corresponding sum of the angles for the weakly coordinated amidine (346.21°). This shows that the strongly coordinated amidine is polarized to a greater extent than the weak one. In the unsymmetrically chelating ligand, the amine C-N bond length in the strongly coordinated amidine (1.356(3)Å) is marginally shorter than that of the weakly coordinated one (1.369(3)Å) (Table 2.4).

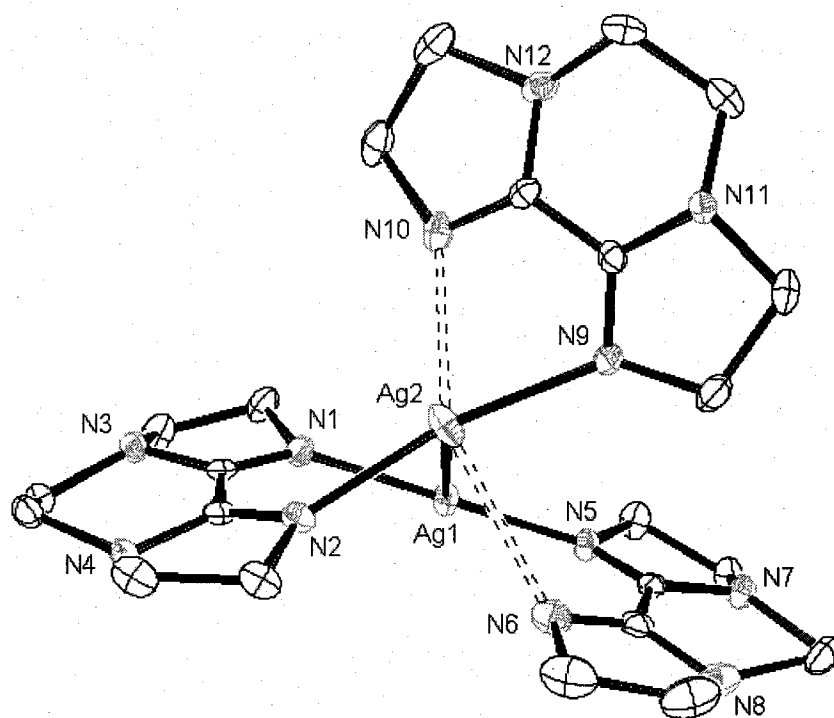


**Figure 2.18** Ortep view of the X-ray Structure of  $[\text{Ag}_2(2,2,2\text{-BisAm})_3](\text{BPh}_4)_2$ , **38**  
(anions and hydrogens not shown for clarity)



**Table 2.4 Selected bond lengths(Å) and angles(°) for [Ag<sub>2</sub>(2,2,2-BisAm)<sub>3</sub>](BF<sub>4</sub>)<sub>2</sub>, 38**

Bond lengths		Bond angles	
Ag(1)-Ag(2)	2.8749(6)	N(1)-Ag(1)-Ag(2)	83.28(8)
Ag(1)-N(1)	2.104(3)	N(5)-Ag(1)-Ag(2)	106.88(8)
Ag(1)-N(5)	2.095(3)	N(2)-Ag(2)-N(9)	163.17(10)
Ag(2)-N(2)	2.209(3)	N(1)-Ag(1)-N(5)	169.21(11)
Ag(2)-N(9)	2.244(3)	N(9)-Ag(2)-N(10)	73.14(10)
Ag(2)-N(10)	2.551(3)	N(2)-Ag(2)-N(10)	119.86(10)
Ag(2)-N(6)	2.820(3)	N(2)-Ag(2)-Ag(1)	84.65(8)
C(10)-N(6)	1.282(3)	N(9)-Ag(2)-Ag(1)	105.27(7)
C(10)-N(8)	1.376(3)	N(10)-Ag(2)-Ag(1)	96.91(7)
C(9)-N(5)	1.304(3)	C(12)-N(7)-C(9)	107.55(7)
C(9)-N(7)	1.352(3)	C(12)-N(7)-C(13)	122.37(7)
C(1)-N(1)	1.297(3)	C(13)-N(7)-C(9)	123.96(7)
C(1)-N(3)	1.359(3)	C(10)-N(8)-C(14)	119.54(7)
C(2)-N(2)	1.292(3)	C(14)-N(8)-C(15)	121.85(7)
C(2)-N(4)	1.373(3)	C(10)-N(8)-C(15)	104.82(7)
C(18)-N(12)	1.369(3)		
C(17)-N(9)	1.280(3)	Dihedral angles	
C(17)-N(11)	1.356(3)	N(5)-C(9)-C(10)-N(6)	-4.30
C(18)-N(10)	1.282(3)	N(2)-C(2)-C(1)-N(1)	15.21
		N(9)-C(17)-C(18)-N(10)	1.65

Esd's are in parentheses.

While a Ag(I)/2,2,2-BisAm ratio of 1:2 yielded the dimeric [Ag<sub>2</sub><sup>I</sup>(2,2,2-BisAm)<sub>3</sub>]<sup>2+</sup> complex with one bridging, one unsymmetrically bridging, and one unsymmetrically chelating BisAm ligand, a similar Ag(I)/3,2,3-BisAm ratio of 1:2 gave a monomeric product with a distorted tetrahedral geometry and two chelating BisAm's. This is another affirmation that 2,2,2-BisAm, with a smaller ideal bite angle, bridges metals readily, while 3,2,3-BisAm has a strong tendency to chelate metals.

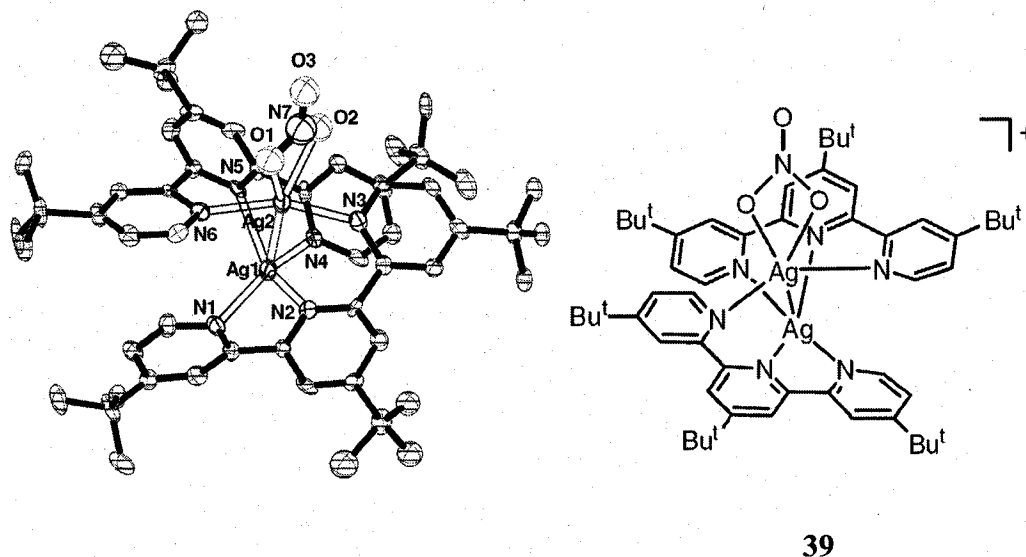


**Figure 2.19** X-ray structure of the cation  $[\text{Ag}_2(\text{tBu}_3\text{tpy})_2(\text{NO}_3)]^+$

Chuan He et al. have described an efficient olefin aziridination reaction catalyzed by a novel disilver(I) compound **39** (Figure 2.19). This was the first report of olefin aziridination reaction mediated by silver ions. In the disilver complex, both silver ions are five-coordinate if the silver-silver interaction is counted. Each ligand bridges two silver(I) ions. The Ag(1)-Ag(2) distance is 2.842(2) Å. The authors hypothesized that the electronic communication between the two silver ions and accessible coordination sites at the terminal positions play an important role in controlling the reactivity of the complex.<sup>36</sup> The complex  $[\text{Ag}_2(2,2,2\text{-BisAm})_3](\text{BPh}_4)_2$  thus has the potential of catalyzing the olefin aziridination reaction since it satisfies these two requirements. Recently, Chuan He and coworkers also prepared a disilver(I) bis(4,7-diphenyl-1,10-phenanthroline) complex and successfully applied it in benzylic C-H activation to form amines.<sup>37</sup>

## G. Copper (II)

For copper(II) 2,2,2-BisAm complexes, an appropriate stoichiometry can result in the formation of either a monomeric or a dimeric complex.<sup>7</sup> Tris(2,2,2-BisAm)copper(II) perchlorate was previously prepared by adding three equivalents of 2,2,2-BisAm to a solution of copper(II) perchlorate hexahydrate in acetonitrile.<sup>7</sup> Forest-green crystals grew from the solution by diethyl ether diffusion. The X-ray structure of this 2,2,2-BisAm complex revealed its copper(II) center in a square-planar geometry featuring one chelating and two monodentate ligands in the equatorial plane (**Figure 2.20**).

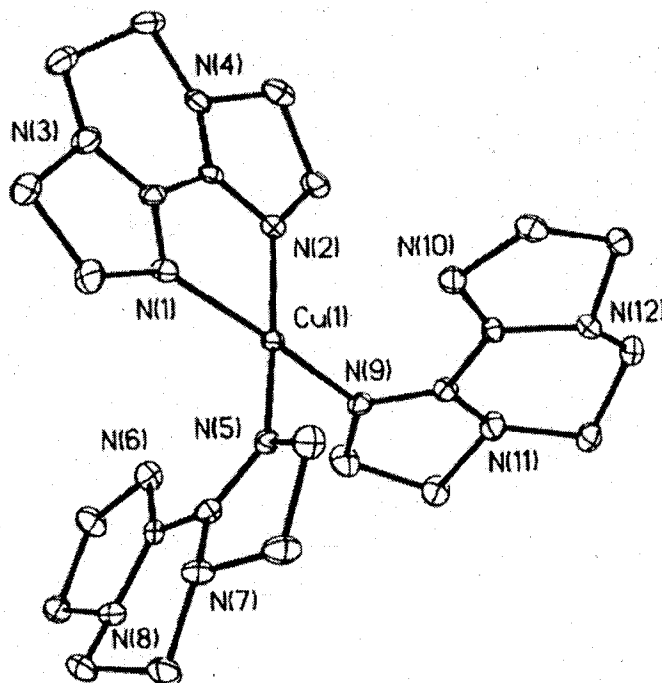
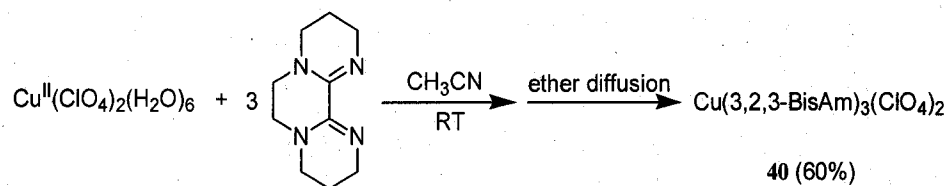


**Figure 2.20** Ortep view of the X-ray structure of [Cu(2,2,2-BisAm)<sub>3</sub>]<sup>2+</sup>

In order to compare with the 2,2,2-BisAm complex, tris(3,2,3-BisAm)copper(II) perchlorate was prepared by mixing three equivalents of 3,2,3-BisAm with copper(II) perchlorate hexahydrate in acetonitrile (**Scheme 2.17**). Upon addition of 3,2,3-BisAm to



**Scheme 2.17 Synthesis of  $[\text{Cu}^{\text{II}}(3,2,3\text{-BisAm})_3](\text{ClO}_4)_2$**

the acetonitrile solution of copper(II) perchlorate hexahydrate, the blue color of the solution became lighter. Diethyl ether was diffused into the solution and after several days, clear green X-ray quality crystals grew from solution. This complex was characterized by elemental analysis and IR. Its IR spectrum contains broad strong C=N stretches around  $1615 \text{ cm}^{-1}$ . The elemental analysis supported an empirical formula of  $[\text{Cu}(\text{C}_{10}\text{H}_{16}\text{N}_4)_3](\text{ClO}_4)_2(\text{H}_2\text{O})$ .

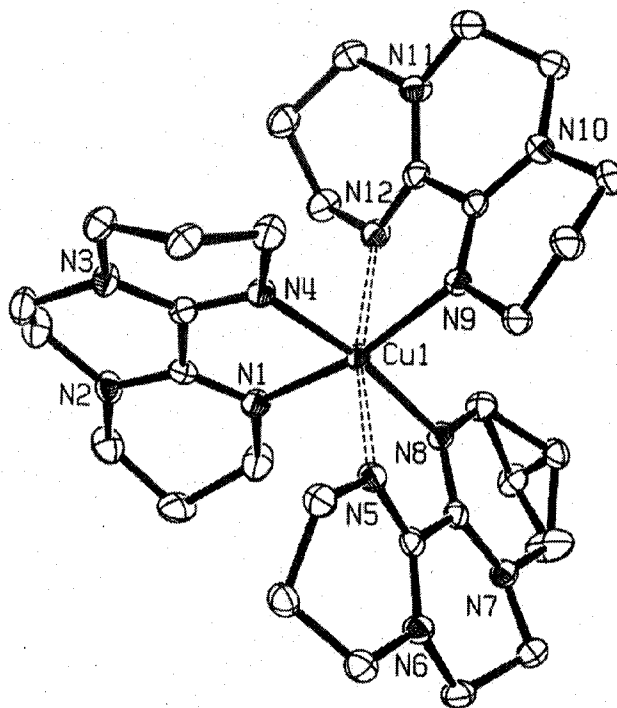


**Figure 2.21 Ortep view of the X-ray structure of  $[\text{Cu}(3,2,3\text{-BisAm})_3](\text{ClO}_4)_2$   
(Perchlorates not shown)**

In its X-ray structure, this complex can be viewed as having a severely Jahn-Teller distorted octahedral geometry (**Figure 2.21**). One symmetric chelating as well as two unsymmetrically chelating ligands complete the copper coordination environment. The equatorial Cu-N bond distances have an average value of 2.027Å. Along the axial direction, the two nitrogen donor atoms are positioned 2.26Å and 2.39Å from the metal center, respectively. The asymmetric chelation mode allows us to compare the

**Table 2.5** Selected bond lengths(Å) and angles(°) for [Cu(3,2,3-BisAm)<sub>3</sub>](ClO<sub>4</sub>)<sub>2</sub>

Bond lengths		Bond angles	
Cu(1)-N(8)	2.0020(18)	N(1)-Cu(1)-N(4)	79.45(8)
Cu(1)-N(4)	2.0116(19)	N(5)-Cu(1)-N(8)	76.39(7)
Cu(1)-N(1)	2.0332(19)	N(9)-Cu(1)-N(12)	73.32(7)
Cu(1)-N(9)	2.0605(19)	N(5)-Cu(1)-N(12)	167.54(7)
Cu(1)-N(5)	2.255(2)	N(4)-Cu(1)-N(9)	94.89(8)
Cu(1)-N(12)	2.394(2)	N(1)-Cu(1)-N(8)	95.09(8)
N(1)-C(10)	1.288(3)	C(30)-N(10)-C(24)	121.4(2)
N(2)-C(10)	1.351(3)	C(30)-N(10)-C(23)	119.97(19)
N(3)-C(9)	1.344(3)	C(23)-N(10)-C(24)	118.27(19)
N(4)-C(9)	1.295(3)	C(29)-N(11)-C(25)	120.9(2)
N(9)-C(30)	1.294(3)	C(29)-N(11)-C(26)	120.3(2)
N(10)-C(30)	1.347(3)	C(25)-N(11)-C(26)	117.05(19)
N(12)-C(29)	1.280(3)		
N(11)-C(29)	1.364(3)	Dihedral angles	
N(2)-C(3)	1.457(3)	N(4)-C(9)-C(10)-N(1)	5.63
		N(9)-C(30)-C(29)-N(12)	-20.88
		N(8)-C(19)-C(20)-N(5)	-9.42

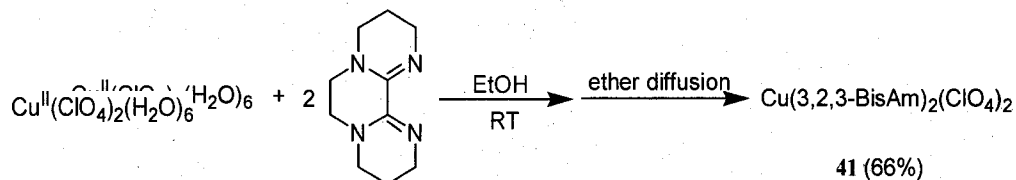
Esd's are in parentheses.

consequence of strong versus weak coordination within the same ligand. Since the longer Cu-N bond distance (Cu(1)-N(12) = 2.394(2)Å) implies weaker coordination, and less amidine polarization, the shorter imine C=N bond distance (N(12)-C(29) = 1.280(3)Å)

and the longer amine C-N bond distance (N(11)-C(29) = 1.364(3)Å) can all be compared to the stronger coordination of Cu(1) to N(9). Although they have different extents of amidine polarization, N(10) and N(11) have very similar amine nitrogen bond angle sum (359.6° vs. 358.3°). The tris-chelated copper complex of a modified bipyridyl ligand also contains two chelates with disparate Cu-N bond distances of 2.045Å and 2.519Å due to the Jahn-Teller distortion.<sup>38</sup>

Thus, in the tris(2,2,2-BisAm)copper(II) perchlorate, the copper center is square planar with one chelating and two monodentate BisAms in the equatorial plane. The 3,2,3-BisAm complex, instead, has a Jahn-Teller distorted tetragonal Cu(II) coordination sphere. This also supports that 3,2,3-BisAm coordinates with metal more readily in a chelating mode than 2,2,2-BisAm.

Treatment of Cu(ClO<sub>4</sub>)<sub>2</sub>·6H<sub>2</sub>O with two equivalents of 3,2,3-BisAm in absolute ethanol gave a blue precipitate immediately. The blue X-ray quality crystals of [Cu<sup>II</sup>(3,2,3-BisAm)<sub>2</sub>](ClO<sub>4</sub>)<sub>2</sub> were obtained after diethyl ether diffusion into CH<sub>3</sub>CN solution of the precipitate (**Scheme 2.18**). Its IR spectrum contained C=N stretch at 1623 cm<sup>-1</sup>. The elemental analysis also supports the formation of Cu(C<sub>10</sub>H<sub>16</sub>N<sub>4</sub>)<sub>2</sub>(ClO<sub>4</sub>)<sub>2</sub>.



**Scheme 2.18** Synthesis of [Cu<sup>II</sup>(3,2,3-BisAm)<sub>2</sub>](ClO<sub>4</sub>)<sub>2</sub>

The X-ray crystal structure of Cu(3,2,3-BisAm)<sub>2</sub>(ClO<sub>4</sub>)<sub>2</sub> reveals that the complex has a distorted square pyramidal geometry around the copper with two chelating 3,2,3-

BisAm ligands (**Figure 2.22**). This is because  $\tau = (\beta - \alpha)/60 = 0.27$ , in which  $\beta$ ,  $\alpha$  are the two largest basal angles. When  $\tau = 1$ , five coordinated complex has a trigonal bipyramidal ( $D_{3h}$ ) geometry; when  $\tau = 0$ , five coordinated complex has a square pyramidal ( $C_{4v}$ ) geometry.<sup>39</sup> The copper cation is coordinated by four N atoms of the two 3,2,3-BisAms, with an average distance of 1.965 Å in the equatorial positions. One perchlorate ( $\text{ClO}_4$ ) anion is weakly coordinated in the axial position with a long Cu-O distance of 2.817 Å. Each imine nitrogen is strongly bound to copper with an average Cu-N distance of 1.965 Å and bite angle of  $82.9^\circ$ . Further, there is good evidence that the amidine has significant polarization with a long C=N bond of 1.300 Å and a short C-N distance of 1.336 Å.

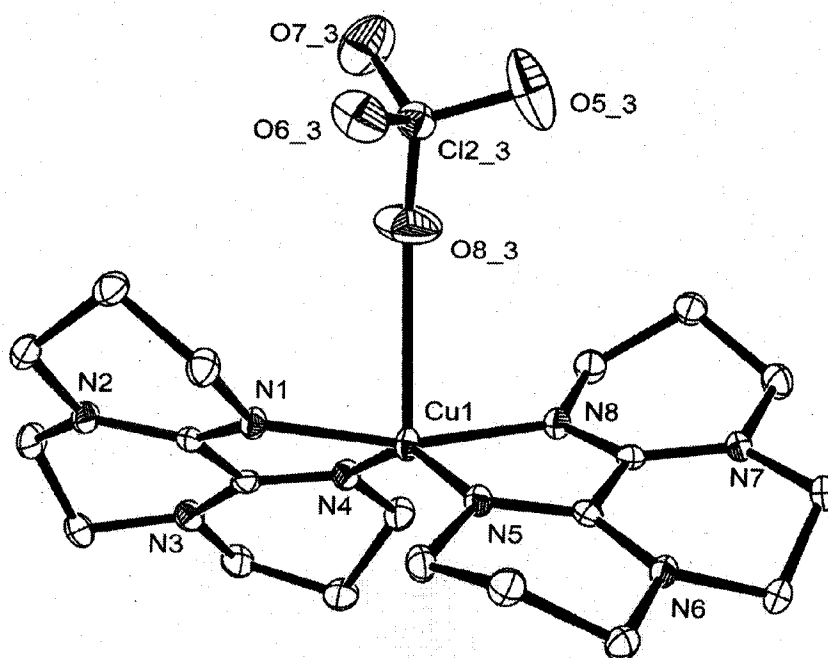


**Figure 2.22** Ortep view of the X-ray structure of  $[\text{Cu}^{\text{II}}(3,2,3\text{-BisAm})_2(\text{ClO}_4)](\text{ClO}_4)$   
(Uncoordinated perchlorate not shown for clarity)

**Table 2.6** Selected bond lengths(Å) and angles(°) for [Cu(3,2,3-BisAm)<sub>2</sub>(ClO<sub>4</sub>)](ClO<sub>4</sub>)

Bond lengths		Bond angles	
Cu(1)-N(1)	1.9532(18)	N(1)-Cu(1)-N(8)	164.37(8)
Cu(1)-N(8)	1.9581(19)	N(1)-Cu(1)-N(4)	83.01(8)
Cu(1)-N(4)	1.9705(19)	N(8)-Cu(1)-N(4)	100.23(8)
Cu(1)-N(5)	1.9797(18)	N(1)-Cu(1)-N(5)	102.76(8)
Cu(1)-O(8)	1.817(3)	N(5)-Cu(1)-N(8)	82.70(8)
N(1)-C(10)	1.302(3)	N(4)-Cu(1)-N(5)	147.91(8)
N(2)-C(10)	1.335(3)	N(4)-Cu(1)-O(8)	100.21(8)
N(3)-C(9)	1.336(3)	N(5)-Cu(1)-O(8)	111.76(8)
N(4)-C(9)	1.297(3)	N(8)-Cu(1)-O(8)	81.31(8)
C(10)-C(9)	1.501(3)	N(1)-Cu(1)-O(8)	83.04(8)
N(2)-C(3)	1.469(3)	C(10)-C(9)-N(4)	114.41(19)
N(2)-C(4)	1.469(3)	C(10)-C(9)-N(3)	118.28(19)
		N(3)-C(9)-N(4)	127.3(2)
		Dihedral angles	
		N(4)-C(9)-C(10)-N(1)	-15.24
		N(5)-C(19)-C(20)-N(6)	-12.13

Esd's are in parentheses.

[Tetrakis(μ-2,2,2-BisAm)dicopper(II)] perchlorate was previously prepared by Widlicka using same procedure.<sup>7</sup> An X-ray study revealed the binuclear [Cu<sub>2</sub>(2,2,2-BisAm)<sub>4</sub>](ClO<sub>4</sub>)<sub>4</sub> complex shown in **Figures 2.23** and **2.24**. The four bridging ligands adopt a pseudo-*C*<sub>4</sub> propeller arrangement down the Cu-Cu axis. Each copper (II) is square pyramidal with four imine N's forming the basal plane. This again shows that 3,2,3-BisAm is the better chelating ligand than 2,2,2-BisAm while it is more facile for 2,2,2-BisAm to form a bridging complex.



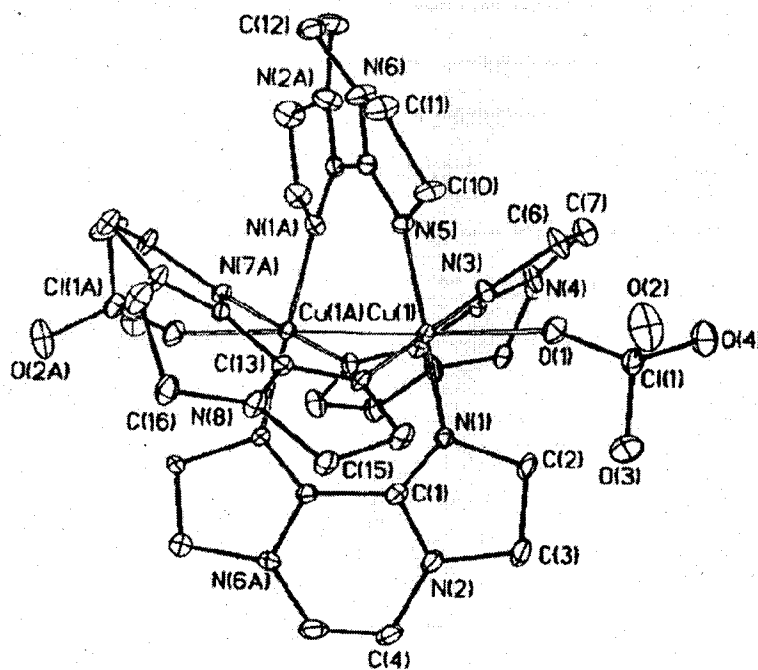


Figure 2.23 Ortep view of the X-ray structure of  $[\text{Cu}_2^{\text{II}}(2,2,2\text{-BisAm})_4(\text{ClO}_4)_2](\text{ClO}_4)_4$

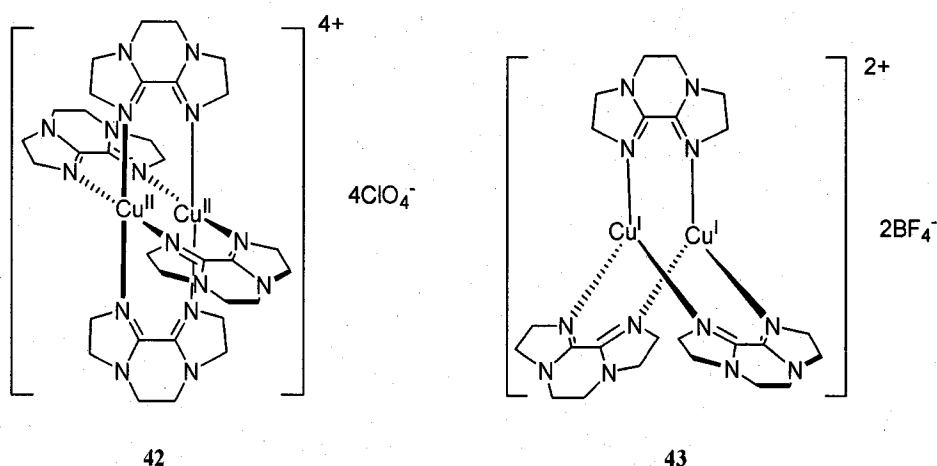
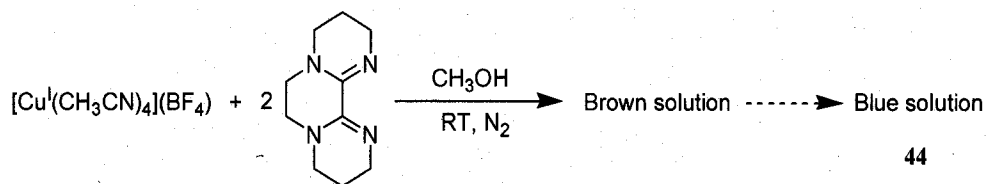


Figure 2.24 Structures of  $[\text{Cu}_2^{\text{II}}(2,2,2\text{-BisAm})_4](\text{ClO}_4)_4$  (left) and  $[\text{Cu}_2^{\text{I}}(2,2,2\text{-BisAm})_3](\text{BF}_4)_2$  (right)<sup>7</sup>

Synthesis of a copper(I) 3,2,3-BisAm complex was attempted by adding two equivalents of 3,2,3-BisAm to a solution of tetrakis(acetonitrile)copper(I)

tetrafluoroborate in degassed methanol under a nitrogen atmosphere using Schlenk techniques (**Scheme 2.19**). Before the reaction, tetrakis(acetonitrile)copper(I) tetrafluoro-



**Scheme 2.19** Attempted Synthesis of  $[\text{Cu}^{\text{I}}(3,2,3\text{-BisAm})_2](\text{BF}_4)$

borate was purified according to a literature procedure.<sup>40</sup> Upon reagent mixing, a brown solution formed immediately. Degassed diethyl ether was used to try to grow X-ray quality crystals by diffusion into this brown solution under nitrogen. Brown cubic crystals were harvested after several days, however, during this recrystallization the solution became pale blue, which meant the complex had been oxidized to copper(II). This was also confirmed by X-ray crystallography. In the resulting X-ray structure, each cation is accompanied by two tetrafluoroborate anions (**Figure 2.25**).

The geometry is distorted square-planar. Two tetrafluoroborates are weakly axially-coordinated to copper with a very long Cu-F distances of 2.9-3.2 Å, within the range of longest Cu-F bonds (3.02 Å).<sup>41</sup> However, a search of the *Cambridge Structural Database* revealed  $\text{Cu}^{\text{II}}\text{-F}(\text{BF}_3)$  bond distances range from 2.31 to 2.84 Å in known complexes. The two BisAm ligands are twisted out of the square planar by  $\sim 25^\circ$ . Each imine nitrogen is strongly bound to copper with an average Cu-N distance of 1.97 Å and there is again good evidence that the amidine unit is significantly polarized with a long C=N bond of 1.296 Å while the C-N distance is shortened to 1.343 Å.

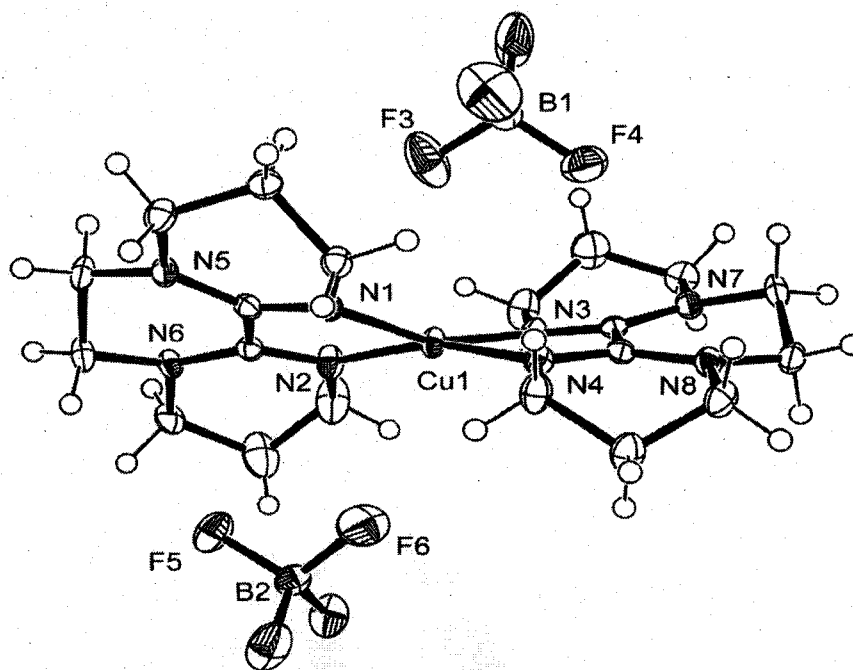


Figure 2.25 Ortep view of the X-ray structure of  $[\text{Cu}^{\text{II}}(3,2,3\text{-BisAm})_2](\text{BF}_4)_2$

Table 2.7 Selected bond lengths(Å) and angles(°) for  $[\text{Cu}(3,2,3\text{-BisAm})_2](\text{BF}_4)_2$

Bond lengths		Bond angles	
Cu(1)-N(1)	1.970(2)	N(1)-Cu(1)-N(2)	82.53(11)
Cu(1)-N(2)	1.970(3)	N(1)-Cu(1)-N(3)	160.13(10)
Cu(1)-N(3)	1.979(3)	N(1)-Cu(1)-N(4)	100.17(11)
Cu(1)-N(4)	1.956(2)	N(2)-Cu(1)-N(3)	100.44(11)
Cu(1)-F(3)	2.897(3)	N(2)-Cu(1)-N(4)	162.37(12)
Cu(1)-F(6)	3.180(3)	N(3)-Cu(1)-N(4)	83.00(11)
N(5)-C(10)	1.343(3)	F(3)-Cu(1)-F(6)	152.81(11)
N(1)-C(10)	1.296(3)	C(3)-N(5)-C(4)	118.38(11)
		C(3)-N(5)-C(10)	120.92(11)
		C(4)-N(5)-C(10)	119.77(11)
		Dihedral angles	
		N(2)-C(9)-C(10)-N(1)	-13.95
		N(4)-C(19)-C(20)-N(5)	-12.19

Esd's are in parentheses.

Widlicka previously carried out a similar reaction using the same stoichiometry of  $\text{Cu}^{\text{I}}(\text{CH}_3\text{CN})_4(\text{BF}_4)$  to 2,2,2-BisAm under the same reaction conditions. After diethyl ether diffusion, yellow crystals were harvested. The X-ray structure revealed a dimeric copper(I) complex with each copper(I) center trigonal pyramidal (**Figure 2.24**). While the  $[\text{Cu}^{\text{I}}_2(2,2,2\text{-BisAm})_3](\text{BF}_4)_2$  solution is stable in air, the  $[\text{Cu}^{\text{I}}(3,2,3\text{-BisAm})_2](\text{BF}_4)$  solution is unstable and easily air-oxidized. The influence of these different BisAm ligands on the oxidation/reduction potential of the central metal  $\text{Cu}^{\text{I}}$  ion in these complexes will be evaluated using cyclic voltammetry in future work by another researcher.

#### H. Europium (III)

Lanthanide coordination chemistry has been studied intensively over the past several decades. Significant progress has been made in applications such as bioactive probes including magnetic resonance, and luminescence studies.<sup>42</sup> However, a search of the *Cambridge Structural Database* showed no europium  $\alpha$ -diimine complexes reported yet. Several years ago, a europium 2,2,2-BisAm complex was prepared by Fichter through the reaction of europium perchlorate and five equivalents of 2,2,2-BisAm in absolute ethanol. The X-ray structure of this complex (Eu(III):2,2,2-BisAm = 1:4) showed this nine-coordinate complex to have a capped square-antiprism geometry with one water coordinated (**Figure 2.26**). This europium complex exhibits phosphorescence, and could potentially be used in biological systems as a luminescent probe.

In order to compare with this 2,2,2-BisAm complex, tetra(3,2,3-BisAm)europium(III) perchlorate was synthesized and characterized. When an amount of europium triflate was added to a solution of five equivalents of 3,2,3-BisAm in EtOH

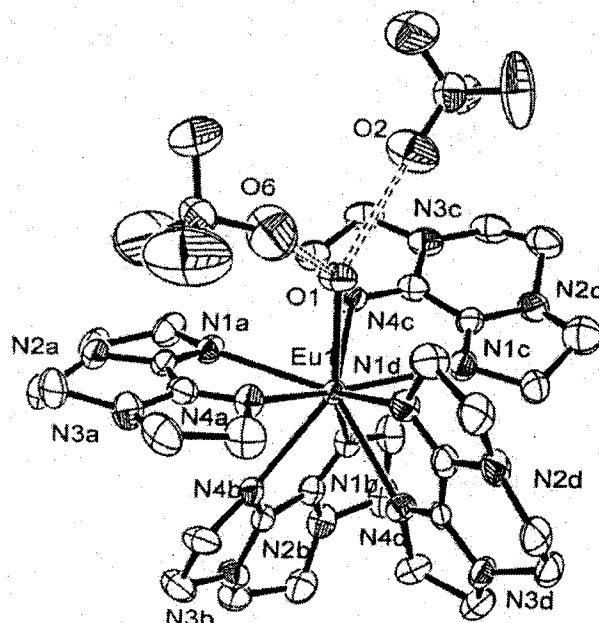
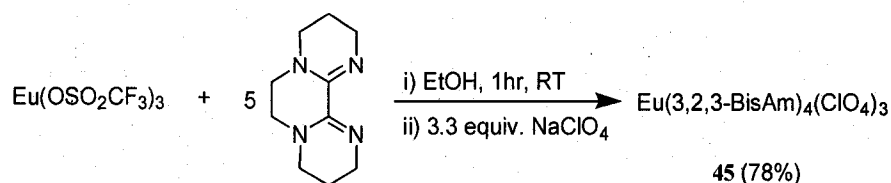


**Figure 2.26** Ortep view of the X-ray structure of  $\text{Eu}(\text{2,2,2-BisAm})_4(\text{H}_2\text{O})(\text{ClO}_4)_3$   
(The third perchlorate not shown)

with stirring, a light yellow solution was formed (Scheme 2.20). Then more than three equivalents of sodium perchlorate were added. A light yellow precipitate formed immediately. This precipitate was collected, washed with additional ethanol then dried under vacuum. Clear, light yellow cubic crystals were harvested after  $\text{Et}_2\text{O}$  diffusion into



**Scheme 2.20** Synthesis of  $[\text{Eu}(\text{3,2,3-BisAm})_4](\text{ClO}_4)_3$

a CH<sub>3</sub>CN solution of this solid over several days.

The X-ray crystal structure revealed that the structure of this complex is approximately square-antiprismatic (**Figure 2.27**). Its four chelating ligands have an average N-Eu-N bite angle of 64.2° and an average Eu-N distance of 2.50Å. The ligands are all nearly planar, with an average diimine torsion angle of only 2.1° and the average sum of their amine nitrogen bond angles is 357°. Eu(2,2,2-BisAm)<sub>4</sub>(H<sub>2</sub>O)(ClO<sub>4</sub>)<sub>3</sub> has an average N-Eu-N bite angle of 66.1° and a slightly longer average Eu-N distance of 2.583Å. Again, polarization of the amidine moiety is observed in the C=N and C-N bond distances (**Table 2.8**). The europium complex of 3,2,3-BisAm is eight-coordinate while the europium complex of 2,2,2-BisAm is nine-coordinate. This may be because 3,2,3-BisAm is the bulkier ligand, which cannot bind in a higher coordination number without prohibitive steric interference between ligands, than 2,2,2-BisAm.

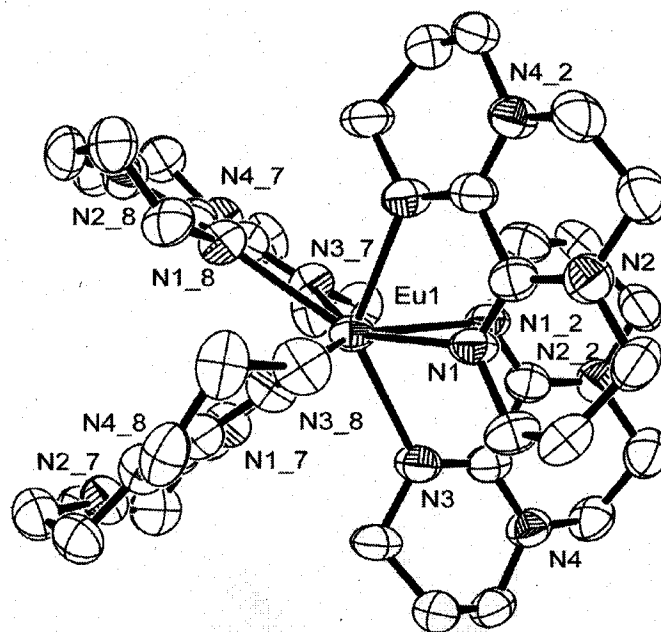


**Figure 2.27** Ortep view of the X-ray structure of Eu(3,2,3-BisAm)<sub>4</sub>(ClO<sub>4</sub>)<sub>3</sub> (Perchlorates not shown)

**Table 2.8 Selected bond lengths(Å) and angles(°) for [Eu(3,2,3-BisAm)<sub>4</sub>](ClO<sub>4</sub>)<sub>3</sub>**

Bond lengths		Bond angles	
Eu(1)-N(3)	2.493(3)	N(1)-Eu(1)-N(3)	64.19(11)
Eu(1)-N(1)	2.512(4)	Eu(1)-N(1)-C(4)	121.8(3)
N(3)-C(9)	1.309(6)	C(4)-N(2)-C(5)	119.9(4)
N(4)-C(9)	1.347(5)	C(3)-N(2)-C(5)	117.2(4)
N(1)-C(4)	1.292(6)	C(4)-N(2)-C(3)	120.0(4)
N(2)-C(4)	1.344(6)		
N(4)-C(8)	1.470(6)	Dihedral angles	
N(4)-C(10)	1.462(6)	N(3)-C(9)-C(4)-N(1)	2.07
		N(2)-C(5)-C(10)-N(4)	56.01

Esd's are in parentheses.

The complex was also characterized by elemental analysis, IR and NMR spectroscopy. Elemental analysis of this complex was consistent with the empirical formula  $\text{Eu}(\text{C}_{10}\text{H}_{16}\text{N}_4)_4(\text{ClO}_4)_3$ . The IR spectrum of  $\text{Eu}(\text{3,2,3-BisAm})_4(\text{ClO}_4)_3$  has one diimine stretching band at  $1595\text{ cm}^{-1}$ . Since NMR signals broaden with the reciprocal of the 6<sup>th</sup> power of the paramagnetic metal-nucleus distance, there is a sphere centered on the paramagnetic metal ion in which proton NMR lines are too broad to be detected, an outer shell in which paramagnetism gives rise to observable but broad lines, and a more remote out shell in which the paramagnetic effect is negligible (**Figure 2.28**).<sup>43</sup> Based on this theory, the  $^{13}\text{C}\{^1\text{H}\}$ -NMR spectrum of this complex can be explained in that the signals are affected to different extents by the  $\text{Eu}^{3+}$  paramagnetic effect (**Figure 2.29**). The signals of the amidine carbon,  $\beta$ -carbon and  $\alpha$ -carbon **a** are greatly shifted to 126.0, 11.5 and 77.8 ppm, respectively while the  $\alpha$ -carbons **b** and **c** are hardly affected. Its  $^1\text{H}$ -NMR spectrum revealed not only the formation of the europium complex but also a slow exchange between coordinated ligands and dissociated ligands at ambient temperature. The broad peaks at 5.36, 2.97, 1.89 and 1.22 ppm correspond to the four sets of protons

on the coordinated 3,2,3-BisAm ligands. The dissociated ligands retain their characteristic NMR signals: a singlet at 3.48 ppm; two triplets at 3.45 and 3.40 ppm. The signals corresponding to  $\beta$ -methylene are overlapping with the solvent residue signal at 1.95 ppm. According to the  $^1\text{H}$ -NMR, the ratio of coordinated ligands to dissociated ligands is  $\sim 10$ .

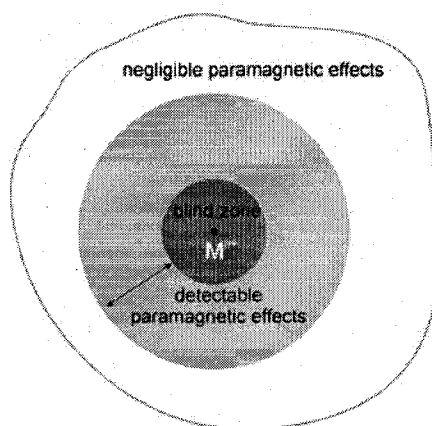


**Figure 2.28 Paramagnetic Effects on an NMR spectrum (from literature 43)**

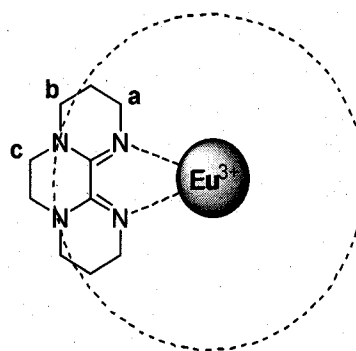
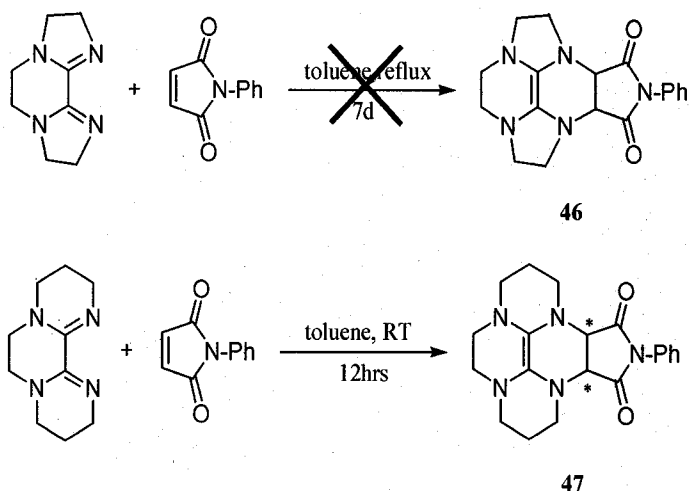


**Figure 2.29 Rationalization of the  $^{13}\text{C}\{^1\text{H}\}$ -NMR spectrum of the Europium complex**



## 2.4 Attempted aza-Diels-Alder reaction of BisAm's



**Scheme 2.21 Attempted aza-Diels-Alder reaction of BisAm's**

It is possible that BisAms can react with suitable dienophiles to form Diels-Alder adducts since the BisAm structure causes the N=C-C=N diene to be held in a *s-cis* conformation. Reed attempted the Diels-Alder reaction between 2,2,2-BisAm and N-phenylmaleimide unsuccessfully (Scheme 2.21).<sup>16</sup> In this research, the Diels-Alder reactions of 2,2,2-BisAm using ethyl acrylate and diphenylacetylene as dienophiles, respectively were attempted. TLC and NMR spectra showed that there are new compounds produced in the former reaction while no reaction had occurred in the latter.

The Diels-Alder reaction of 3,2,3-BisAm and N-phenylmaleimide was attempted. A red solid was produced after stirring the reactants in toluene at room temperature which was characterized by IR and NMR spectroscopy. The IR spectrum showed a slight red shift of the C=O stretching band to 1707 from 1710  $\text{cm}^{-1}$  compared to N-phenylmaleimide. There was no resonance around 5.8 ppm in the  $^1\text{H-NMR}$  spectrum, which indicated absence of alkene H's in the product. All the Hs' on the 3,2,3-BisAm

part of the product had slight upfield shifts relative to those of 3,2,3-BisAm. The product tetraaminoethylene may be easily oxidized by oxygen under light to form colorless imidazolidinones.<sup>44,45</sup> Further purification and characterization are still needed.

## 2.5 Conclusions and Future work

In summary, tricyclic bisamidine 3,2,3-BisAm can be readily prepared from the respective linear tetraamine. In addition, by comparison of their coordination chemistry, it was demonstrated that 2,2,2-BisAm has both symmetrical and unsymmetrical chelating as well as metal-bridging coordination modes; 3,2,3-BisAm, with a substantially larger bite angle, has been found to date only in the chelating mode.

Much more novel work is worthwhile for BisAm ligands and their transition metal complexes in future. For example, more BisAm derivatives such as the unsymmetric 3,2,2-BisAm and their complexes need to be synthesized and characterized. Copper(I) complexes with different BisAm ligands have different air stability. Studying the influence of BisAm ligands on Cu<sup>I</sup> redox chemistry is attractive. Some transition metal complexes of BisAm's have great potential as catalysts in organic reactions. The palladium(II) dimer complex of 2,2,2-BisAm may be oxidized to a palladium(III) dimer, reduced to a palladium(I) dimer, or even mixed-valent species. The luminescence properties of lanthanide complexes of BisAm's should be studied due to their potential as probes in biological systems.

## CHAPTER 3

### SYNTHESIS OF CHIRAL BISAM

#### 3.1 Introduction

Many pharmaceuticals and agrochemicals are chiral and enantiomerically pure. Development of effective methods for synthesis of enantiomerically-pure compounds continues to be of great academic and industrial importance.<sup>46</sup> There are several ways to produce enantiopure compounds. Asymmetric catalysis is the most efficient and appealing one. Historically, enantiomerically-pure compounds have been generated either by chemical transformation of a cheap enantiomerically-pure starting material or by resolving a racemic mixture of the two enantiomers. Both of these approaches suffer from potentially severe drawbacks. The former requires stoichiometric amounts of a suitable precursor from the chiral pool; the latter yields only up to 50% of the desired enantiomer. Asymmetric synthesis and asymmetric catalysis in particular, in which each molecule of chiral catalyst, by virtue of being continually regenerated, can yield many molecules of chiral product, has significant potential advantages over those older procedures.<sup>47</sup> In 2001, the Nobel Prize in chemistry was conferred on three chemists: Knowles, Noyori and Sharpless, who made major contributions in the field of asymmetric catalysis, especially asymmetric catalytic hydrogenation and asymmetric catalytic oxidation.

Most asymmetric catalysts consist of metal complexes with chiral ligands. To make an efficient transition metal catalyst, researchers must possess interdisciplinary knowledge including organic, inorganic, organometallic and biomimetic chemistry. The greatest challenge usually is the first step, designing and synthesizing chiral ligands.<sup>48</sup>

Of the thousands of chiral ligands prepared so far, most of them possess  $C_2$  symmetry. Due to their broad applicability, some  $C_2$ -symmetric chiral ligands have been called “privileged ligands” (Figure 3.1).<sup>49</sup>  $C_2$ -symmetric chiral ligands have many advantages compared with fully asymmetric ligands. The most obvious one is in mechanistic studies since it can reduce remarkably the number of possible reaction intermediates, which facilitates analysis of the ligand-substrate interactions.<sup>50</sup>

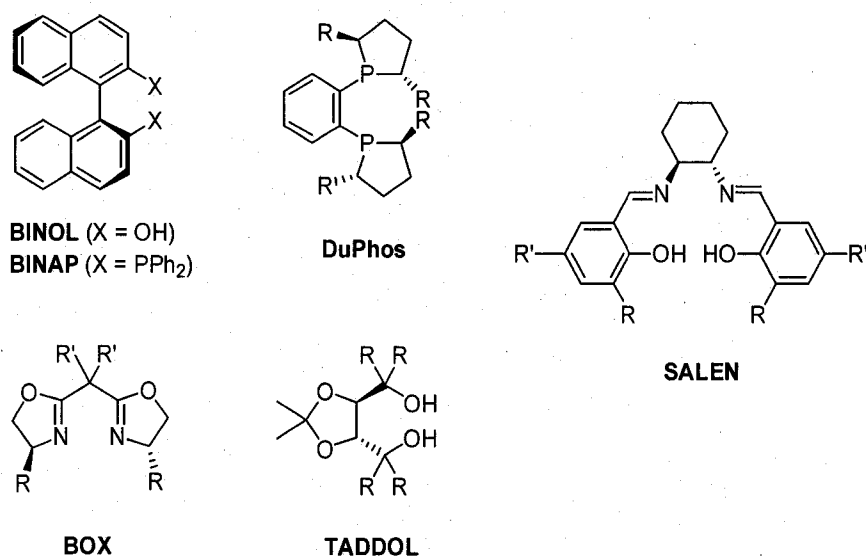


**Figure 3.1 Structures of some privileged ligands**

$C_2$ -symmetric bis(oxazolines) (BOX) are one of the most popular classes of chiral

ligands, and have received a great deal of attention as ligands in coordination chemistry and in asymmetric catalysis. The BOX ligands quickly became widely adopted bidentate ligands as a consequence of their easy and flexible synthesis and for the excellent enantioselectivity exhibited in asymmetric cyclopropanation of alkenes, enantioselective Diels-Alder reactions, aziridination reactions, aldol and aldol-like reactions, allylic substitution reactions, Michael reactions, 1,3-Dipolar cycloaddition reactions, and other reactions.<sup>51-53</sup>

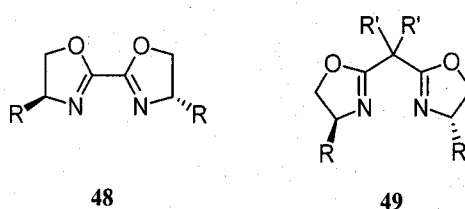
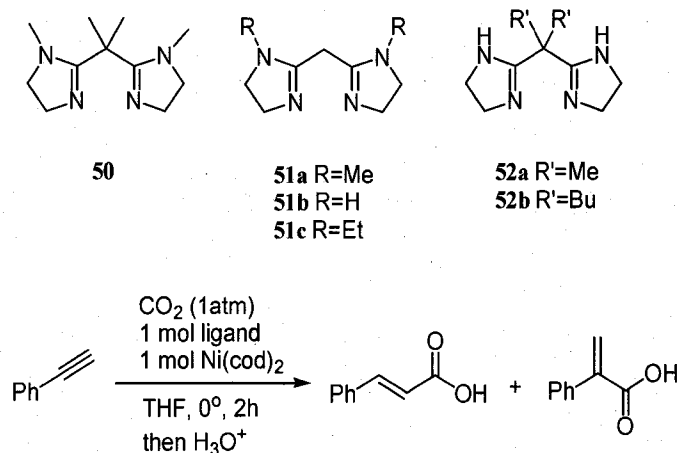


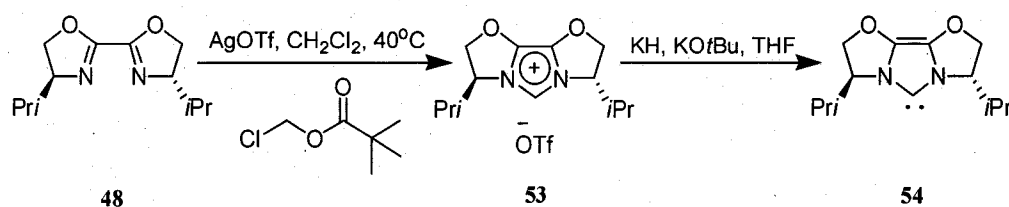
**Figure 3.2 Structures of bis(oxazolines)**

On the basis of successful synthesis of tricyclic bisamidines and their complexes, we are interested in synthesis of  $C_2$  symmetric chiral tricyclic bisamidines. There are two principal reasons for this. First of all,  $C_2$  symmetric chiral BisAm is a conformationally restricted analogue of the chiral Bis(oxazoline) ligand. As discussed above, the oxazolines are highly successful ligands, and  $C_2$  bis(oxazoline)s such as **48** and **49** (BOX) are widely used in transition metal-catalyzed reactions (**Figure 3.2**). Like bisoxazolines, BisAms are also tunable. Their electronic and conformational properties can be tuned by varying their substituents and ring sizes. BisAm has a greater conformational rigidity and donor strength which will promote metal coordination. Recently, Iwasawa and coworkers

designed and synthesized novel achiral bisamidine ligands **50**, **51**, and **52** for Ni(0)-mediated coupling of carbon dioxide with alkynes or allenes. High regioselectivity was achieved even for the carboxylation of aryl-substituted internal alkynes (Scheme 3.1).<sup>54</sup> Therefore, C<sub>2</sub> symmetric chiral BisAm might be expected to be another successful ligand family in metal-catalyzed asymmetric catalysis. In addition, chiral BisAms are synthetic precursors for chiral cyclens and may be synthetic precursors for chiral carbenes. In 2002, Glorius et al. reported a method to transform bioxazolines and oxazolineimines into a new class of N-heterocyclic carbenes for asymmetric catalysis.<sup>55</sup> (Scheme 3.2).



**Scheme 3.1** Iwasawa's bisamidine ligands and the catalyzed coupling reaction



**Scheme 3.2** Oxazolines as chiral building blocks for N-heterocyclic carbene ligands

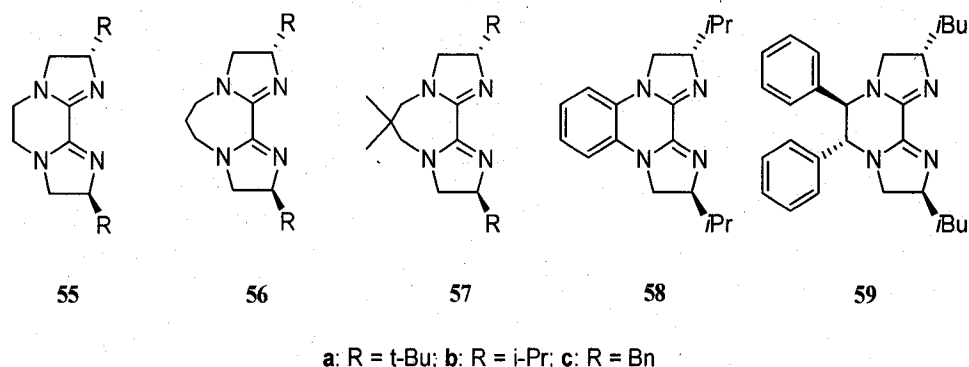
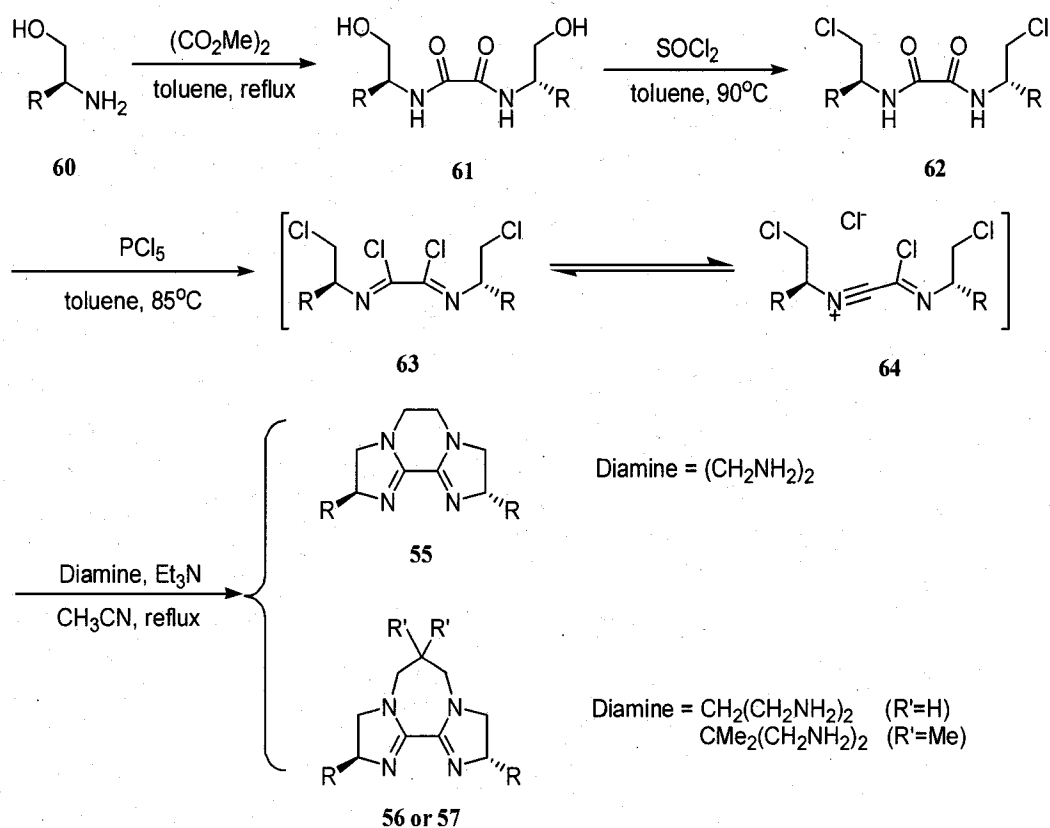


**Figure 3.3  $C_2$  symmetric chiral 2,b,2-BisAm**  
(b is number of bridging carbons in the middle ring, here b = 2 or 3)

In 2004, Casey and coworkers reported the synthesis of several chiral 2,b,2-BisAm's<sup>14</sup> (Figure 3.3). They used the chiral  $\beta$ -amino alcohols **60** as starting materials to react with dimethyl oxalate, and obtained bishydroxy amides **61**. The bishydroxy amides **61** were then converted to chloroamides **62** by reaction with thionyl chloride. These compounds are familiar precursors for bisoxazolines. Their treatment with phosphorous pentachloride in toluene at 85°C gave intermediates **63**, which were reacted with various diamines to yield different versions of chiral 2,b,2-BisAm's (Scheme 3.3).<sup>14</sup>

Although Casey and coworkers successfully synthesized these chiral BisAm's, there are some limitations in their method. Firstly, the starting enantiopure  $\beta$ -amino alcohols are expensive. It is also not economical to synthesize  $C_2$  symmetric chiral 3,b,3-BisAm using this method since this method requires expensive enantiopure  $\gamma$ -amino alcohols as starting materials. Secondly, it is not feasible for synthesizing unsymmetrical BisAms, like chiral 3,2,2-BisAm.

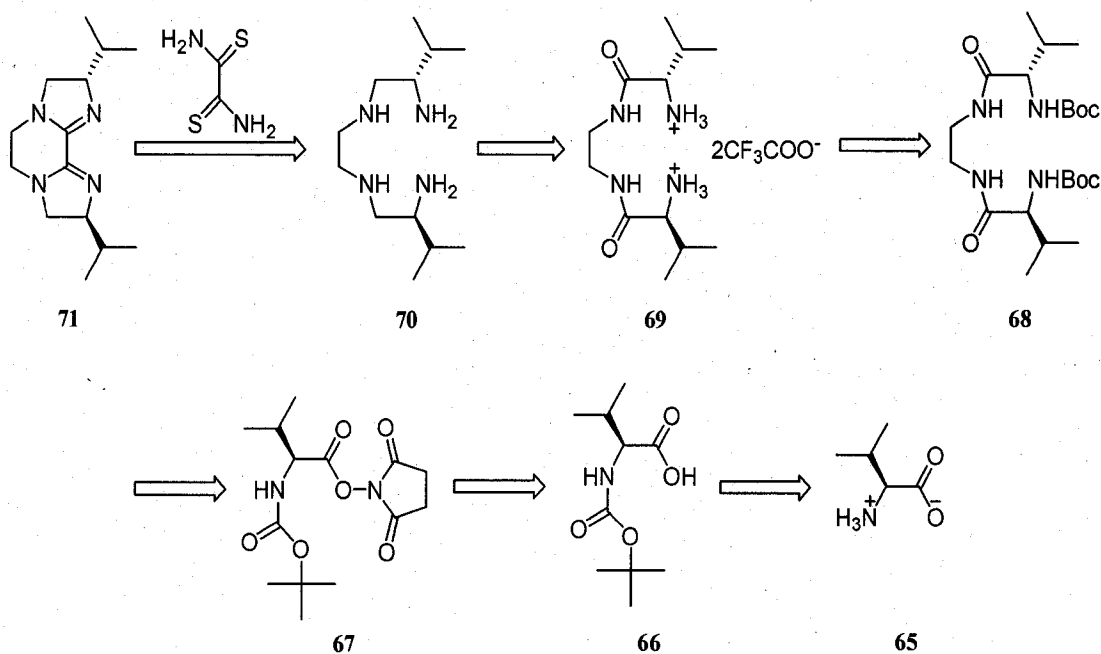


### Scheme 3.3 Casey's synthetic route to $C_2$ symmetric chiral 2,b,2-BisAm<sup>14</sup>

Earlier, in 2002, Weisman had designed a different synthetic route to  $C_2$  symmetric chiral 2,2,2-BisAms from cheap natural enantiopure  $\alpha$ -amino acids (**Scheme 3.4**).<sup>56</sup> This route utilized the condensation reaction with dithiooxamide developed earlier by Weisman and Reed, requiring the corresponding chiral tetraamine to be synthesized.<sup>56</sup> The chiral tetraamine can be prepared from the protected amino acid (Boc-protected *S*-valine was first utilized). In 2002, the challenge came from the reduction of the chiral amide **69** to yield the chiral tetraamine **70**. As part of her senior thesis research project, Kwan tried to reduce the chiral amide **69** with excess  $\text{BH}_3\cdot\text{THF}$ , but the reaction was

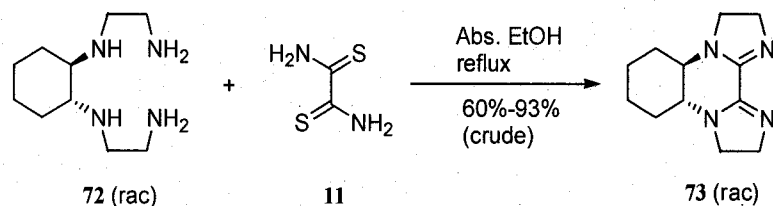


unsuccessful, probably due to incomplete reduction. Nonetheless, this synthetic route remains a viable strategy to synthesize  $C_2$  symmetric chiral BisAm's as an alternative to Casey's route.



**Scheme 3.4 Retrosynthetic analysis of ligand 71**

In 1999, Young had prepared the tetraamine **72** with a diaminocyclohexane ring incorporated into it following Saburi and Yoshikawa's procedure.<sup>78</sup> Then he utilized Weisman and Reed's methodology to synthesize successfully a racemic  $C_2$ -symmetric BisAm **73** containing the backbone of 2,2,2-BisAm (Scheme 3.5).<sup>57</sup>



**Scheme 3.5 Synthesis of 73**

We are interested in the use of chiral BisAms as ligands to exploit metal-catalyzed asymmetric reactions. In this chapter, the synthesis of Kwan's  $C_2$  symmetric chiral 2,2,2-BisAm **71** was finally completed according to the retrosynthetic analysis in the **Scheme 3.4**; and the  $C_2$  symmetric chiral 3,2,3-BisAm **74** synthesis was initiated by adopting the same strategy (**Figure 3.4**).

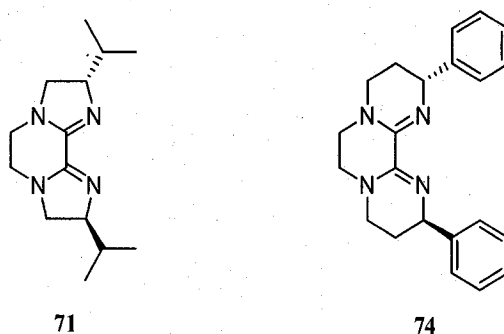
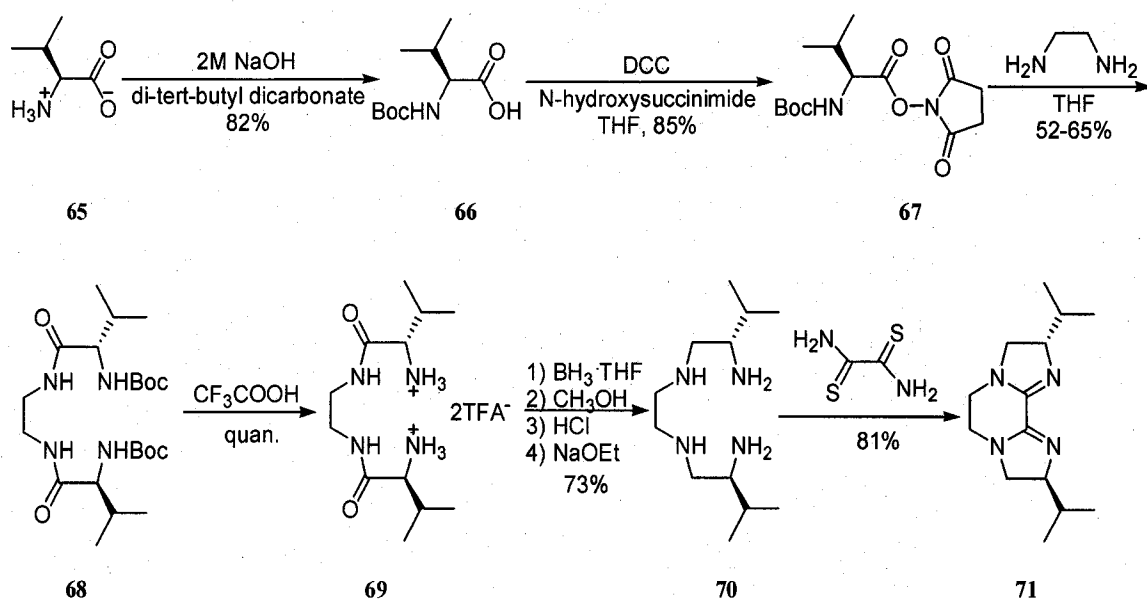


**Figure 3.4** Target molecules in this work

### 3.2 Synthesis of $C_2$ symmetric chiral 2,2,2-BisAm **71**

The reaction sequence in the synthesis of **71** is shown in **Scheme 3.6**. Based on the retrosynthetic analysis in **Scheme 3.4**, the amino group in the starting material (*S*)-valine **65** needs to be protected using di-*tert*-butyl dicarbonate ((Boc)<sub>2</sub>O) in the first step. A pair of rotamers of the Boc-protected (*S*)-valine **66** was observed in the <sup>1</sup>H-NMR spectrum (**Figure 3.5**). Then a 1,3-dicyclohexylcarbodiimide (DCC) coupling of Boc-protected amino acid with *N*-hydroxysuccinimide (NHS) produced the compound **67**. In the <sup>1</sup>H-NMR spectrum of **67**, the appearance of a new singlet signal at 2.85 ppm for the methylene group of succinimide indicated the formation of compound **67**.



**Scheme 3.6 Synthesis of ligand 71**

Rotamers of **67** were also observed in the  $^1\text{H-NMR}$  spectrum. Upon addition of ethylenediamine to **67**, a white precipitate immediately formed. The crude white solid

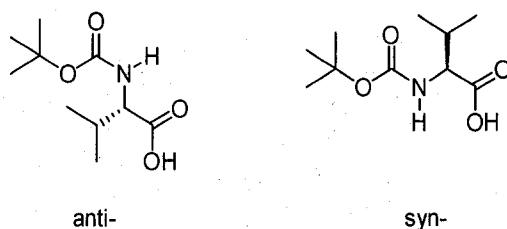


**Figure 3.5 Syn- and anti-rotamer of Boc-protected (S)-valine**

was purified by recrystallization from acetone to afford white needle crystals of **68**. In the  $^1\text{H-NMR}$  spectrum of **68**, the singlet at 2.85 ppm for the ethylene group of succinimide disappeared. This confirmed the complete displacement of the NHS group

by ethylenediamine. The  $^{13}\text{C}\{^1\text{H}\}$ -NMR spectrum of **68** afforded further support by exhibiting two characteristic carbonyl peaks, not three. The compound **68** was deprotected using trifluoroacetic acid (TFA) without solvent to generate amide TFA salt **69** in quantitative yield. The Boc carbonyl signal at  $\sim 156$  ppm disappeared, which indicated a successful deprotection. The structure of amide **69** was confirmed by  $^1\text{H}$ -NMR spectrum in which the strong *tert*-butyl group signal disappeared.

The diamide-diamine **69** was then reduced to the tetraamine **70** with  $\text{BH}_3\cdot\text{THF}$  directly. The solubility issue of the TFA salt didn't affect the completion of this reduction. An excess of borane was needed in order to complete not only the reduction of amide but also the neutralization of the TFA salt as well as reduction of TFA itself. After the reaction, the acidic workup was carried out by adding methanol followed by concentrated HCl to hydrolyze the Borane amine complex. Then the solvents were removed by evaporation under reduced pressure. Although column chromatography can be employed to separate and purify the crude amine,<sup>58</sup> this is not convenient for realizing a large scale synthesis. After neutralizing with fresh sodium ethoxide, Kugelrohr distillation at  $120^\circ\text{C}$  and 200 millitorr was carried out to distill **70** as a light yellow oil.<sup>59</sup> This oil was employed in the next step without further purification since its purity was confirmed by its  $^1\text{H}$ -NMR spectrum.

In the  $^1\text{H}$ -NMR spectrum of the chiral tetraamine **70**, the two geminal hydrogens  $\text{H}_a$  on the methylene **D** groups from the reduction of amide generate two doublets of doublets, which are centered at 2.69 and 2.37 ppm (**Figure 3.6**). The geminal coupling

constant is 11.5 Hz. The diastereotopic ethylene protons produce an AA'BB' multiplet signal at 2.65-2.81 ppm (Table 3.1). Successful reduction of **69** with borane was also proved by the  $^{13}\text{C}\{^1\text{H}\}$ -NMR spectrum of this  $C_2$  symmetric product, in which six carbon signals appear in the upfield region. Absence of the amide carbon peak at  $\sim 170$  ppm and appearance of new methylene **D** peak confirmed the formation of the tetraamine.

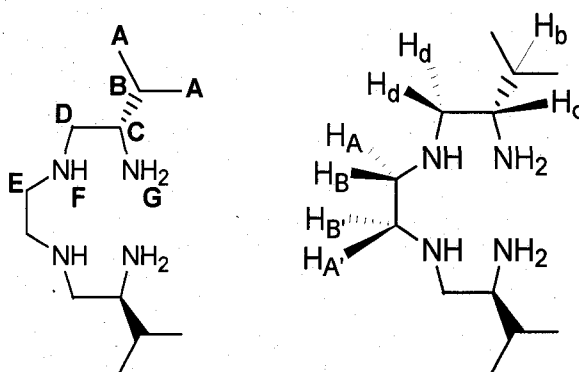


Figure 3.6 Structure of  $C_2$  symmetric chiral tetraamine **70**

Table 3.1  $^1\text{H}$ -NMR data for synthetic intermediate **70**

ppm	Multiplicity	Integration	Proton Assignment
0.89, 0.91	2 doublets ( $J = 6.9, 7.0$ Hz)	12	Diastereotopic $-\text{CH}_3$ on isopropyl group
1.55-1.63	m ( $J = 5.5, 6.8$ Hz)	2	$\text{H}_b$
1.43-1.64	broad	6	$-\text{NH}_2$ and $-\text{NH}$
2.34-2.40	dd ( $J = 9.4, 11.5$ Hz)	2	$\text{H}_d$
2.55-2.62	ddd ( $J = 3.5, 5.5, 9.4$ Hz)	2	$\text{H}_c$
2.65-2.81	AA'BB'	4	$-\text{CH}_2\text{CH}_2-$
2.67-2.71	dd ( $J = 3.5, 11.5$ Hz)	2	$\text{H}_d$

With the chiral tetraamine **70** in hand, the condensation reaction with one equivalent of dithiooxamide was performed according to Weisman and Reed's procedure

to obtain the  $C_2$  symmetric chiral 2,2,2-BisAm **71**. The crude product is dark orange, which means the crude product contains some impurity dithiooxamide. The observed optical rotation at 27°C of crude product **71** (0.51g/100mL  $CHCl_3$ ) in a 1 dm tube was +0.346°, so the specific rotation  $[\alpha]_D^{27}$  is +67.5°. ( $[\alpha]_D^T = 100\alpha_D^T/lc$ ,  $l$  is length of sample tube in decimeters;  $c$  is concentration of solution in grams per 100 mL) Casey et al. reported a **71**'s specific rotation  $[\alpha]_D^{20}$  of +111.6° (2g/100mL  $CHCl_3$ ).<sup>14</sup> These data cannot be directly compared since our sample is not pure enough and they were measured at different concentrations and temperature. This is because the variation of rotation with concentration is not necessarily linear and the temperature also affects optical rotation. Further purification needs to be done.

In the  $^1H$ -NMR spectrum of the chiral 2,2,2-BisAm **71**, there are two separated doublets centered at 0.82 and 1.02 ppm respectively, corresponding to the hydrogens of the diastereotopic methyl groups on the isopropyl group. The octet resonance centered at 1.76 ppm corresponds to the methine hydrogen ( $H_b$ ) on the isopropyl group (**Figure 3.7**). Two geminal hydrogens  $H_d$  on the methylene **D** generate two doublet of doublets signals at two different chemical shifts 2.76 and 3.43 ppm. The geminal coupling constant is ~8.8 Hz. The diastereotopic ethylene protons produce an AA'BB' multiplet signal centered at 3.15 ppm (**Table 3.2**). The  $^{13}C\{^1H\}$ -NMR spectrum of the  $C_2$  symmetric compound exhibited seven major peaks with a small impurity peak. The seven peaks include two diastereotopic methyl signals at 20.3 and 19.0 ppm, respectively, and the characteristic signal of amidine carbons at 154.5 ppm.

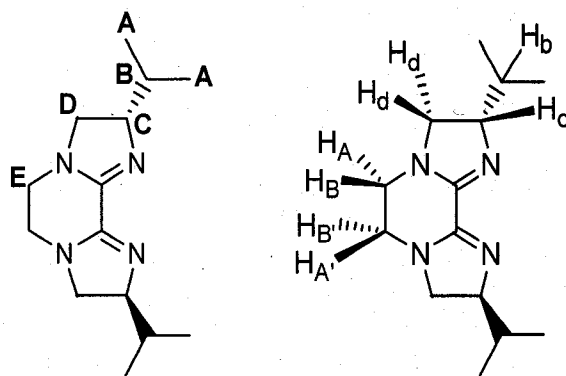
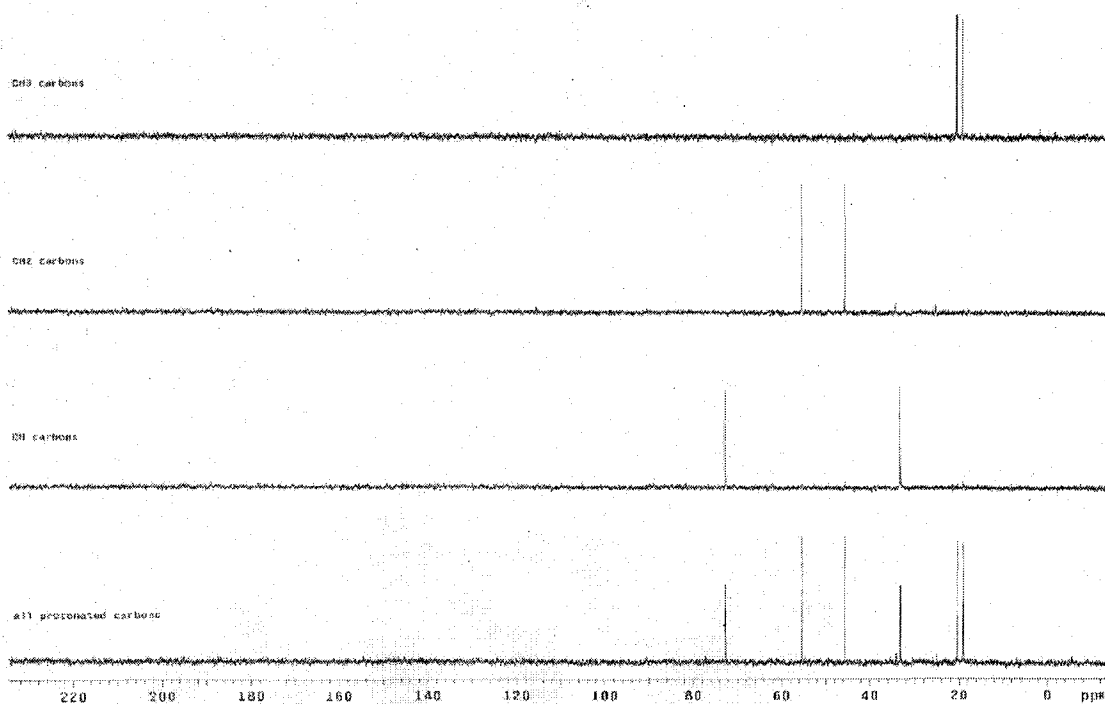


Figure 3.7 Structure of  $C_2$  symmetric chiral 2,2,2-BisAm 71

Table 3.2  $^1\text{H-NMR}$  data for  $C_2$  symmetric chiral 2,2,2-BisAm 71

ppm	Multiplicity	Integration	Proton Assignment
0.83, 1.02	2 doublets ( $J = 6.7, 6.8$ Hz)	12	Diastereotopic $-\text{CH}_3$ on isopropyl group
1.70-1.82	octet ( $J = 6.8$ Hz)	2	$\text{H}_b$
2.74-2.79	dd ( $J = 8.8, 12.5$ Hz)	2	$\text{H}_d$
3.10-3.21	$\text{AA}'\text{BB}'$	4	$-\text{CH}_2\text{CH}_2-$
3.41-3.46	dd ( $J = \sim 9.1$ Hz)	2	$\text{H}_d$
3.66-3.73	ddd ( $J = 7.7, 9.4, 12.5$ Hz)	2	$\text{H}_c$

A DEPT experiment was performed for further elucidation of the assignments of carbon signals (Figure 3.8). The spectrum identified the methine carbons **B** at 33.2 ppm and **C** at 72.6 ppm.



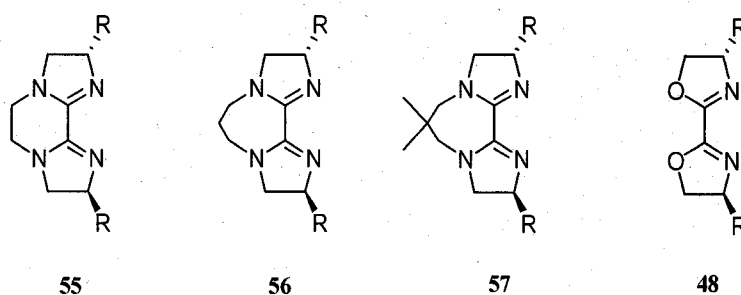
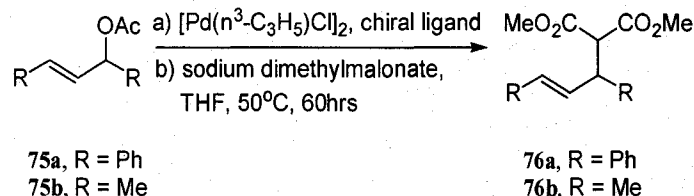
**Figure 3.8 DEPT spectra of  $C_2$  symmetric chiral 2,2,2-BisAm 71**

### 3.3 Attempted Synthesis of chiral 3,2,3-BisAm

With  $C_2$  symmetric chiral 2,2,2-BisAm 71 in hand, its metal complexes of palladium or copper can be expected to be available and tested as catalysts in many asymmetric reactions. In 2004 when Casey and coworkers reported the synthesis of chiral 2,2,2-BisAms (**Figure 3.3**), they had applied these chiral BisAms as ligands to the asymmetric Pd-catalyzed allylic alkylation reactions.<sup>14</sup> They found that the tricyclic bisamidine ligands are more effective ligands than the bicyclic bisoxazolines in this reaction. Bisoxazoline ligands **48a** and **48b** showed no apparent activity under their conditions<sup>60</sup> while the allylation reaction proceeded successfully with all the tricyclic



bisamidines. However, only moderate enantioselectivity (less than 80%) was obtained (Scheme 3.7).



a: R = t-Bu; b: R = i-Pr; c: R = Bn

### Scheme 3.7 Pd-catalyzed asymmetric allylic alkylation reaction

As a  $C_2$  symmetry ligand, chiral 3,2,3-BisAm has some advantages over chiral 2,2,2-BisAm in asymmetric catalysis since it can shield the metal center more effectively. This is because the two sterically-hindered substituents on chiral 3,2,3-BisAm are more convergent than the two same substituents on chiral 2,2,2-BisAm (Figure 3.9),  $\beta < \alpha$ . This places the two substituents on chiral 3,2,3-BisAm in closer proximity to influence the coordination site than those on the 2,2,2-BisAm ligand.

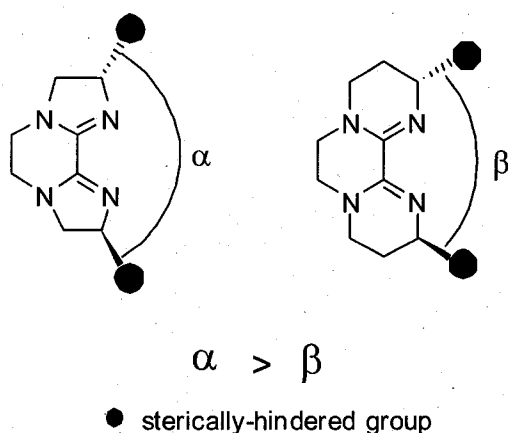
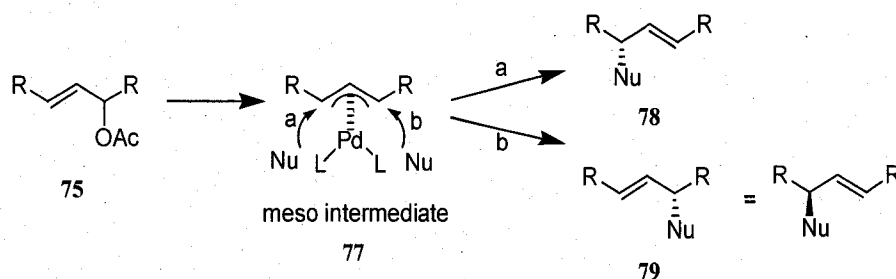


**Figure 3.9 Structural comparison of chiral 2,2,2-BisAm and 3,2,3-BisAm**

Using the asymmetric allylic alkylation reaction as an example (**Scheme 3.8**), the asymmetric allylic alkylation reaction proceeds via a meso intermediate. The identity of the product produced depends on which end of the allyl group the nucleophile attacks.<sup>61</sup> If the nucleophile attacks side **a**, the product **78** will be formed; otherwise, the enantiomer **79** will be generated. Therefore, directing the approach of the nucleophile is critical. Both  $C_2$ -chiral BisAm ligands can perturb the symmetry of the allyl group by direct steric interactions<sup>62</sup> (**Figure 3.10**). However, the same substituent groups on 3,2,3-BisAm can hinder the approach of the nucleophile more effectively than those on 2,2,2-BisAm due to the fact that  $\beta < \alpha$ . So better enantioselective results can be expected using chiral 3,2,3-BisAm.



**Scheme 3.8** The asymmetric allylic alkylation reaction

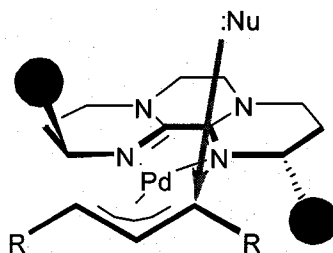
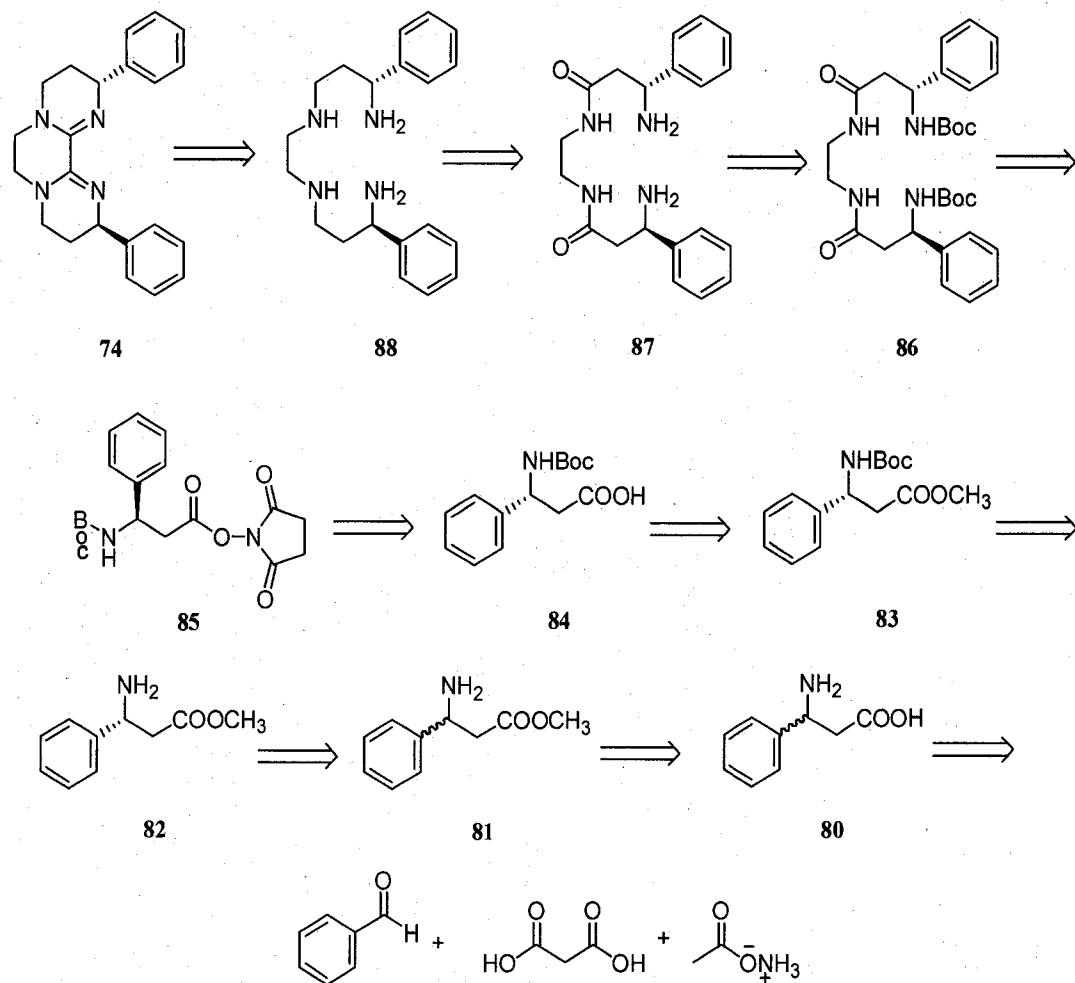


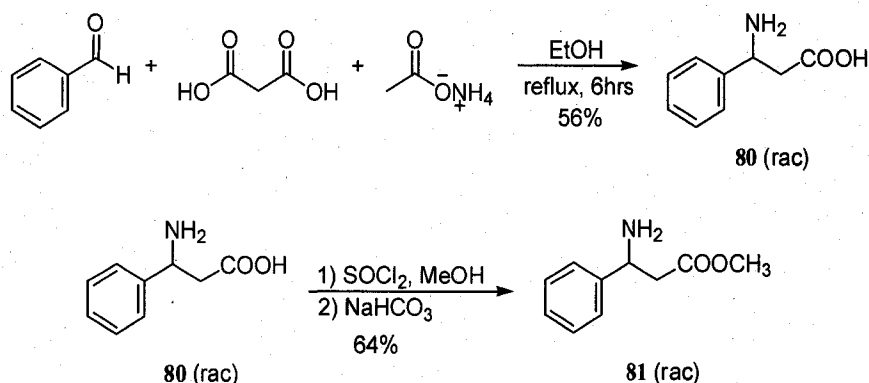
**Figure 3.10** Steric interactions during alkylation

The same synthetic strategy of chiral 2,2,2-BisAm **71** can be employed to synthesize chiral 3,2,3-BisAm (**Scheme 3.9**). The difference is that enantiopure  $\beta$ -amino acids will be needed as starting materials. There are many approaches to the synthesis of enantiomeric  $\beta$ -amino acids and esters for large-scale production. These include the asymmetric Michael additions, homologation of  $\alpha$ -amino acids, stereoselective reduction of enantiomeric enamines, as well as addition of Reformatsky reagents and ester enolates to imines etc.<sup>63</sup> 3-amino-3-phenylpropanoic acid **80** was chosen because it is easily prepared in a one-pot Mannich reaction and is conveniently resolved into two highly pure enantiomers with *L*-tartaric acid by classical resolutions.



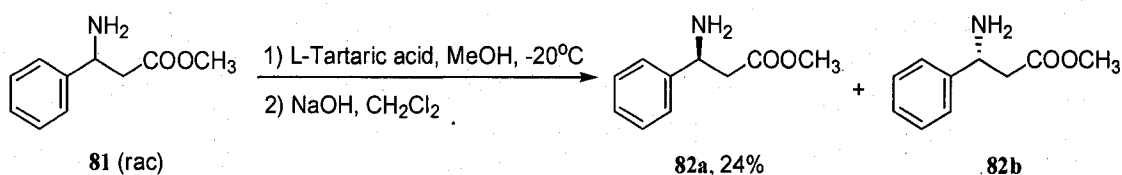
**Scheme 3.9 Retrosynthetic analysis of ligand 74**

The racemic  $\beta$ -amino acid, 3-amino-3-phenylpropanoic acid was prepared by reaction of benzaldehyde with malonic acid and ammonium acetate in ethanol and was isolated as a white precipitate by filtration, without need for any further purification<sup>64</sup> (Figure 3.11). Then racemic  $\beta$ -amino acid **80** was transformed to racemic methyl ester **81** by slow addition of  $\text{SOCl}_2$  into its methanol solution (Scheme 3.10).



### Scheme 3.10 Synthesis of racemic 3-amino-3-phenylpropanoic acid & derivative

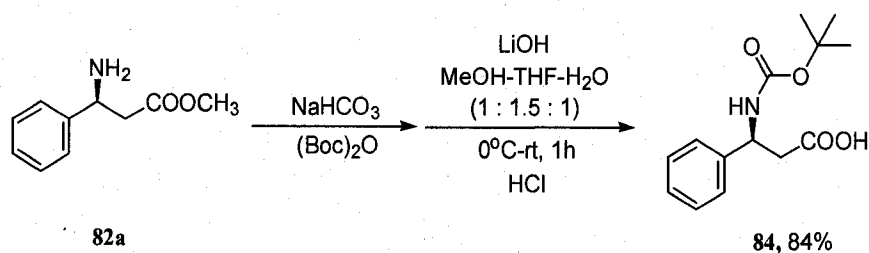
The methyl ester **81** was extracted using ethyl acetate after neutralization. The yield was 64%. Then the resolution of the racemic methyl ester **81** with *L*-tartaric acid by recrystallization gave (*S*)-methyl ester **82a**, the yield was 24% and the resolution of the filtrate with *D*-tartaric acid yielded the (*R*)-methyl ester **82b**<sup>65</sup> (Scheme 3.11). The specific rotation  $[\alpha]_D^{27}$  of **82a** is  $-23.9^\circ$  (conc. 1.9 g/100ml, CHCl<sub>3</sub>). More than 98% enantiomeric excess value was obtained comparing its optical rotation with the literature.<sup>66,67</sup>



### Scheme 3.11 Resolution of racemic methyl 3-amino-3-phenylpropanoate 81

The amino group of (*S*)-methyl ester **82a** was then protected by reaction with (Boc)<sub>2</sub>O followed by hydrolysis of the methyl ester using lithium hydroxide<sup>68</sup> (Scheme 3.12). With the enantioenriched Boc-protected β-amino acid **84** in hand, the chiral

3,2,3-BisAm **67** can be anticipated.

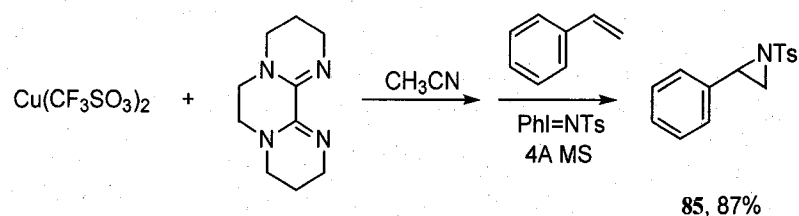


**Scheme 3.12** Synthesis of Boc-protected (*S*)-3-amino-3-phenylpropanoic acid **84**

### 3.4 Preliminary study of Cu(II)-BisAm catalyzed aziridination

Aziridines are important intermediates because they can be converted into other nitrogen-containing functional groups.<sup>69,70</sup> The protocol for the formation of aziridines from diverse aromatic and aliphatic olefins by *N*-(*p*-toluenesulfonylimino)phenyliodinane (PhI=NTs), mediated by transition metals such as Rh, Cu, have been well established.<sup>71,72</sup> In the 1990s, Evans reported the use of bis(oxazolines) as ligands in asymmetric aziridination, which afforded good yields and enantioselectivities.<sup>73,74</sup> As was discussed above, BisAms are conformationally restricted analogues of bis(oxazolines). We are interested in asymmetric aziridination reaction using chiral BisAms as ligands. Before the study of asymmetric aziridination, a preliminary study of Cu(II)-3,2,3-BisAm-catalyzed aziridination reaction of styrene was performed which gave a promising yield (**Scheme 3.13**). In this study, a conventional reaction protocol was adopted.<sup>36</sup> This initial result demonstrated that a copper complex of 3,2,3-BisAm could be an efficient catalyst for the aziridination of olefins, so development of

copper(II)-catalyzed enantioselective aziridination reaction using chiral 3,2,3-BisAms as ligands is expected.



**Scheme 3.13 Preliminary study of  $\text{Cu}^{\text{II}}$ -BisAm catalyzed aziridination**

### 3.5 Conclusion and Future work

In summary, the  $C_2$  symmetric chiral 2,2,2-BisAm **71** was successfully prepared in a multistep syntheses and confirmed by spectroscopic analysis. In addition, the synthesis of  $C_2$  symmetric chiral 3,2,3-BisAm **74** was initiated by adopting the same synthetic strategy (Figure 3.4). On the basis of the studies above, a general synthetic route can be developed to  $C_2$ -symmetric tricyclic bisamidines (BisAm) from chiral amino acids. In order to investigate broadly the asymmetric catalytic ability of chiral BisAms, more novel chiral BisAms with different substituents and ring sizes should be designed and prepared. In addition to transition metal-catalyzed allylic alkylation reaction and aziridination reaction, other interesting asymmetric reactions such as Aldol additions, Michael addition should also be tested.





## CHAPTER 4

### EXPERIMENTAL SECTION

#### A. General Procedures

All other reagents and solvents were obtained from commercial sources and used without further purification. Deuterated solvents were obtained from Cambridge Isotope Laboratories and stored over 3 Å molecular sieves.

All  $^1\text{H}$ -NMR and  $^{13}\text{C}\{^1\text{H}\}$ -NMR spectra were acquired on a Varian *Mercury* 400 MHz spectrometer operating at 399.75 and 100.51 MHz respectively or on a Varian *Unity INOVA* 500 MHz spectrometer operating at 500 and 125.67 MHz respectively. IR spectra were recorded from KBr pellets on a Nicolet MX-1 FT Spectrophotometer. ESI-MS was performed on a Thermofinnigan LCQ Mass Spectrometer coupled to a Picoview electrospray source. FAB-MS was performed on the JEOL JMS-AX505HA Mass Spectrometer in the University of Notre Dame. Electronic Spectra were measured on a Cary 219 spectrophotometer. Elemental analysis was performed at the Atlantic Microlab, Inc. Norcross, GA. X-ray structures were solved by the Crystallography Laboratory at the University of California-San Diego. Optical rotations were measured on a Rudolph Research AUTOPOL III automatic polarimeter in specified solutions and concentrations.

#### B. Preparation of 3,2,3-BisAm and its transition metal complexes

All reactions were performed in standard Schlenk glassware. Recrystallizations were conducted in closed containers without special precautions to remove either air or

moisture. Bulk solvent removal was by rotary evaporation under reduced pressure and trace solvent removal from solids was by vacuum pump. 2,2,2-BisAm was prepared as described by Reed. N, N'-bis-(3-aminopropyl)-1,2-ethylenediamine was obtained from Aldrich Chemical Co. Dithiooxamide was obtained from Fluka Chemical Co.

**Caution!** Perchlorate salts of metal complexes of organic ligands in organic solvents are potentially explosive. Although no detonations of the described salts have occurred in our laboratories, cautious handling of only small amounts of these compounds is strongly recommended.

### **3,2,3-BisAm (9)**

(2,3,4,6,7,9,10,11-Octahydro-pyrazino[1,2-a:4,3-a']dipyrimidine)

A 250mL three-necked round-bottomed flask equipped with a reflux condenser with N<sub>2</sub> inlet tube, a fritted gas dispersion tube (initially closed) and a pressure-equalizing addition funnel was charged with dithiooxamide (2.0g, 16.64mmol) suspended in absolute EtOH (30 mL). A solution of N, N'-bis-(3-aminopropyl)-1,2-ethylenediamine (2.90g, 16.64mmol) in absolute EtOH (20 mL) was added by syringe. The nitrogen manifold exit line was routed through two scrubbing towers charged with 30% aq. NaOH solution in order to trap the gases evolved. The reaction mixture was heated at 80°C for 2 hrs. The reaction mixture was then cooled to room temperature and EtOH (30 mL) was then added in order to immerse the fritted gas dispersion tube. Residual gaseous byproducts were purged from the solution by entrainment with nitrogen for 24 hours. Then the solvent was removed by rotary evaporation leaving a dark-red thick liquid. The thick liquid was taken up in CHCl<sub>3</sub> (100 mL) and then filtered through glass wool. Then

the solution was concentrated and toluene (100 mL) was added and heated. The near-boiling mixture was filtered through glass wool. The toluene extracts were azeotropically distilled for 2 days and evaporation of the corresponding bright dark yellow solution under reduced pressure afforded a yellow solid (1.745 g, yield 55%).  $^1\text{H}$  NMR ( $\text{CDCl}_3$ , 399.75MHz):  $\delta$  1.82-1.88 (m, 4H), 3.19-3.22 ('t', 4H), 3.22 (s, 4H), 3.52-3.55 ('t', 4H);  $^{13}\text{C}\{^1\text{H}\}$  NMR ( $\text{CDCl}_3$ , 100.51 MHz, ref center line of  $\text{CHCl}_3$  set at 77.3)  $\delta$  21.52, 45.00, 47.66, 48.06, 148.04;  $^1\text{H}$  NMR ( $\text{CD}_3\text{CN}$ , 399.75 MHz):  $\delta$  1.73-1.78 (m, 4H), 3.18-3.20 ('t', 4H), 3.18 (s, 4H), 3.33-3.36 ('t', 4H);  $^{13}\text{C}\{^1\text{H}\}$  NMR ( $\text{CD}_3\text{CN}$ , 100.51 MHz, ref center line of  $\text{CD}_3\text{CN}$  set at 117.61)  $\delta$  21.56, 44.43, 47.47, 47.63, 148.03; The NMR spectra in  $\text{CD}_3\text{CN}$  is used to compare with the NMR spectra of the 3,2,3-BisAm complexes. IR (KBr):  $1601\text{cm}^{-1}$  (C=N); UV-Vis ( $\text{CH}_3\text{CN}$ ): 248 nm ( $\epsilon = 7500\text{ M}^{-1}\text{cm}^{-1}$ ); *Anal. Calc.* for  $\text{C}_{10}\text{H}_{16}\text{N}_4 \cdot (\text{H}_2\text{O})_{0.8}$ : C, 58.12; H, 8.58; N, 27.11. Found: C, 58.18; H, 8.66; N, 26.79%. The crude yellow solid was recrystallized from hexane or heptane to give white solid (yield 26% in heptane), followed by sublimation at  $115^\circ\text{C}$  and  $\sim 800$  millitorr to give white crystals (yield 40%).  $^1\text{H}$  NMR ( $\text{CDCl}_3$ , 399.75MHz):  $\delta$  1.82-1.88 (m, 4H), 3.19-3.22 ('t', 4H), 3.22 (s, 4H), 3.52-3.55 ('t', 4H);  $^{13}\text{C}\{^1\text{H}\}$  NMR ( $\text{CDCl}_3$ , 100.51 MHz, ref center line of  $\text{CHCl}_3$  set at 77.3)  $\delta$  21.49, 44.94, 47.62, 48.02, 148.03.

### **[Pd(3,2,3-BisAm)(CH<sub>3</sub>CN)<sub>2</sub>](BF<sub>4</sub>)<sub>2</sub> (23)**

$\text{Pd}(\text{CH}_3\text{CN})_4(\text{BF}_4)_2$  is an air sensitive yellow solid, thus this reaction was performed under  $\text{N}_2$ . Addition of an amount of  $\text{Pd}(\text{CH}_3\text{CN})_4(\text{BF}_4)_2$  (250mg, 0.563mmol) to a solution of 3,2,3-BisAm (101mg, 0.525mmol) in  $\text{CH}_3\text{CN}$  (15mL) resulted in the formation of a dark orange solution. After stirring for 2hrs, 25mL diethyl ether was added

into the reaction mixture to precipitate the Pd complex. Workup of the yellow solid by recrystallization (CH<sub>3</sub>CN/diethyl ether diffusion) gave yellow crystals (214 mg, 69% yield). <sup>1</sup>H NMR (CD<sub>3</sub>CN, 399.75MHz): δ 1.96(m, 4H), 1.99(s, 6H), 3.30(t, 4H), 3.40(t, 4H), 3.47(s, 4H); <sup>13</sup>C{<sup>1</sup>H} NMR (CD<sub>3</sub>CN, 100.52MHz, ref CD<sub>3</sub>CN set at 117.6 ppm) δ 20.20, 46.31, 46.37, 47.58, 146.46; IR (KBr): 2320 (CN), 2259 (CN), 1621 (C=N), 1000-1150 (B-F), 762 (B-F)cm<sup>-1</sup>; FAB-MS: 467.0978amu {[Pd(3,2,3-BisAm)(CH<sub>3</sub>CN)<sub>2</sub>(BF<sub>4</sub>)<sub>2</sub>]<sup>+</sup>}; *Anal.* Calc. for [Pd(3,2,3-BisAm)(CH<sub>3</sub>CN)<sub>2</sub>](BF<sub>4</sub>)<sub>2</sub>: C, 30.33; H, 4.00; N, 15.16. Found: C, 30.10; H, 4.09; N, 14.75%.

#### **[Pd(3,2,3-BisAm)<sub>2</sub>](BF<sub>4</sub>)<sub>2</sub> (24)**

An amount of Pd(CH<sub>3</sub>CN)<sub>4</sub>(BF<sub>4</sub>)<sub>2</sub> (250mg, 0.563mmol) was dissolved in CH<sub>3</sub>CN (5 mL). Addition of 4.4 mL (222mg, 0.5mmol) CH<sub>3</sub>CN of this solution of Pd(CH<sub>3</sub>CN)<sub>4</sub>(BF<sub>4</sub>)<sub>2</sub> by syringe to 3,2,3-BisAm (194mg, 1.01mmol) in a flask resulted in a yellow solution. The reaction mixture was stirred at room temperature for 4 hours. The solution was then transferred to test tubes for crystallization by slow Et<sub>2</sub>O diffusion. Yellow needles (236mg, 71% yield) were harvested. <sup>1</sup>H NMR (CD<sub>3</sub>CN, 399.75MHz): δ 1.95(m, 4H), 3.39(t, 4H), 3.40(t, 4H), 3.45(s, 4H); <sup>13</sup>C{<sup>1</sup>H} NMR (CD<sub>3</sub>CN, 100.51MHz, ref CD<sub>3</sub>CN set at 117.6 ppm): δ 20.1, 46.3, 46.8, 48.7, 155.0; IR (KBr): 1612cm<sup>-1</sup> (C=N); ESI-MS: 557.1amu {[Pd(3,2,3-BisAm)<sub>2</sub>(BF<sub>4</sub>)<sub>2</sub>]<sup>+</sup>}; *Anal.* Calc. for Pd(C<sub>10</sub>H<sub>16</sub>N<sub>4</sub>)<sub>2</sub>(BF<sub>4</sub>)<sub>2</sub>·(H<sub>2</sub>O)<sub>1.5</sub>: C, 34.74; H, 5.10; N, 16.20. Found: C, 34.78; H, 4.84; N, 16.30%.

### **[Pd(3,2,3-BisAm)<sub>2</sub>]Cl<sub>2</sub> (26)**

PdCl<sub>2</sub>·2PhCN was prepared according to a literature method.<sup>[9]</sup> An amount of PdCl<sub>2</sub>·2PhCN (56.6mg, 0.148mmol) and 3,2,3-BisAm (56.9mg, 0.295mmol) were combined in a flask. CH<sub>3</sub>CN (5 mL) was added to the flask and stirred at room temperature. After 4 hours, some initially insoluble yellow solid had disappeared. The reaction mixture was then transferred to test tubes for crystallization by slow diethyl ether diffusion. Yellow opaque solids (63mg, 76% yield) were obtained. <sup>1</sup>H NMR (CD<sub>3</sub>CN, 399.75MHz): δ 1.95(m, 4H), 3.40(t, 4H), 3.42(t, 4H), 3.46(s, 4H); <sup>13</sup>C{<sup>1</sup>H} NMR (CD<sub>3</sub>CN, 100.51MHz, ref CD<sub>3</sub>CN set at 117.6 ppm) δ 20.1, 46.4, 46.8, 48.7, 155.0;

### **W(3,2,3-BisAm)(CO)<sub>4</sub> (27)**

An amount of W(CO)<sub>6</sub> (351mg, 1.0mmol) and 3,2,3-BisAm (148mg, 0.767mmol) were combined in a flask. Toluene (8 mL) was added to the flask and the reaction mixture was heated to reflux for one hour. The solution became dark-red with the formation of a bright red precipitate. The reaction mixture was evaporated and then placed under reduced pressure to remove excess W(CO)<sub>6</sub> by sublimation at 50-70°C. The red solid residue was washed with hexane and dried under reduced pressure to give 220 mg (82% yield) of product. <sup>1</sup>H NMR (d<sup>7</sup>-DMF, 399.75MHz): δ 1.97(m, 4H), 3.43(t, 4H), 3.48(s, 4H), 3.70(t, 4H); <sup>13</sup>C{<sup>1</sup>H} NMR (d<sup>7</sup>-DMF, 100.52MHz, ref central line of DC(=O)N(CD<sub>3</sub>)<sub>2</sub> set at 164.9 ppm) δ 23.6, 48.8, 49.6, 54.5, 154.7, 204.9, 218.6; IR (KBr): 2000 (C=O<sub>sym</sub>), 1851, 1787 (C=O<sub>asym</sub>), 1625, 1603cm<sup>-1</sup> (C=N).

### **Zn(3,2,3-BisAm)<sub>2</sub>(ClO<sub>4</sub>)<sub>2</sub> (28)**

Addition of an amount of Zn(ClO<sub>4</sub>)<sub>2</sub>·6H<sub>2</sub>O (88.0mg, 0.236mmol) to a solution of 3,2,3-BisAm (87.2mg, 0.454mmol) in CH<sub>3</sub>CN (25 mL) formed a light yellow solution. After stirring for 3hrs, the solution was transferred to vials for crystallization by diethyl ether diffusion. White solids (139mg, 85% yield) were harvested over several days. <sup>1</sup>H-NMR (CD<sub>3</sub>CN, 399.75MHz): δ 1.90-1.93 (~pentet, 4H), 3.36-3.39 (t, 4H) 3.40-3.43 (t, 4H) 3.50 (s, 4H); <sup>13</sup>C{<sup>1</sup>H}-NMR (CD<sub>3</sub>CN, 100.53MHz, ref CD<sub>3</sub>CN set at 117.59 ppm) δ 19.64, 43.20, 46.31, 47.37, 149.78; IR (KBr): 1614.1cm<sup>-1</sup> (C=N); *Anal.* Calc. for Zn(C<sub>10</sub>H<sub>16</sub>N<sub>4</sub>)<sub>2</sub>(ClO<sub>4</sub>)<sub>2</sub>(H<sub>2</sub>O): C, 36.02; H, 5.14; N, 16.08; Cl, 10.63. Found: C, 36.02; H, 5.18; N, 16.56; Cl, 10.72%.

### **[Zn(3,2,3-BisAm)<sub>3</sub>]Cl<sub>2</sub> (29)**

An amount of ZnCl<sub>2</sub>·xH<sub>2</sub>O (19.1mg, ~0.14mmol) and a slight excess of three equivalents of 3,2,3-BisAm (88.2mg, 0.458mmol) were dissolved in MeCN (5 mL). The reactants slowly dissolved to give a clear solution. A small portion of the solution was transferred to a vial for crystallization by diethyl ether diffusion. The remaining solution was concentrated by rotary evaporation and dried by vacuum to give a white solid (63.8mg, 71% yield). <sup>1</sup>H NMR (CD<sub>3</sub>CN, 499.78MHz): δ 1.72(m, 5H), 1.87(m, 7H), 3.10-3.56(m, 12x3H); <sup>13</sup>C{<sup>1</sup>H} NMR (CD<sub>3</sub>CN, 100.52MHz, ref CD<sub>3</sub>CN set at 117.7 ppm) δ 20.4, 42.5, 46.6, 47.3, 147.3; IR (KBr): 1607-1619(b)cm<sup>-1</sup> (C=N); *Anal.* Calc. for Zn(C<sub>10</sub>H<sub>16</sub>N<sub>4</sub>)<sub>3</sub>Cl<sub>2</sub>·(H<sub>2</sub>O)<sub>4</sub>: C, 45.89; H, 7.19; N, 21.41; Cl, 9.03. Found: C, 45.72; H, 7.12; N, 21.22; Cl, 9.23%.

### **Zn(3,2,3-BisAm)<sub>3</sub>(ClO<sub>4</sub>)<sub>2</sub> (30)**

Addition of an amount of Zn(ClO<sub>4</sub>)<sub>2</sub>·6H<sub>2</sub>O (38.6mg, 0.104mmol) to a solution of 3,2,3-BisAm (61.2mg, 0.318mmol) in CH<sub>3</sub>CN (20 mL) formed a colorless solution. After stirring for 2hrs, this solution was transferred to vials for crystallization by diethyl ether diffusion. X-ray quality colorless crystals were harvested over several days. <sup>1</sup>H NMR (CD<sub>3</sub>CN, 399.75MHz): δ 1.70-1.85(2 multiplets, 3x4H), 3.02-3.60(m, 3x12H); <sup>13</sup>C{<sup>1</sup>H} NMR (CD<sub>3</sub>CN, 100.53MHz, ref CD<sub>3</sub>CN set at 117.7 ppm) δ 20.4, 42.5, 46.6, 47.3, 147.3; IR (KBr): 1613.6cm<sup>-1</sup> (C=N); *Anal. Calc.* for Zn(C<sub>10</sub>H<sub>16</sub>N<sub>4</sub>)<sub>3</sub>(ClO<sub>4</sub>)<sub>2</sub>: C, 42.84; H, 5.75; N, 19.78; Cl, 8.43. Found: C, 42.61; H, 5.81; N, 19.71; Cl, 8.64%.

### **[Cd(3,2,3-BisAm)<sub>3</sub>](ClO<sub>4</sub>)<sub>2</sub> (32)**

An amount of Cd(ClO<sub>4</sub>)<sub>2</sub>(H<sub>2</sub>O)<sub>6</sub> (54.4 mg, 0.130 mmol) was dissolved in MeOH (5 mL). Slightly over three equivalents of 3,2,3-BisAm (80.1 mg, 0.417 mmol) were dissolved in MeOH (10 mL). The mixture of two solutions resulted in the formation of a light yellow solution. The solution was transferred to small vials for recrystallization by diethyl ether diffusion. Clear, colorless needle crystals were harvested after one night. The total yield of the crystals collected was 58.4 mg (50.6% yield). <sup>1</sup>H NMR (CD<sub>3</sub>CN, 399.75MHz): δ 1.81(m, 4H), 3.26(t, 4H), 3.34(t, 4H), 3.36(s, 4H); <sup>13</sup>C{<sup>1</sup>H} NMR (CD<sub>3</sub>CN, 100.52MHz, ref CD<sub>3</sub>CN set at 117.6 ppm) δ 20.4, 43.8, 46.7, 47.6, 148.0; IR (KBr pellet): 1606 (C=N), 1362, 1315, 1091 (ClO<sub>4</sub><sup>-</sup>) cm<sup>-1</sup>; *Anal. Calc.* for Cd(C<sub>10</sub>H<sub>16</sub>N<sub>4</sub>)<sub>3</sub>(ClO<sub>4</sub>)<sub>2</sub>: C, 40.57; H, 5.41; N, 18.93; Cl, 7.98. Found: C, 40.10; H, 5.48; N, 18.61; Cl, 8.16%.

**[Hg(3,2,3-BisAm)<sub>2</sub>](HgCl<sub>4</sub>) (33)**

Addition of an amount of HgCl<sub>2</sub> (95.3mg, 0.351mmol) to a solution of 3,2,3-BisAm (71.1mg, 0.370mmol) in MeOH (15 mL) resulted in the precipitation of a white solid. After filtration, the product was washed with additional MeOH and dried under reduced pressure to give a white powder. Clear, colorless cubic crystals were harvested after Et<sub>2</sub>O diffusion into a DMF solution of this powder over several days. <sup>1</sup>H NMR (CD<sub>3</sub>CN, 399.75MHz): δ 1.93(m, 4H), 3.37(t, 4H), 3.42(s, 4H), 3.51(t, 4H); <sup>13</sup>C{<sup>1</sup>H} NMR (CD<sub>3</sub>CN, 100.52MHz, ref CD<sub>3</sub>CN set at 117.6 ppm) δ 20.1, 44.9, 46.6, 47.4, 148.0; MS (EI): 429.3amu {[Hg(3,2,3-BisAm)Cl]<sup>+</sup>}; IR (KBr): 1608cm<sup>-1</sup> (C=N); *Anal.* Calc. for Hg(C<sub>10</sub>H<sub>16</sub>N<sub>4</sub>)Cl<sub>2</sub>: C, 25.90; H, 3.48; N, 12.08; Cl, 15.29. Found: C, 25.99; H, 3.50; N, 11.93; Cl, 15.10%.

**[Hg(3,2,3-BisAm)<sub>3</sub>](BPh<sub>4</sub>)<sub>2</sub> (34)**

An amount of slightly over five equivalents of 3,2,3-BisAm (192.6mg, 1.002mmol) was dissolved in MeOH (10 mL). Addition of HgCl<sub>2</sub> (53.8mg, 0.198mmol) solution in MeOH (5 mL) to this 3,2,3-BisAm solution formed a slight yellow solution. The reaction mixture was stirred at room temperature overnight. Then an excess of two equivalents of NaBPh<sub>4</sub> (138.6mg, 0.405mmol) was added into the solution to obtain a white precipitate. After filtration, the product was washed with additional CH<sub>3</sub>CN and dried under reduced pressure to give a white powder 196.4mg (yield 70%). <sup>1</sup>H NMR (d<sup>6</sup>-DMSO, 399.75MHz): δ 1.76 (m, 4H), 3.27-3.31 (m, 8H), 3.34 (s, 4H), 6.78 (t, 8H), 6.92 (t, 16H), 7.15-7.20 (m, 16H); <sup>13</sup>C{<sup>1</sup>H} NMR (d<sup>6</sup>-DMSO, 100.52MHz, ref (CD<sub>3</sub>)<sub>2</sub>SO set at 40.2 ppm) δ 20.63, 44.98, 46.77, 47.67, 122.19, 125.97, 136.22, 147.14, 163.31, 163.80,



164.29, 164.78; IR (KBr):  $1602\text{cm}^{-1}$  (C=N); *Anal.* Calc. for  $[\text{Hg}(\text{C}_{10}\text{H}_{16}\text{N}_4)_3][\text{B}(\text{C}_6\text{H}_5)_4]_2$ : C, 66.17; H, 6.26; N, 11.87. Found: C, 66.55; H, 6.19; N, 11.36%.

**[Ag(3,2,3-BisAm)<sub>2</sub>](BF<sub>4</sub>) (35)**

Addition of an amount of AgBF<sub>4</sub> (28.9mg, 0.148mmol) to a solution of 3,2,3-BisAm (62.1mg, 0.323mmol) in MeCN (6 mL) generated a light yellow solution. This MeCN solution was transferred to test tubes for recrystallization by ether diffusion. Light yellow crystals (38.9mg, 45% yield) were harvested from the solution after several days in the dark. <sup>1</sup>H NMR (CD<sub>3</sub>CN, 399.75MHz, ref CD<sub>2</sub>H<sub>2</sub>CN set at 1.96 ppm): δ 1.85(m, 4H), 3.30(t, 4H), 3.32(s, 4H), 3.46(t, 4H); <sup>13</sup>C{<sup>1</sup>H} NMR (CD<sub>3</sub>CN, 100.52MHz, ref CD<sub>3</sub>CN set at 117.6 ppm) δ 20.7, 46.95, 46.98, 47.6, 148.4; IR (KBr):  $1626, 1596\text{cm}^{-1}$  (C=N); *Anal.* Calc. for Ag(C<sub>10</sub>H<sub>16</sub>N<sub>4</sub>)<sub>2</sub>(BF<sub>4</sub>): C, 41.47; H, 5.57; N, 19.35. Found: C, 41.58; H, 5.64; N, 19.28%.

**[Ag(3,2,3-BisAm)<sub>2</sub>](BPh<sub>4</sub>) (36)**

Addition of a solution of AgBF<sub>4</sub> (48.8mg, 0.251mmol) in EtOH (2 mL) to a solution of 3,2,3-BisAm (99.2mg, 0.516mmol) in EtOH (3 mL) produced a cloudy light yellow solution. After stirring for 3 hrs in the dark, a solution of NaBPh<sub>4</sub> (88.1mg, 0.257mmol) in EtOH was added to exchange the counter anion BF<sub>4</sub><sup>-</sup>. Immediately, a white precipitate was formed. The white precipitate was filtered off and washed with additional EtOH, followed by drying under vacuum in the dark to give a white powder (144.0mg, 71% yield). Clear, colorless cubic crystals were harvested after Et<sub>2</sub>O diffusion into a DMF solution of this white powder in the dark over several days. <sup>1</sup>H-NMR

(CD<sub>3</sub>)<sub>2</sub>SO, 399.75MHz): δ 1.75(m, 4H), 3.25(t, 4H), 3.29(s, 4H), 3.37(t, 4H), 6.78(t, 4H), 6.92(s, 4H), 7.17(m, 4H); <sup>13</sup>C{<sup>1</sup>H}-NMR ((CD<sub>3</sub>)<sub>2</sub>SO, 100.52MHz, ref (CD<sub>3</sub>)<sub>2</sub>SO set at 40.2 ppm) δ 20.8, 46.7, 47.0, 47.6, 122.3, 126.0, 136.0, 148.3; IR (KBr): 1614cm<sup>-1</sup> (C=N); *Anal.* Calc. for Ag(C<sub>10</sub>H<sub>16</sub>N<sub>4</sub>)<sub>2</sub>(BC<sub>24</sub>H<sub>20</sub>)[Ag(BC<sub>24</sub>H<sub>20</sub>)]<sub>0.9</sub>: C, 65.88; H, 5.90; N, 9.37. Found: C, 65.59; H, 5.82; N, 9.14%.

**[Ag<sub>2</sub>(2,2,2-BisAm)<sub>4</sub>](BF<sub>4</sub>)<sub>2</sub> (37)**

Addition of an amount of AgBF<sub>4</sub> (155.7mg, 0.800mmol) to a solution of 2,2,2-BisAm (268.0mg, 1.632mmol) in MeCN (20 mL) generated a light yellow solution. The reaction mixture was stirred overnight. After centrifugation, then MeCN solution was transferred to test tubes for recrystallization by ether diffusion. Colorless cubic crystals (308mg, 74% yield) were harvested from the solution after several days in the dark. <sup>1</sup>H-NMR (CD<sub>3</sub>CN, 399.75MHz, ref CD<sub>2</sub>H<sub>2</sub>CN set at 1.96 ppm): δ 3.37 (s, 4H), 3.53-3.58 (t, 4H), 3.79-3.85 (t, 4H); <sup>13</sup>C{<sup>1</sup>H}-NMR (CD<sub>3</sub>CN, 100.52MHz, ref CD<sub>3</sub>CN set at 117.6 ppm) δ 44.21, 51.98, 53.90, 156.19; IR (KBr): 1630cm<sup>-1</sup> (C=N); *Anal.* Calc. for Ag(C<sub>8</sub>H<sub>12</sub>N<sub>4</sub>)<sub>2</sub>BF<sub>4</sub>: C, 36.74; H, 4.62; N, 21.42. Found: C, 36.58; H, 4.83; N, 21.16%.

**[Ag<sub>2</sub>(2,2,2-BisAm)<sub>3</sub>](BPh<sub>4</sub>)<sub>2</sub> (38)**

Addition of an amount of AgBF<sub>4</sub> (151.4mg, 0.778mmol) to a solution of 2,2,2-BisAm (274.3mg, 1.670mmol) in MeCN (40 mL) yielded a colorless solution with a brown precipitate. After stirring for 6 hrs in the dark, one equivalent of NaBPh<sub>4</sub> (267.0mg, 0.780mmol) was added to exchange the counteranion. Then the solution was stirred for 2 hrs in the dark. After filtering the insoluble brown solid off, the filtrate was concentrated

to 20 mL. Then 100 mL of ethanol was added to produce a white precipitate. This white precipitate was collected and washed with additional EtOH, then dried under vacuum overnight to give a white solid (434.6mg, 74% yield). Clear, colorless crystals were harvested after Et<sub>2</sub>O diffusion into CH<sub>3</sub>CN solution of this white solid in the dark over several days. <sup>1</sup>H NMR (CD<sub>3</sub>CN, 399.75MHz, ref CD<sub>2</sub>H<sub>2</sub>CN set at 1.96 ppm): δ 3.38(s, 3x4H), 3.57(t, 3x4H), 3.84(t, 3x4H), 6.87(t, 8H), 7.02(t, 16H), 7.29(m, 16H); <sup>13</sup>C{<sup>1</sup>H} NMR (CD<sub>3</sub>CN, 100.52MHz, ref CD<sub>3</sub>CN set at 117.6 ppm) δ 44.0, 51.8, 54.0, 122.1, 125.9, 136.0, 156.1; IR (KBr): 1621cm<sup>-1</sup> (C=N); *Anal.* Calc. for Ag<sub>2</sub>(C<sub>8</sub>H<sub>12</sub>N<sub>4</sub>)<sub>3</sub>(BC<sub>24</sub>H<sub>20</sub>)<sub>2</sub>: C, 64.21; H, 5.69; N, 12.48. Found: C, 64.21; H, 5.58; N, 12.50%.

#### [Cu(3,2,3-BisAm)<sub>3</sub>](ClO<sub>4</sub>)<sub>2</sub> (40)

Addition of an amount of Cu(ClO<sub>4</sub>)<sub>2</sub>(H<sub>2</sub>O)<sub>6</sub> (37.2mg, 0.101mmol) to a solution of 3,2,3-BisAm (58.3mg, 0.303mmol) in MeCN (5 mL) resulted in the formation of a light blue solution. After stirring for 1 hr, the solution was transferred to small vials for crystallization by diethyl ether diffusion. Clear, green X-ray quality crystals were harvested after several days. A total mass of 51.0 mg (60.3% yield) of the crystals were collected. IR (KBr pellet): 1615 cm<sup>-1</sup> (C=N); *Anal.* Calc. for Cu(C<sub>10</sub>H<sub>16</sub>N<sub>4</sub>)<sub>3</sub>(ClO<sub>4</sub>)<sub>2</sub>(H<sub>2</sub>O): C, 42.03; H, 5.88; N, 19.61; Cl, 8.27. Found: C, 42.05; H, 5.83; N, 19.35; Cl, 8.18%.

#### [Cu(3,2,3-BisAm)<sub>2</sub>](ClO<sub>4</sub>)<sub>2</sub> (41)

An amount of Cu(ClO<sub>4</sub>)<sub>2</sub>(H<sub>2</sub>O)<sub>6</sub> (58.2mg, 0.157mmol) and two equivalents of 3,2,3-BisAm (59.6mg, 0.310mmol) were combined in a flask. A blue precipitate formed

immediately when EtOH (5 mL) was added into the flask. The product was collected by filtration and washed with additional MeOH, dried under reduced pressure to give a blue powder (65.7mg, 66% yield). Clear, dark blue needle crystals were harvested after Et<sub>2</sub>O diffusion into a CH<sub>3</sub>CN solution of this powder over several days. IR (KBr): 1623 cm<sup>-1</sup> (C=N); *Anal.* Calc. for Cu(C<sub>10</sub>H<sub>16</sub>N<sub>4</sub>)<sub>2</sub>(ClO<sub>4</sub>)<sub>2</sub>: C, 37.13; H, 4.99; N, 17.32; Cl, 10.96. Found: C, 37.61; H, 5.00; N, 17.45%.

#### **Cu(3,2,3-BisAm)<sub>2</sub>(BF<sub>4</sub>)<sub>2</sub> (44)**

Cu(3,2,3-BisAm)<sub>2</sub>(BF<sub>4</sub>)<sub>2</sub> was obtained due to the undesired oxidation of Cu(3,2,3-BisAm)<sub>2</sub>(BF<sub>4</sub>). IR (KBr): 1614-1627 cm<sup>-1</sup> (C=N); *Anal.* Calc. for Cu(C<sub>10</sub>H<sub>16</sub>N<sub>4</sub>)<sub>2</sub>(BF<sub>4</sub>)<sub>2</sub>: C, 25.90; H, 3.48; N, 12.08; Cl, 15.29. Found: C, 25.99; H, 3.50; N, 11.93; Cl, 15.10%.

Below is the synthetic procedure of Cu(3,2,3-BisAm)<sub>2</sub>(BF<sub>4</sub>): Addition of an amount of Cu<sup>I</sup>(CH<sub>3</sub>CN)<sub>4</sub>BF<sub>4</sub> (31.8mg, 0.101mmol) to a solution of 3,2,3-BisAm (40.2mg, 0.209mmol) in degassed MeCN (3 mL) in glove box filled with N<sub>2</sub> resulted in the formation of a brown solution. After stirring for 15 minutes, the brown solution was transferred to a vial for crystallization by degassed diethyl ether diffusion in the glove box. Brown cubic crystals were harvested after several days, but the supernatant was blue in color.

#### **[Eu(3,2,3-BisAm)<sub>4</sub>](ClO<sub>4</sub>)<sub>3</sub> (45)**

Addition of an amount of Eu(OSO<sub>2</sub>CF<sub>3</sub>)<sub>3</sub> (75.3mg, 0.126mmol) to a solution of 3,2,3-BisAm (115.8mg, 0.602mmol) in EtOH (20mL) with stirring for 1 hr. resulted in the formation of light yellow solution. Then more than 3 equivalents of NaClO<sub>4</sub> (50.9mg,

0.416mmol) was added into this solution. An off-white precipitate formed immediately. After another 1 hour of stirring, the off-white precipitate was collected and washed by additional EtOH followed by drying under reduced pressure to give a white solid (119.4mg, 78% yield). Clear, colorless cubic crystals were harvested after Et<sub>2</sub>O diffusion into a CH<sub>3</sub>CN solution of the white solid over several days. <sup>1</sup>H-NMR (CD<sub>3</sub>CN, 399.75MHz): δ 1.22 (broad, 4H), 1.88 (broad s, 4H), 2.97 (broad, 4H), 5.36 (broad, 4H); <sup>13</sup>C{<sup>1</sup>H}-NMR (CD<sub>3</sub>CN, 100.52MHz, ref CD<sub>3</sub>CN set at 117.59 ppm) δ 11.48, 40.40, 47.42, 77.78, 125.95; IR (KBr): 1595 cm<sup>-1</sup> (C=N); *Anal.* Calc. for Eu(C<sub>10</sub>H<sub>16</sub>N<sub>4</sub>)<sub>4</sub>(ClO<sub>4</sub>)<sub>3</sub>: C, 39.40; H, 5.29; N, 18.38; Cl, 8.72. Found: C, 39.25; H, 5.38; N, 18.21; Cl, 8.49%.

### C. Preparation of chiral BisAm's

#### Reagents

Borane-Tetrahydrofuran complex was obtained from Lancaster Synthesis, Inc.

Di-*tert*-butyl dicarbonate was obtained from Lancaster Synthesis, Inc.

Dicyclocarbodiimide was obtained from Aldrich Chemical Company, Inc.

Ethylenediamine was obtained from Aldrich Chemical Company, Inc.

Hydrochloric acid was obtained from EMD Chemical Inc.

N-Hydroxysuccinimide was obtained from Acros Organics.

Sodium sulfate was obtained from EMD Chemical Inc.

(*S*)-Valine was obtained from Lancaster Synthesis, Inc

Benzaldehyde was obtained from Aldrich Chemical Company, Inc.

*L*-tartaric acid was obtained from Aldrich Chemical Company, Inc.

Malonic acid was obtained from Sigma Chemical Company.

Ammonia acetate was obtained from J. T. Baker Chemical Company.

Lithium hydroxide was obtained from Aldrich Chemical Company, Inc.

Sodium Bicarbonate was obtained from Fisher Scientific Co.

Trifluoroacetic acid was obtained from Alfa Aesar.

Dithiooxamide was obtained from Fluka Chemical Co.

(*N*-(*p*-toluenesulfonyl)imino)phenyliodinane, PhI=NTs, was prepared by the published method<sup>75</sup> and recrystallized from methanol/water at 5°C.

#### **(*S*)-(+)-*N*-(*tert*-butyloxycarbonyl)valine (66)**

According to a procedure in the literature<sup>76</sup>, NaHCO<sub>3</sub> (7.20g, 85.67mmol) was added to a solution of *S*-valine (5.02g, 42.83mmol) in water (60 mL) with stirring at 0°C, followed by the addition of a solution of di-*tert*-butyl dicarbonate (9.35g, 42.85mmol) in THF (64mL). After 30 minutes, the ice bath was removed and the reaction solution was heated to reflux for 16 hours. The reaction solution was then concentrated to remove THF. The aqueous solution was extracted with EtOAc (45mL). Then the aqueous layer was cooled to 10°C and acidified with saturated aqueous NaHSO<sub>4</sub> solution (27mL) to pH = 3. The layers were separated, and the aqueous layer was extracted with EtOAc (40mL). The combined organic layers were washed with water (20mL) and brine (20mL), dried over MgSO<sub>4</sub> and concentrated using rotary evaporation and vacuum to give a clear sticky liquid. This crude product was triturated with ether to yield white solids (6.84g, 74% yield). <sup>1</sup>H NMR (399.75 MHz, CDCl<sub>3</sub>) δ 0.93-0.94 (d, 3H, J = 6.8 Hz, (CH<sub>3</sub>)(CH<sub>3</sub>)HC-), 1.00-1.01 (d, 3H, J = 6.8 Hz, (CH<sub>3</sub>)(CH<sub>3</sub>)HC-), 1.45 (s, 9H, (CH<sub>3</sub>)<sub>3</sub>C-), 2.10-2.26 (m, 1H,

(CH<sub>3</sub>)<sub>2</sub>HC-), 4.01-4.07 and 4.25-4.28 (2m, 1:3, 1H, -CHRNH-), 5.02-5.04 and 6.09-6.14 (2m, 3:1, 1H, -CHRNH-), 9.50-10.60 (broad s, 1H, -COOH); <sup>13</sup>C{<sup>1</sup>H}-NMR (100.52 MHz, CDCl<sub>3</sub>) δ 17.68, 19.26, 28.52, 31.22, 58.64, 80.30, 156.04, 177.42.

**(*tert*-Butyloxycarbonyl)-*L*-valylsuccinimide (67)**

To a stirred solution of **66** (5.82g, 26.77mmol) in dry tetrahydrofuran solution (140 mL) at 0°C was added *N*-hydroxysuccinimide (3.09g, 26.80mmol) followed by dicyclohexylcarbodiimide (5.53g, 26.80mmol). The reaction solution was stirred for six hours at 0-5°C and then left to stand in the refrigerator overnight. The reaction solution was then filtered to remove the urea and the organic solvent was then removed under reduced pressure. The resulting white solid was dissolved in methylene chloride and filtered to give a colorless filtrate which was concentrated and dried under vacuum to afford a white solid (8.25g, 98% yield). This product was used in the following steps without further purification. <sup>1</sup>H NMR (399.75 MHz, CDCl<sub>3</sub>) δ 1.03-1.05 (d, 3H, J = 6.8 Hz, (CH<sub>3</sub>)(CH<sub>3</sub>)HC-), 1.00-1.01 (d, 3H, J = 6.8 Hz, (CH<sub>3</sub>)(CH<sub>3</sub>)HC-), 1.46 (s, 9H, (CH<sub>3</sub>)<sub>3</sub>C-), 2.26-2.35 (m, 1H, (CH<sub>3</sub>)<sub>2</sub>HC-), 2.84(s, 4H, -CH<sub>2</sub>CH<sub>2</sub>-), 4.30-4.35 and 4.58-4.62 (2m, ~1:4, 1H, -CHRNH-), 4.72-4.74 and 5.00-5.03 (2m, ~1:4, 1H, -CHRNH-); <sup>13</sup>C{<sup>1</sup>H}-NMR (100.52 MHz, CDCl<sub>3</sub>) δ 17.55, 18.92, 25.80, 28.48, 31.92, 57.27, 80.65, 155.32, 168.19, 168.82.

**{1-[2-(2-tert-butoxycarbonylamino-3-methyl-butyrylamino)-ethylcarbamoyl]-2-methyl-propyl}-carbamic acid tert-butyl ester (68)**

To a solution of **67** (2.29g, 7.27mmol) in dry THF (40 mL) was added ethylenediamine (0.219g, 244 $\mu$ L, 3.64mmol) in dry THF (10 mL) drop-wise at 0°C. The reaction solution was allowed to stir at 0°C for one hour and for 16 hours at room temperature under nitrogen. The solvent was then evaporated. The crude white solid was recrystallized from acetone to give white needle-like crystals (1.10g, 66% yield). <sup>1</sup>H NMR (399.75 MHz, CDCl<sub>3</sub>)  $\delta$  0.92-0.94 (d, 2x3H, J = 6.8 Hz, (CH<sub>3</sub>)(CH<sub>3</sub>)HC-), 0.95-0.97 (d, 2x3H, J = 6.8 Hz, (CH<sub>3</sub>)(CH<sub>3</sub>)HC-), 1.44 (s, 2x9H, (CH<sub>3</sub>)<sub>3</sub>C-), 2.04-2.09 (m, 2x1H, (CH<sub>3</sub>)<sub>2</sub>HC-), 3.20-3.53 (AA'BB', 4H, -CH<sub>2</sub>CH<sub>2</sub>-), 3.81-3.86 (~t, 2x1H, -CH<sub>2</sub>CH<sub>2</sub>-), 5.14-5.16 (~d, 2x1H, -CH<sub>2</sub>CH<sub>2</sub>-), 6.94-7.01 (b, 2x1H, -CH<sub>2</sub>NHC(=O)-); <sup>13</sup>C{<sup>1</sup>H}-NMR (100.52 MHz, CDCl<sub>3</sub>)  $\delta$  18.37, 19.57, 28.55, 30.66, 39.37, 60.90, 80.24, 156.44, 173.08.

**(S, S)-2-Amino-N-[2-(amino-3-methyl-butyrylamino)-ethyl]-3-methyl-butyramide ditrifluoroacetate salt (69)**

To 9 mL (13.77g, 120.76mmol) of trifluoroacetic acid was added **68** (715.2mg, 1.56mmol). The mixture was allowed to stir at room temperature for 4 hrs. The excess trifluoroacetic acid was evaporated under reduced pressure to give an off-white solid. 3x20 mL diethyl ether was used to wash the crude solids then followed by drying under vacuum overnight to give a white solid (749.6mg, 99%). <sup>1</sup>H NMR (399.75 MHz D<sub>2</sub>O)  $\delta$  0.86 (d, 2x3H, J = 6.9 Hz, (CH<sub>3</sub>)(CH<sub>3</sub>)HC-), 0.87-0.88 (d, 2x3H, J = 6.9 Hz, (CH<sub>3</sub>)(CH<sub>3</sub>)HC-), 2.00-2.09 (apparent octet, 2x1H, J = 6.0, 6.9 Hz, (CH<sub>3</sub>)<sub>2</sub>HC-), 3.19-



3.34 (AA'BB', 4H, -CH<sub>2</sub>CH<sub>2</sub>-), 3.60-3.61 (d, 2x1H, J = 6.0 Hz, -CHRNH<sub>2</sub>); <sup>13</sup>C{<sup>1</sup>H}-NMR (100.52 MHz, D<sub>2</sub>O) δ 16.97, 17.79, 29.92, 38.69, 58.86, 112.07, 114.96, 117.86, 120.76, 162.85, 163.21, 169.69.

**(S, S)-2-Amino-N-[2-(amino-3-methyl-butrylamino)-ethyl]-3-methyl-butane-1,2-diamine (70)**

To 25 mL of a 1M borane-THF complex was added slowly **69** (1.17g, 2.40mmol). The mixture was refluxed for 18 hours. The temperature was maintained at -10°C during the addition of the borane-THF complex. After cooling to room temperature, methanol (15 mL) was added slowly. Then the reaction mixture was refluxed for 3 days, followed by removal of the solvent by rotary evaporation. To the residue was added methanol (20 mL) and concentrated HCl (0.7 mL, 11.3M). After the mixture was stirred at the room temperature for 4 hours, the solvent and excess HCl were evaporated to give a light orange solid 1.11g, which was added into a fresh NaOEt solution (430 mg sodium in 45 mL ethanol) and stirred at room temperature for 1 hour. During this period a white solid was formed. The white solid was filtered off, followed by removing the solvent in the filtrate to afford a yellow residue 2.23g. The product was isolated from the residue by Kugelrohr distillation at 120°C and 200 millitorr to give a light yellow oil (405.7mg, 73% yield). <sup>1</sup>H NMR (399.75 MHz, CDCl<sub>3</sub>) δ 0.89-0.90 (d, 6H, J = 6.9 Hz, (CH<sub>3</sub>)(CH<sub>3</sub>)HC-), 0.90-0.92 (d, 6H, J = 7.0 Hz, (CH<sub>3</sub>)(CH<sub>3</sub>)HC-), 1.43-1.64 (broad, 6H, NH, NH<sub>2</sub>), 1.55-1.63 (m, 2H, J = 5.5, 6.8 Hz, (CH<sub>3</sub>)<sub>2</sub>HC-), 2.37 (dd, 2H, J = 9.4, 11.5 Hz, -NHCH<sub>2</sub>HC-), 2.58 (ddd, 2H, J = 3.5, 5.5, 9.4 Hz, -CH<sub>2</sub>CH(NH<sub>2</sub>)-), 2.70 (dd, 2H, J = 3.5, 11.5 Hz, -NHCH<sub>2</sub>HC-), 2.73 (AA'BB', 4H, -CH<sub>2</sub>CH<sub>2</sub>-); <sup>13</sup>C{<sup>1</sup>H}-NMR (100.52, CDCl<sub>3</sub>) δ 18.00,

19.59, 32.59, 49.88, 54.32, 56.74; IR (KBr): 3297, 2937, 1677, 1593, 1467, 1386, 1201, 1135, 1055, 801, 721  $\text{cm}^{-1}$ .

### 2,9-Diisopropyl-2,3,5,6,8,9-hexahydro-diimidazo[1,2-a;2',1'-c]pyrazine (71)

A 100 mL three-necked round-bottomed flask equipped with a reflux condenser with  $\text{N}_2$  inlet tube, a fritted gas dispersion tube (initially closed) and a pressure-equalizing addition funnel was charged with dithiooxamide (71.1mg, 0.591mmol) suspended in absolute EtOH (20mL). A solution of **70** (130.3mg, 0.566mmol) in absolute EtOH (20 mL) was added drop by drop into the dithiooxamide solution. The nitrogen manifold exit line was routed through two scrubbing towers charged with 30% aq. NaOH solution in order to trap the gases evolved. An orange-red solution formed after stirring and heating. The reaction mixture was heated at  $80^\circ\text{C}$  for 4 hours during which a constant flow of  $\text{N}_2$  purged the system. The reaction mixture was then cooled to room temperature and residual gaseous byproducts were purged from the solution by entrainment with nitrogen overnight using fritted gas dispersion tube. Then the solvent was removed under reduced pressure leaving a dark red-brown oil, which was washed with  $\text{Et}_2\text{O}$  (40 mL) to afford a red solution. Then the solution was concentrated and dried under reduced pressure to give an orange solid (114mg, yield 81%).  $[\alpha]_{\text{D}}^{27} = +67.5^\circ$  (conc. 0.51 g/100ml,  $\text{CHCl}_3$ );  $^1\text{H}$  NMR (399.75 MHz,  $\text{CDCl}_3$ )  $\delta$  0.82-0.84 (d, 6H,  $J = 6.8$  Hz,  $(\text{CH}_3)(\text{CH}_3)\text{HC-}$ ), 1.02-1.03 (d, 6H,  $J = 6.7$  Hz,  $(\text{CH}_3)(\text{CH}_3)\text{HC-}$ ), 1.76 (octet, 2H,  $J = 6.8$  Hz,  $(\text{CH}_3)_2\text{HC-}$ ), 2.77 (dd, 2H,  $J = 12.5, 8.8$  Hz,  $-\text{NHCHHCH-}$ ), 3.10-3.21 (AA'BB', 4H,  $-\text{CH}_2\text{CH}_2-$ ), 3.43 (dd, 2H,  $J = \sim 9.1$  Hz,  $-\text{NHCHHCH-}$ ), 3.70 (ddd, 2H,  $J = 12.5, 9.4, 7.7$  Hz,  $-\text{CH}_2\text{CH}(\text{NH}_2)-$ );

$^{13}\text{C}\{^1\text{H}\}$ -NMR (100.52,  $\text{CDCl}_3$ )  $\delta$  19.02, 20.33, 33.22, 45.61, 55.47, 72.55, 154.53.

Further purification needs to be done.

#### **( $\pm$ )-3-Amino-3-phenylpropanoic Acid (80)**

Benzaldehyde (21.2g, 200mmol) and  $\text{NH}_4\text{OAc}$  (30.8g, 400mmol) were dissolved in EtOH (200 mL). The solution was stirred at  $45^\circ\text{C}$ . A solution of malonic acid (20.8g, 200mmol) in EtOH (100mL) was added. The mixture was stirred and at reflux for 6hrs. After cooling to  $5^\circ\text{C}$ , the resulting precipitate was collected by filtration and washed with ice-cold EtOH. The white solid was dried in vacuum to give 18.34g (yield 56%), which was used in the following steps without further purification.  $^1\text{H}$  NMR (399.75 MHz,  $\text{D}_2\text{O}$ )  $\delta$  2.65-2.79 (2dd, AMX, 2H,  $-\text{CH}_2$ ,  $J = 6.5, 16.2\text{Hz}$ ;  $J = 8.0, 16.2\text{Hz}$ ), 4.48-4.52 (dd, 1H,  $-\text{N}(\text{Ph})\text{CH}-$ ,  $J = 6.7, 8.0\text{Hz}$ ), 7.30-7.34 (m, 5H,  $\text{C}_6\text{H}_5-$ );  $^{13}\text{C}\{^1\text{H}\}$ -NMR (100.52,  $\text{D}_2\text{O}$ )  $\delta$  40.59, 52.88, 127.05, 129.40, 136.11, 177.37.

#### **( $\pm$ )-Methyl 3-Amino-3-phenylpropanoate (81)**

( $\pm$ )-3-Amino-3-phenylpropanoic Acid **80** (18.34g, 111.0mmol) was dissolved in MeOH (220 mL) and cooled to  $5^\circ\text{C}$ . To this mixture was added dropwise  $\text{SOCl}_2$  (10mL) and the mixture was stirred overnight at room temperature. The solution was refluxed for 2 hrs and subsequently concentrated to dryness. To the white residue was added saturated  $\text{NaHCO}_3$  to neutral and the mixture was extracted with EtOAc (4x120mL). The combined organic layers were dried over  $\text{Na}_2\text{SO}_4$  and concentrated through rotary evaporation and dried under vacuum to obtain yellow oil (12.70g, yield 64%), which was used in the following steps without further purification.  $^1\text{H}$  NMR (399.75 MHz,  $\text{CD}_3\text{CN}$ )

$\delta$  1.74 (s, 2H, NH<sub>2</sub>-), 2.62-2.64 (ABX, 2H, -CH<sub>2</sub>(C=O)O-), 3.63 (s, 3H, CH<sub>3</sub>-), 4.31-4.35 (dd, 1H, -N(Ph)CH-), 7.25-7.41 (m, 5H, C<sub>6</sub>H<sub>5</sub>-); <sup>13</sup>C{<sup>1</sup>H}-NMR (100.52, CD<sub>3</sub>CN)  $\delta$  44.27, 51.28, 53.05, 126.52, 127.25, 128.63, 146.05, 172.35.

### **(3*S*)-Methyl 3-Amino-3-phenylpropanoate (82a)**

A solution of ( $\pm$ )-methyl ester **81** (14.50g, 80.91mmol) in MeOH (20 mL) was added to a boiling solution of *L*-tartaric acid (12.15g, 80.95mmol) in MeOH (40 mL). The product was allowed to crystallize overnight at -20°C. The precipitate was collected and recrystallized two times in MeOH (60mL) to give an overall yield of 12.21g (yield 45.8%) of the (3*S*)-Methyl 3-Amino-3-phenylpropanoate *L*-Tartrate Salt. <sup>1</sup>H NMR (399.75 MHz, D<sub>2</sub>O)  $\delta$  2.98-3.13 (m, 2H), 3.55 (s, 3H), 4.37 (s, 2H), 4.68 (t, 1H), 7.33-7.39 (m, 5H); <sup>13</sup>C{<sup>1</sup>H}-NMR (100.52, D<sub>2</sub>O)  $\delta$  37.94, 51.62, 52.82, 72.98, 127.16, 129.58, 129.87, 135.24, 172.25, 176.52. The above crystalline *L*-tartrate salt (12.21g, 37.08mmol) was dissolved in 1M NaOH (70 mL) and CH<sub>2</sub>Cl<sub>2</sub> (40 mL). The aqueous phase was extracted with CH<sub>2</sub>Cl<sub>2</sub> (3x100 mL) and the extract dried and evaporated to get a colorless oil (3.44g, 24% total yield), which solidified in the refrigerator.  $[\alpha]_D^{27} = -23.9^\circ$  (conc. 1.9 g/100ml, CHCl<sub>3</sub>); <sup>1</sup>H NMR (399.75 MHz, CD<sub>3</sub>CN)  $\delta$  1.70 (broad, 2H, NH<sub>2</sub>-), 2.61-2.63 (ABX, 2H, -CH<sub>2</sub>(C=O)O-), 3.62 (s, 3H, CH<sub>3</sub>-), 4.31-4.34 (dd, ABX, 1H, -N(Ph)CH-), 7.24-7.41 (m, 5H, C<sub>6</sub>H<sub>5</sub>-); <sup>13</sup>C{<sup>1</sup>H}-NMR (100.52, CD<sub>3</sub>CN)  $\delta$  44.29, 51.28, 53.06, 126.52, 127.25, 128.63, 146.08, 172.35.

**(3S)-Methyl-3-*tert*-Butoxycarbonylamino-3-phenylpropanoate (83)**

To an aqueous solution (60 mL) of NaHCO<sub>3</sub> (3.19g, 38.00mmol) was added **82** (3.44g, 18.97mmol) at 0°C, followed by the addition of di-*tert*-butyl dicarbonate (8.29g, 38.00mmol). After the mixture was stirred at 0°C for 0.5 hr, the ice bath was removed. The reaction solution was stirred at room temperature for another 16 hours. Then the reaction mixture was diluted and extracted with CH<sub>2</sub>Cl<sub>2</sub> (3x50 mL). The organic layer was washed with brine and dried over anhydrous Na<sub>2</sub>SO<sub>4</sub>. Then the CH<sub>2</sub>Cl<sub>2</sub> solution was concentrated using rotary evaporation to afford a white solid, which was used in the following steps without further purification. <sup>1</sup>H-NMR (399.75 MHz, CDCl<sub>3</sub>) δ 1.35 (s, 9H, -C(CH<sub>3</sub>)<sub>3</sub>), 2.76-2.77 (m, 2H, CH<sub>2</sub>), 3.55 (s, 3H, -CH<sub>3</sub>), 5.03 (broad, 1H, -CH), 5.37 (broad, 1H, -NH), 7.17-7.27 (m, 5H, -C<sub>6</sub>H<sub>5</sub>); <sup>13</sup>C{<sup>1</sup>H}-NMR (100.52, CDCl<sub>3</sub>) δ 27.31, 39.77, 50.18, 50.74, 78.69, 125.08, 126.48, 127.62, 140.14, 154.00, 170.33.

**(3S)-3-*tert*-Butoxycarbonylamino-3-phenylpropanoic acid (84)**

The above compound **83** and lithium hydroxide (1.14g, 47.50mmol) were dissolved in the solvent mixture (MeOH : THF : H<sub>2</sub>O = 1 : 1.5 : 1, 105 mL) at 0°C with stirring. The reaction mixture was continued to stirred for 2 hrs. Then the solvents were removed by rotary evaporation to obtain a white residue, which was dissolved in a mixture of CH<sub>2</sub>Cl<sub>2</sub> (70 mL) and water (50 mL). The mixture was extracted with CH<sub>2</sub>Cl<sub>2</sub> (2x50 mL). After extraction, the aqueous layer was acidified with concentrated HCl to pH = 2 and extracted with EtOAc (3x70 mL). The organic layers from these two extractions were combined and dried over anhydrous Na<sub>2</sub>SO<sub>4</sub>. Then CH<sub>2</sub>Cl<sub>2</sub> and EtOAc were removed to yield a white solid (4.23g, 84.0% yield). <sup>1</sup>H NMR (399.75 MHz,

CD<sub>3</sub>CN)  $\delta$  1.40 (s, 9H, -C(CH<sub>3</sub>)<sub>3</sub>), 2.74-2.77 (m, 2H, -CH<sub>2</sub>), 4.98-5.00 (broad, 1H, -CH), 5.98-5.99 (broad, 1H, -NH), 7.35 (m, 5H, -C<sub>6</sub>H<sub>5</sub>); <sup>13</sup>C{<sup>1</sup>H}-NMR (100.52, CD<sub>3</sub>CN)  $\delta$  27.83, 40.58, 51.62, 78.98, 126.56, 127.56, 128.75, 142.81, 155.42, 171.92.

#### **Preliminary aziridination reaction of styrene catalyzed by Cu(II)-3,2,3-BisAm**

In a 10 mL dry capped tube, a mixture of Cu(OTf)<sub>2</sub> (9.0mg, 0.025mmol) and 3,2,3-BisAm (4.8mg, 0.025mmol) was stirred in 3 mL of CH<sub>3</sub>CN for 10 minutes, and then 4Å activated molecular sieves (0.5g) were added. The resulting green mixture was cooled to 0°C and PhI=NTs (186.5mg, 0.5mmol) was then added. The suspension solution turned green. Styrene (260.5mg, 2.5mmol, 5 equiv) was added by syringe and the solution stirred at 0°C for 0.5 hour and then warmed to room temperature, after another stirring for 12 hours, the suspension became dark khaki. The reaction mixture was diluted with 10 mL of CH<sub>2</sub>Cl<sub>2</sub> and filtered through Celite. The filter cake was washed thoroughly with (2x5 mL) CH<sub>2</sub>Cl<sub>2</sub> and the combined filtrates were concentrated under reduce pressure. The isolated materials were purified by chromatography on silica gel using hexane/EtOAc = 9:1 as the eluent solvent to yield aziridine **85** (119.4mg, 87% yield). <sup>1</sup>H NMR (399.75 MHz, CD<sub>3</sub>Cl)  $\delta$  2.38-2.39 (d, 1H, CH<sub>2</sub>, J = 4.3Hz), 2.43 (s, 3H, CH<sub>3</sub>), 2.97-2.99 (d, 1H, CH, J = 7.2Hz), 3.76-3.79 (dd, 1H, -CHPh, J = 4.5, 7.2Hz); 7.20-7.34 (m, 7H, Ar-H), 7.86-7.88 (~d, 2H, Ar-H); <sup>13</sup>C{<sup>1</sup>H}-NMR (100.52, CD<sub>3</sub>Cl)  $\delta$  21.87, 36.15, 41.27, 126.78, 128.17, 128.52, 128.78, 129.97, 135.29, 144.85.

## LIST OF REFERENCES

1. *Comprehensive Coordination Chemistry II*; McCleverty, J. A.; Meyer, T. J., Eds.; Elsevier Pergamon: Boston, **2004**; Vol. 1, p. 1.
2. Reedjik, J. *Comprehensive Coordination Chemistry*; Wilkinson, G.; Gillard, R. D.; McCleverty, J. A. Eds.; Pergamon: Oxford, **1987**; Vol. 2, p. 73.
3. Gomez, M.; Muller, G.; Rocamora, M. *Coord. Chem. Rev.* **1999**, *193-195*, 769-835.
4. Zou, X. H.; Li, H.; Yang, G.; Deng, H.; Liu, R. H.; Zeng, Q. L.; Xiong, Y.; Ji, L. N. *Inorg. Chem.* **2001**, *40*, 7091-7095.
5. Kaes, C.; Katz, A.; Hosseini, M. W. *Chem. Rev.* **2000**, *100*, 3553-3590.
6. Constable, E.C. *Adv. Inorg. Chem.* **1989**, *34*, 1-63.
7. Widlicka, D. W.; Wong, E. H.; Weisman, G. R.; Lam, K. C.; Sommer, R. D.; Incarvito, C. D.; Rheingold, A. L. *Inorg. Chem. Commun.* **2000**, *3*, 648-652.
8. Widlicka, D. W.; E.H. Wong, Weisman, G. R.; Sommer, R. D.; Incarvito, C. D.; Rheingold, A. L. *Inorg. Chim. Acta.* **2002**, *341*, 45-53.
9. Jena, S.; Rath, N.; Dash, K. C. *Indian J. Chem.* **1977**, *55*, 1213; Thummel, R. P.; Gouille, V.; Chen, B. *J. Org. Chem.* **1989**, *54*, 3057-3061.
10. Weisman, G. R.; Reed, D. P. *J. Org. Chem.* **1996**, *61*, 5186-5187; **1997**, *62*, 4548.
11. Reed, D. P. Weisman, G. R. *Org. Synth.* **2002**, *78*, 73-81.
12. Widlicka, D. W. MS thesis, University of New Hampshire, **2002**.
13. Fichter, K. A. MS thesis, University of New Hampshire, **2004**.
14. Boland, N. A.; Casey, M.; Hynes, S. J.; Matthews, J. W.; Müller-Bunz, H.; Wilkes, P. *Org. Biomol. Chem.* **2004**, *2*, 1995-2002.
15. Raebiger, J. W.; Miedaner, A.; Curtis, C. J.; Miller, S. M.; Anderson, O. P.; DuBois, D. L., *J. Am. Chem. Soc.* **2004**, *126*, 5502-5514.
16. Reed, D. P. Ph.D dissertation, University of New Hampshire, **1998**.
17. Lees, A. J. *Coord. Chem. Rev.* **1998**, *177*, 3-35.
18. Van Staveren, D. R.; Metzler-Nolte, N. *Chem. Commun.* **2002**, 1406-1407.

19. Kanis, D. R.; Ratner, M. A.; Marks, T. J. *J. Am. Chem. Soc.* **1990**, *112*, 8203-8204.
20. Zou, R. Q.; Xu, Q. *Acta Crystallogr., Sect. E: Struct. Rep. Online*, **2005**, *61*, m1075-1076.
21. Bock, C.W.; Katz, A. K.; Glusker, J.P. *J. Am. Chem. Soc.* **1995**, *117*, 3754-3763.
22. Sigel, H.; Martin, R.B. *Chem. Soc. Rev.* **1994**, *23*, 83-91.
23. Crabtree, R. H. *The Organometallic Chemistry of the Transition Metals* 3<sup>rd</sup> ed., John Wiley & Sons, New York, **2001**.
24. Patra, G. K.; Goldberg, I.; Sarkar, A.; Chowdhury, S.; Datta, D. *Inorg. Chim. Acta.* **2003**, *344*, 7-14.
25. Tirosh, E.; Maman, R.; Goldberg, I. *Acta Crystallogr., Sect. E: Struct. Rep. Online* **2005**, *61*, m541.
26. Chen, H.; Xu, X. Y.; Gao, J.; Yang, X. J.; Lu, L. D.; Wang, X. *Chinese J. Struct. Chem.* **2005**, *24*, 1276-1281.
27. Pervukhina, N. V.; Vasil'ev, V. I.; Naumov, D. Y.; Borisov, S. V. Magarill, S. A. *Can. Mineral.* **2004**, *42*, 87-94.
28. McEwen, R. S.; Sim, G. A.; Johnson, C. R. *Chem. Commun.* **1967**, *17*, 885-886.
29. *Eur. J. Inorg. Chem.* **2006**, 1260-1267.
30. Yang, S. P.; Chen, X. M.; Ji, L. N. *J. Chem. Soc., Dalton Trans.* **2000**, 2337-2343.
31. Cotton, F. A.; Walton, R. A., *Multiple Bond Between Metal Atoms*, 2<sup>nd</sup> ed.; Oxford University Press: Oxford, U. K., **1992**.
32. Cotton, F. A.; Feng, X.; Matusz, M.; Poli, R. *J. Am. Chem. Soc.* **1988**, *110*, 7077-7083.
33. Cotton, F. A.; Feng, X.; Timmons, D. J. *J. Am. Chem. Soc.* **1998**, *120*, 4066-4069.
34. Bondi, A. *J. Phys. Chem.* **1964**, *68*, 441-451.
35. Jansen, M. *Angew. Chem., Int. Ed.* **1987**, *26*, 1098-1111.
36. Cui, Y.; He, C., *J. Am. Chem. Soc.* **2003**, *125*, 16202-16203.
37. Li, Z. G.; Capretto, D. A.; Rahaman, R.; He, C. *Angew. Chem. Int. Ed.* **2007**, *46*, 5184-5186.



38. Menon, S.; Rajasekharan, M. V. *Inorg. Chem.* **1997**, *36*, 4983-4987.
39. Addison, A. W.; Rao T. N.; Reedijk, J.; Rijn, J. V.; Verschoor, G. C. *J. Chem. Soc., Dalton Trans.* **1984**, 1349-1356.
40. Kubas, G. J. *Inorg. Synth.* **1990**, *28*, 68-70.
41. Korybut-Daszkiewicz, B.; Taraszewska, J.; Zieba, K.; Makal, A.; Wozniak, K. *Eur. J. Inorg. Chem.* **2004**, 3335-3344.
42. Woods, M.; Monald, E. W. C.; Sherry, A. D. *Chem. Soc. Rev.* **2006**, *35*, 500-511.; Gunnlaugsson, T.; Leonard, J. P. *Chem. Commun.* **2005**, *25*, 3114-3131.; Faulkner, S.; Pope, S. J. A.; Burton-Pye, B. P. *Appl. Spectrosc. Rev.* **2005**, *40*, 1-31.
43. Bertini, I.; Luchinat, C.; Parigi, G.; Pierattelli, R. *ChemBioChem* **2005**, 1536-1549.
44. Bulent, A.; Engin, C.; Bekir, C.; Dincer, U.; Nawaz, T. M. *J. Chem. Res, Synopses*, **1996**, *12*, 516-517.
45. Shi, Z.; Thummel, R. P. *Tetrahedron Lett.* **1994**, *35*, 33-36.
46. Morrison J. D. *Asymmetric Synthesis*, Vol. 5, Academic Press Inc. **1985**.; Seyden-Penne, J. *Chiral Auxiliaries and Ligands in Asymmetric Synthesis*, John Wiley & Sons, Inc: New York, **1995**; Williams, J. M. J. *Catalysis in Asymmetric Synthesis*, Blackwell Science, Inc. **1999**.
47. Halpern, J.; Trost, B. M., *PNAS*, **2004**, *101*, 5347.
48. Zhang, X. M. *C&EN*, **2001**, *March 26*, 142.
49. Yoon, P. Y.; Jacobsen, E. N. *Science*, **2003**, *299*, 1691-1693.
50. Pfaltz, A.; Drury III, W. J. *PNAS*, **2004**, *101*, 5723-5726.
51. Johnson, J. S.; Evans, D. A. *Acc. Chem. Res.* **2000**, *33*, 325-335.
52. McManus, H. A.; Guiry, P. J. *Chem. Rev.* **2004**, *104*, 4151-4202.
53. Desimoni, G.; Faita, G.; Jørgensen, K. A. *Chem. Rev.* **2006**, *106*, 3561.
54. Aoki, M.; Kaneko, M.; Izumi, S.; Ukai, K.; Iwasawa, N. *Chem. Commun.* **2004**, 2568-2569.
55. Glorius, F.; Altenhoff, G.; Goddard R.; Lehmann, C. *Chem. Commun.* **2002**, 2704-2705.

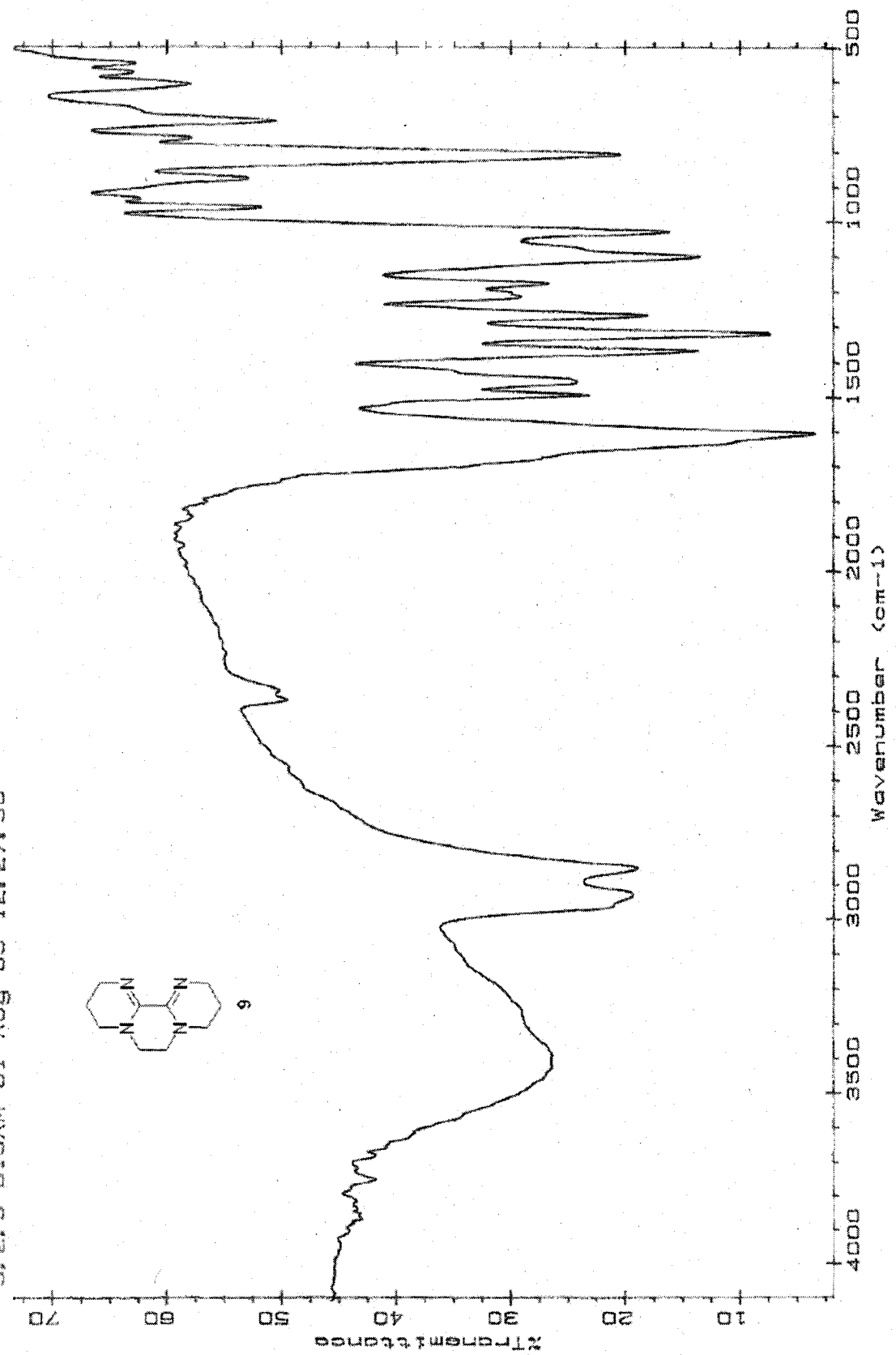
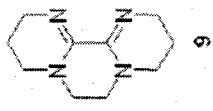
56. Kwan, K. K. BS thesis, University of New Hampshire, **2002**.
57. Young, M. J. MS thesis, University of New Hampshire, **1999**.
58. Ali, M. S.; Quadri, S. M. *Bioconjugate Chem.* **1996**, *7*, 576-583.
59. Sun, J. H.; Matos, J. R.; Park, C. H.; Clifton, R. G. Jr. *U.S. 5329048*, **1995**, 20.
60. Muller, D.; Umbrecht, G.; Weber, B.; Pfaltz, A. *Helv. Chim. Acta.* **1991**, *74*, 232-240.
61. *Catalysis in Asymmetric Synthesis*; Williams, J. M. J. Ed; Blackwell Science, **1999**, p154.
62. Saitoh, A.; Achiwa, K.; Tanaka, K.; Morimoto, T. *J. Org. Chem.* **2000**, *65*, 4227-4240.
63. Abdel-Magid, A. F.; Cohen, J. H.; Maryanoff, C. A. *Current Medicinal Chemistry*, **1999**, *6*, 955-970.
64. Tan, C. Y. K.; Weaver, D. F. *Tetrahedron* **2002**, *58*, 7449-7461.
65. Liu, S. Y.; Müller, J. F. K.; Neuburger, M.; Schaffner, S.; Zehnder, M. *Helv. Chim. Acta.* **2000**, *83*, 1256-1267.
66. Tse, M. K.; Bhor, S.; Klawonn, M.; Anilkumar, G.; Jiao, H.; Doebler, C.; Spannenberg, A.; Maegerlein, W.; Hugl, H.; Beller, M. *Chem. Eur. J.* **2006**, *12*, 1855-1874.;
67. Hsiao, Y.; Rivera, N. R.; Rosner, T.; Krska, S. W.; Njolito, E.; Wang, F.; Sun, Y. K.; Armstrong, J. D. III; Grabowski, E. J. J.; Tillyer, R. D.; Spindler, F.; Malan, C. *J. Am. Chem. Soc.* **2004**, *126*, 9918-9919.
68. Price, D. A.; Gayton, S.; Selby, M. D.; Ahman, J.; Haycock-Lewandowski, S.; Stammen, B. L.; Warren, A. *Tetrahedron Lett.* **2005**, 5005-5007.
69. Trost, B. M.; Fandrick, D. R. *Org. Lett.* **2005**, *7*, 823-826.
70. Galonic, D. P.; Ide, N. D.; van der Donk, W. A.; Gin, D. Y. *J. Am. Chem. Soc.* **2005**, *127*, 7359-7369.
71. Lebel, H.; Leogane, O.; Huard, K.; Lectard, S. *Pure Appl. Chem.* **2006**, *78*, 363-375.
72. Halfen, J. A. *Curr. Org. Chem.* **2005**, *9*, 657-669.
73. Evans, D. A.; Faul, M. M.; Bilodeau, M. T. *J. Org. Chem.* **1991**, *56*, 6744-6746.
74. Evans, D. A.; Bilodeau, M. T.; Faul, M. M. *J. Am. Chem. Soc.* **1994**, *116*, 2742-2753.

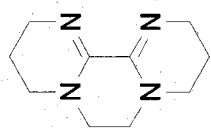
75. Yamada, Y.; Yamamoto, T.; Okawara, M. *Chem. Lett.* **1975**, 361-362.
76. Chen, J.; Corbin, S. P.; Holman, N. J. *Org. Process Res. Dev.* **2005**, *9*, 185-187.
77. Nakamoto, K. *Advances in the Chemistry of Coordination Compounds*, MacMillan: New York, **1961**.
78. Saburi, M.; Yoshikawa, S. *Bull. Chem. Soc. Jpn.* **1974**, *47*, 1184-1189.

## APPENDICES

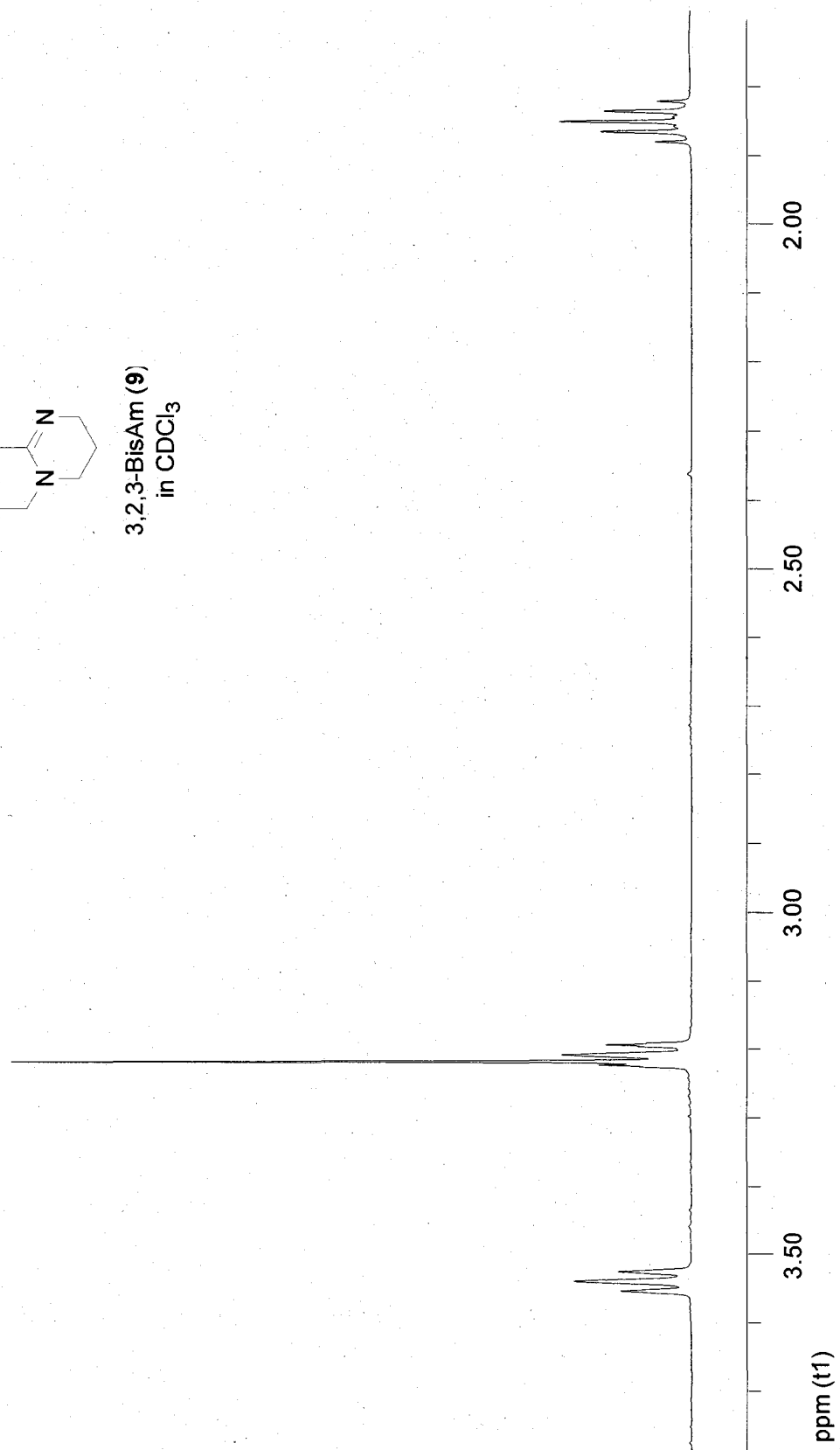
**APPENDIX A**  
**SELECTED SPECTRA**

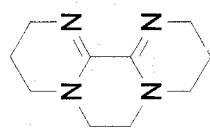
3, 2, 3-BISAM 01 AUG 05 12:27:36



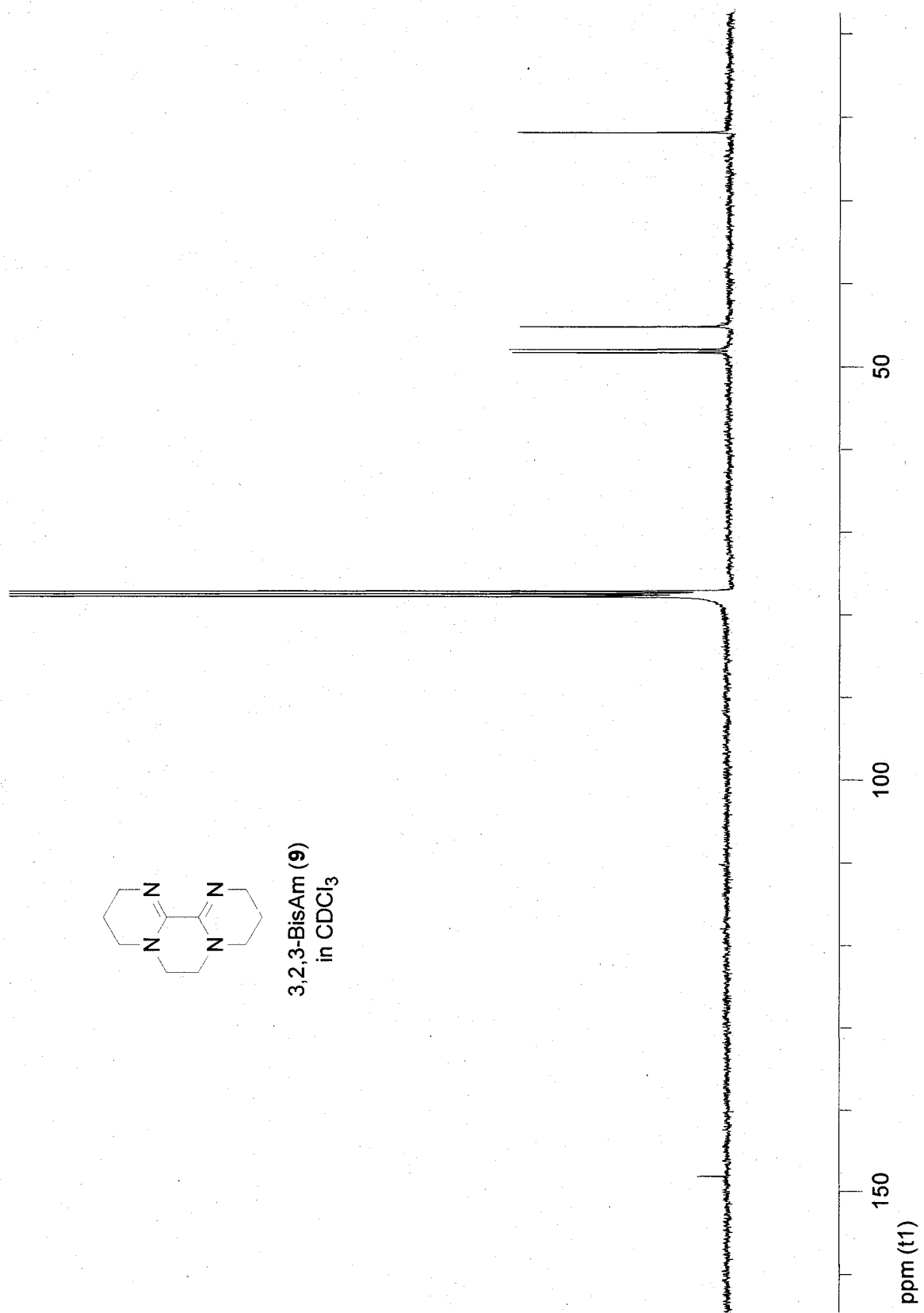


3,2,3-BisAm (9)  
in CDCl<sub>3</sub>

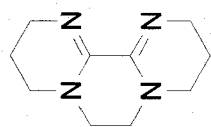




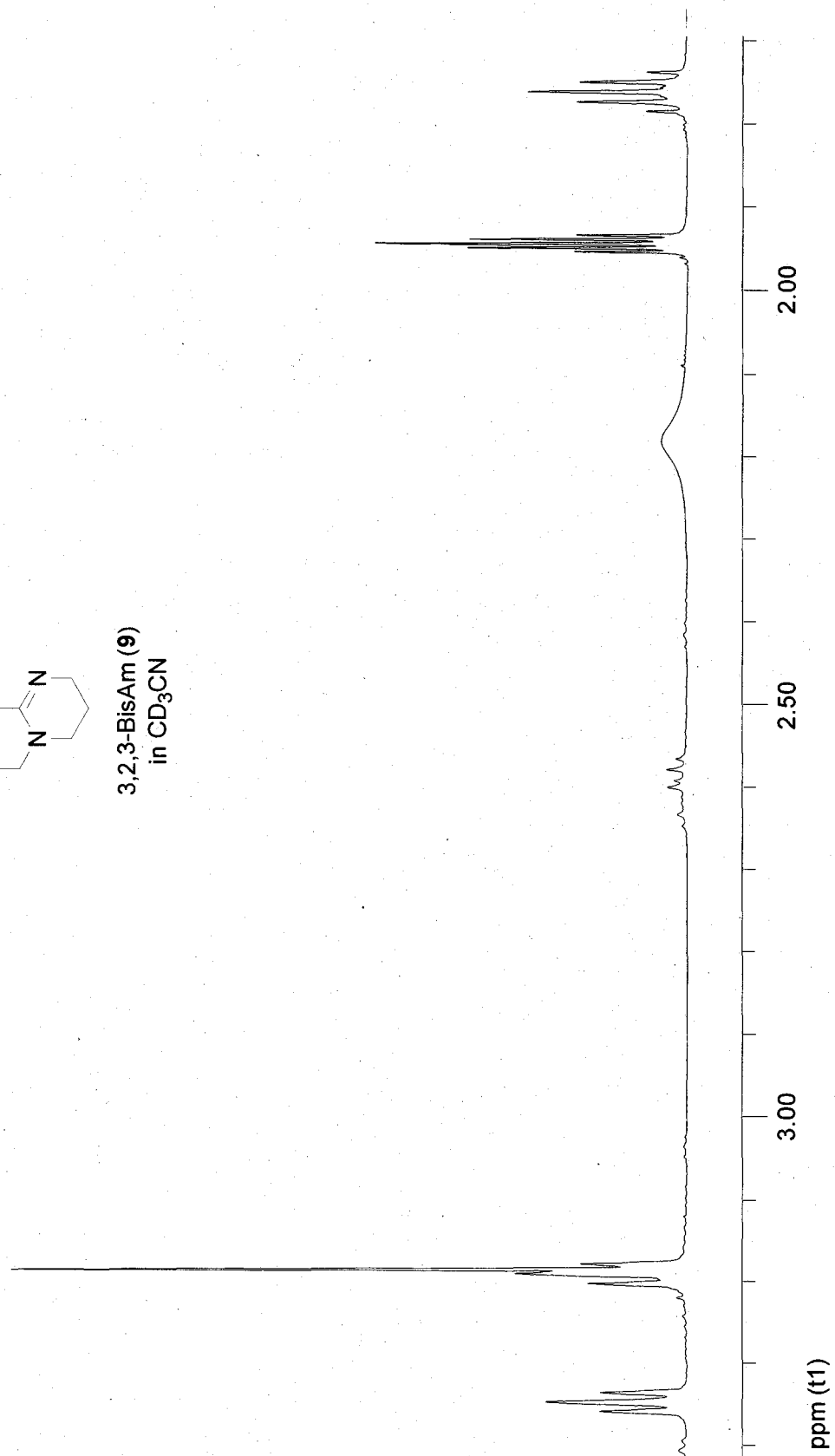
3,2,3-BisAm (9)  
in CDCl<sub>3</sub>

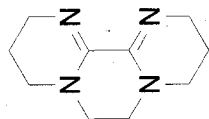




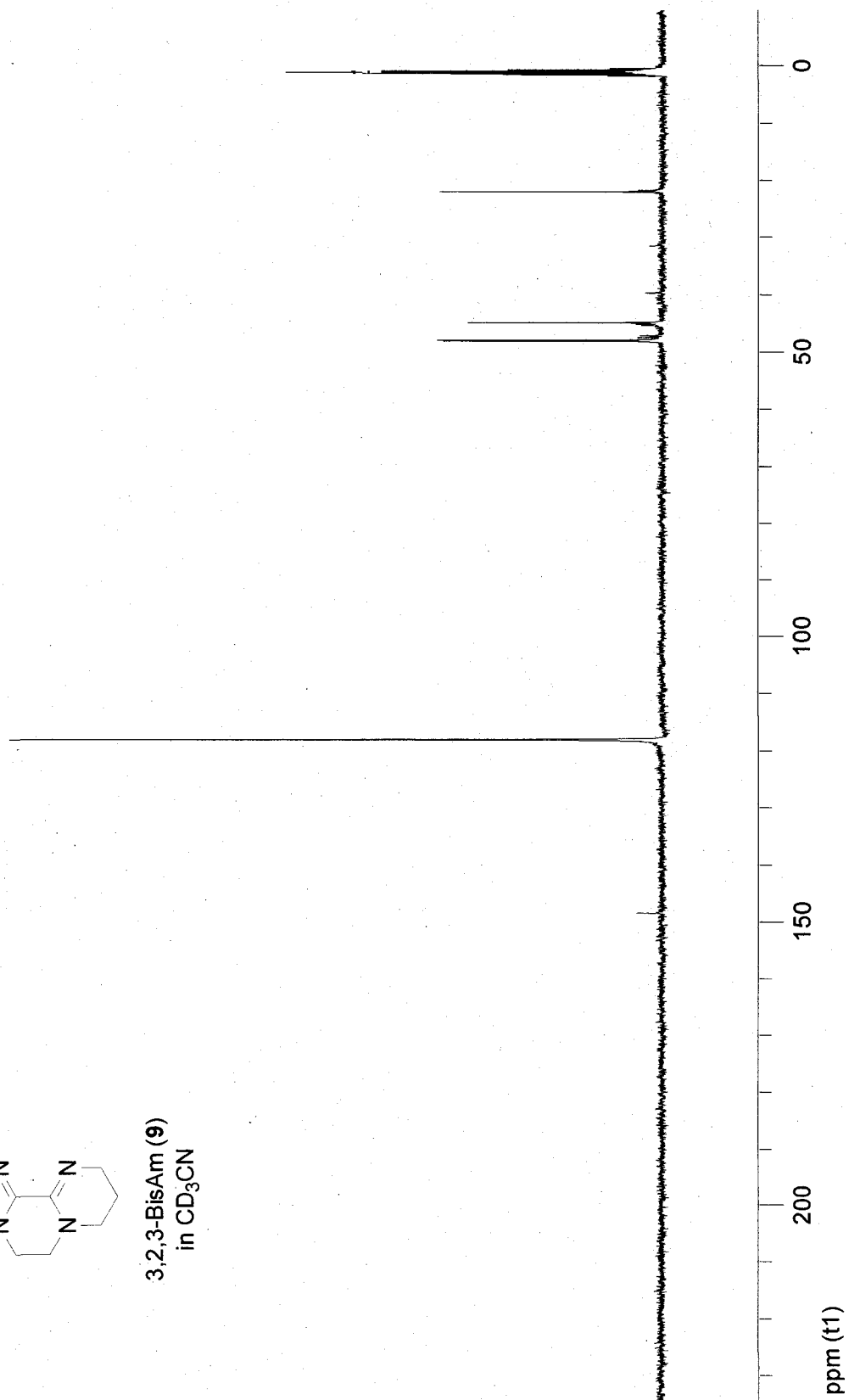


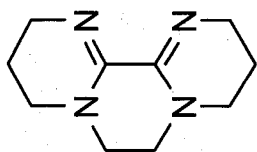
3,2,3-BisAm (9)  
in CD<sub>3</sub>CN



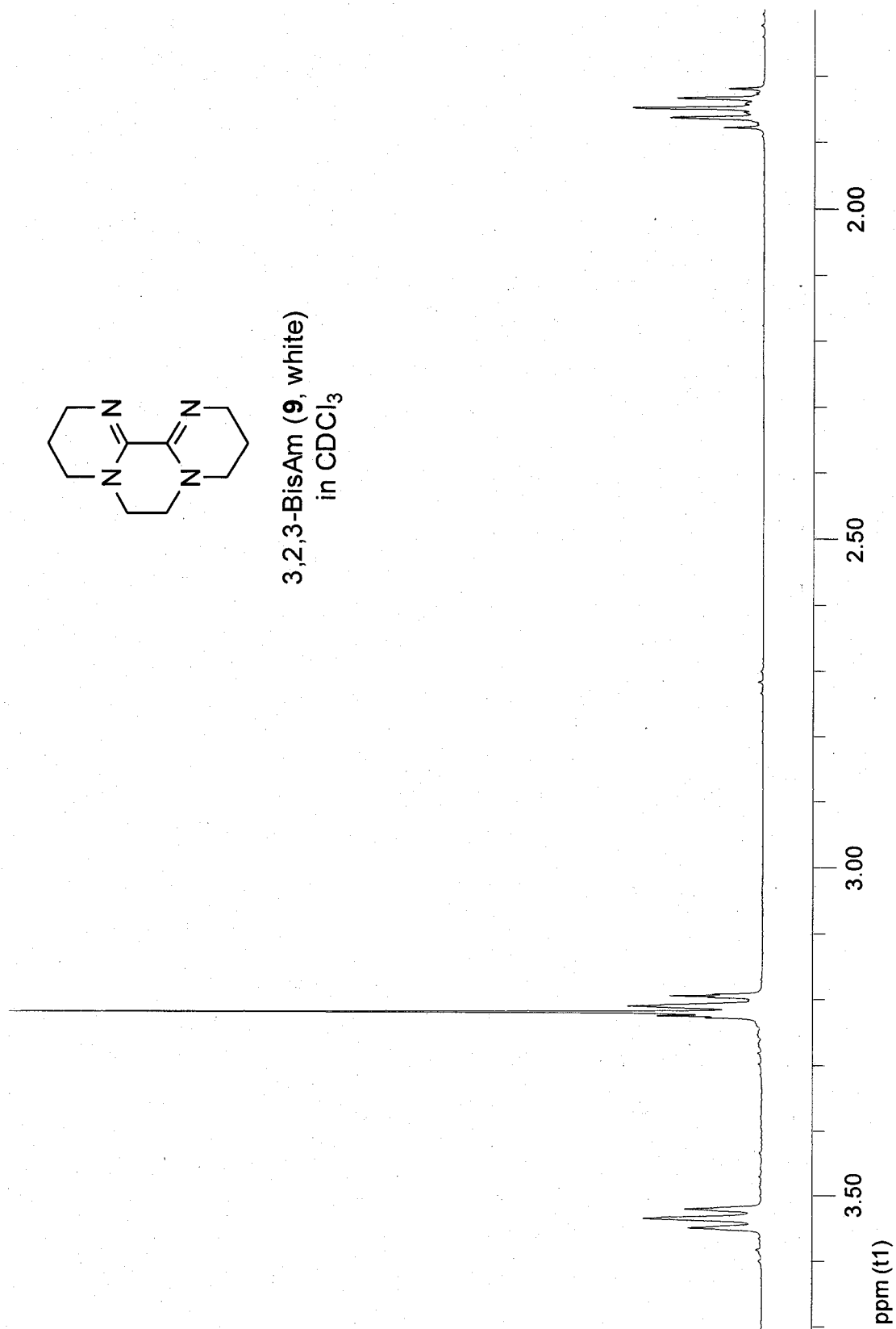


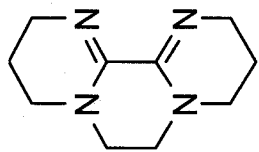
3,2,3-BisAm (9)  
in CD<sub>3</sub>CN



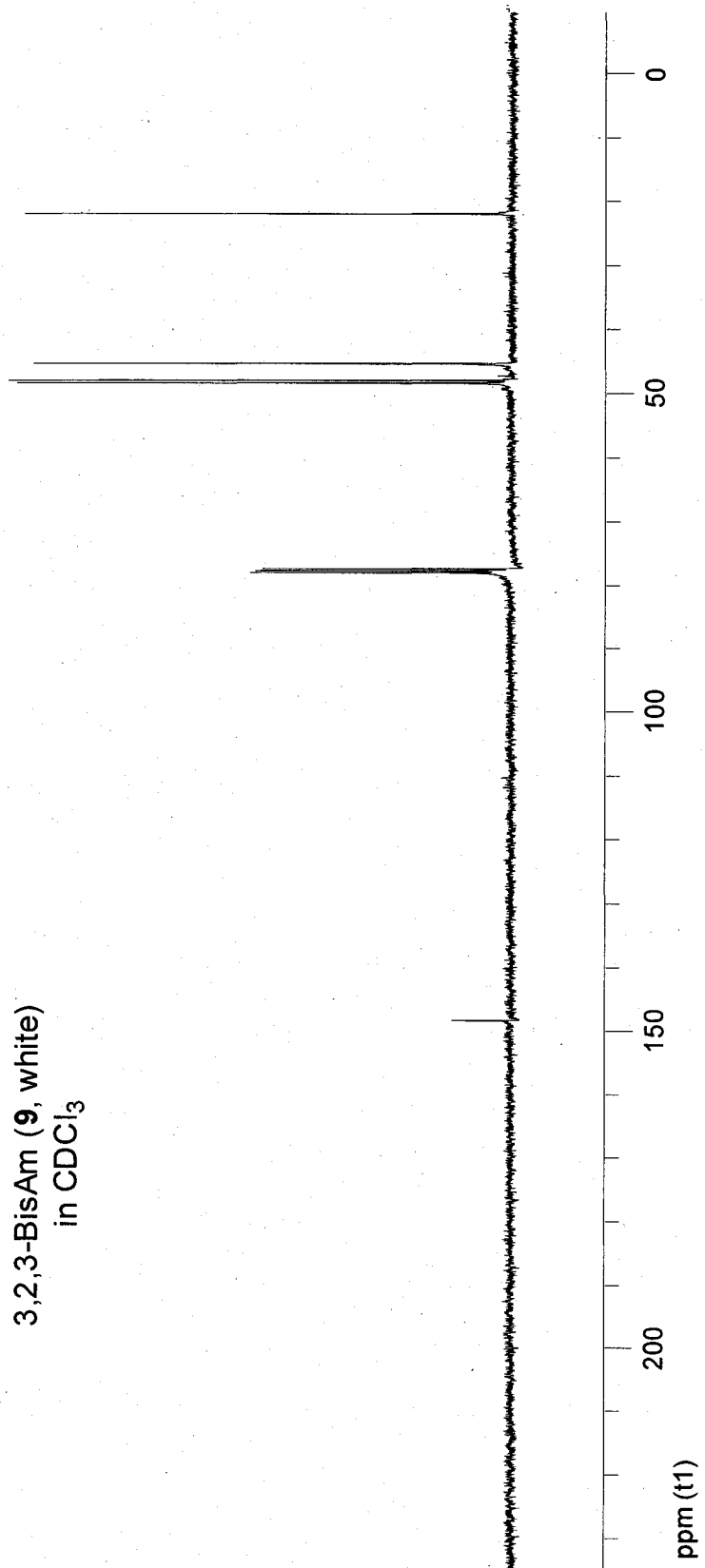


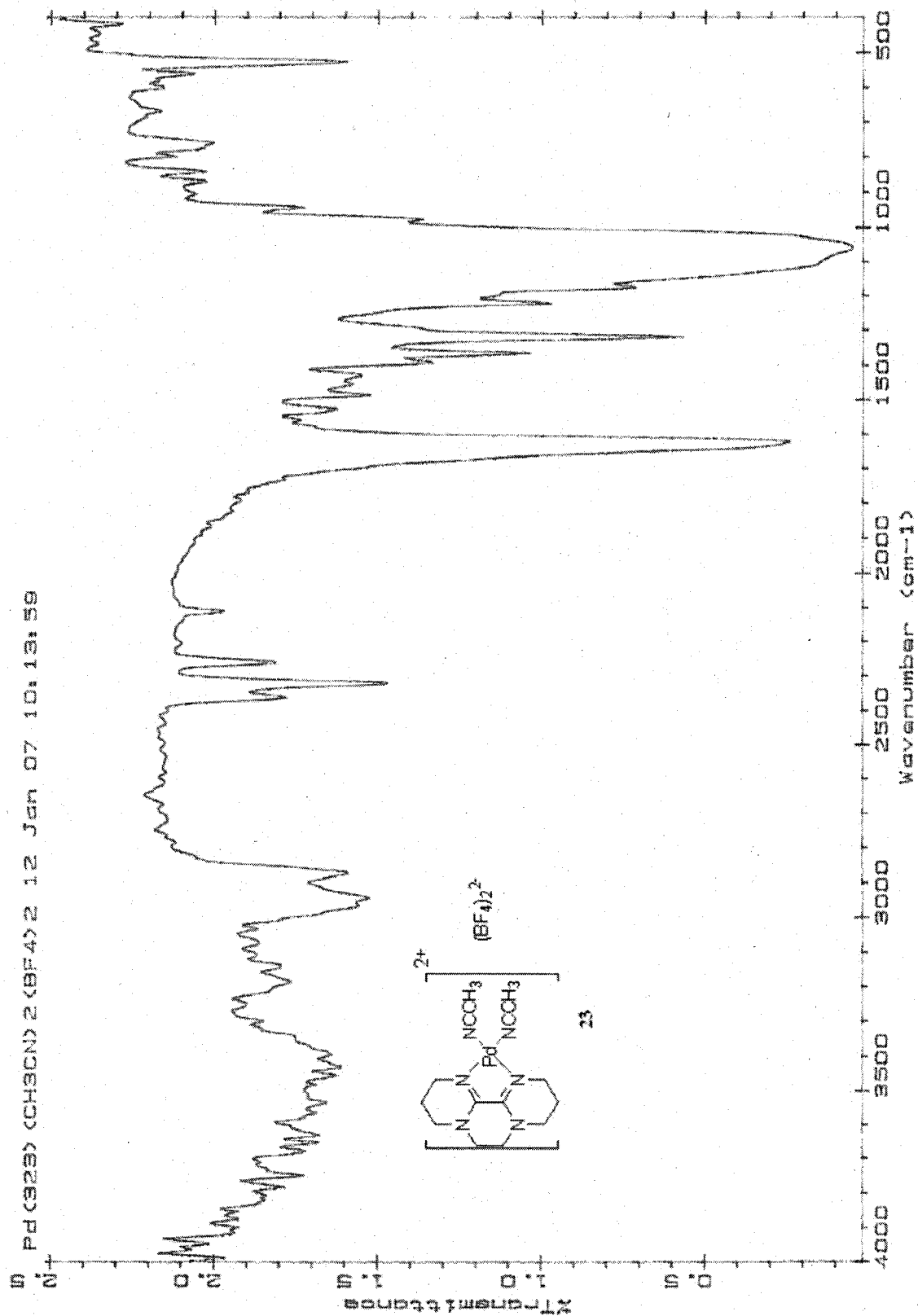
3,2,3-BisAm (9, white)  
in CDCl<sub>3</sub>

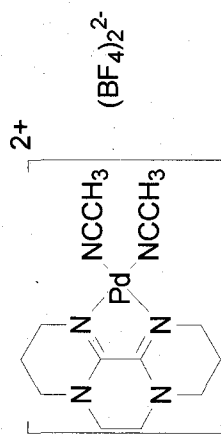




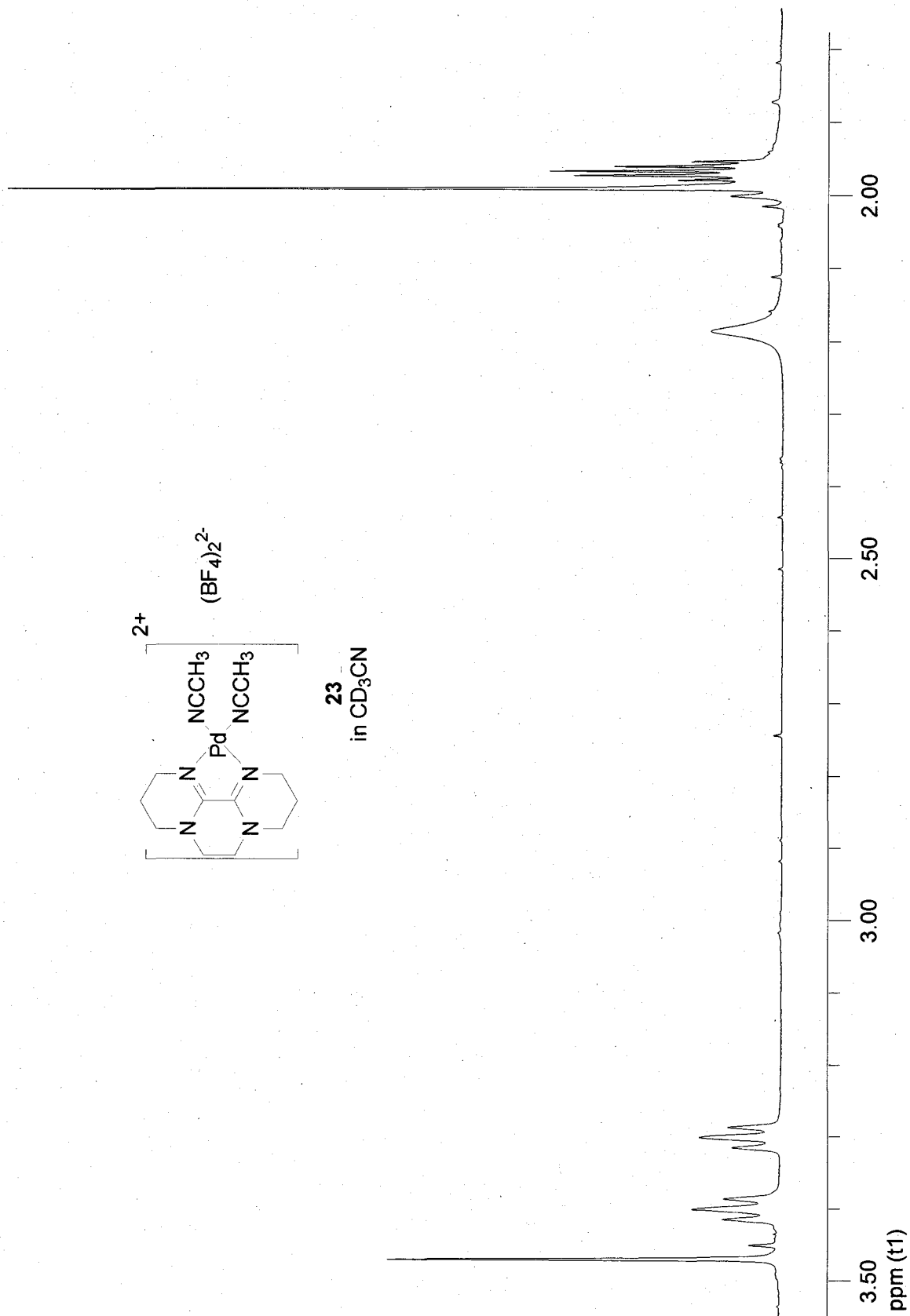
3,2,3-BisAm (9, white)  
in CDCl<sub>3</sub>

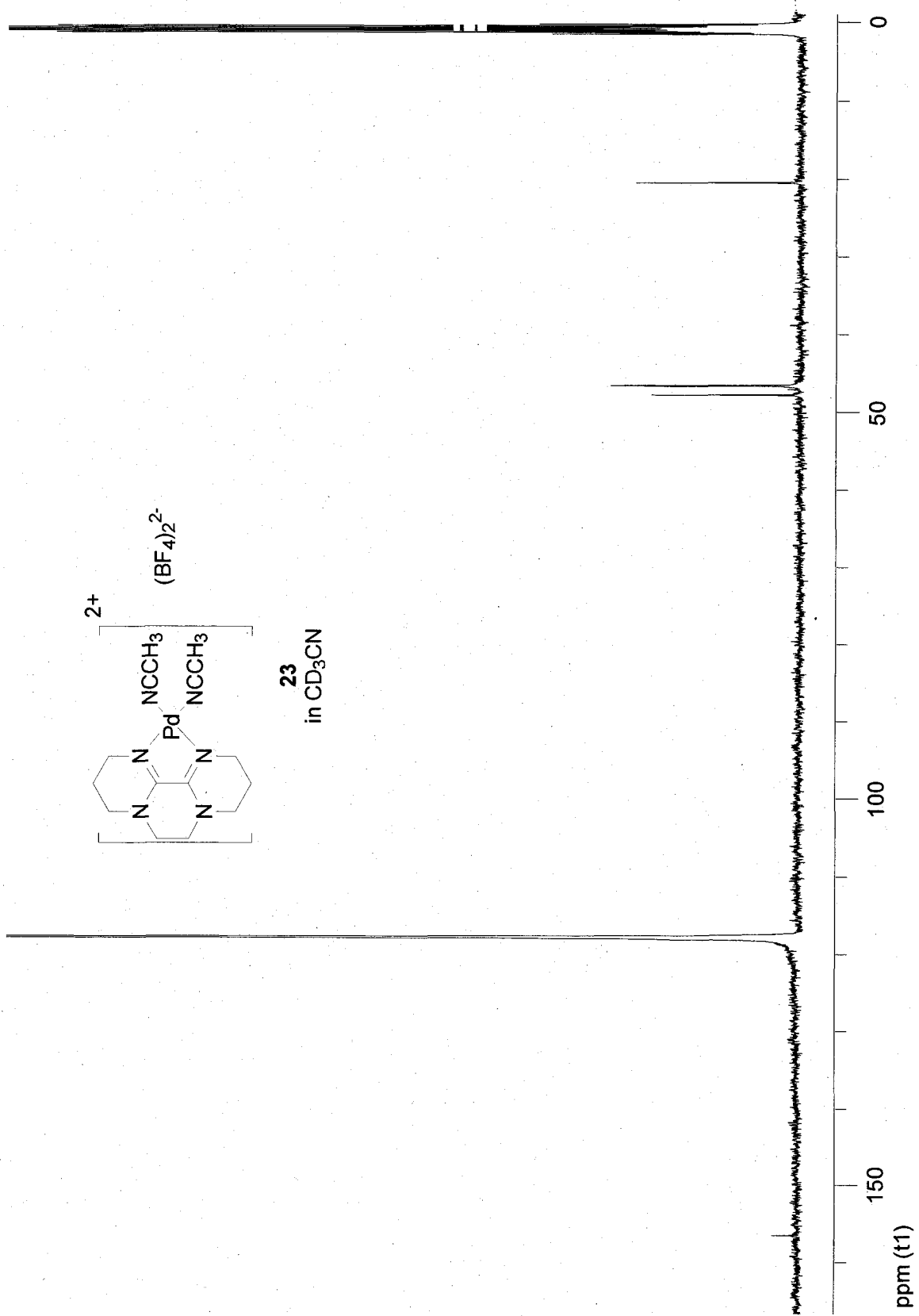




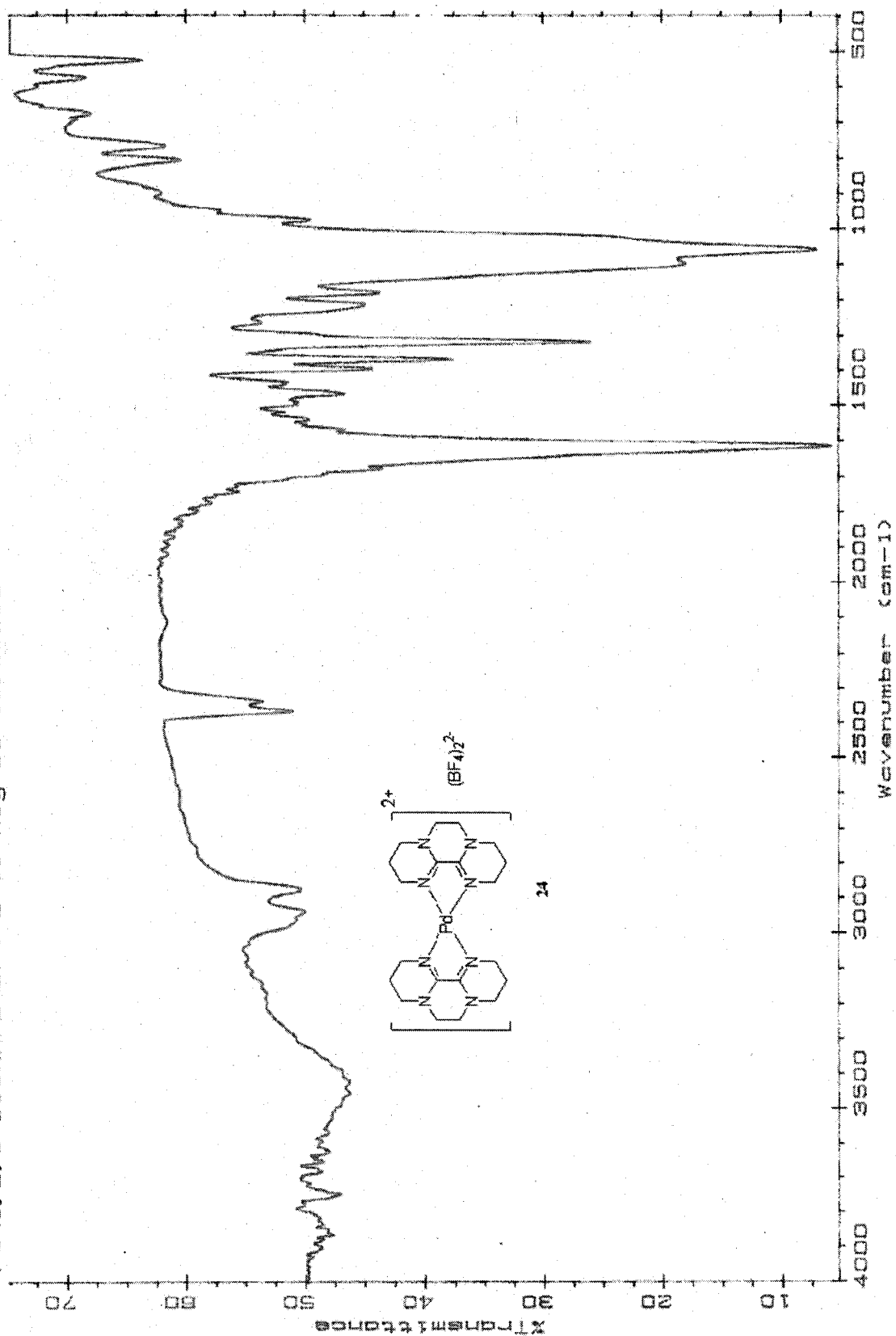


**23**  
in  $CD_3CN$

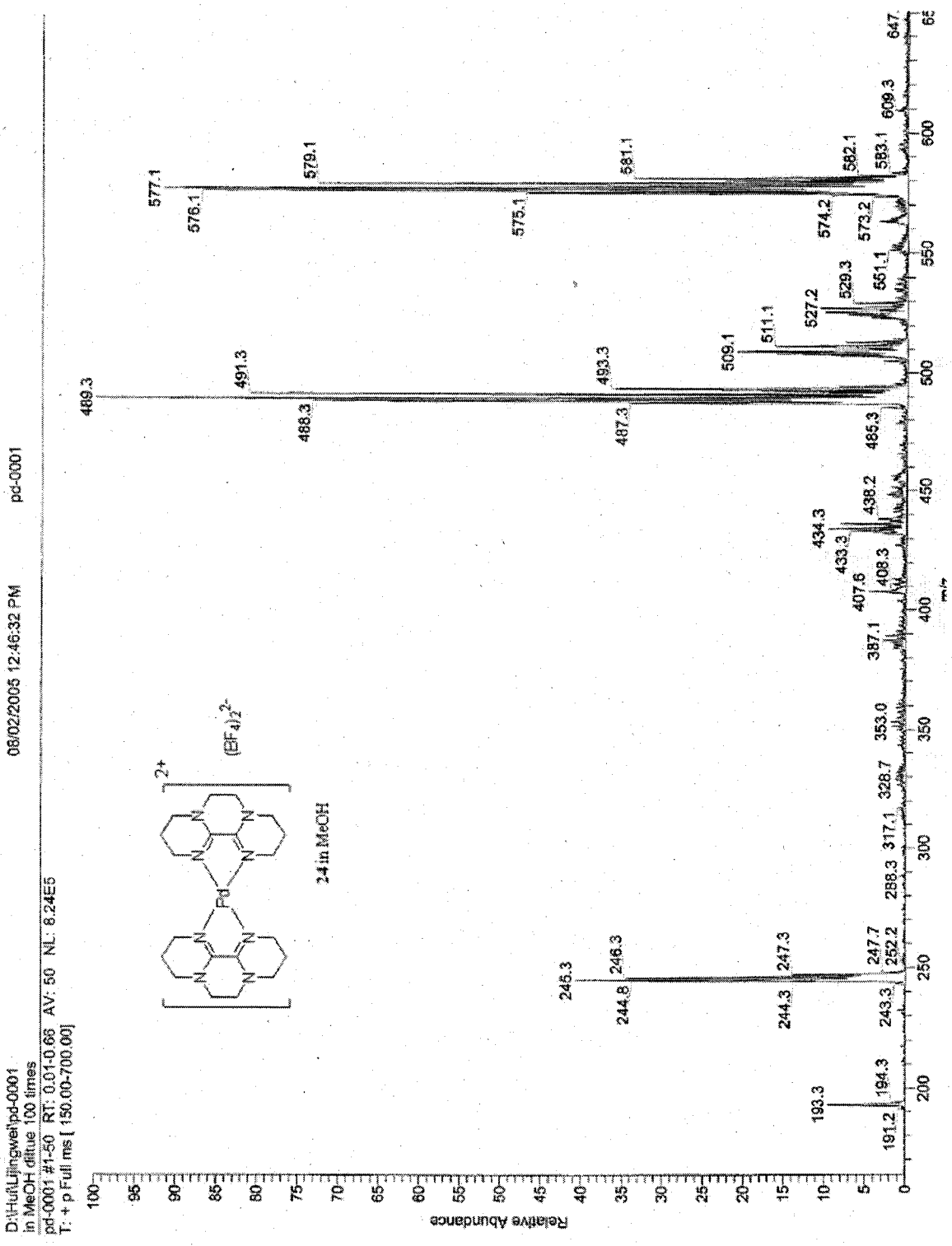


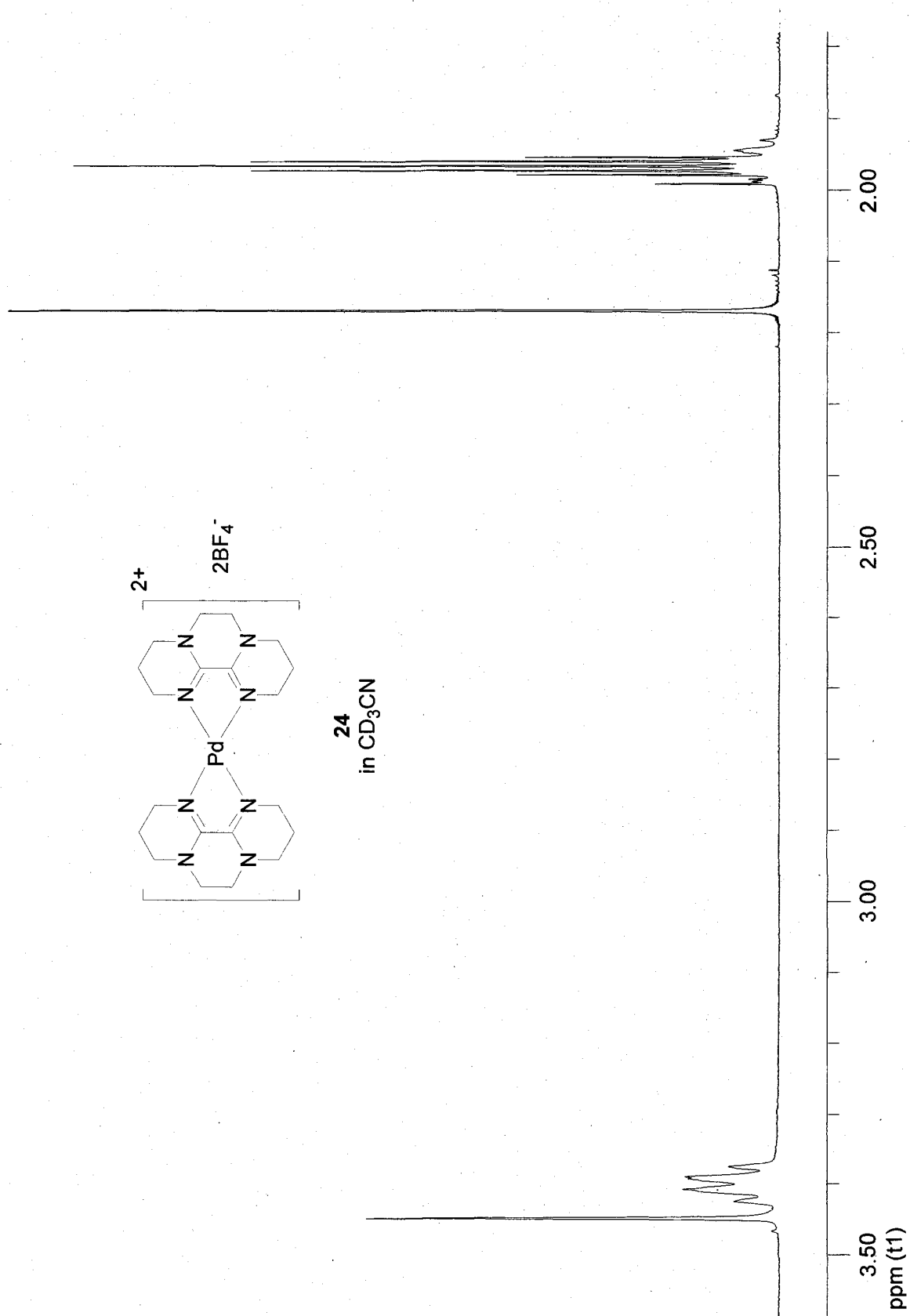


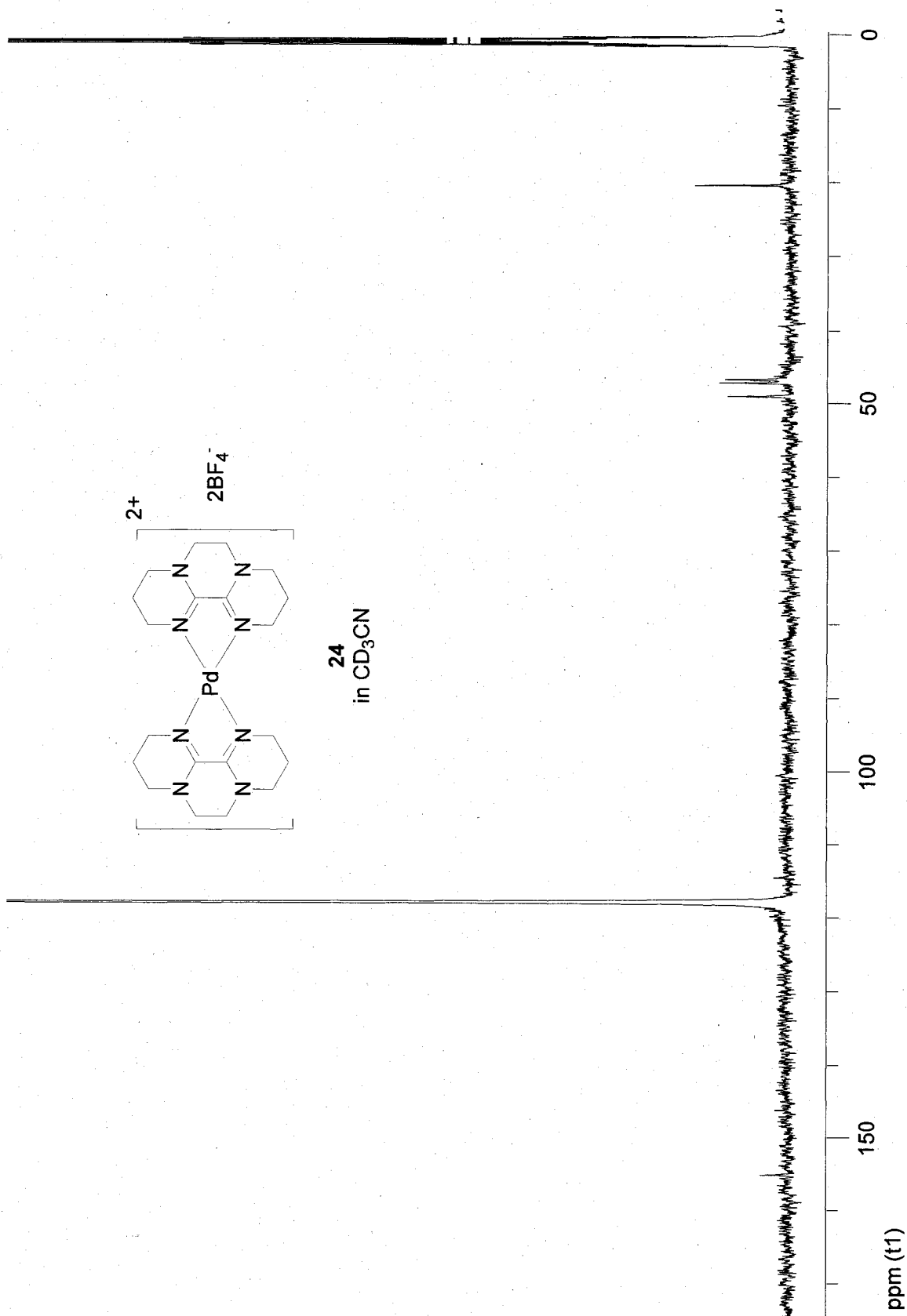
Pd(3,2,3-BISAM)2(BF4)2 01 AUG 05 15:00:10

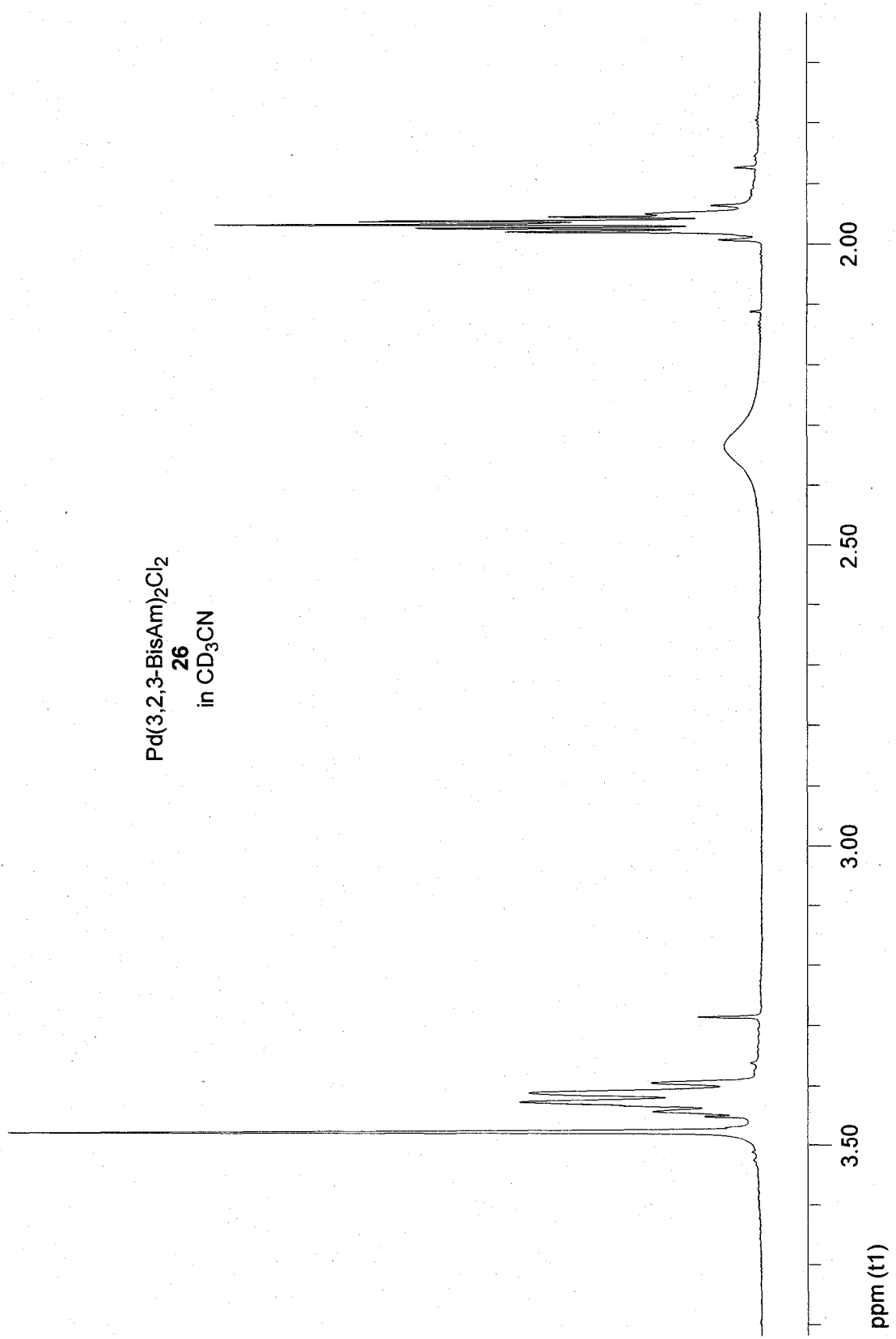


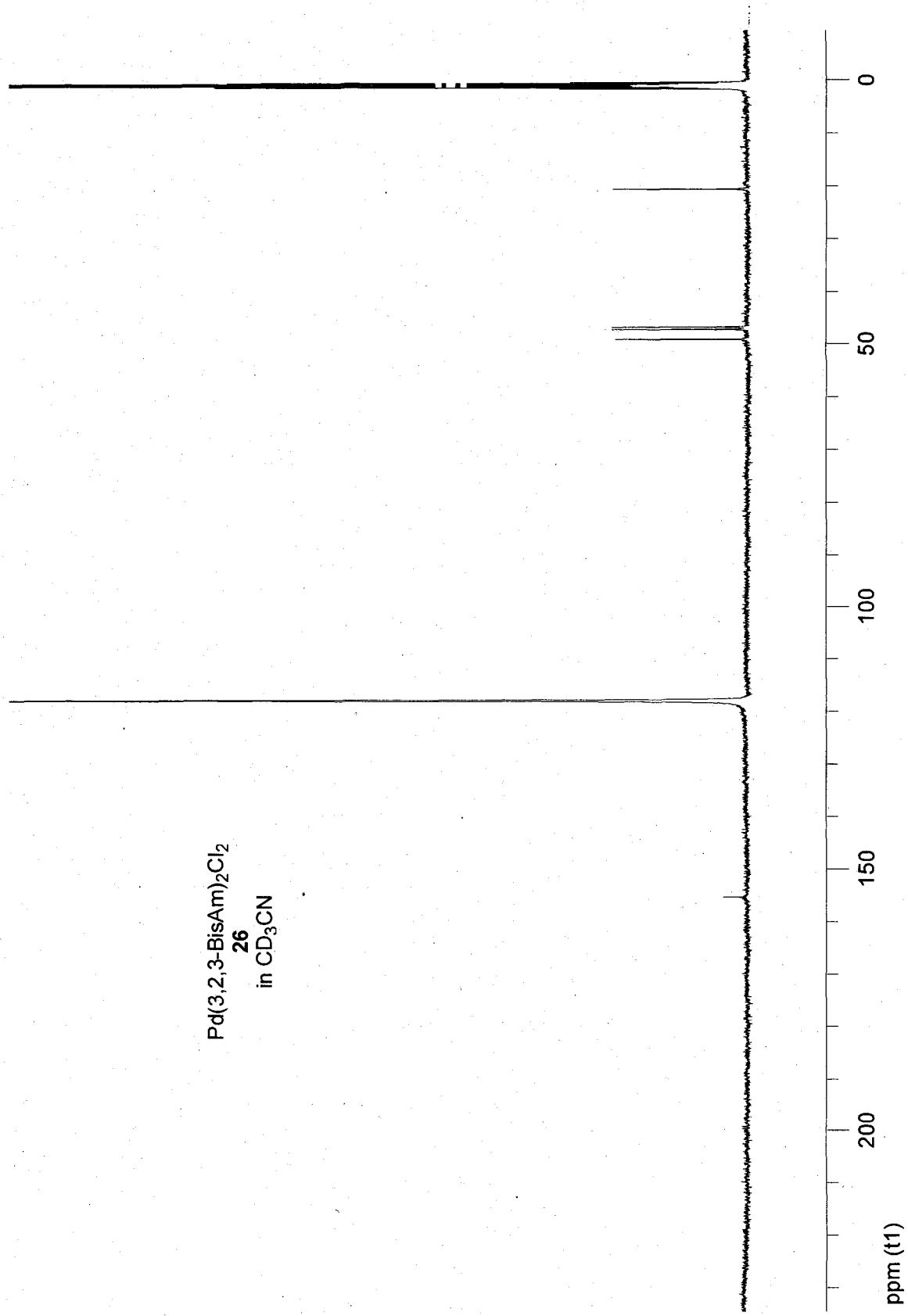




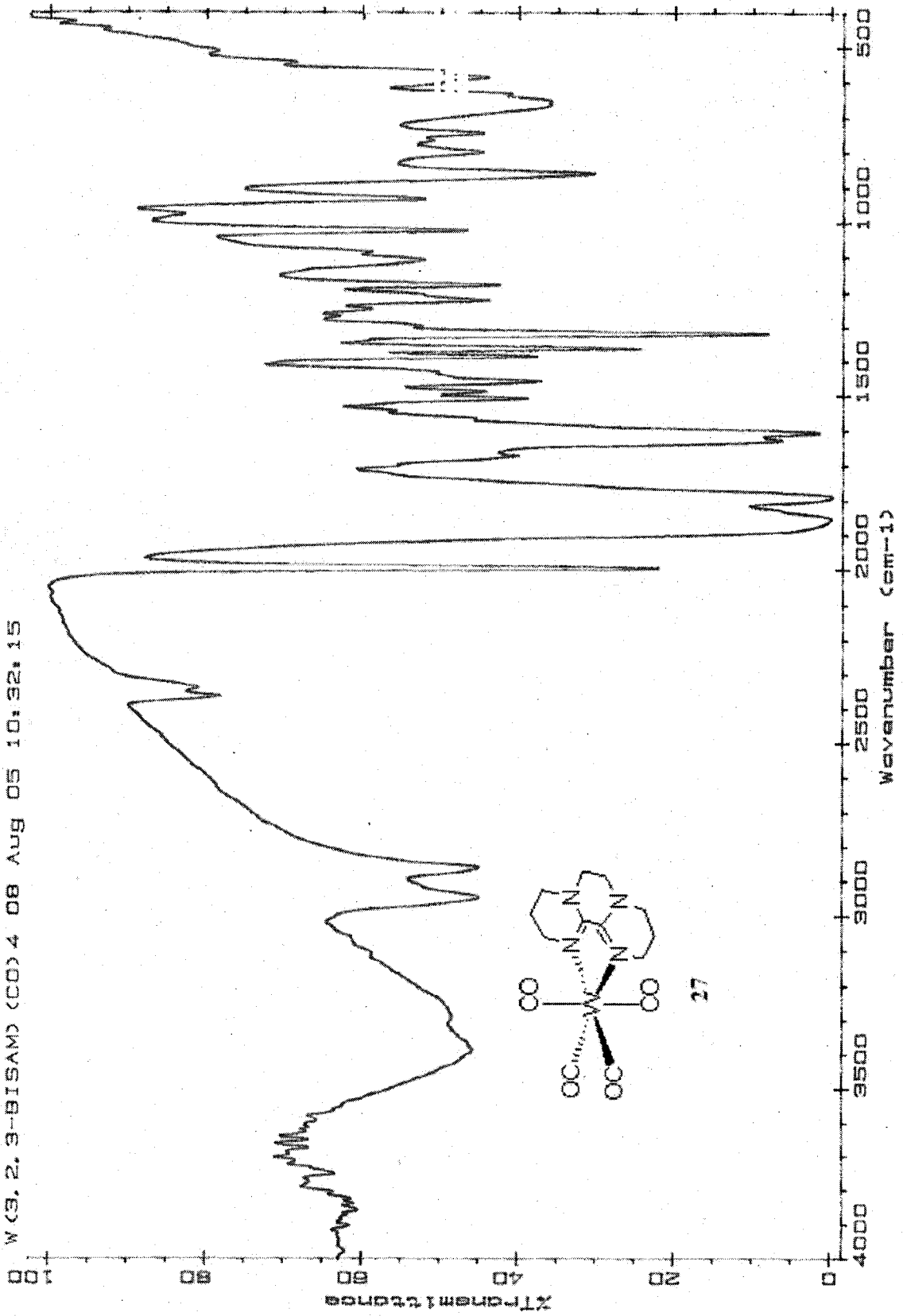


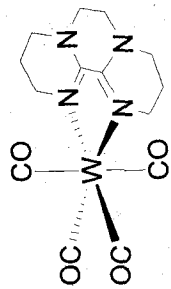




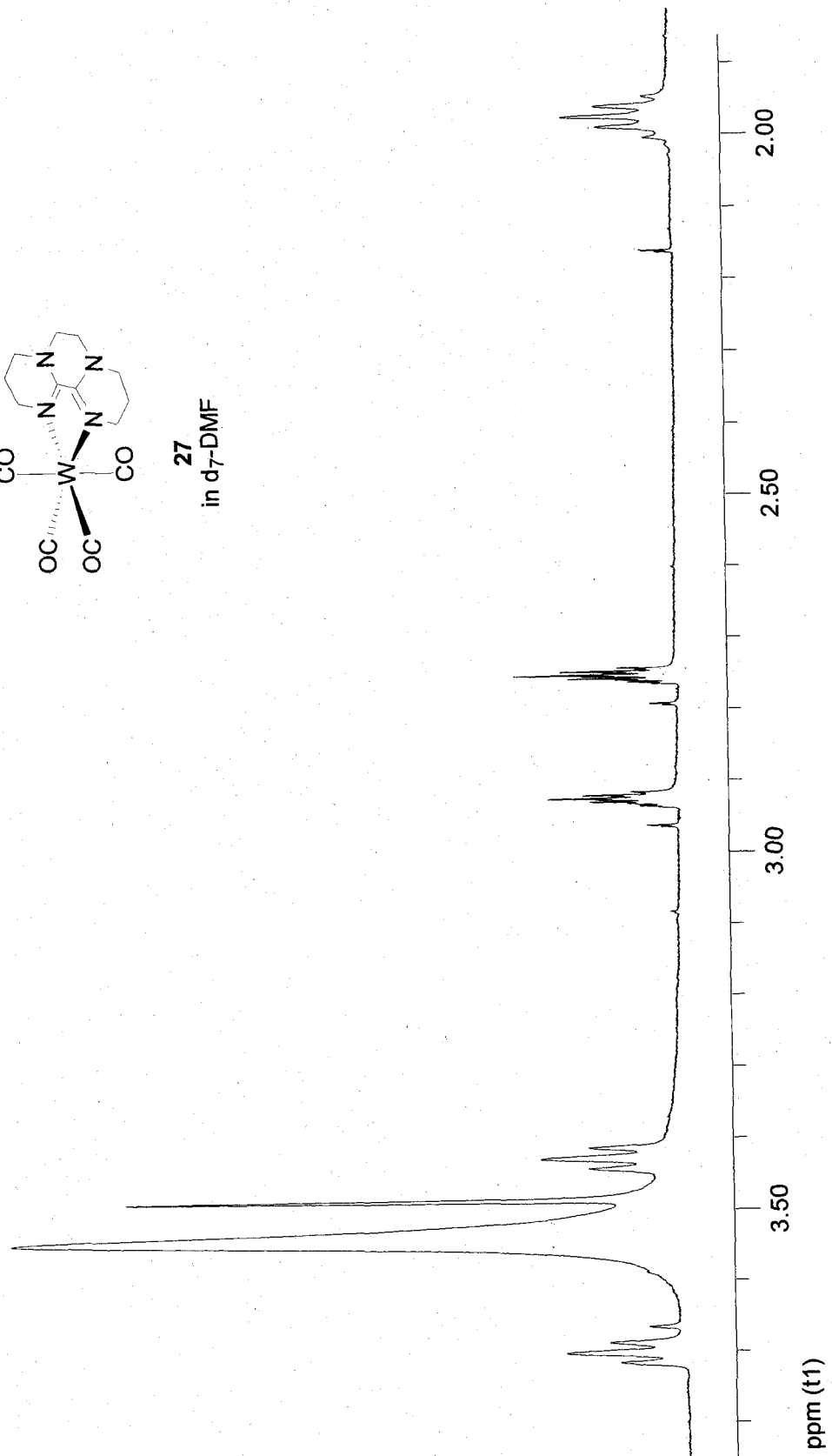


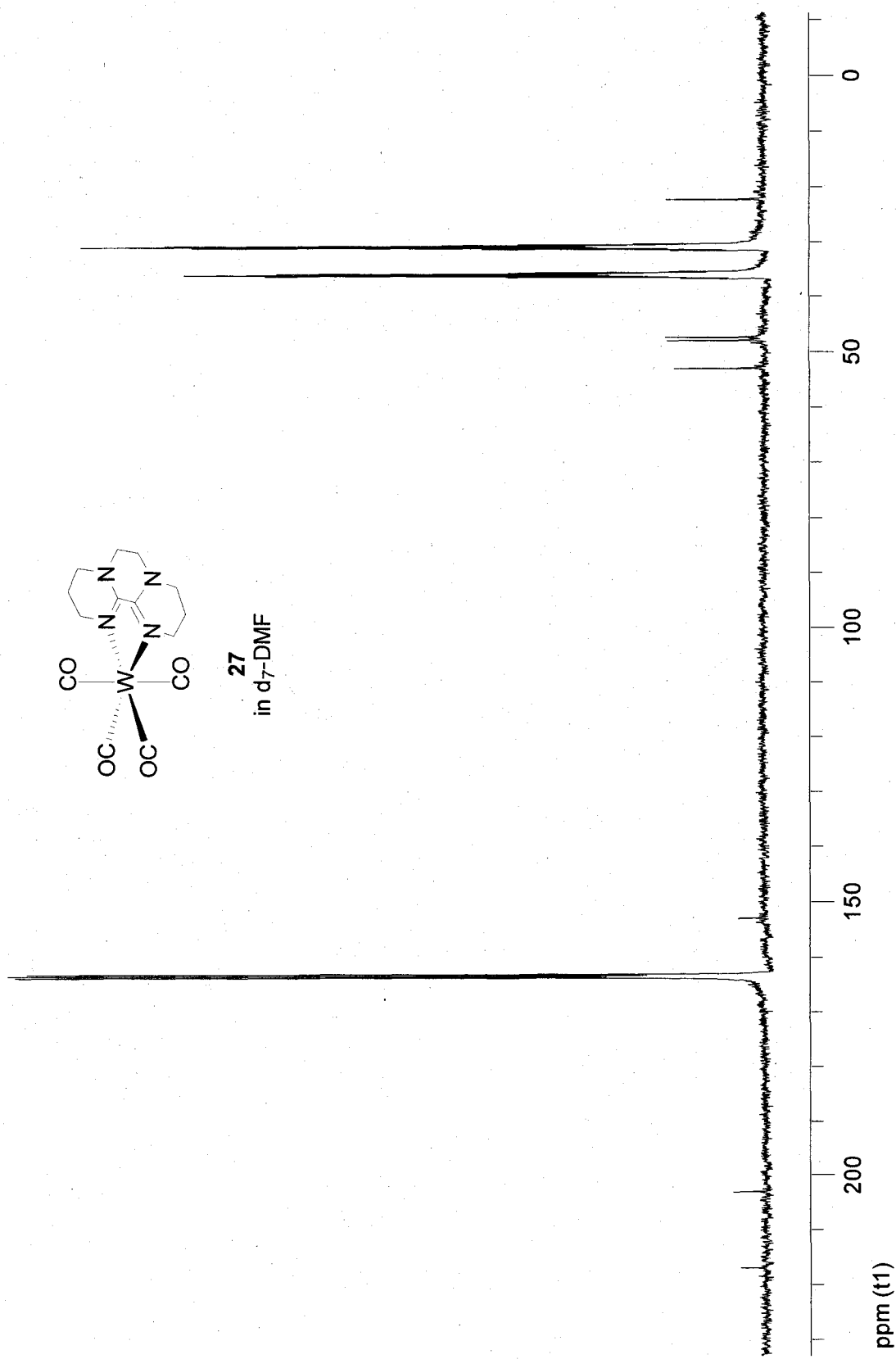
W (3. 2. 3-BISAM) (CO) 4 08 AUG 05 10:32:15



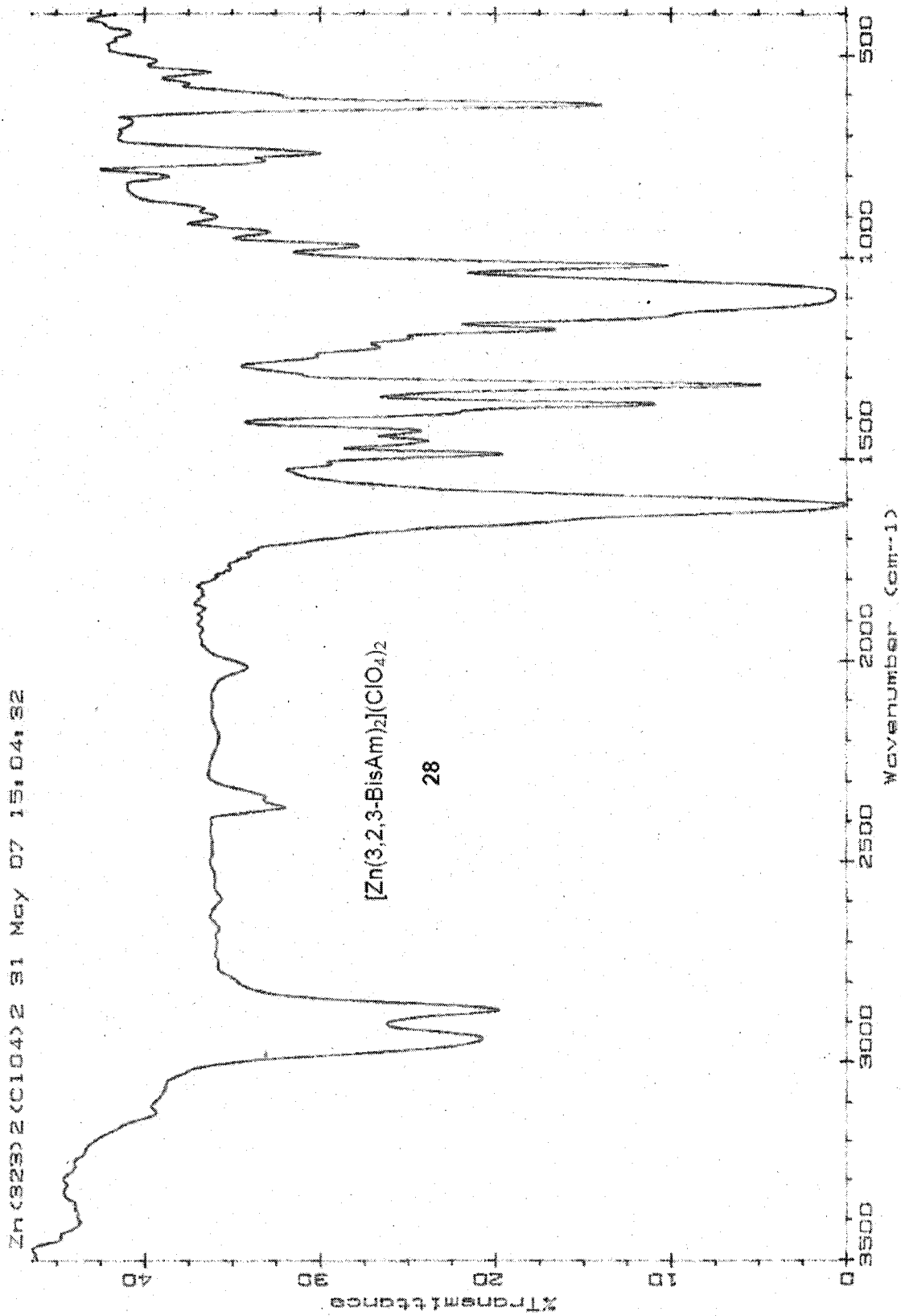


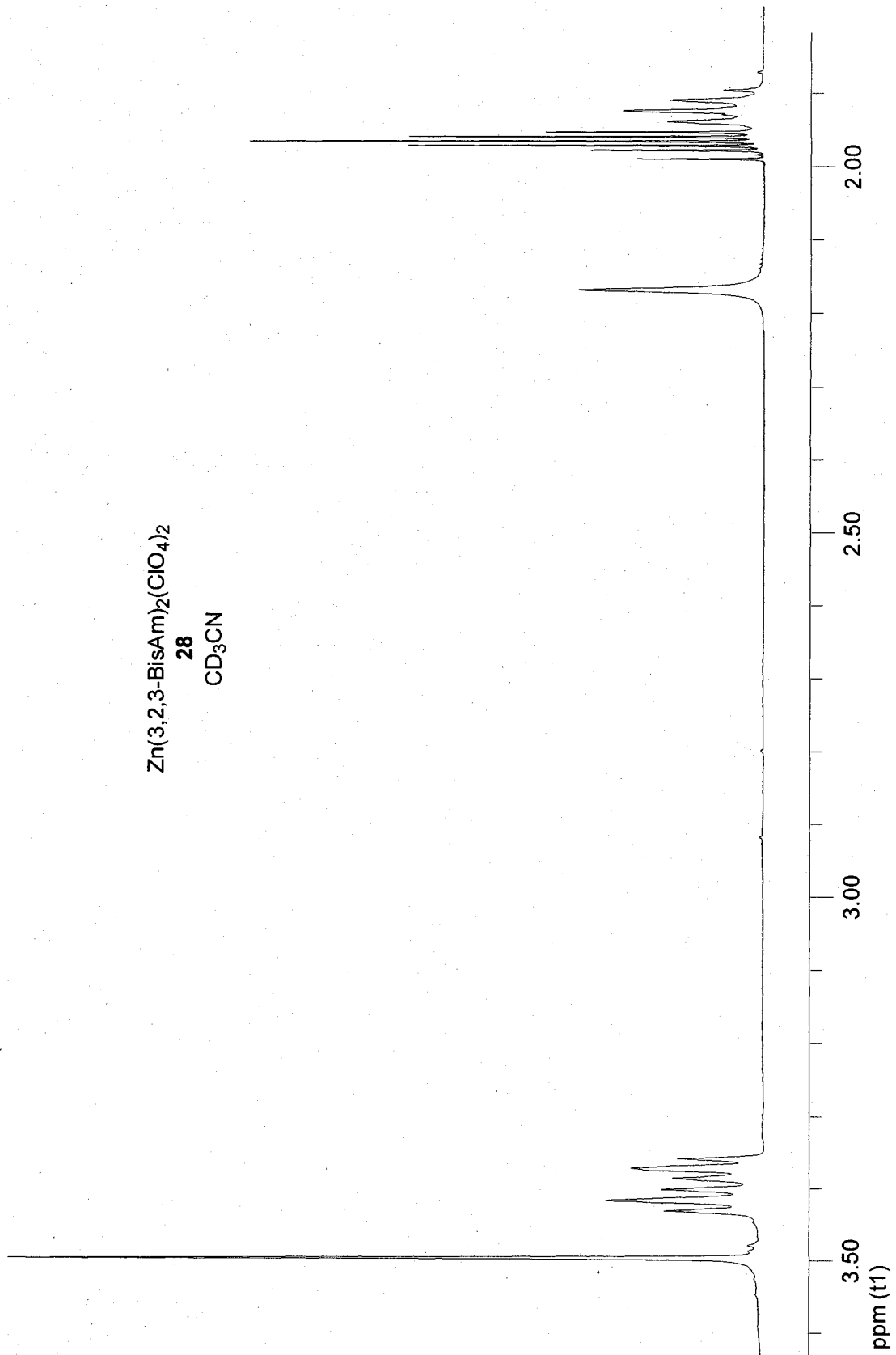
27  
in d<sub>7</sub>-DMF

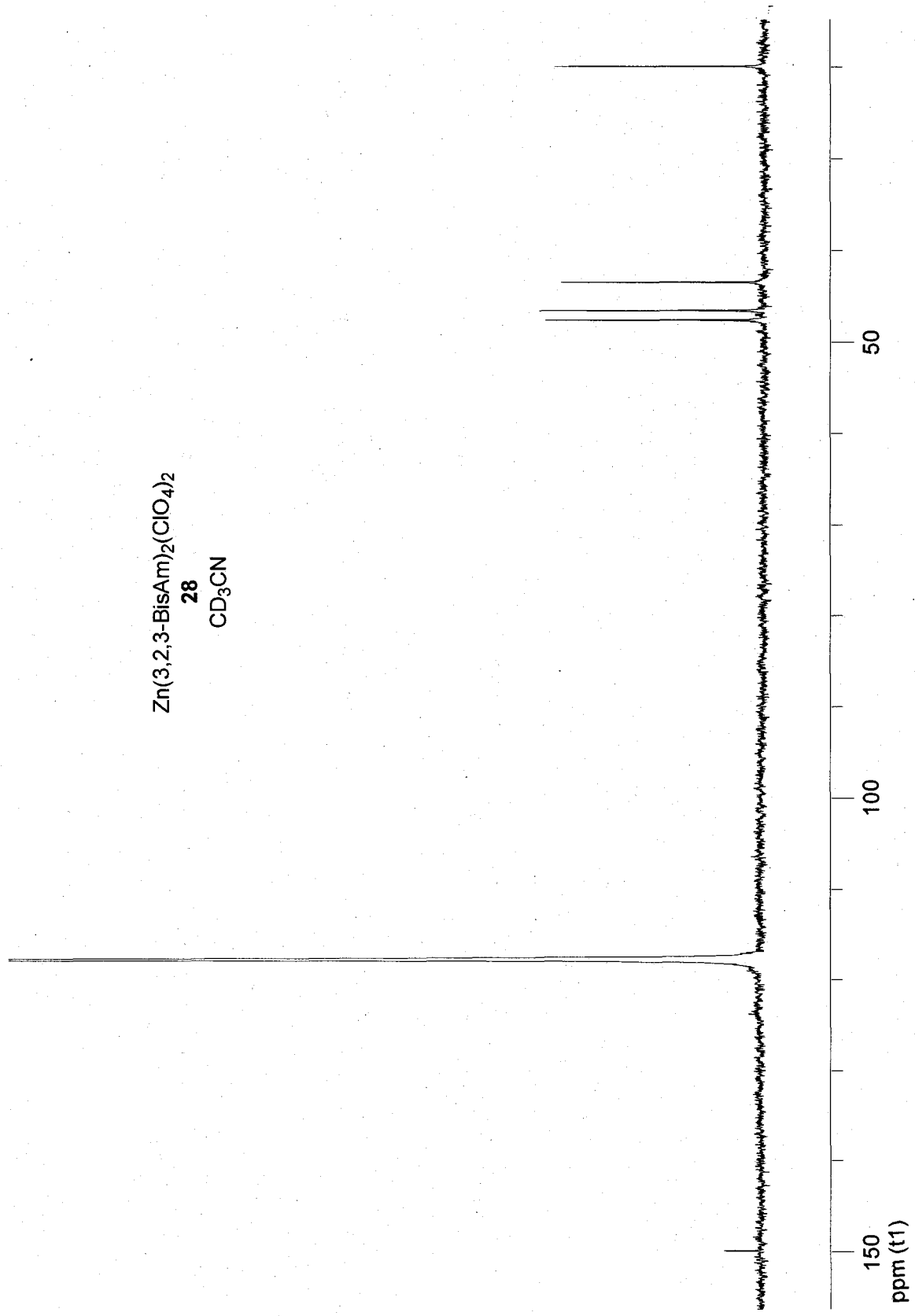




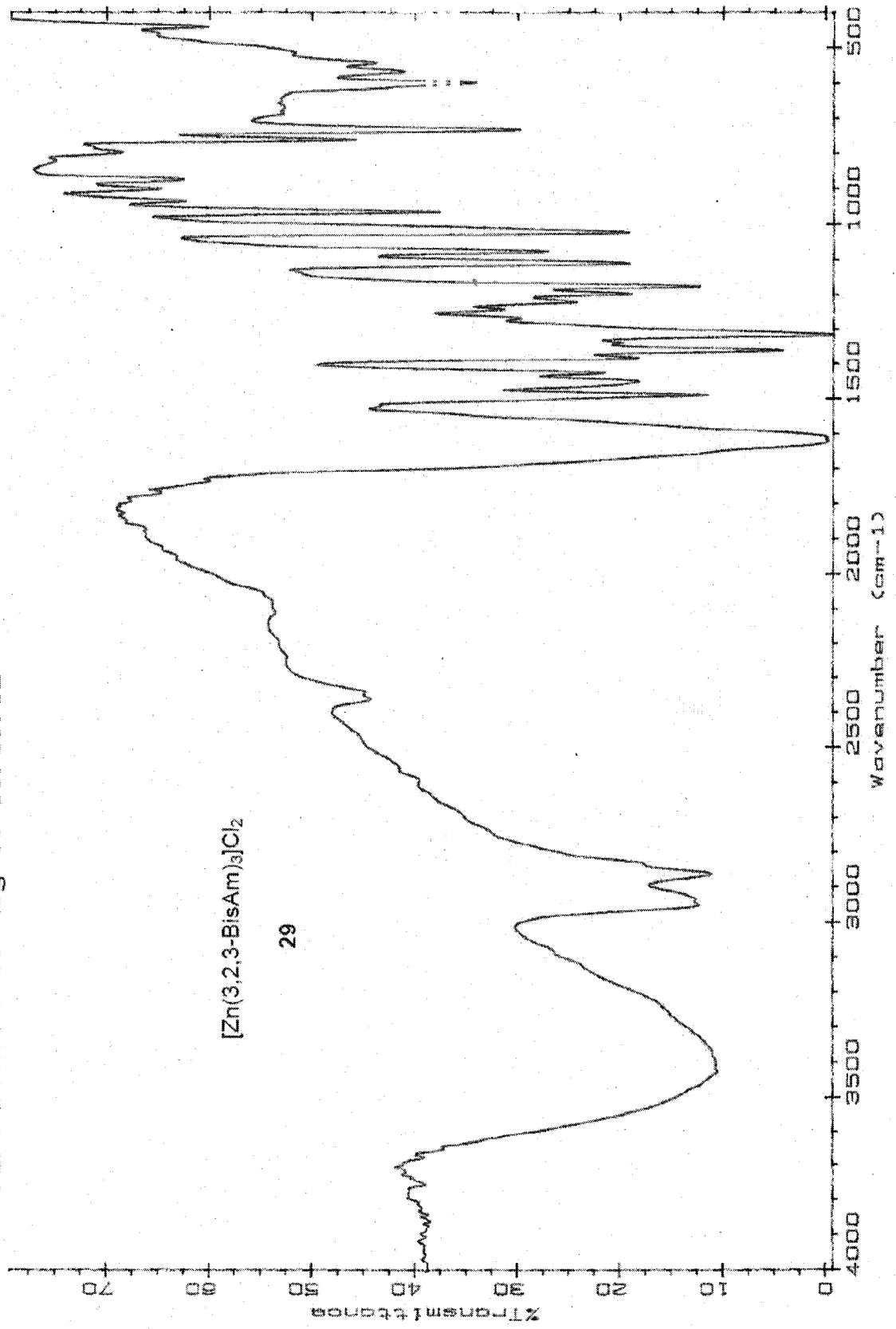


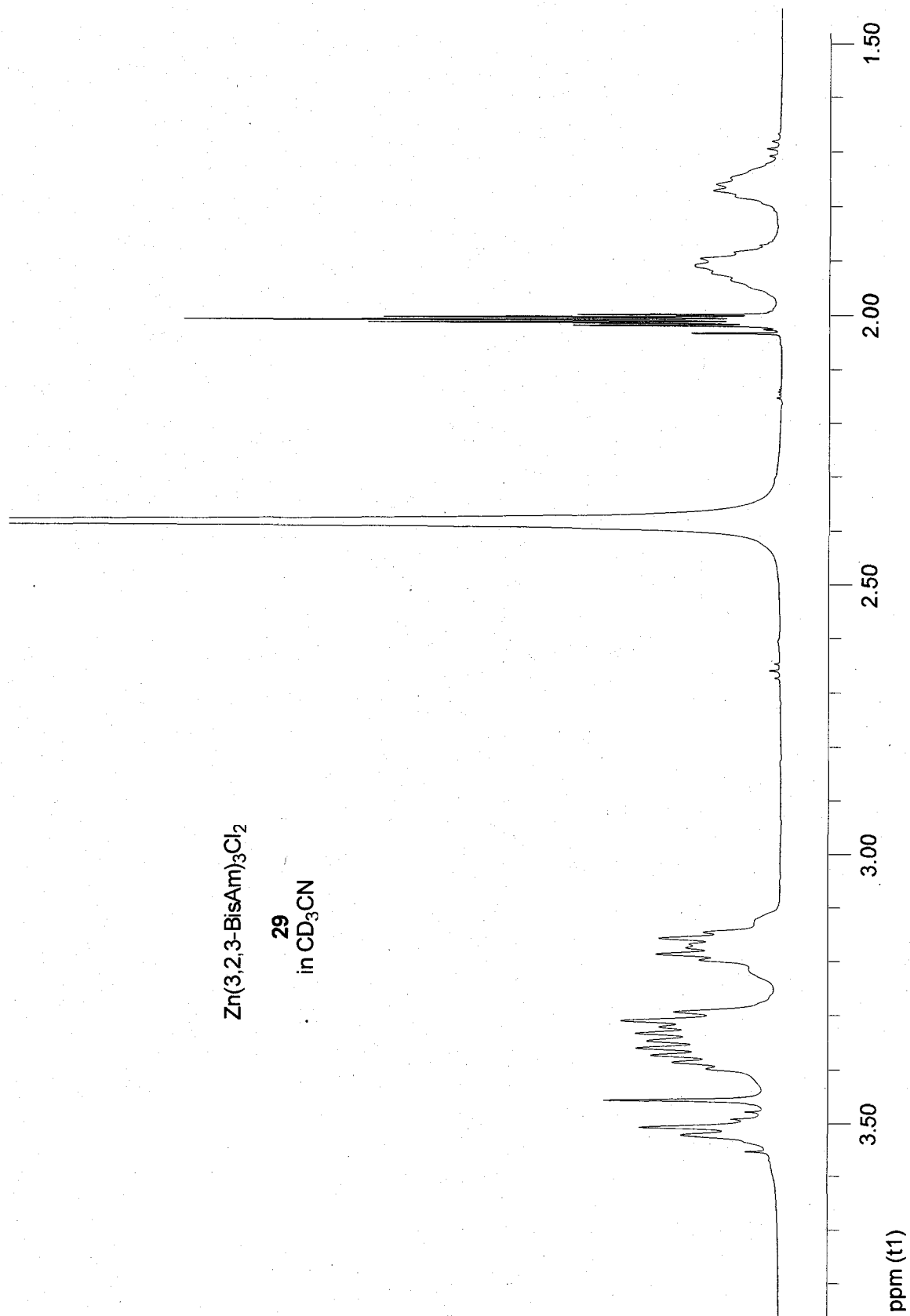




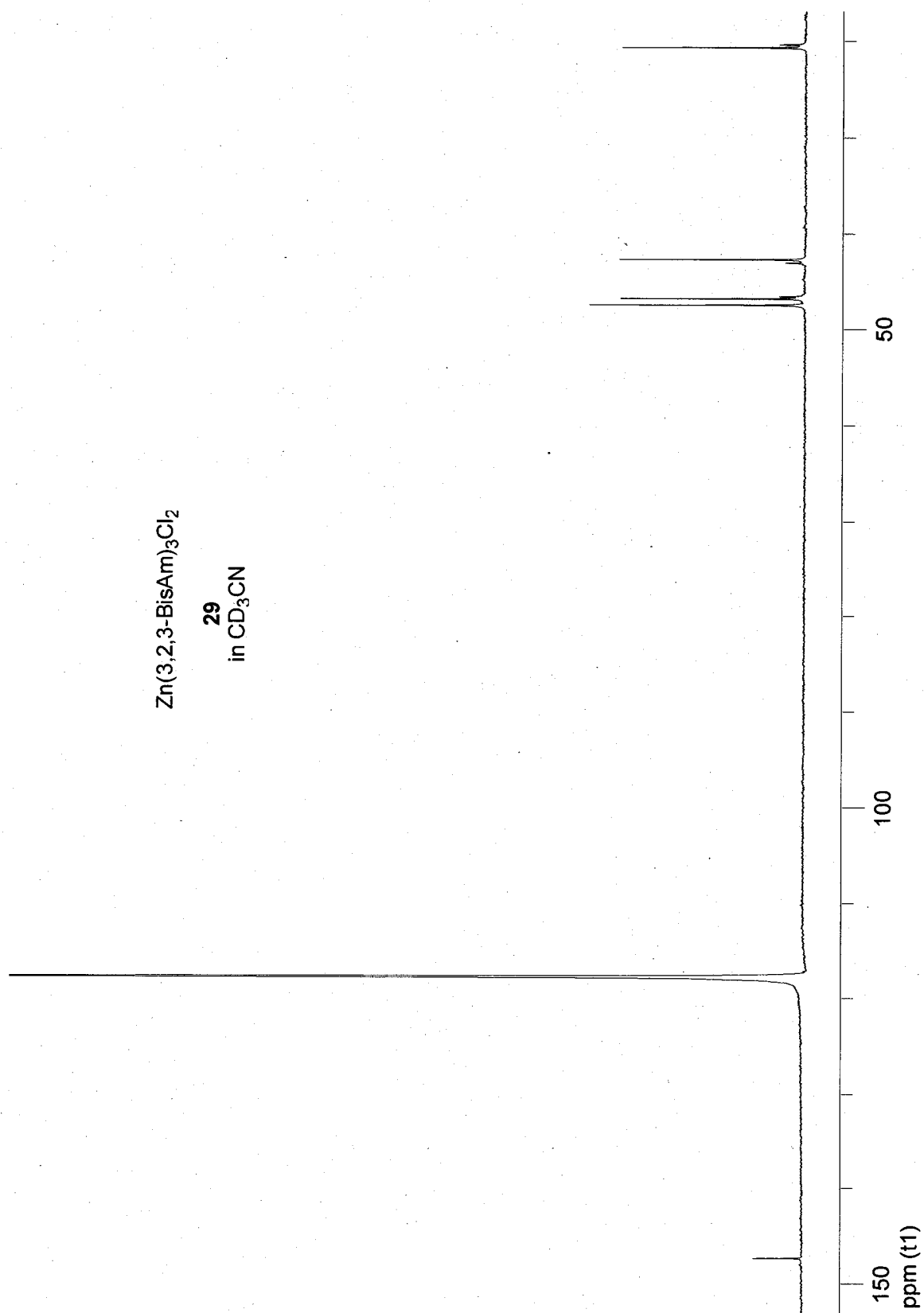


Zn(3,2,3-BISAM)3 19 Aug 05 09:59:32

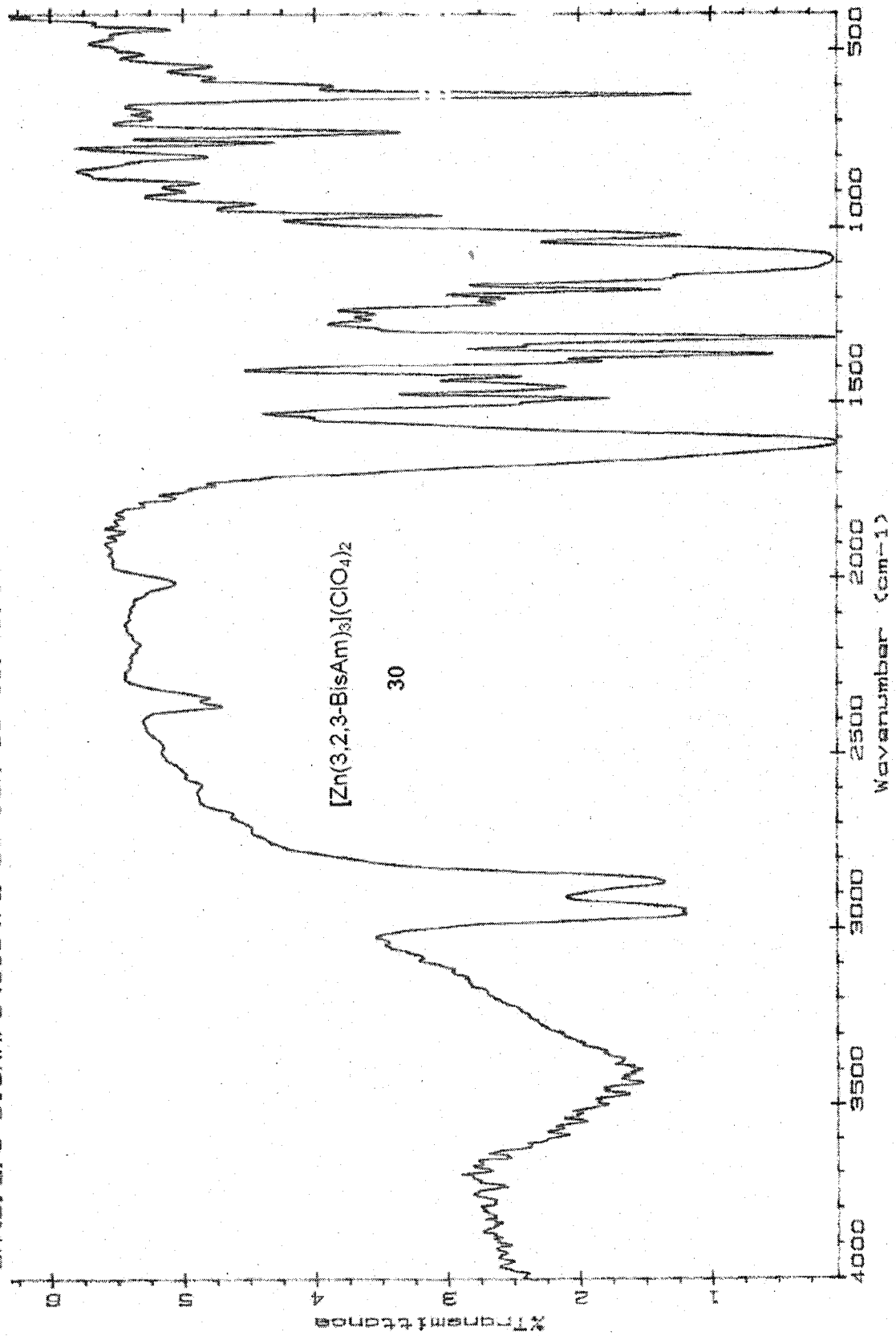


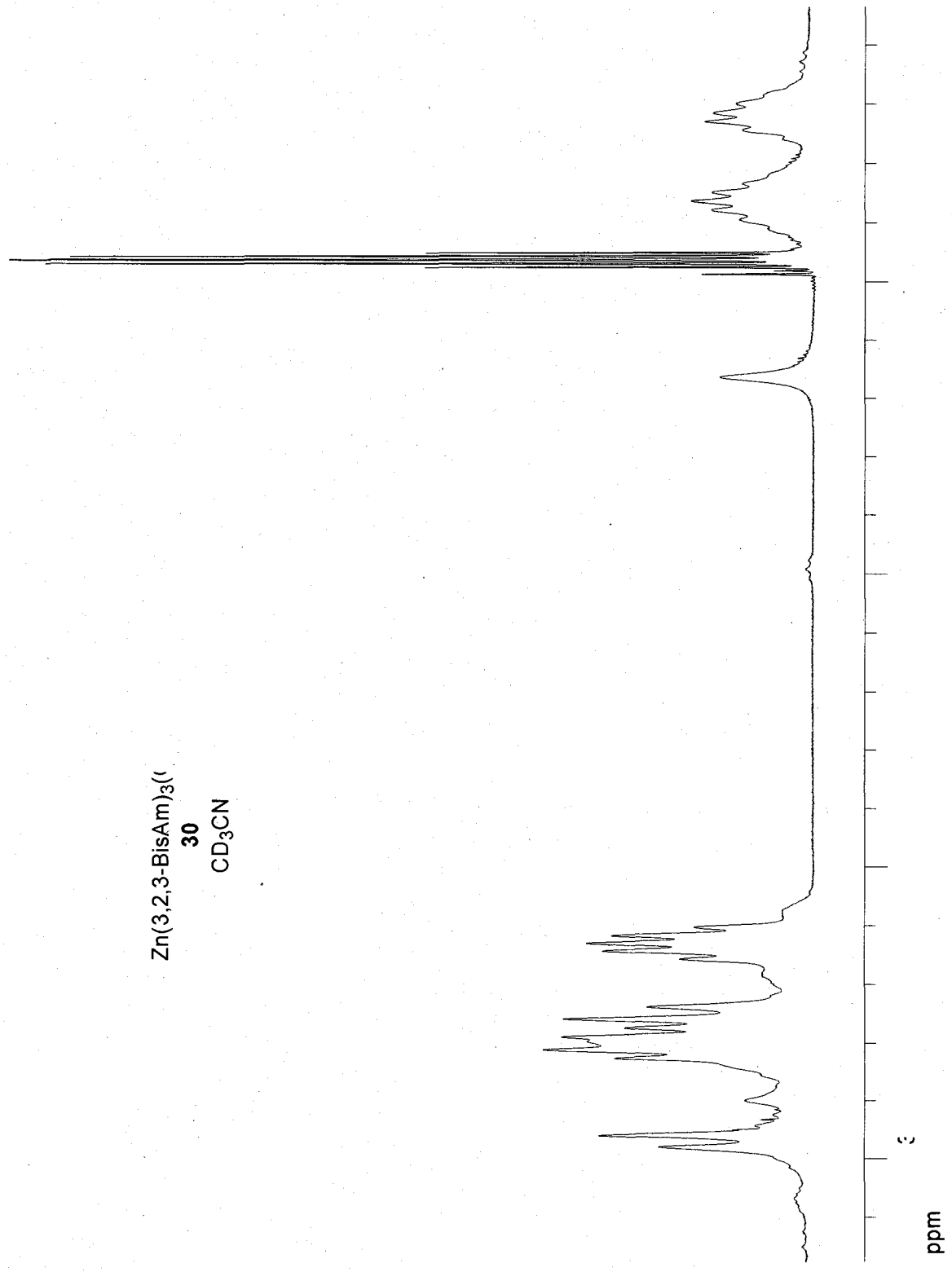


Zn(3,2,3-BisAm)<sub>3</sub>Cl<sub>2</sub>  
**29**  
in CD<sub>3</sub>CN

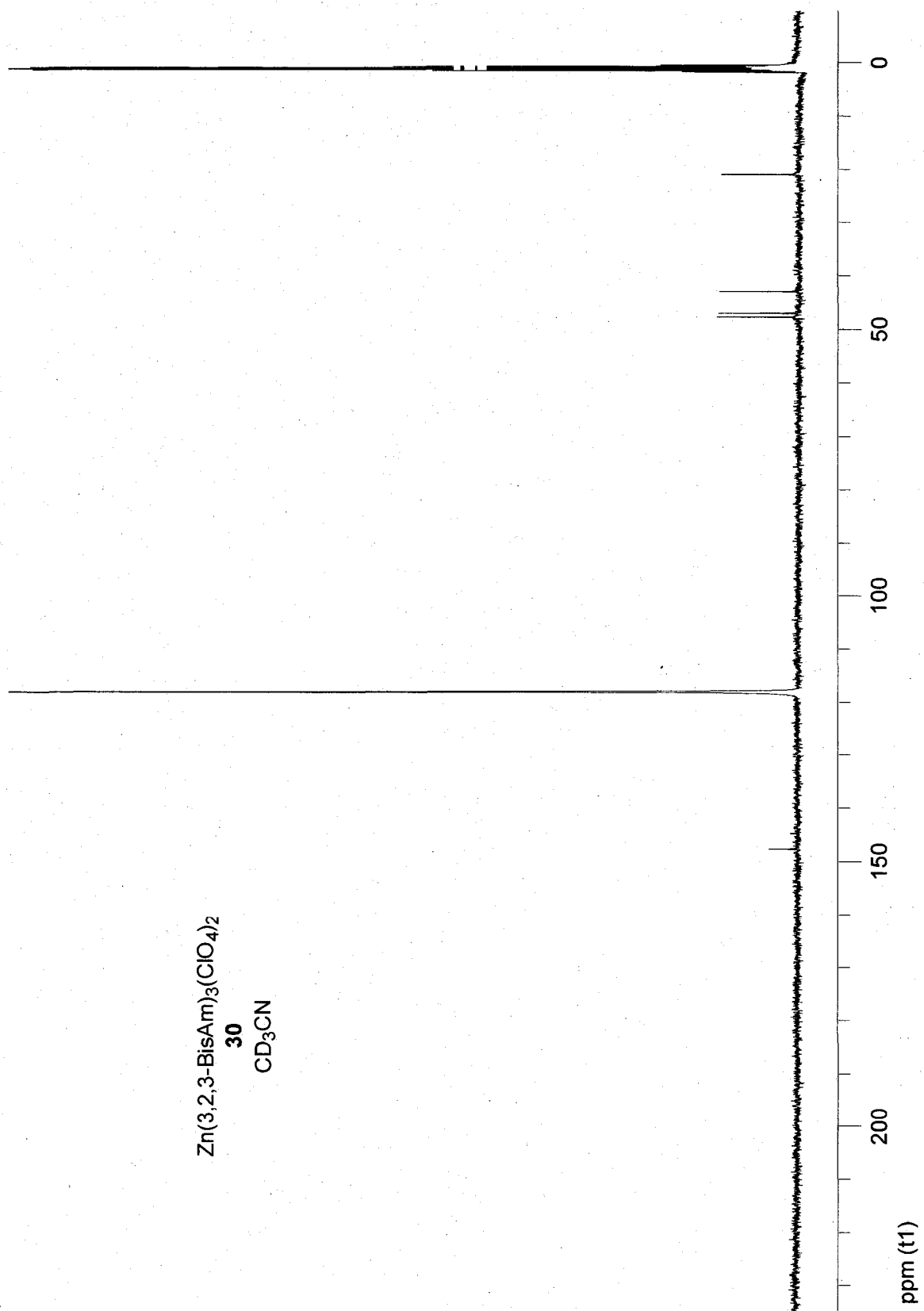


Zn(3,2,3-BISAM)3(ClO4)2 08 JUN 06 10:41:34

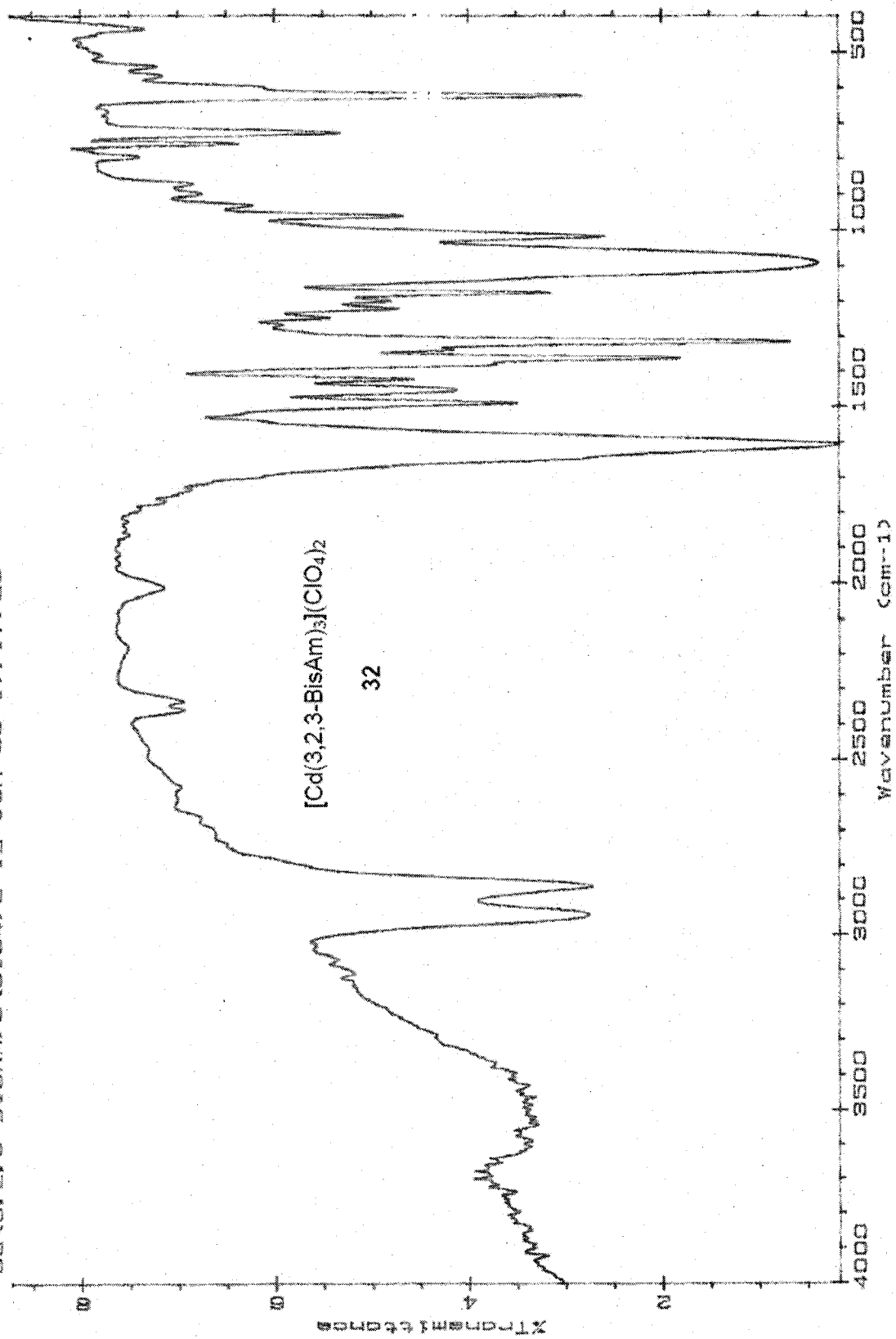




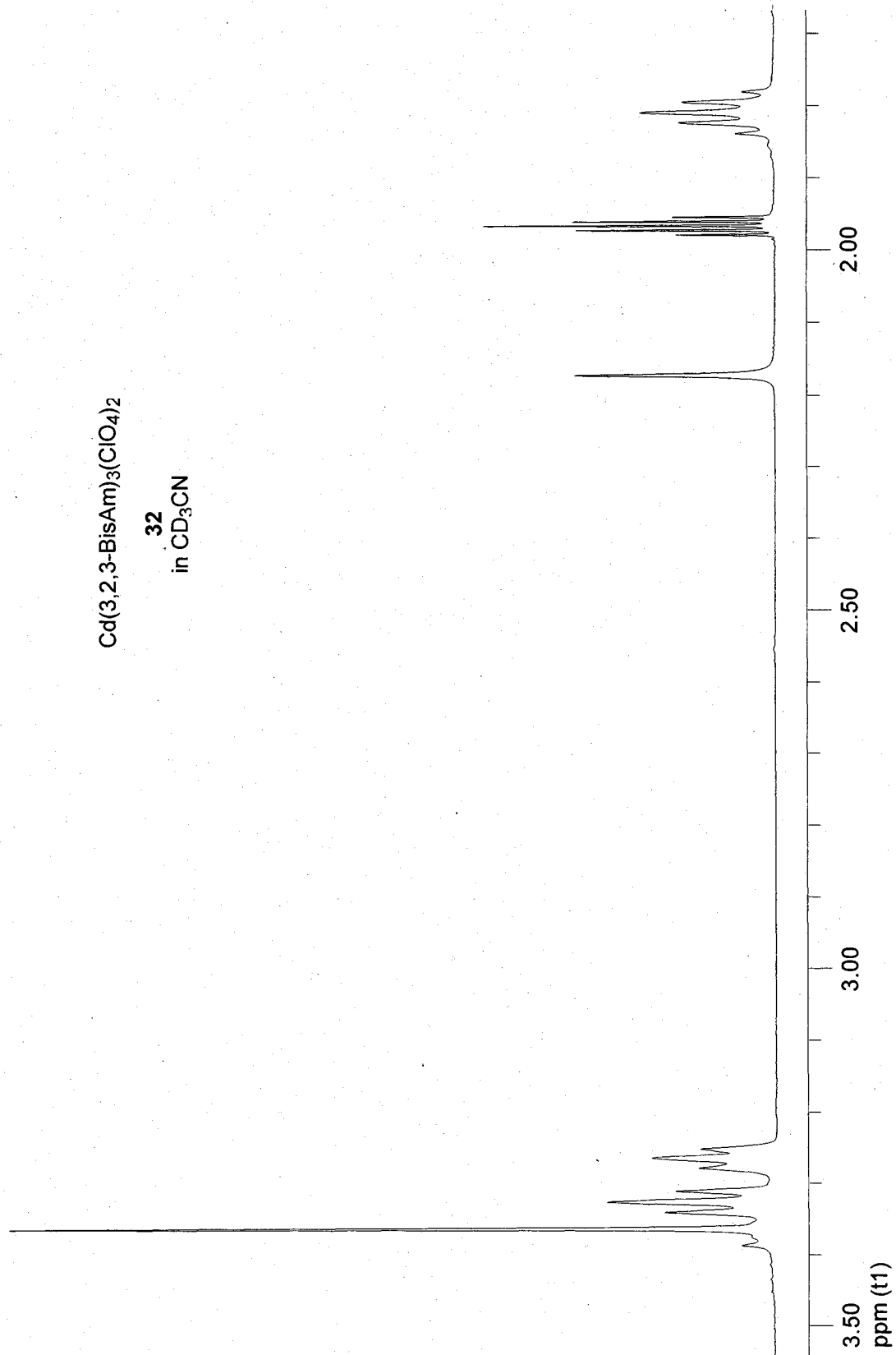


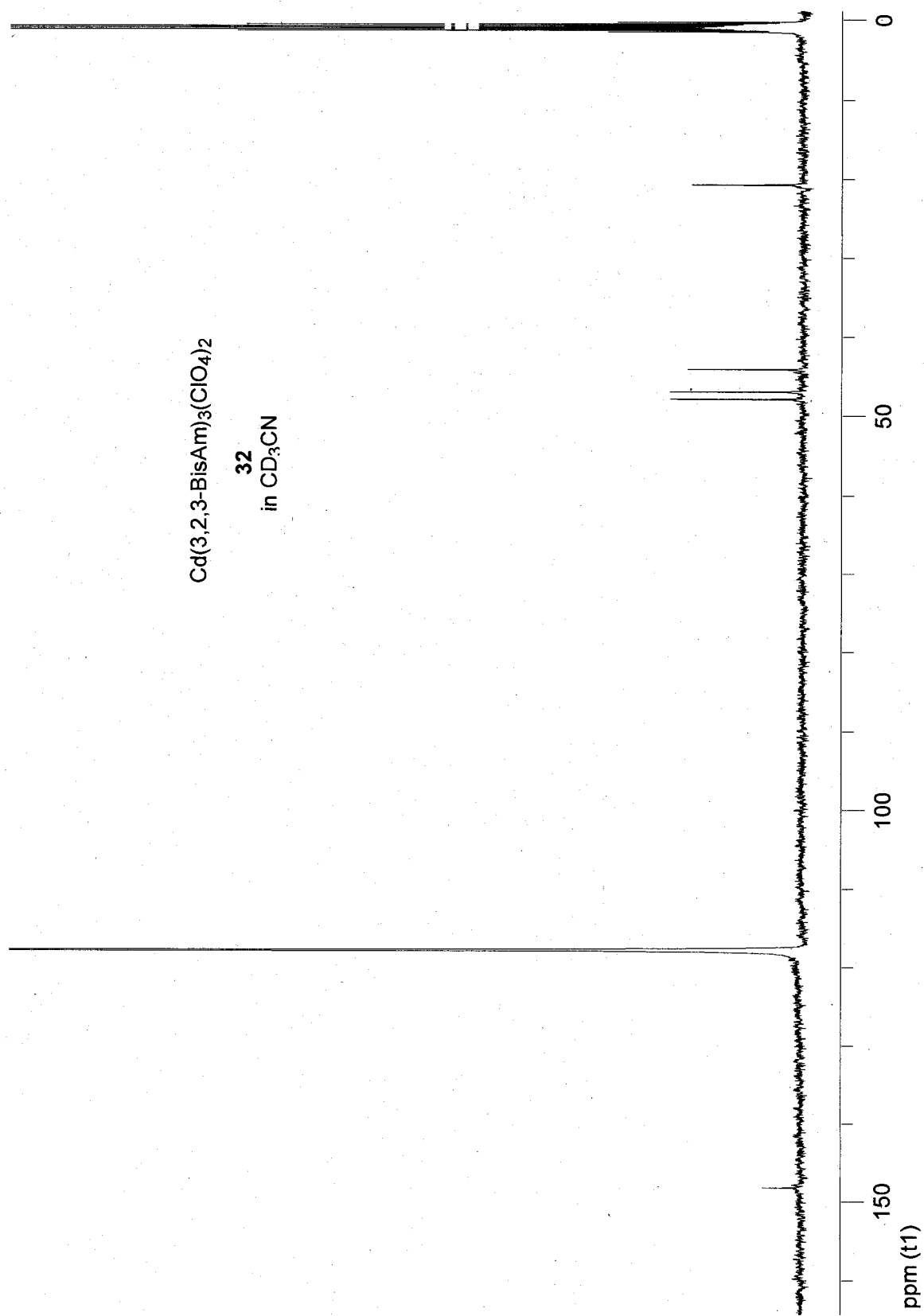


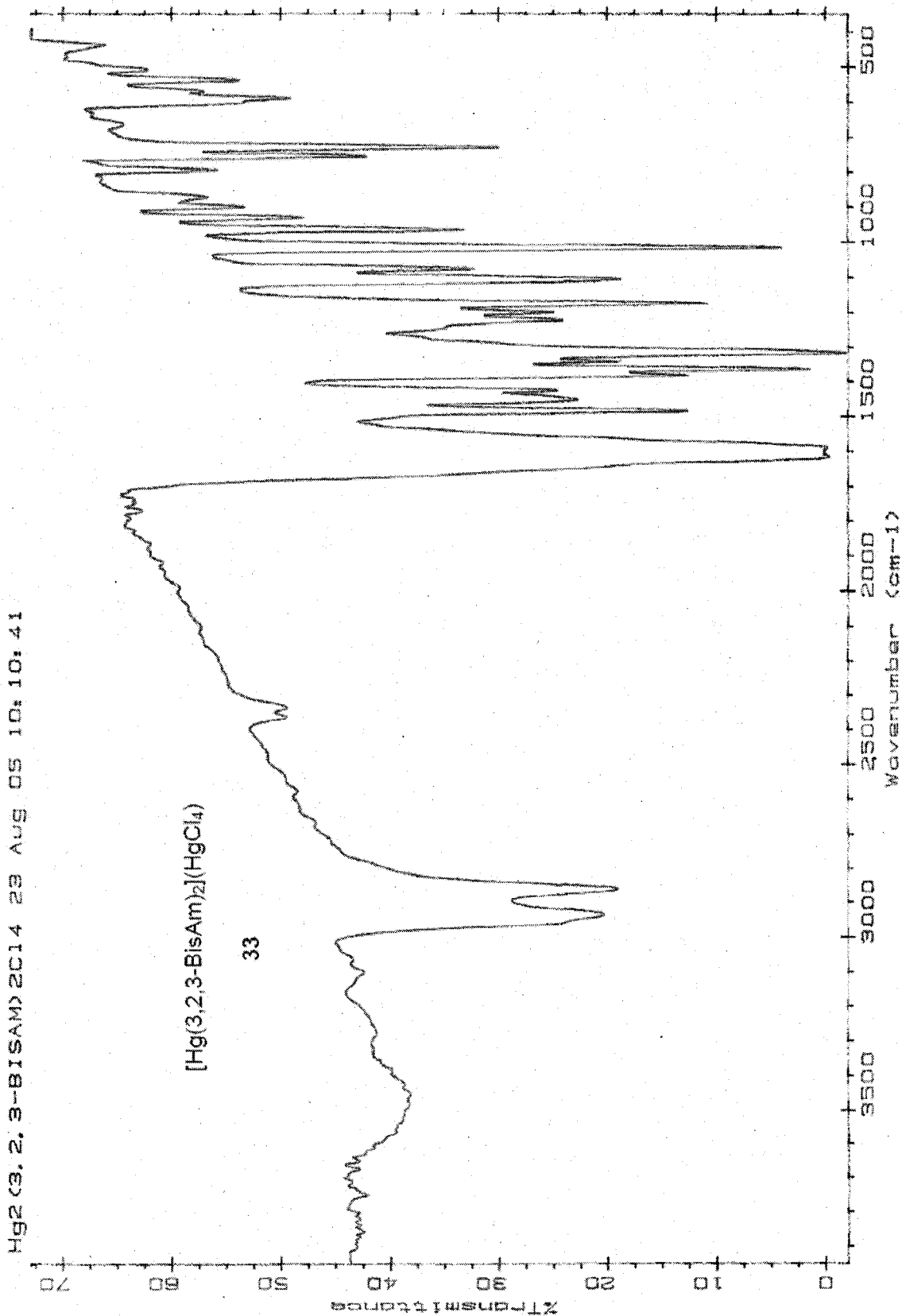
Cd(3,2,3-BISAM)3(ClO4)2 12 Jun 68 17:17:23

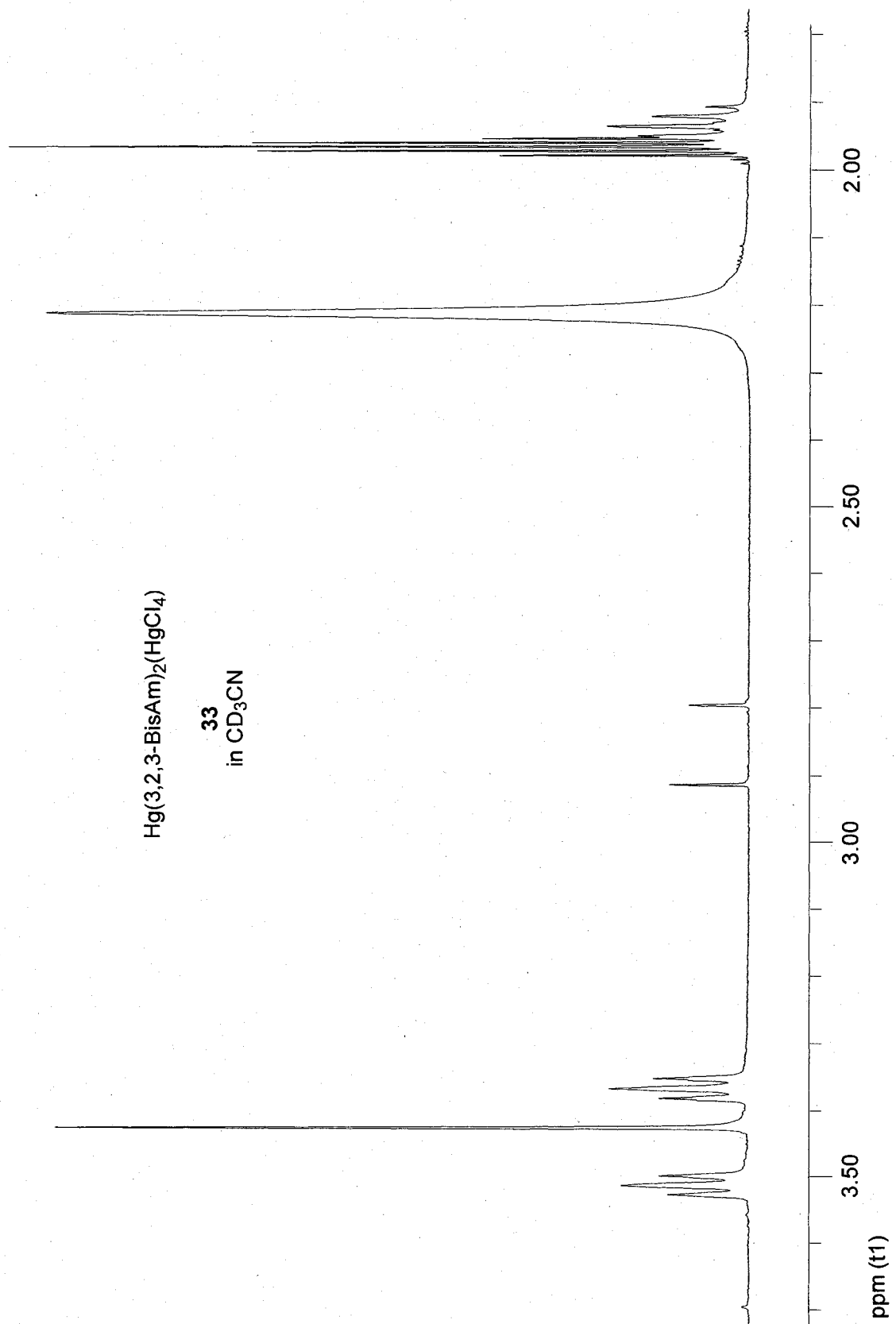


$\text{Cd}(\text{3,2,3-BisAm})_3(\text{ClO}_4)_2$   
**32**  
in  $\text{CD}_3\text{CN}$



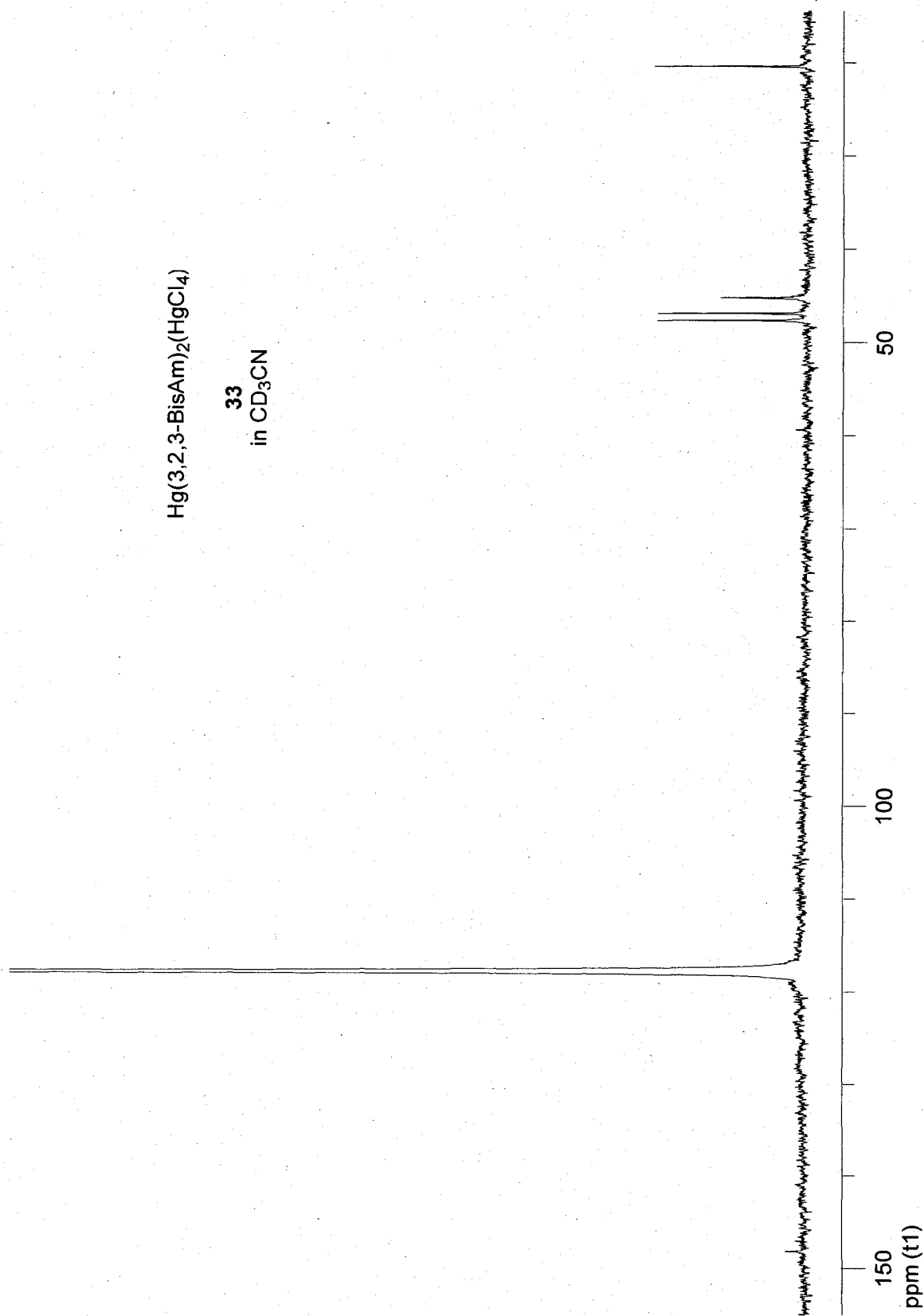


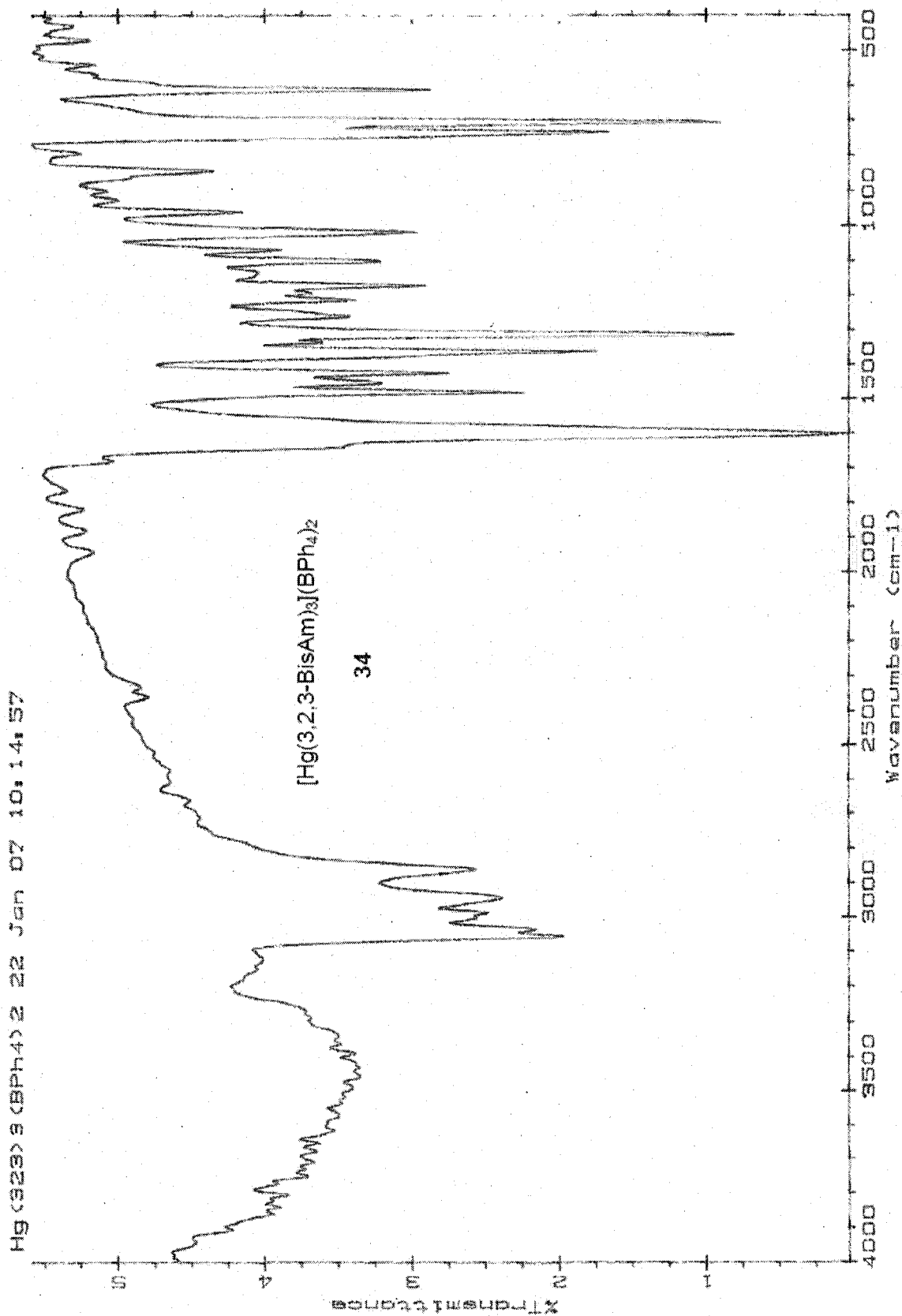




Hg(3,2,3-BisAm)<sub>2</sub>(HgCl<sub>4</sub>)

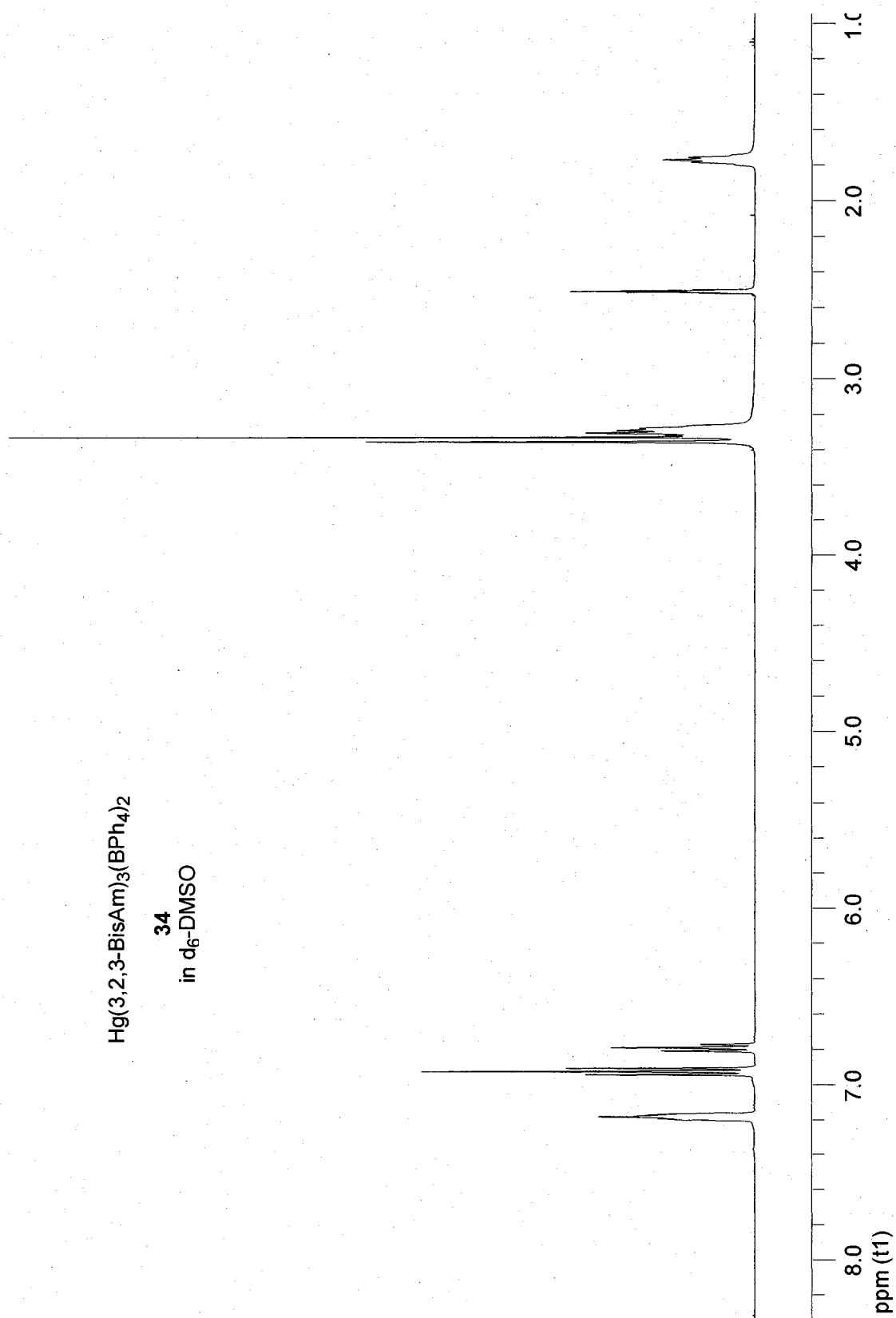
<sup>33</sup>  
in CD<sub>3</sub>CN



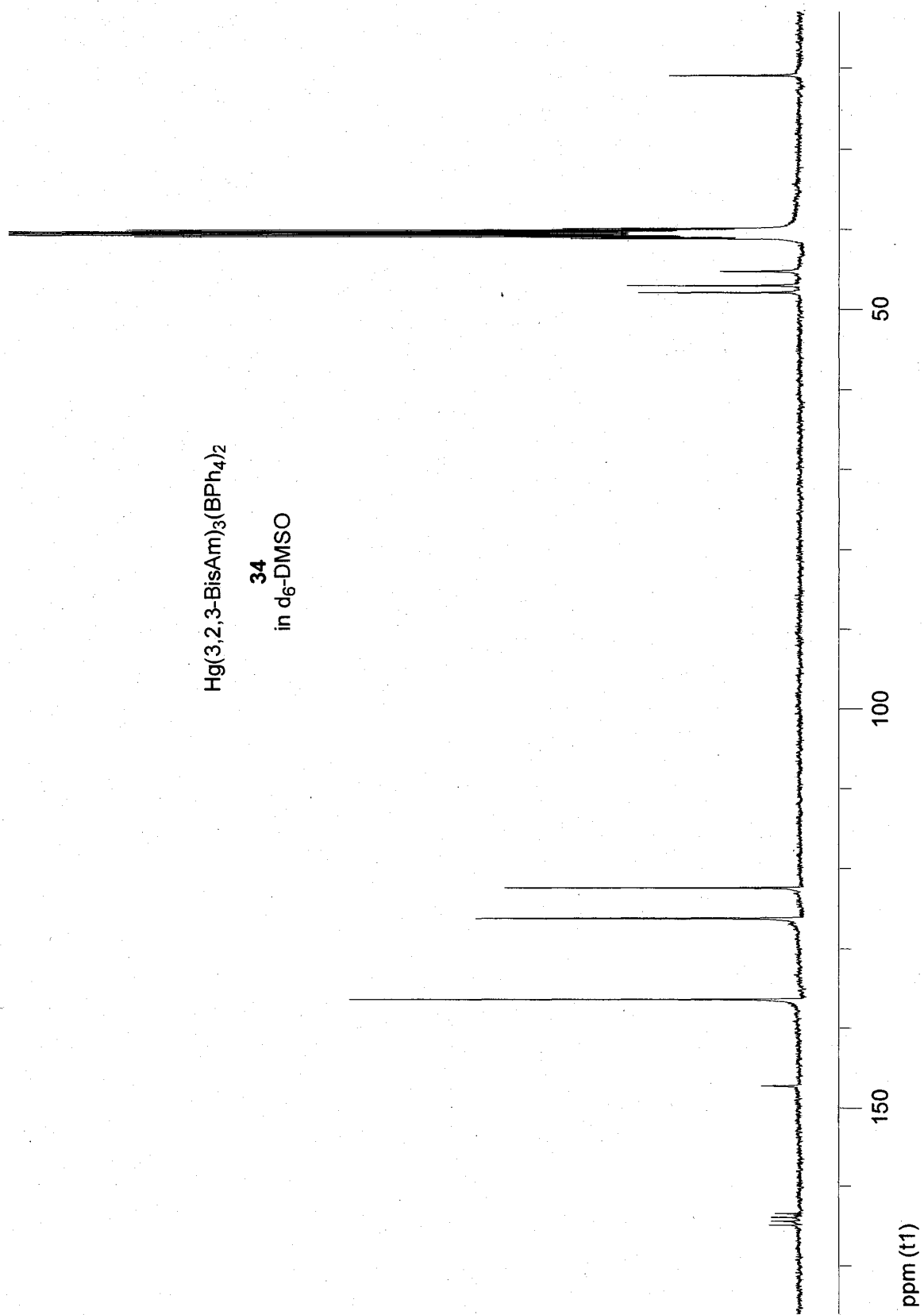


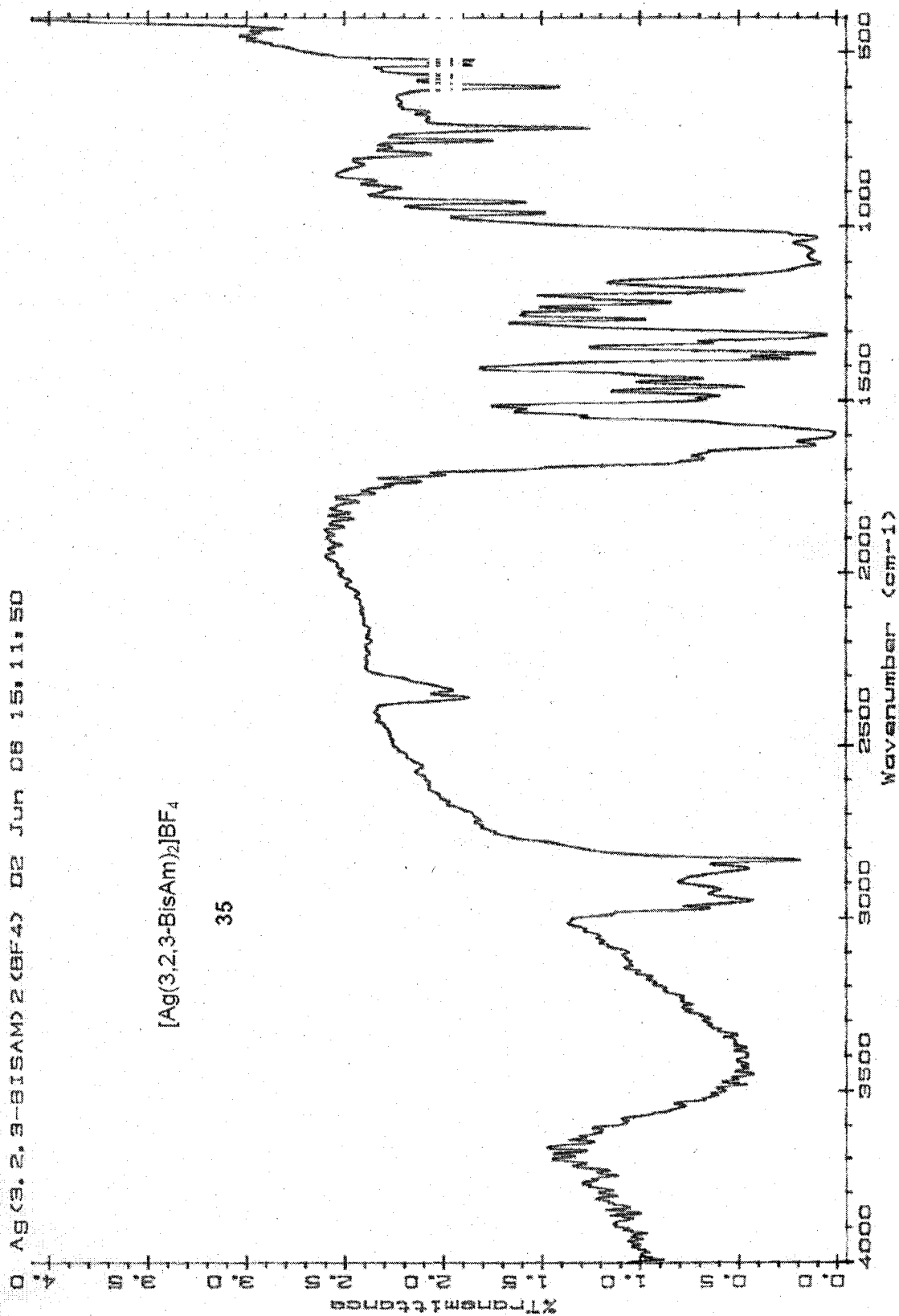


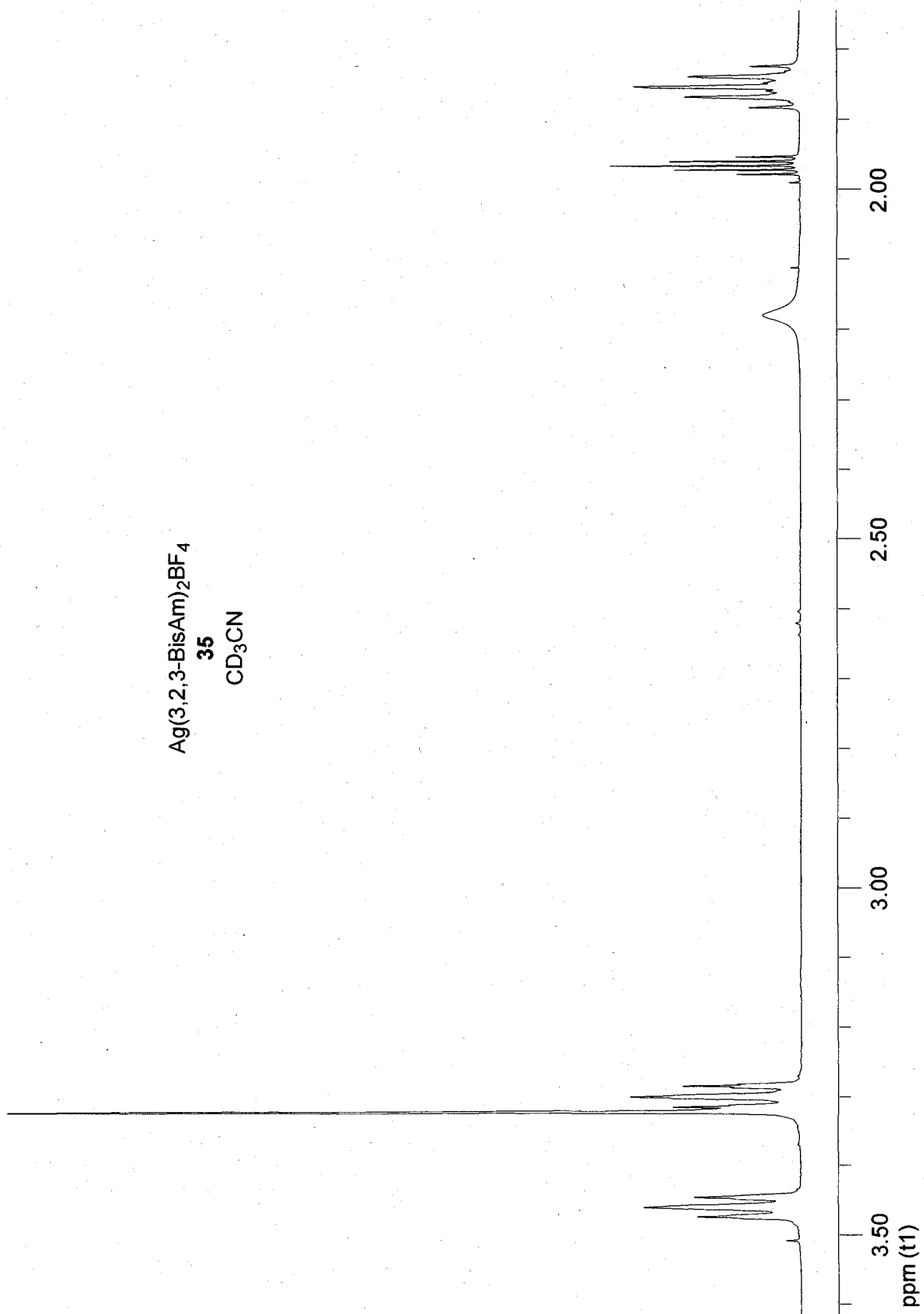
Hg(3,2,3-BisAm)<sub>3</sub>(BPh<sub>4</sub>)<sub>2</sub>  
**34**  
in d<sub>6</sub>-DMSO



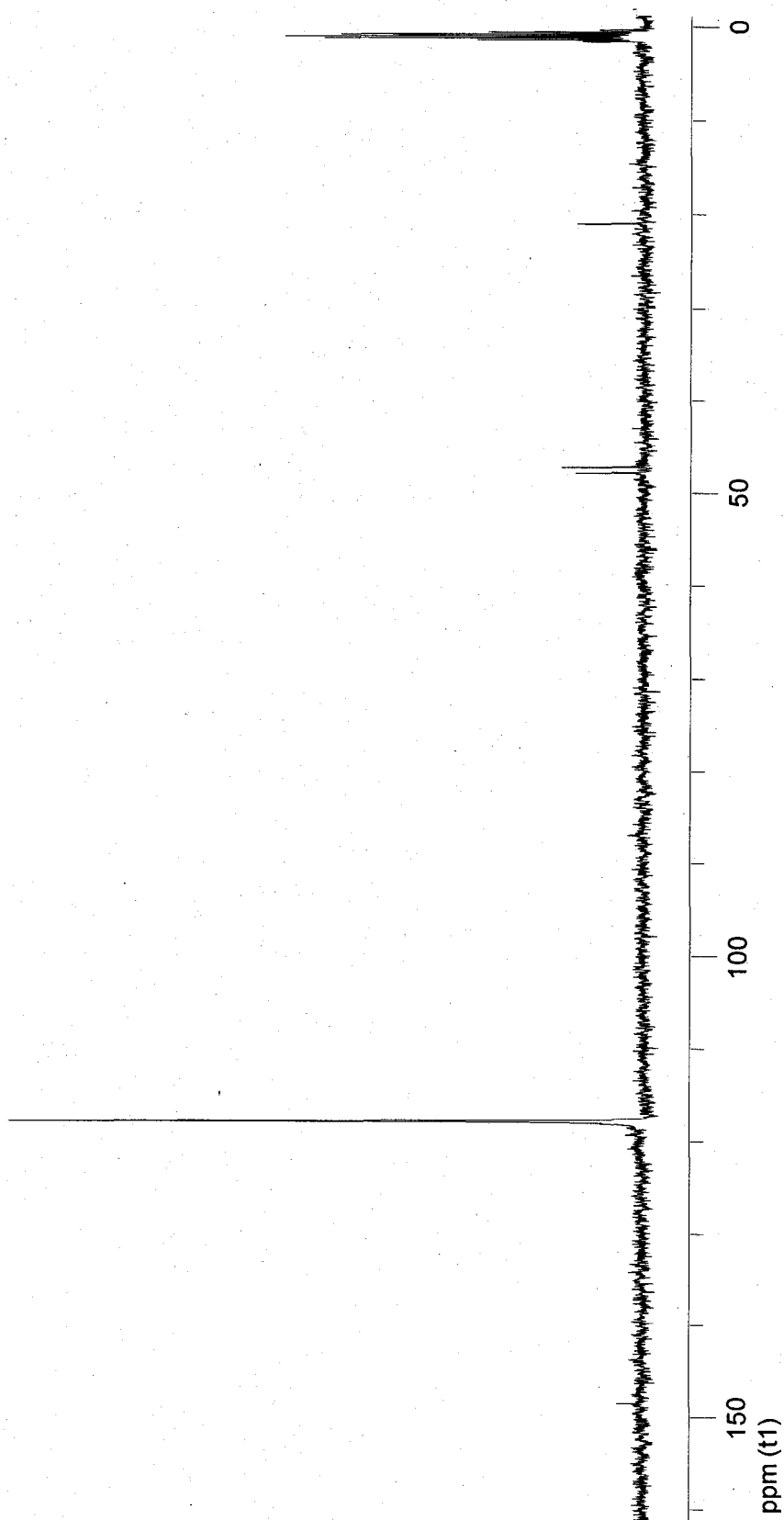
Hg(3,2,3-BisAm)<sub>3</sub>(BPh<sub>4</sub>)<sub>2</sub>  
34  
in d<sub>6</sub>-DMSO

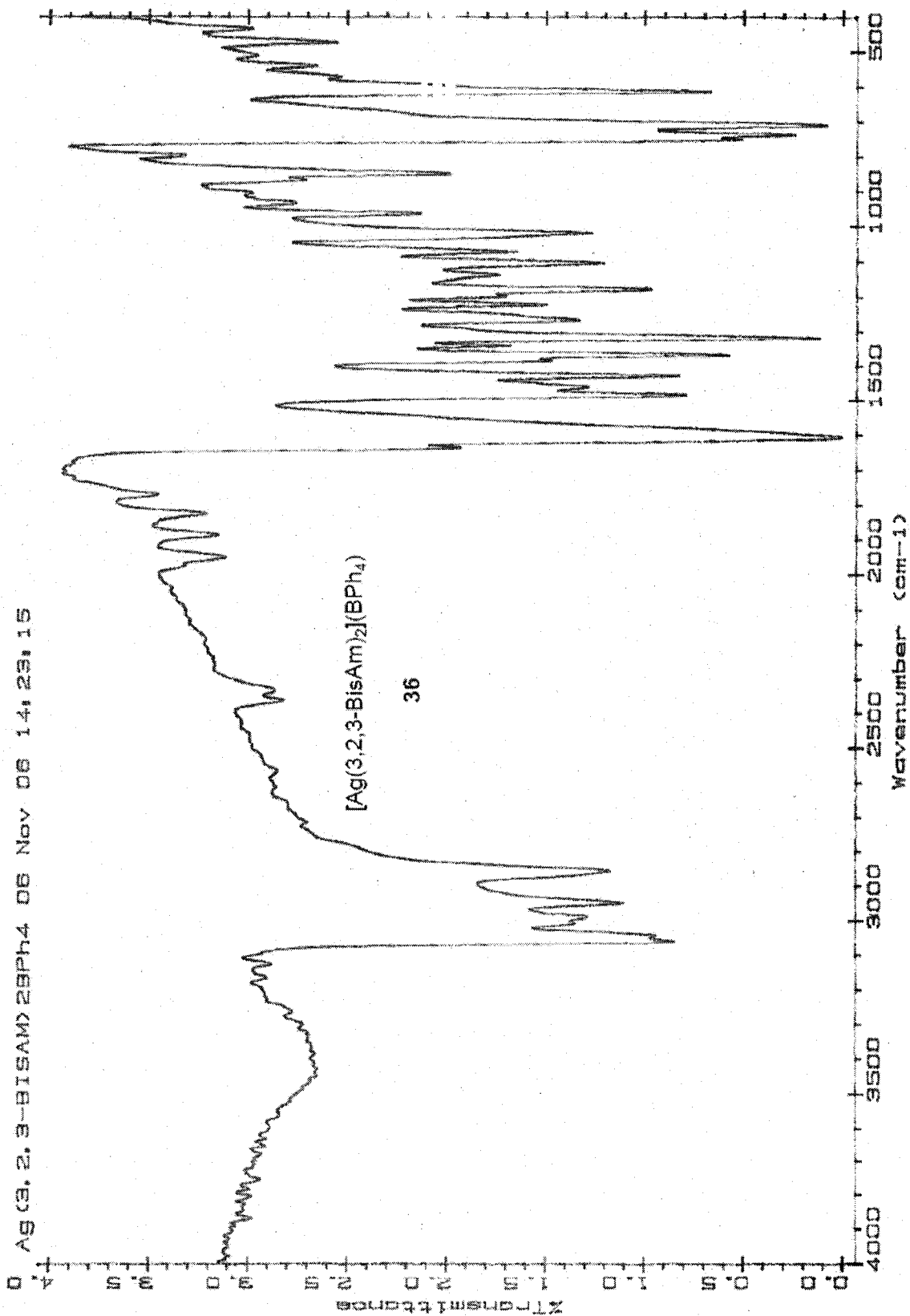




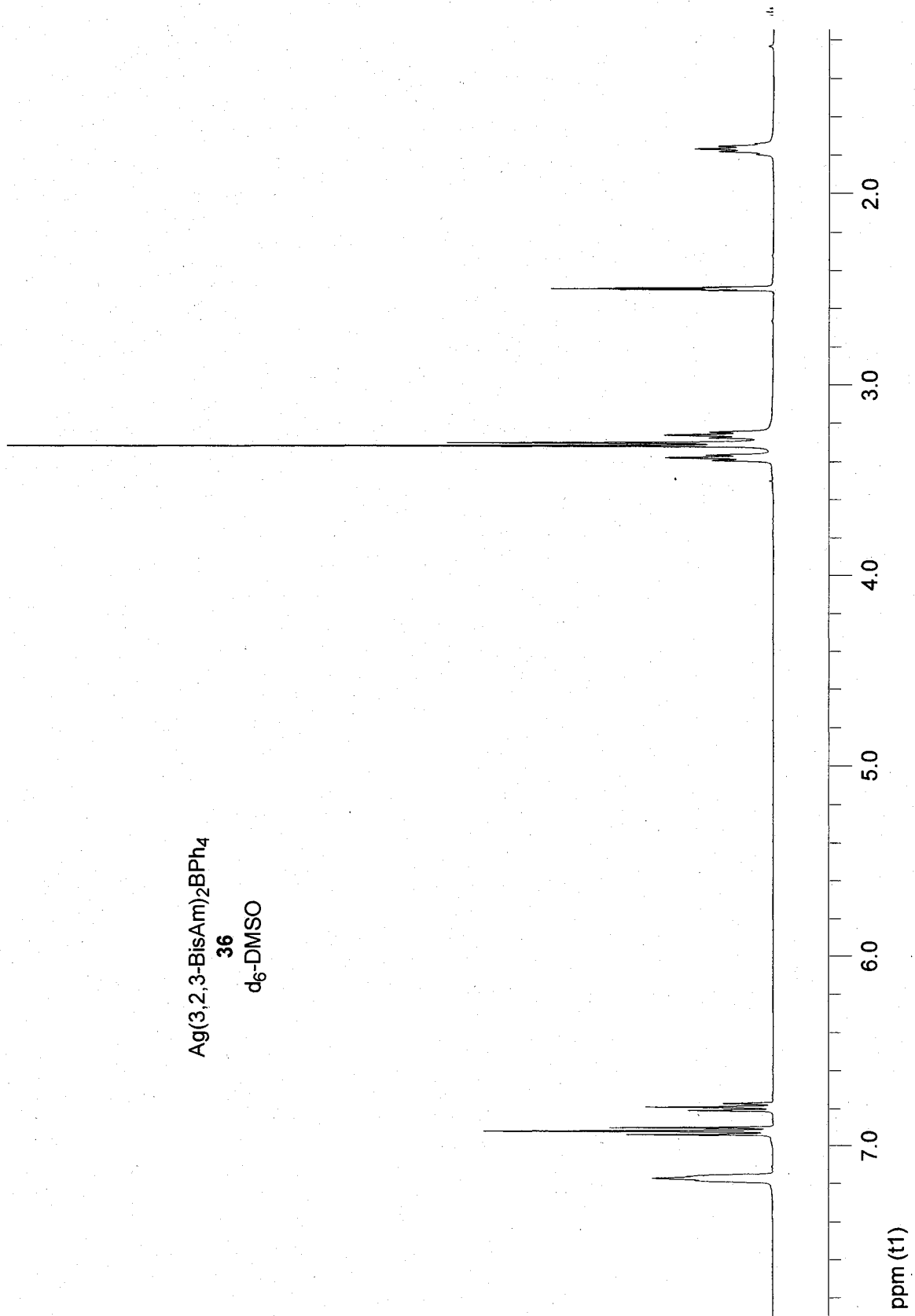


Ag(3,2,3-BisAm)<sub>2</sub>BF<sub>4</sub>  
35  
CD<sub>3</sub>CN

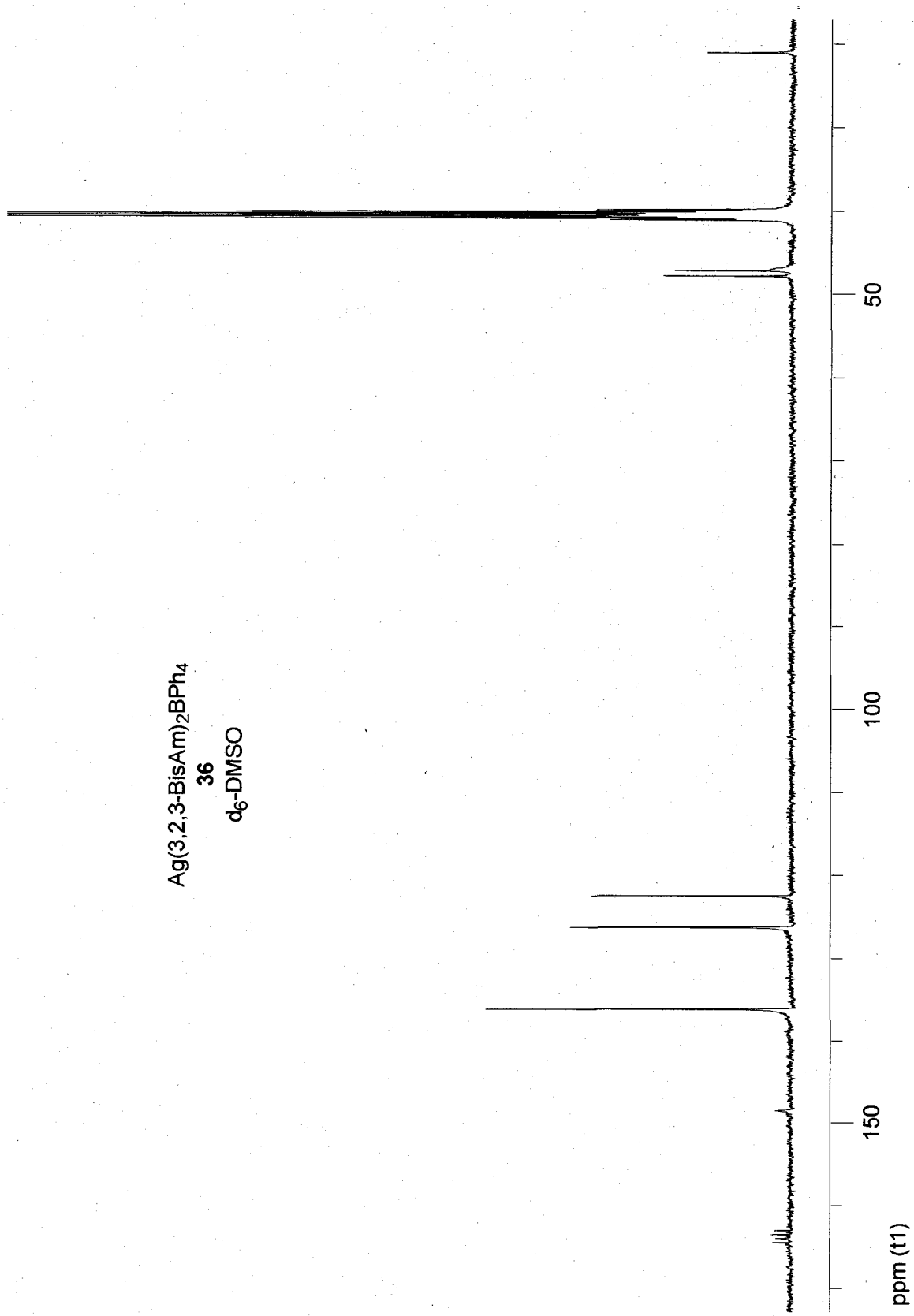




Ag(3,2,3-BisAm)<sub>2</sub>BPh<sub>4</sub>  
36  
d<sub>6</sub>-DMSO



Ag(3,2,3-BisAm)<sub>2</sub>BPh<sub>4</sub>  
36  
d<sub>6</sub>-DMSO

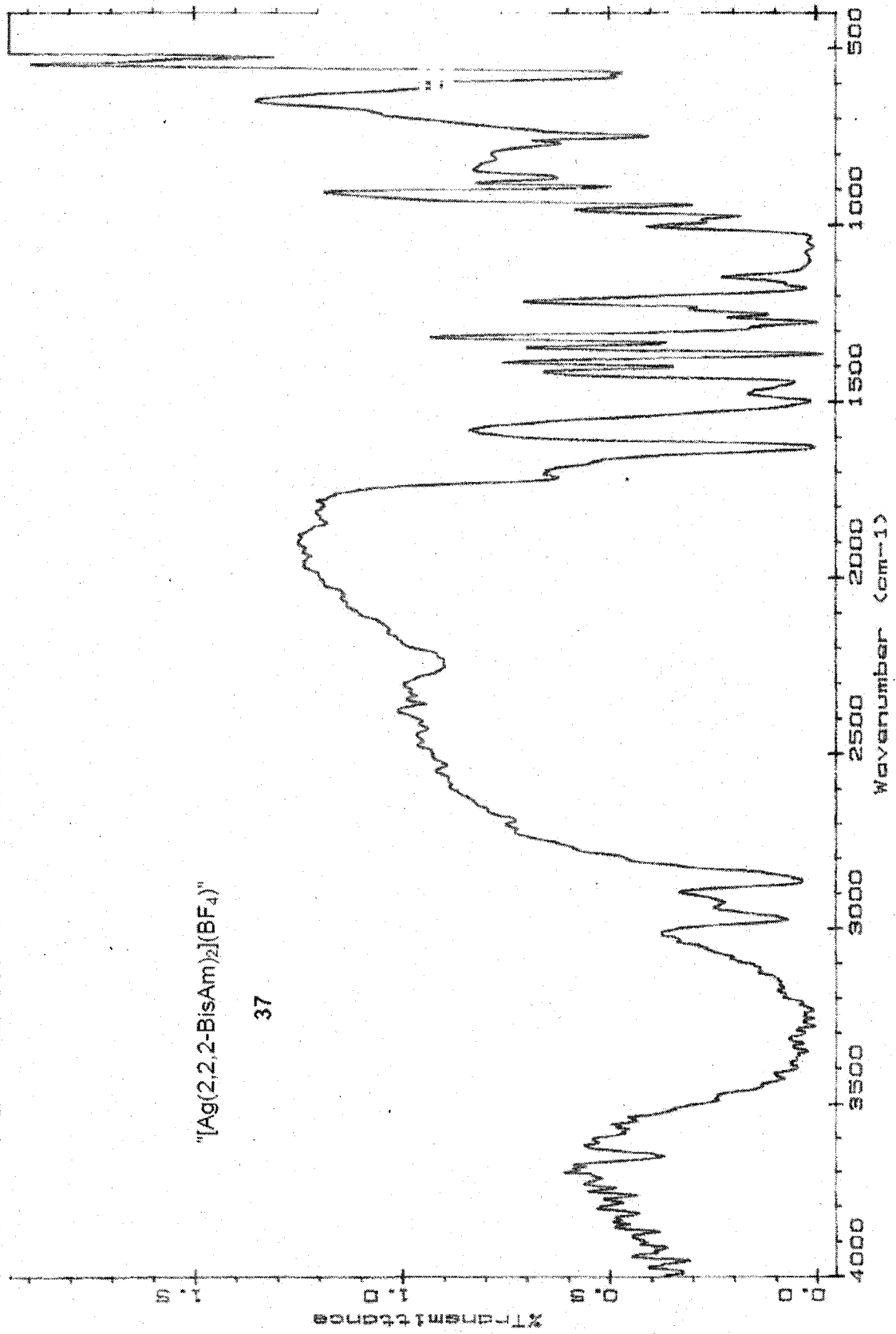


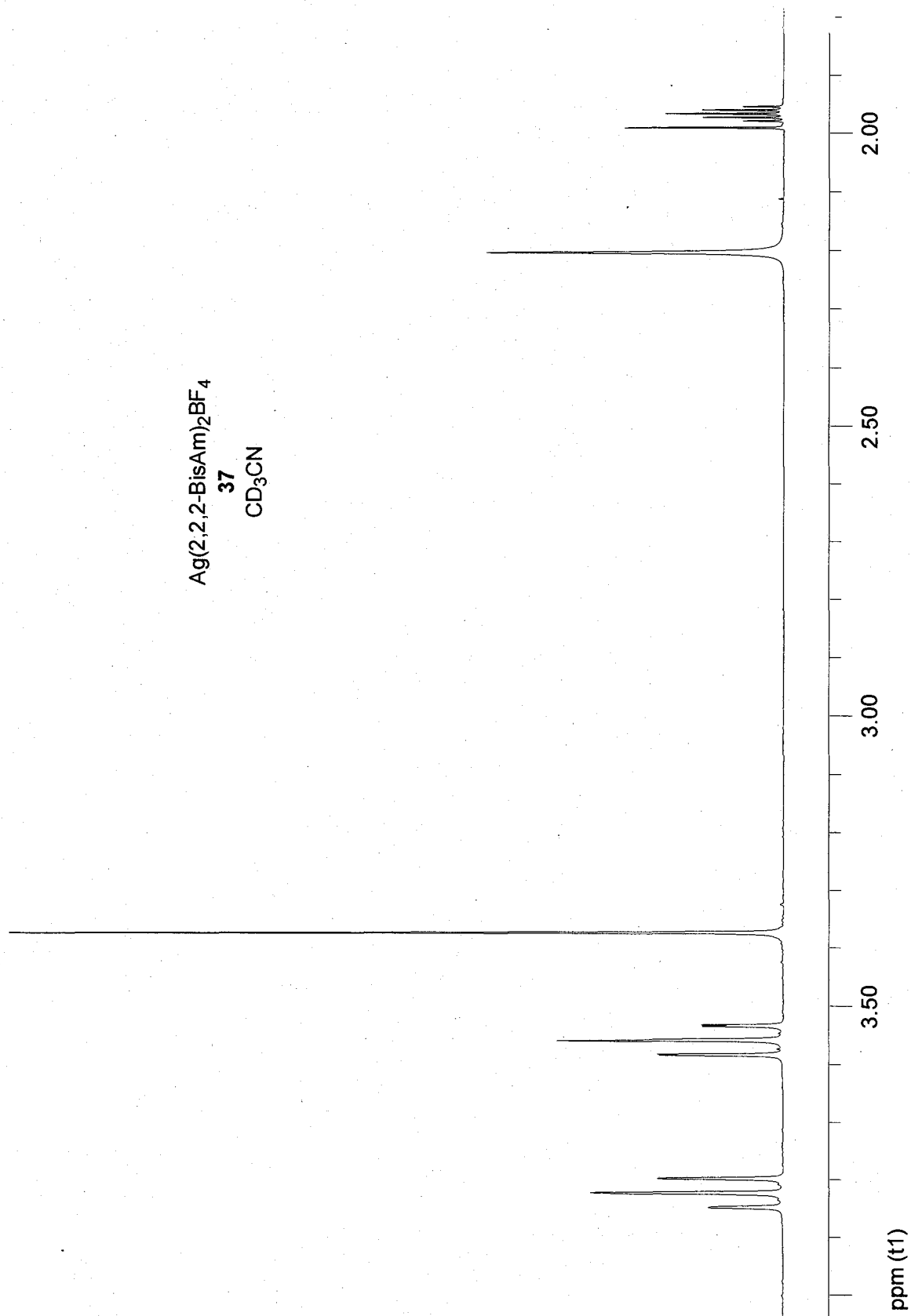


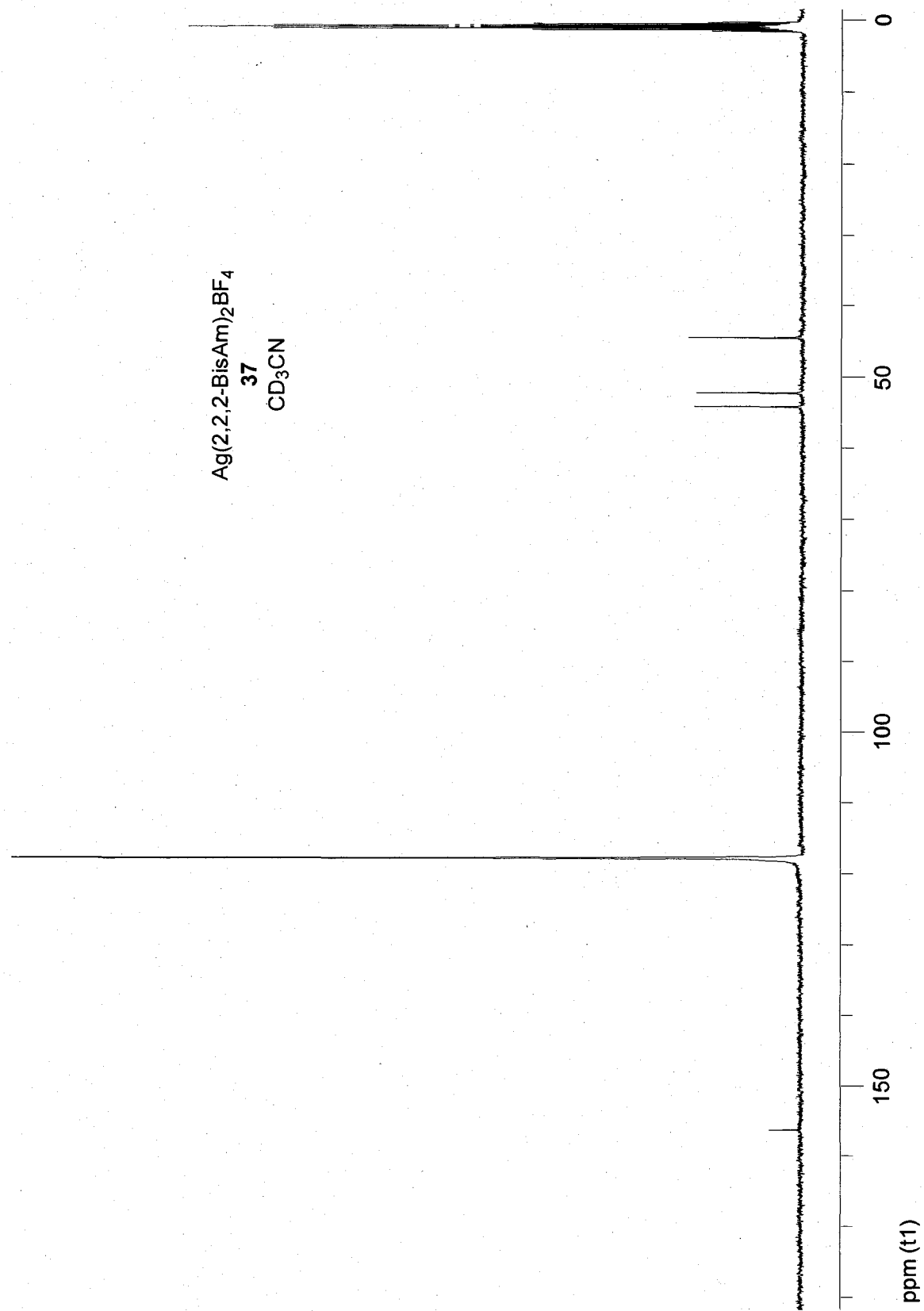
Nicolet 205 02 Jun 88 15:48:01

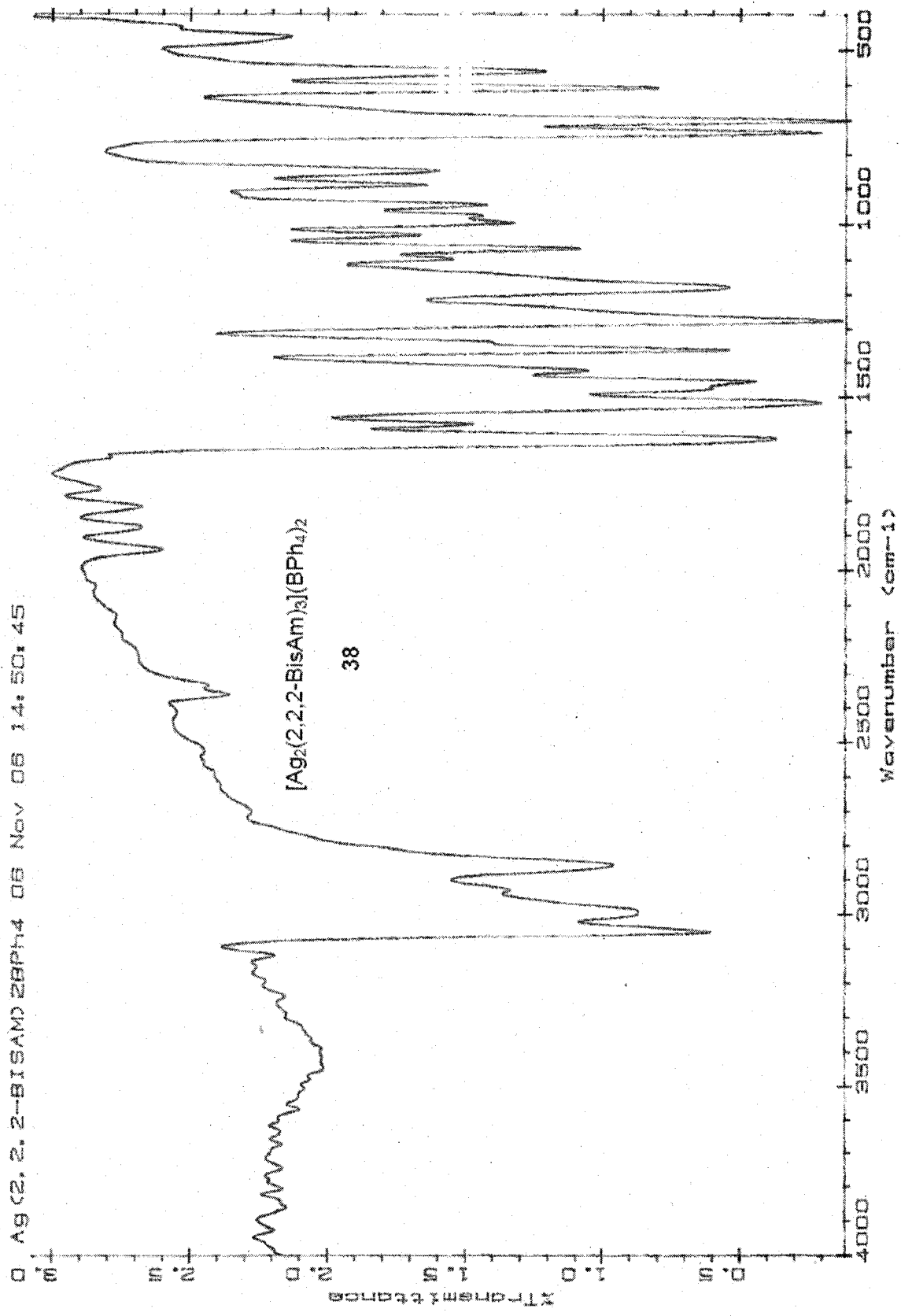
"[Ag(2,2-BisAm)<sub>2</sub>](BF<sub>4</sub>)"

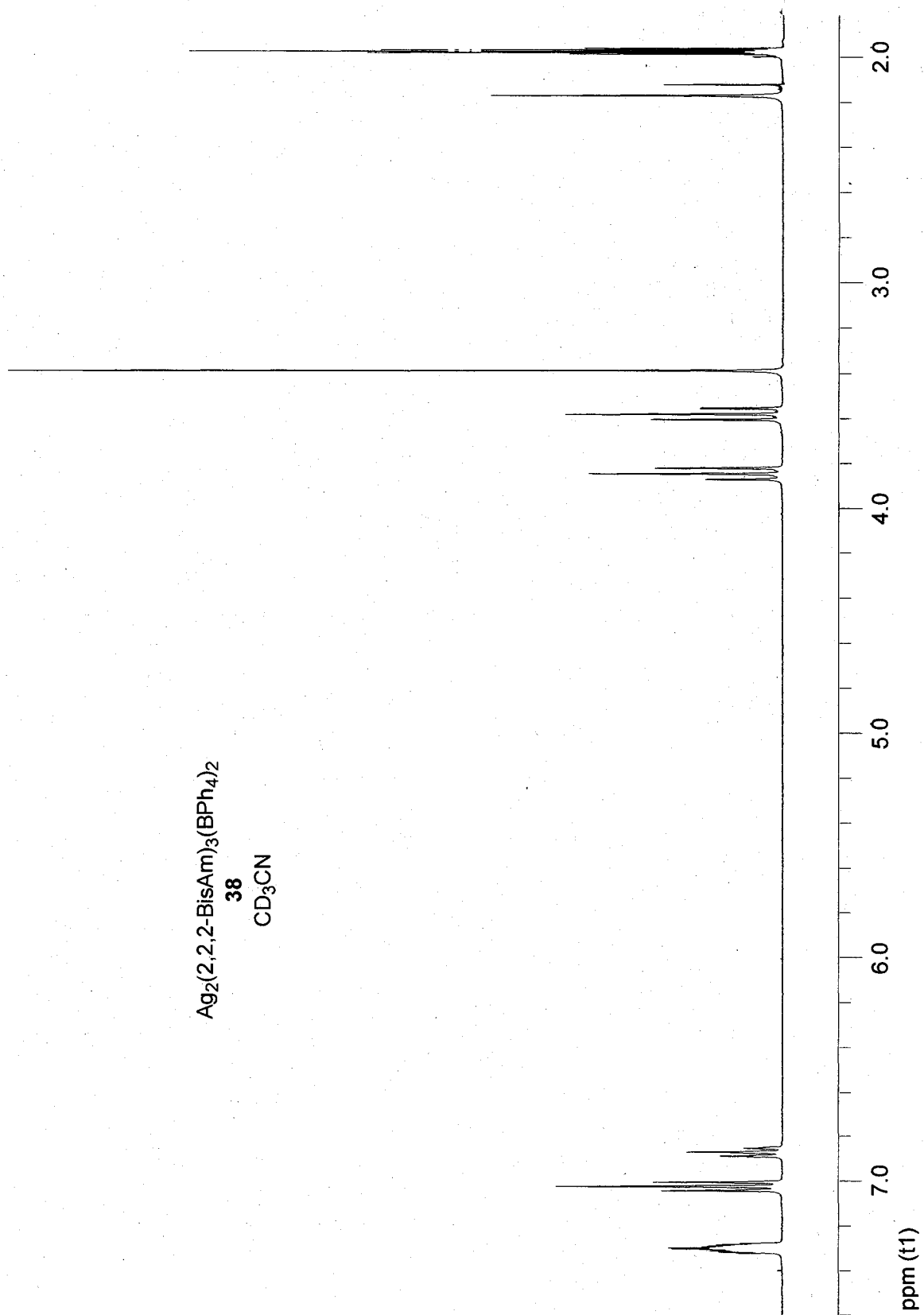
37



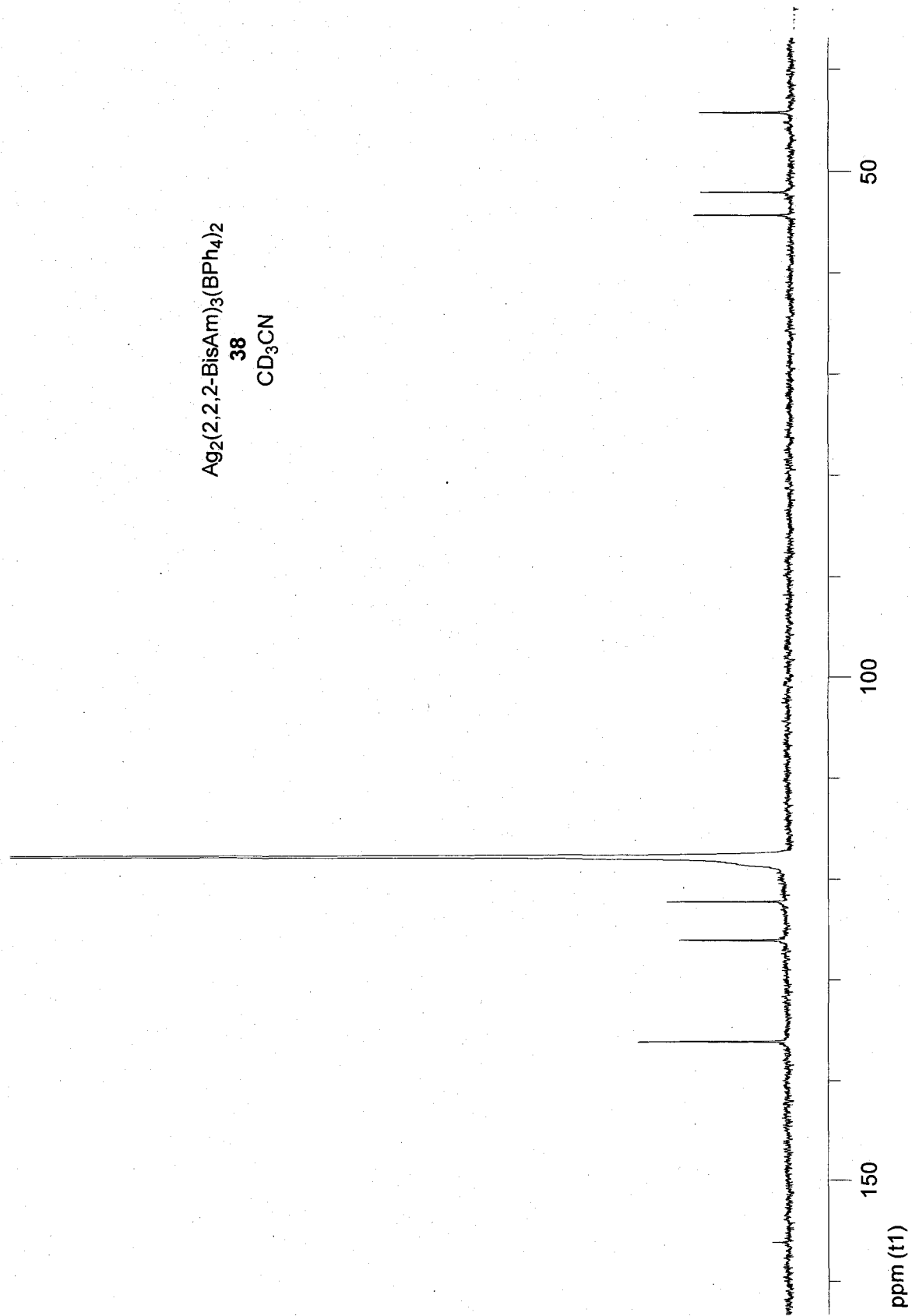


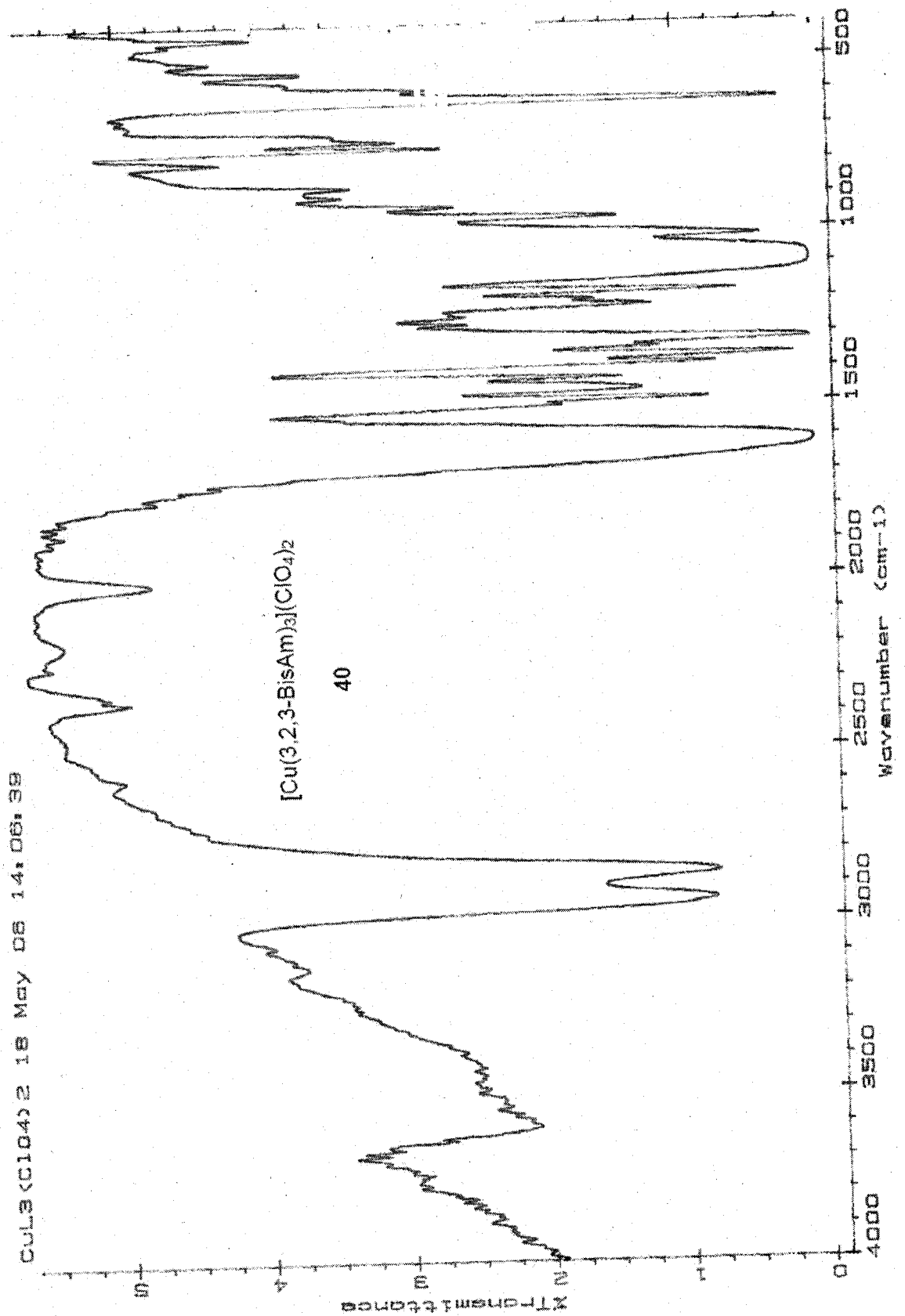


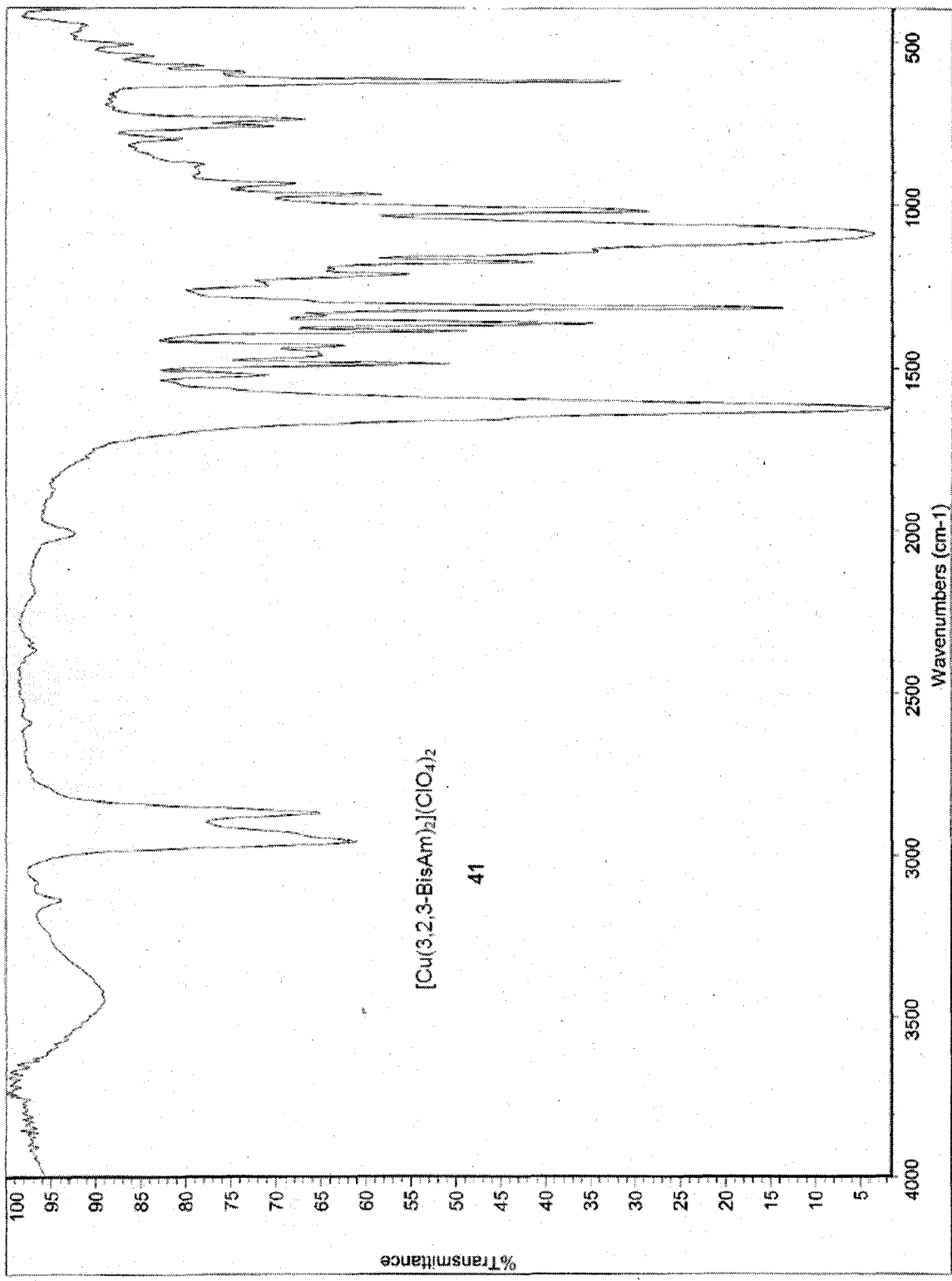




Ag<sub>2</sub>(2,2,2-BisAm)<sub>3</sub>(BPh<sub>4</sub>)<sub>2</sub>  
38  
CD<sub>3</sub>CN

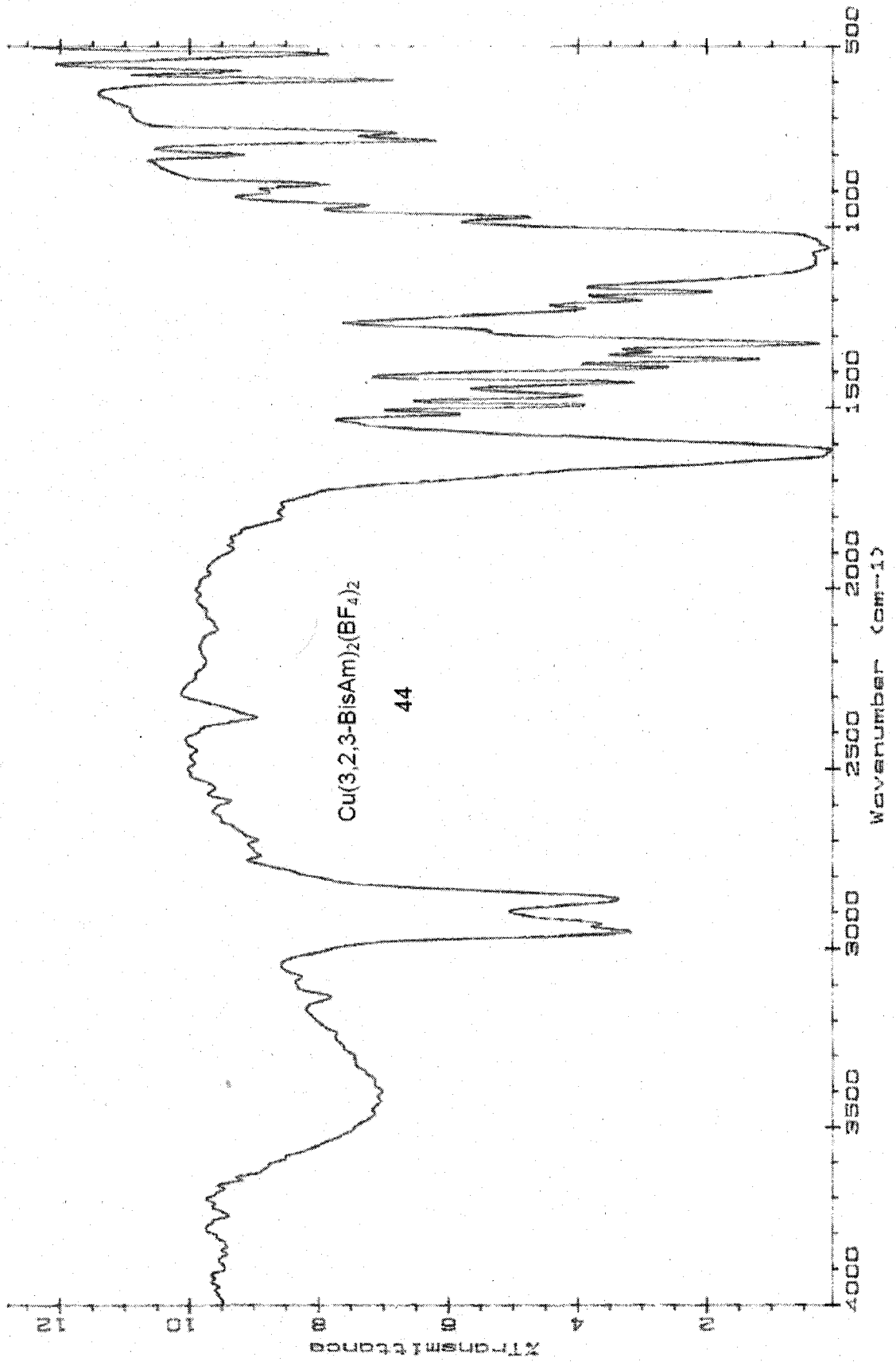




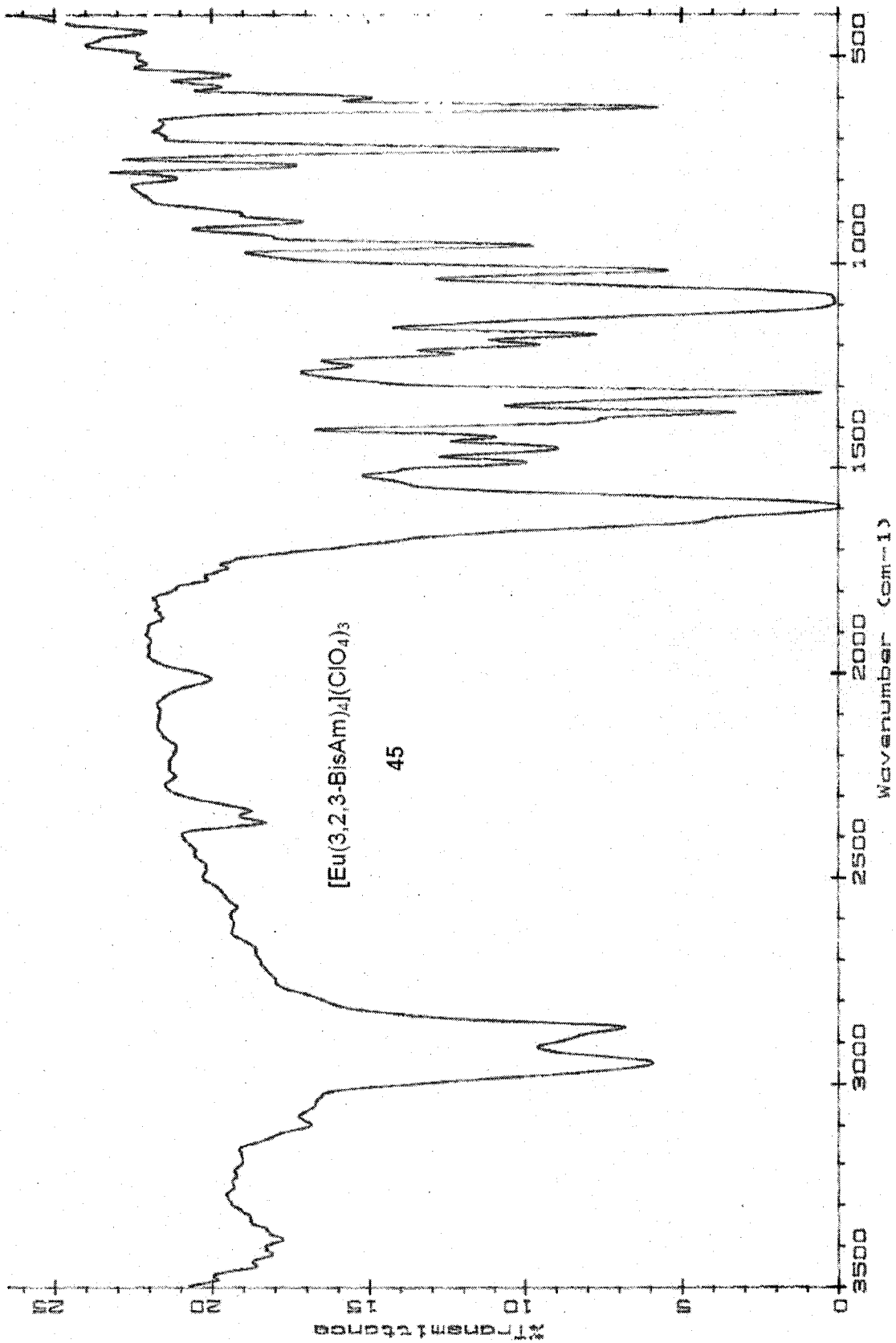


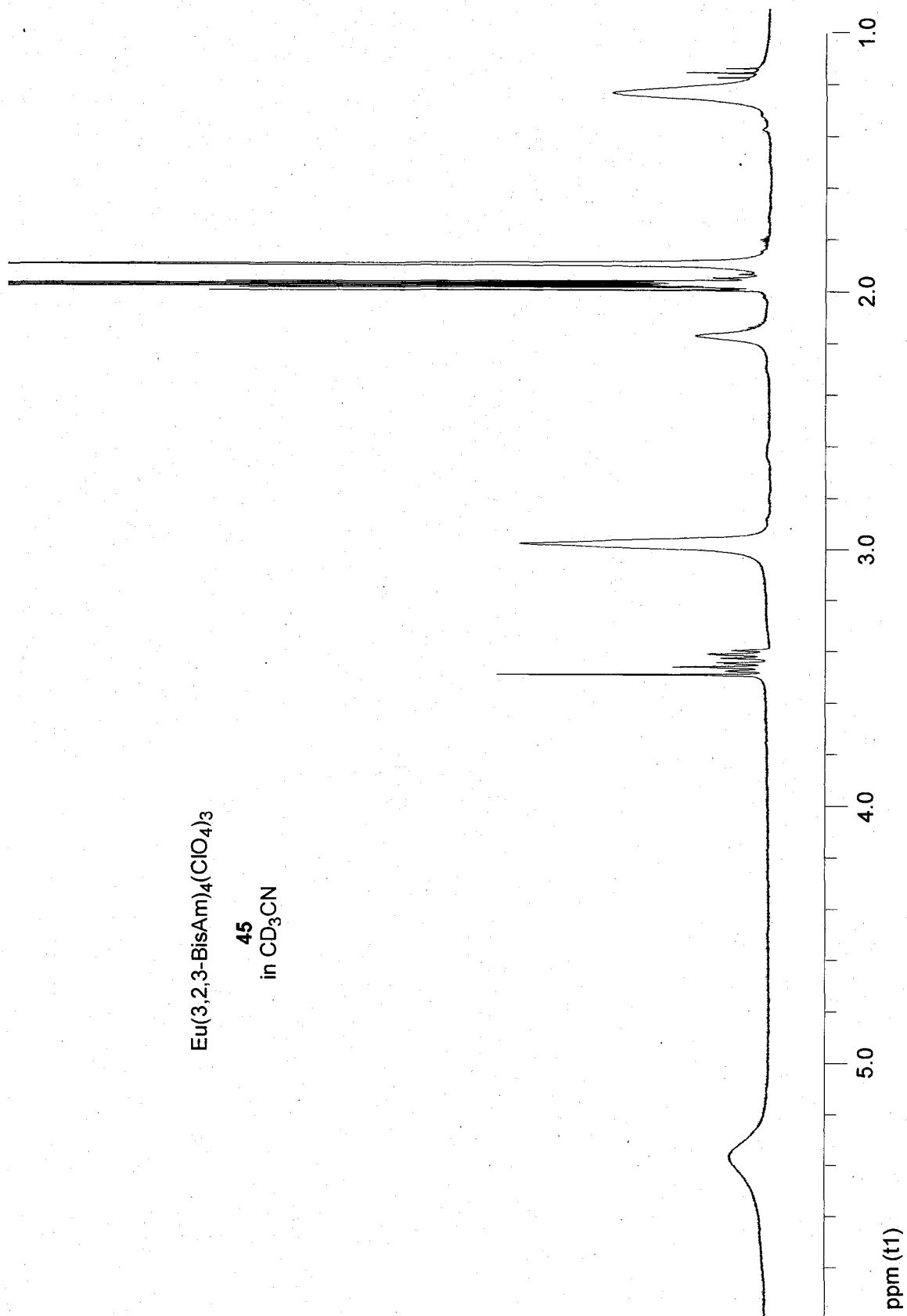


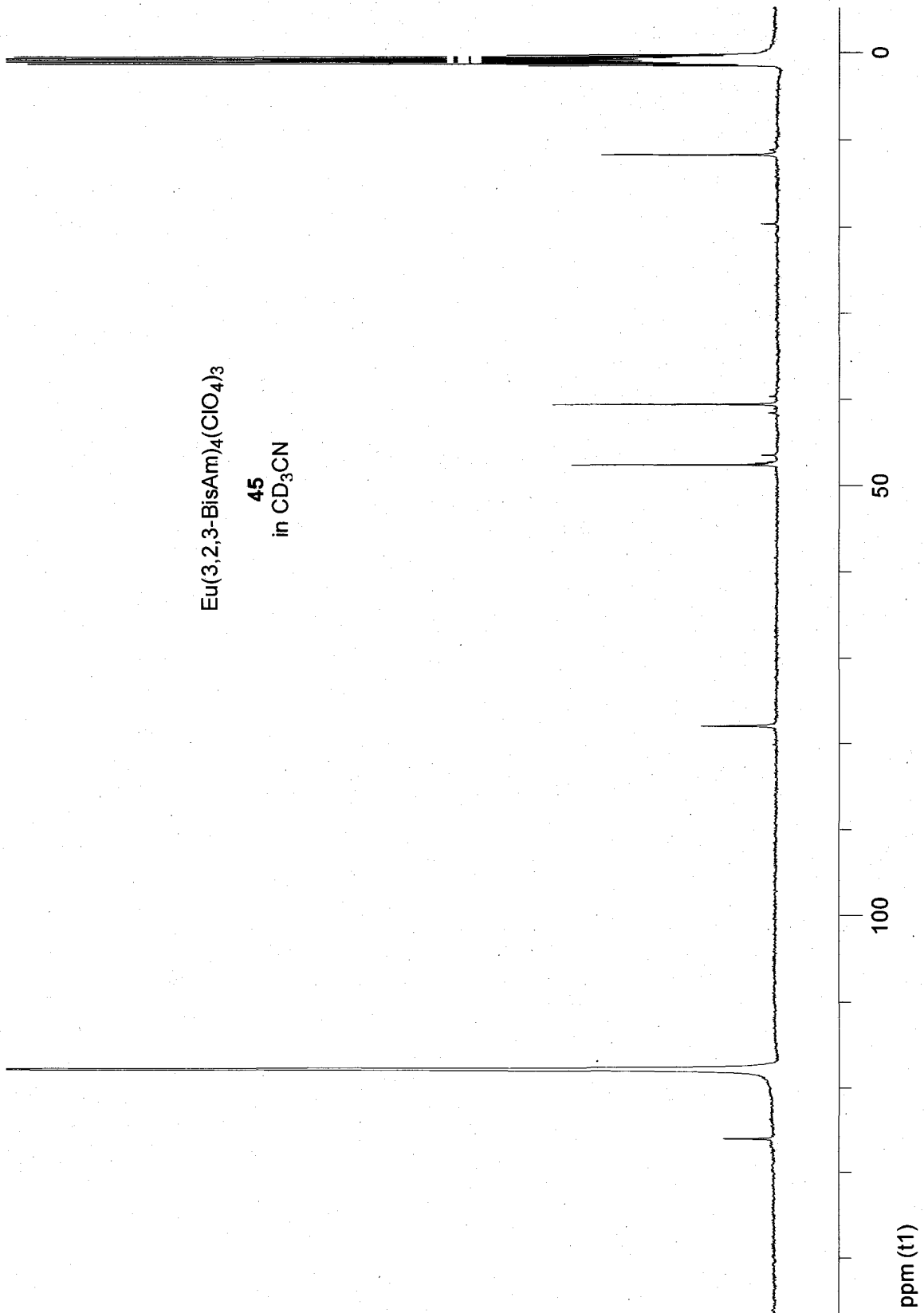
Cu(323)2(BF4)2 08 Jul 07 09:18:15

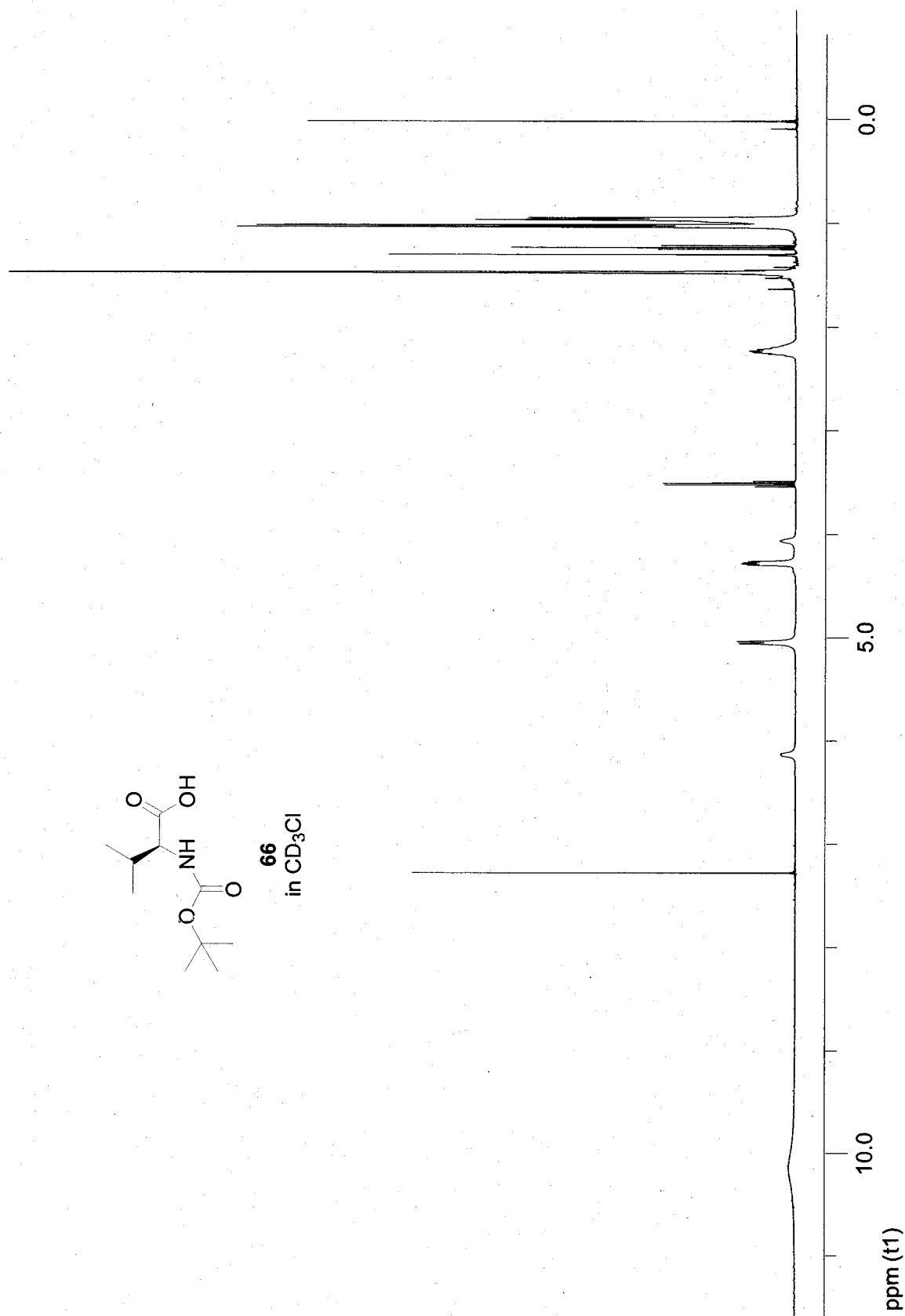
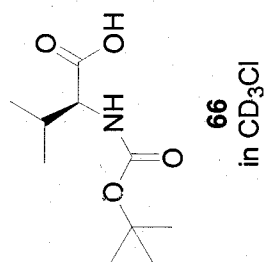


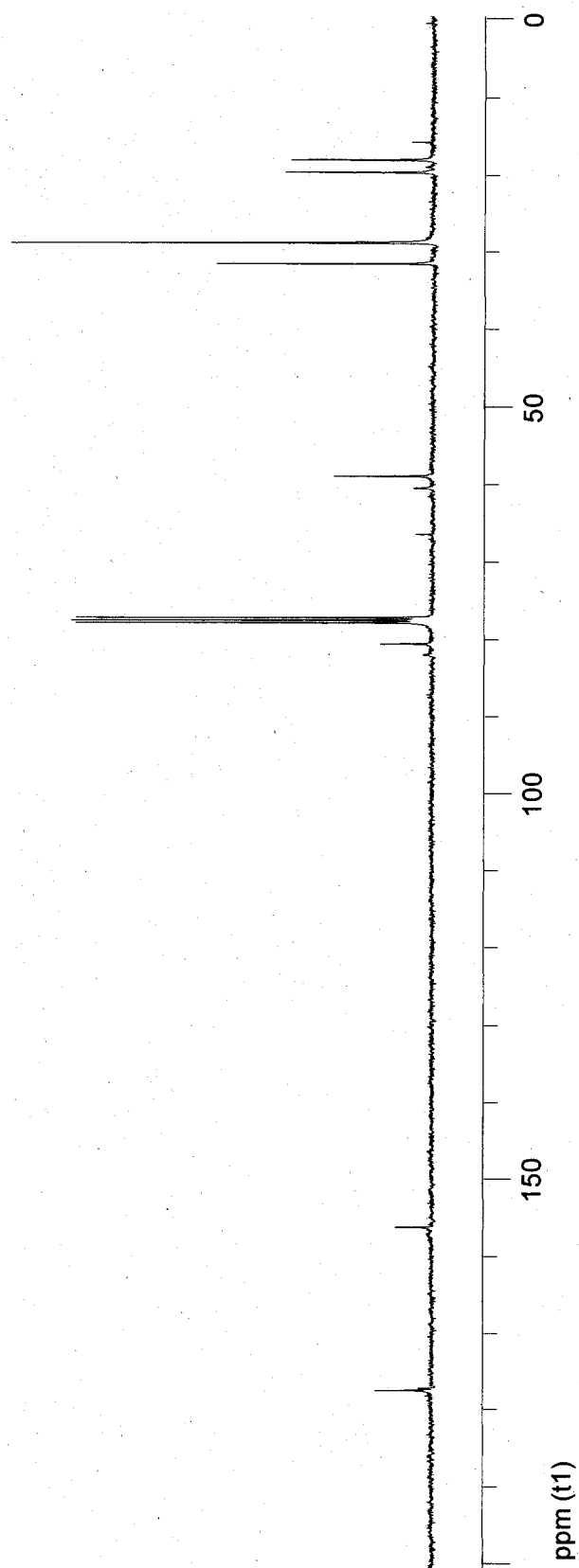
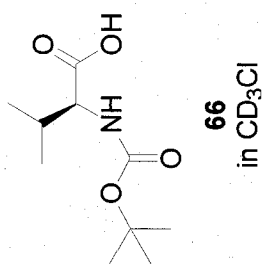
EUL4(C104)3 03 Jun 07 19:40:33

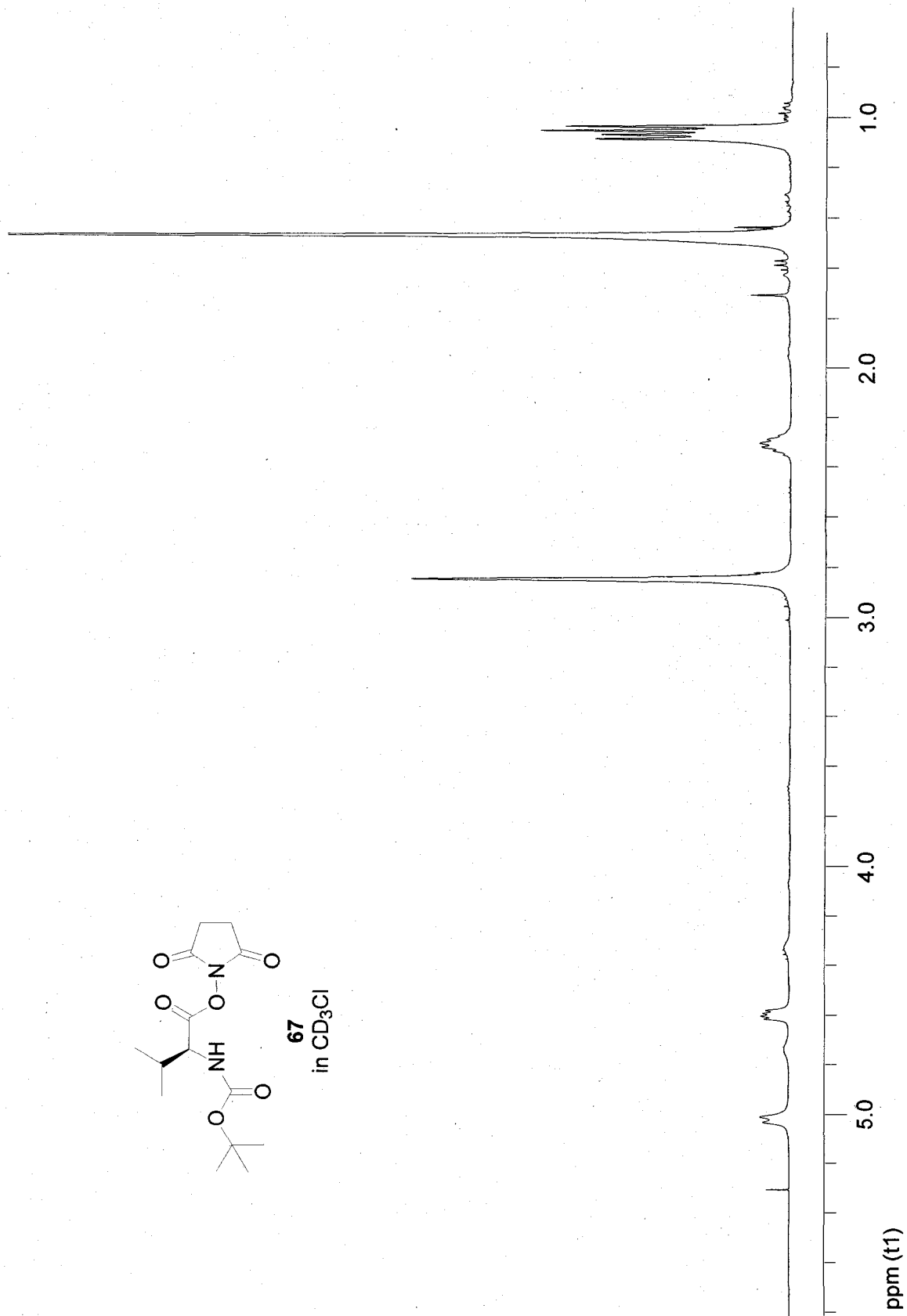
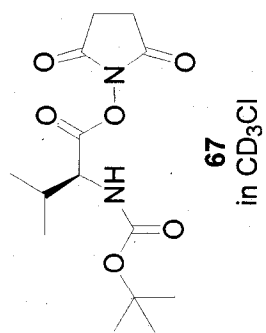


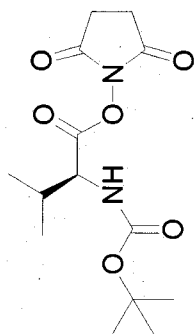




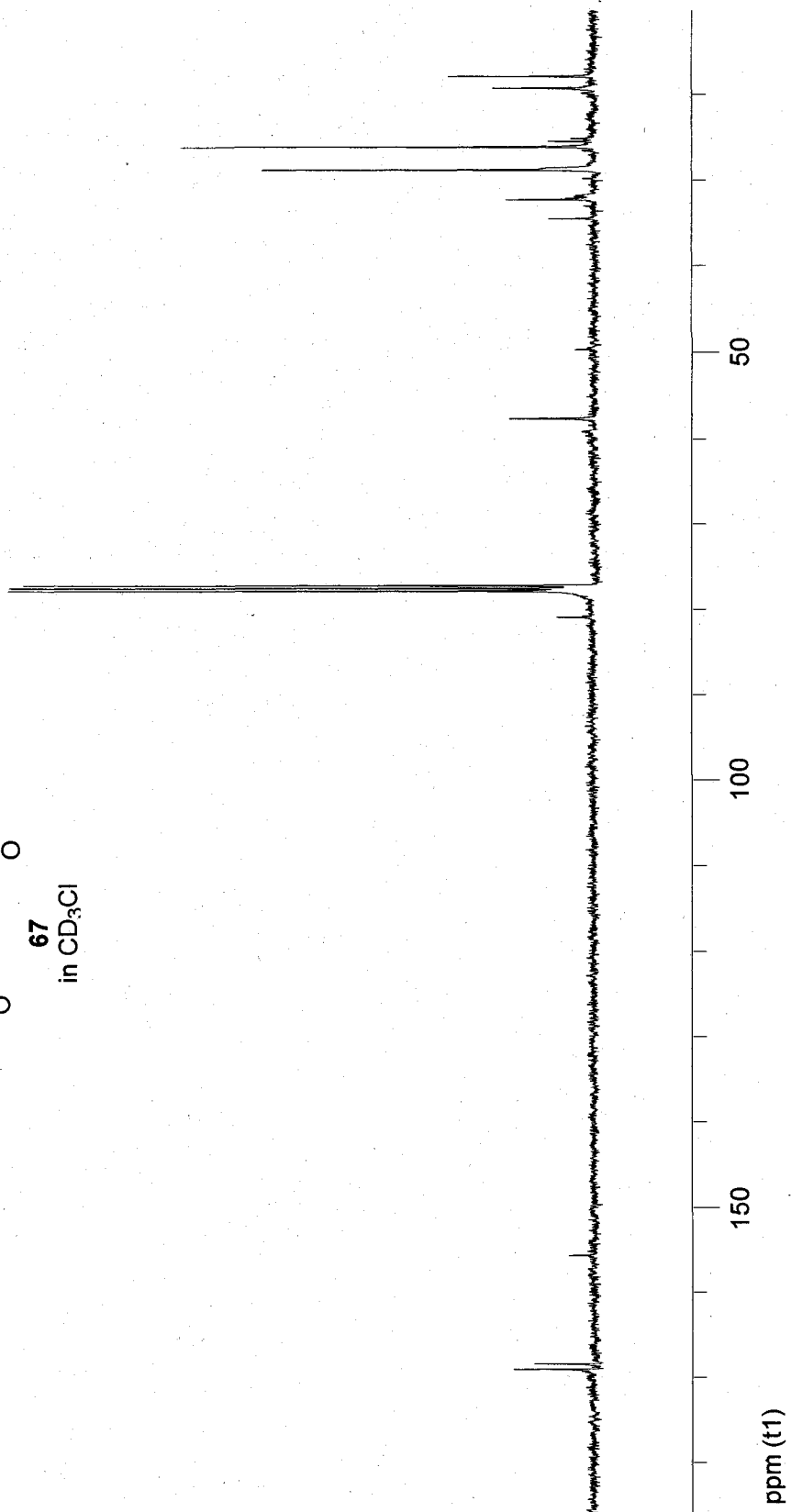




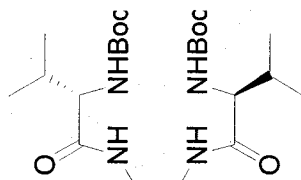




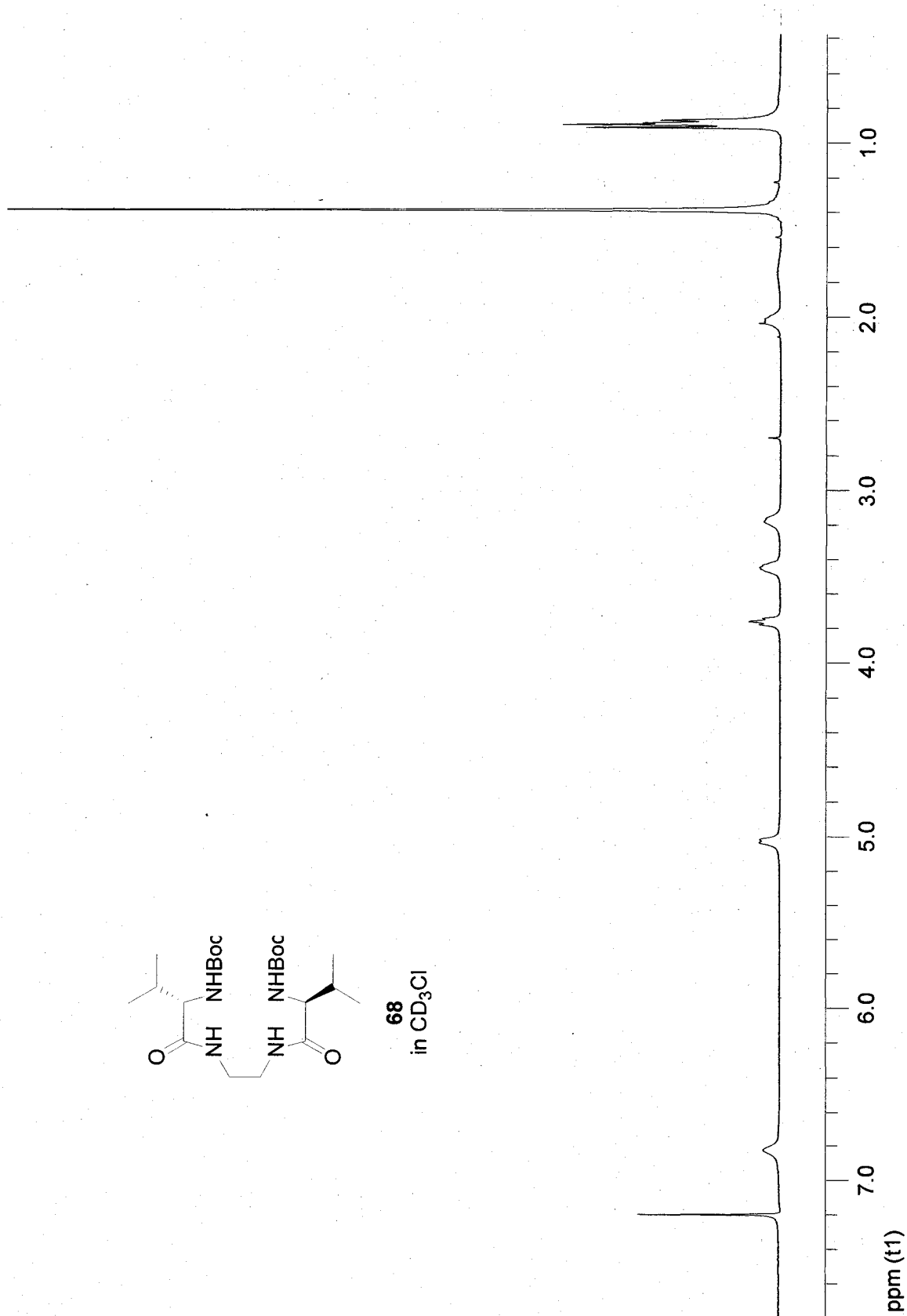
**67**  
in CD<sub>3</sub>Cl

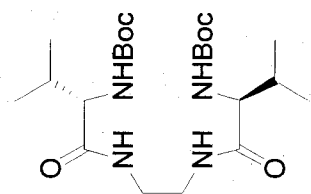




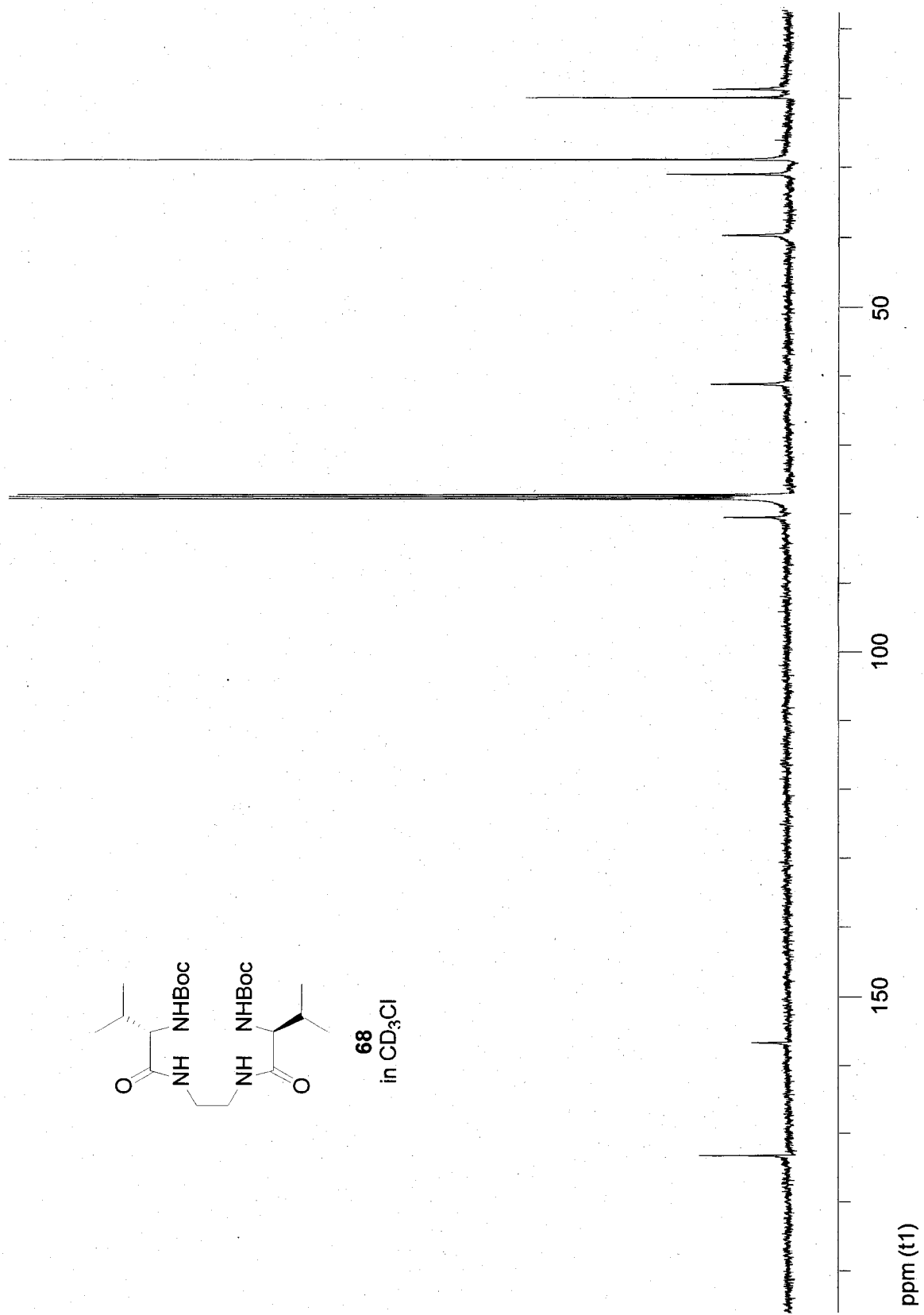


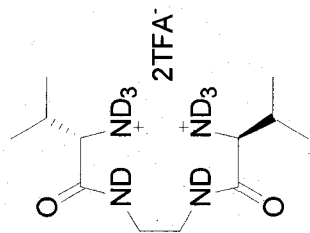
**68**  
in CD<sub>3</sub>Cl



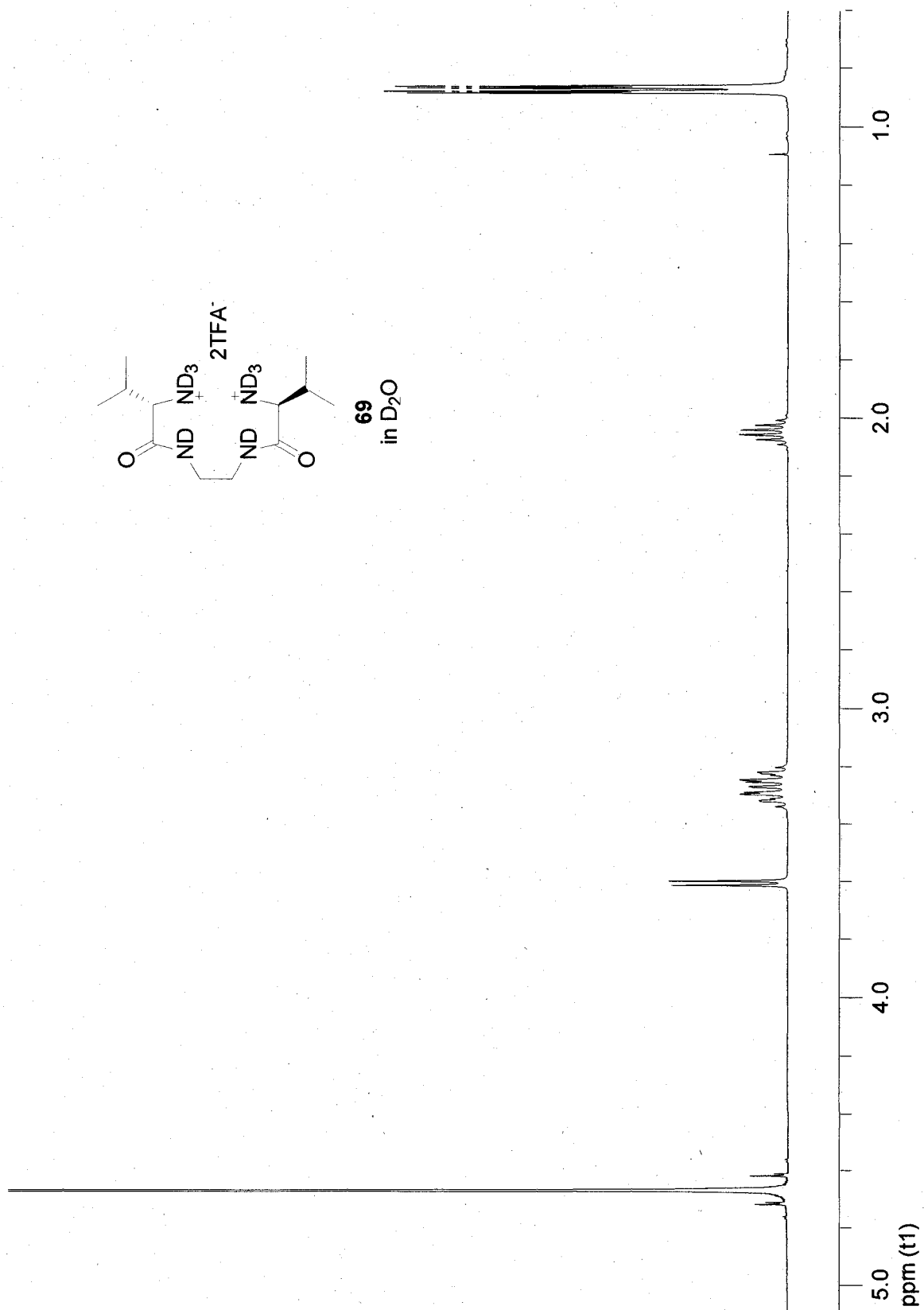


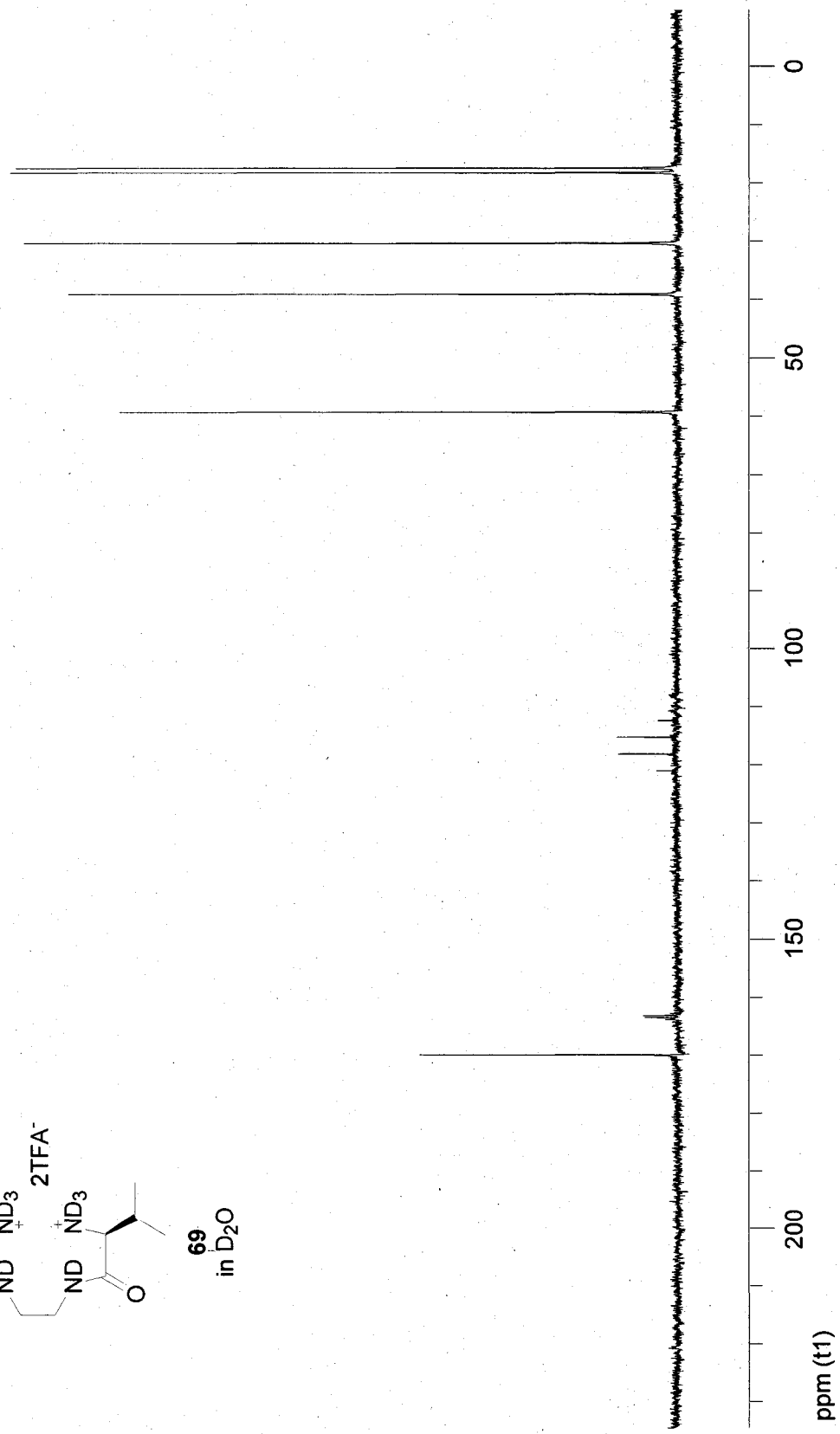
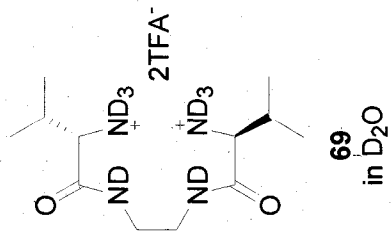
**68**  
in CD<sub>3</sub>Cl

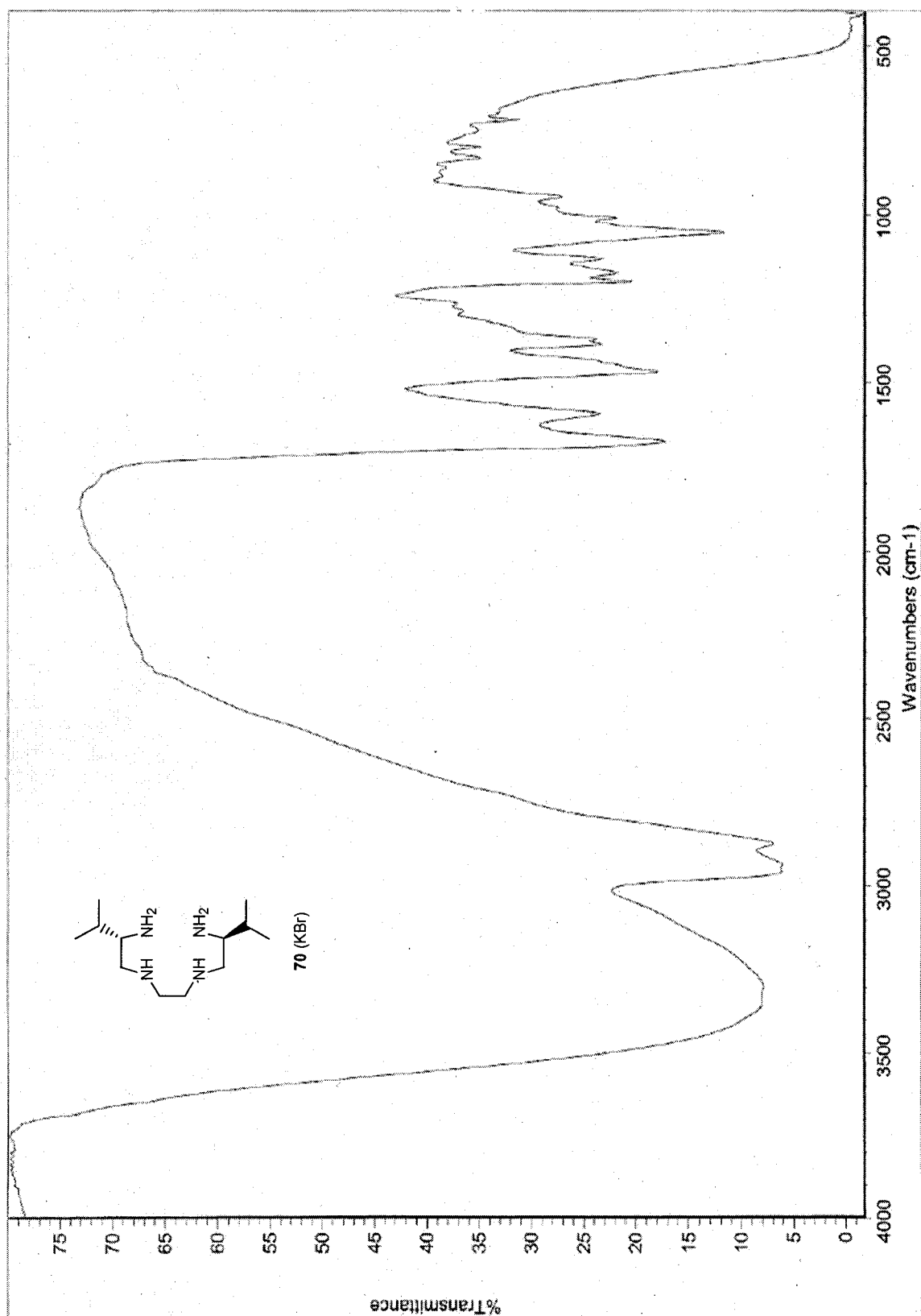


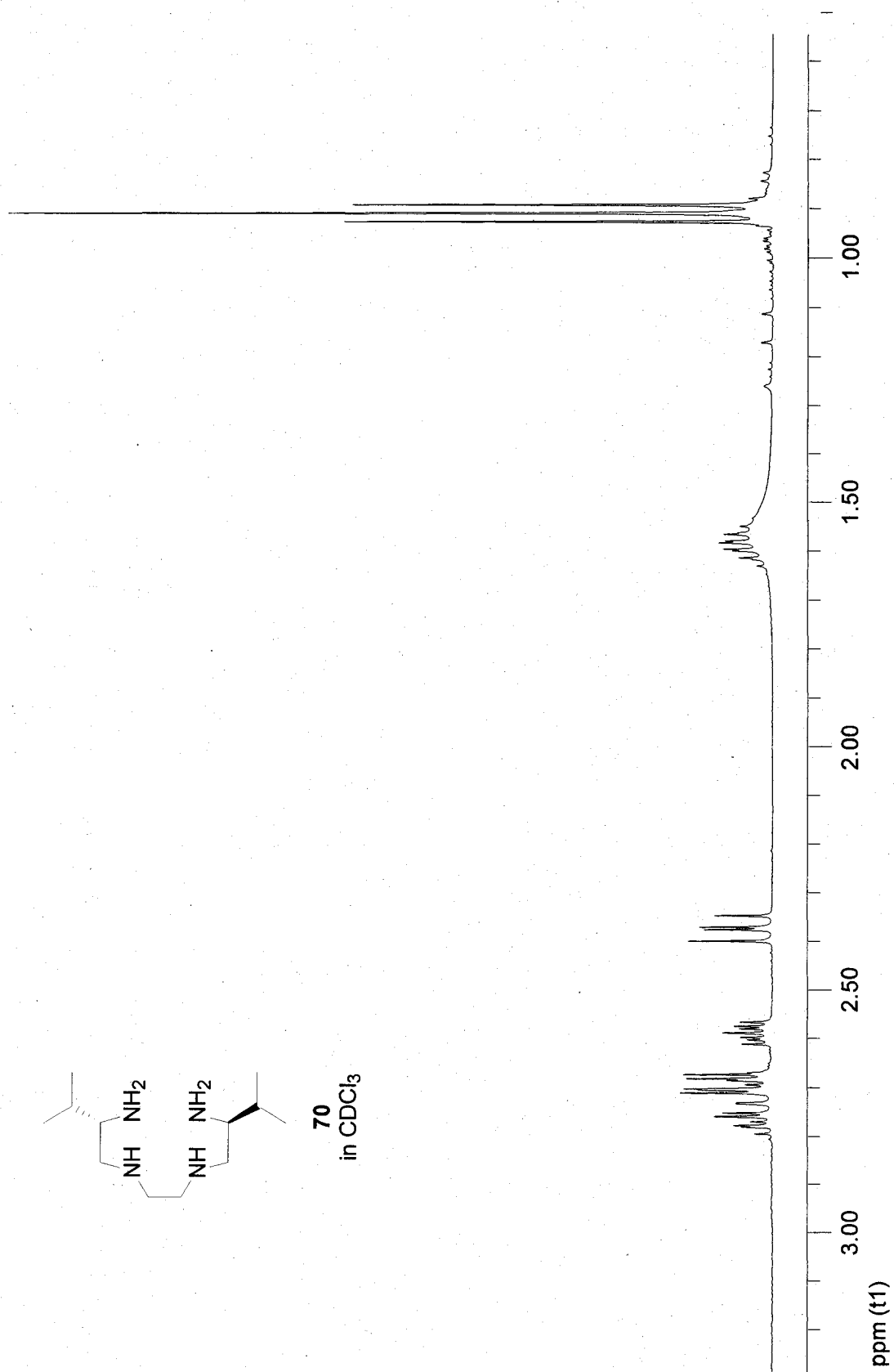
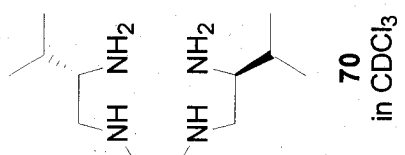


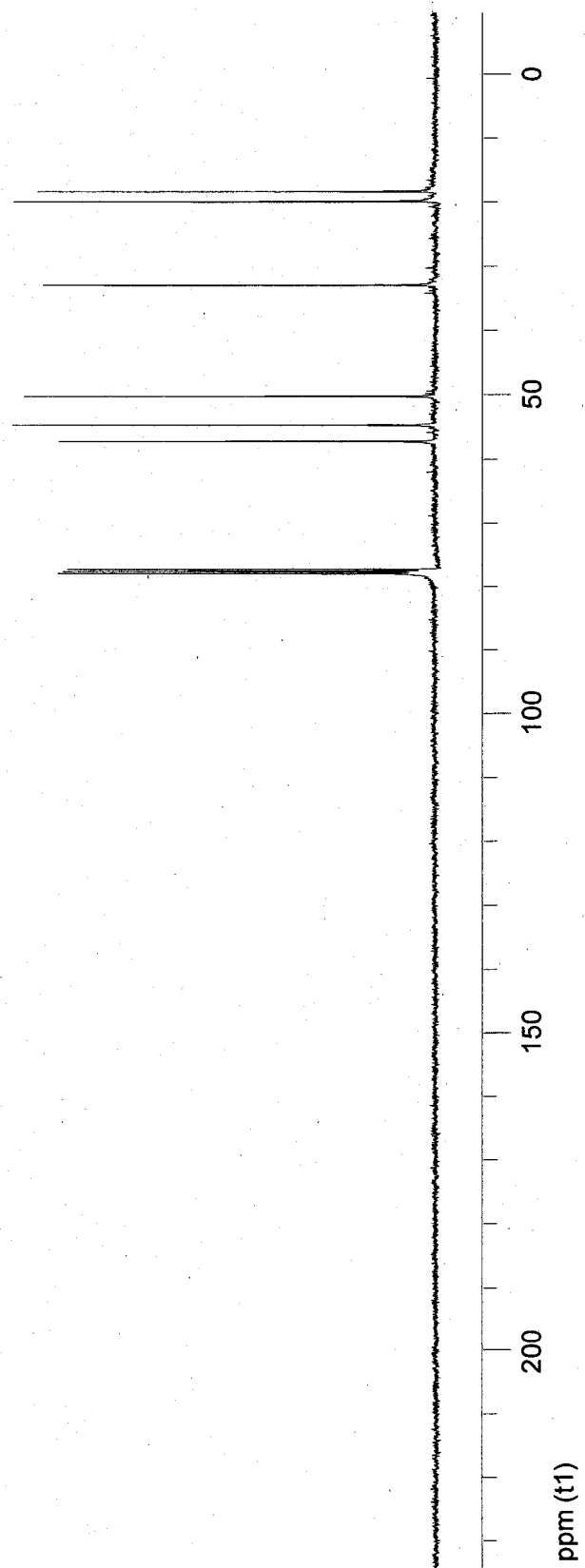
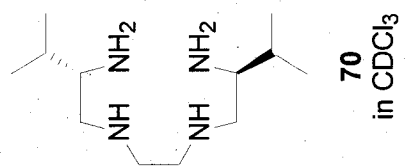
69  
in D<sub>2</sub>O

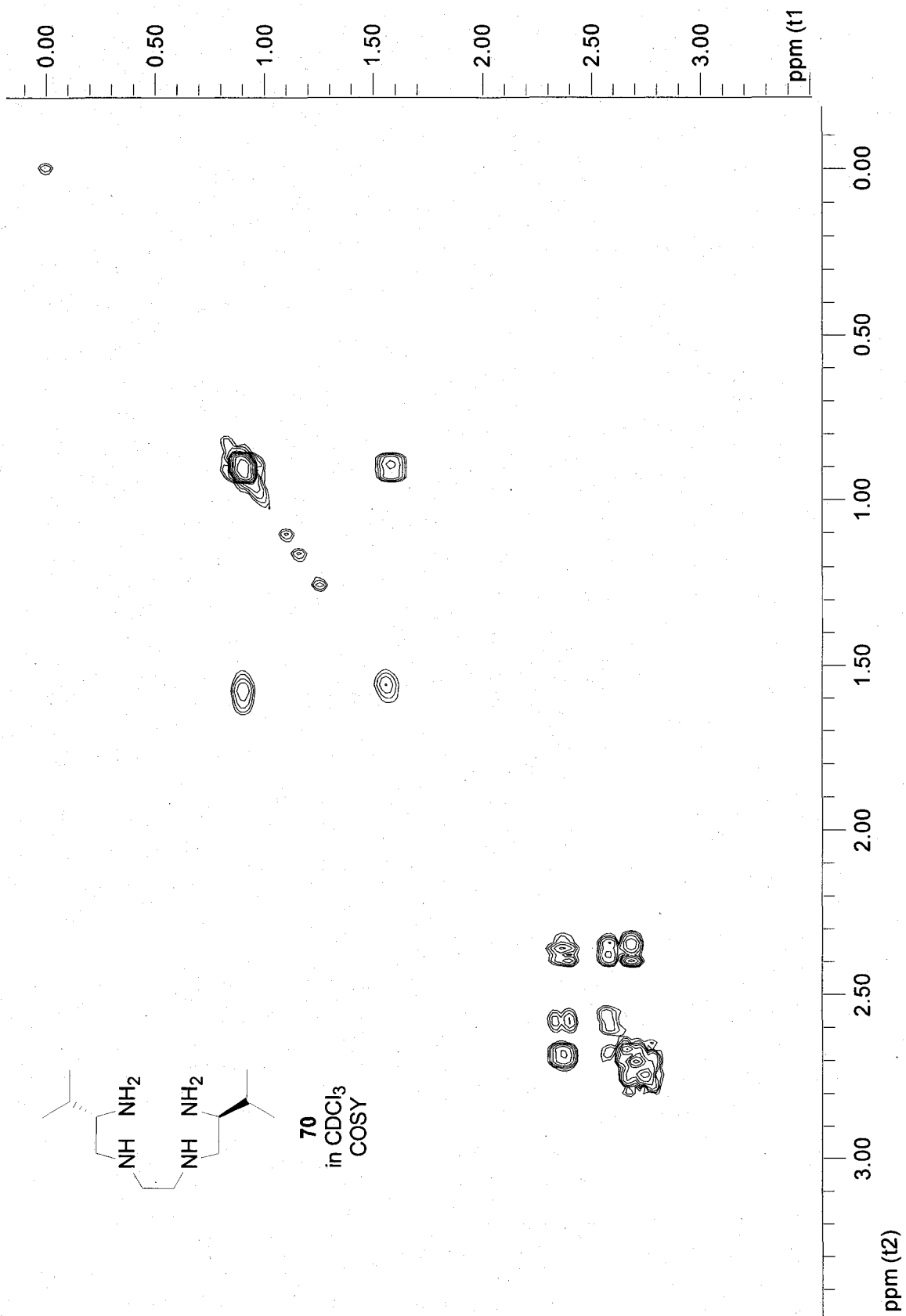




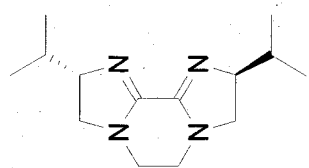






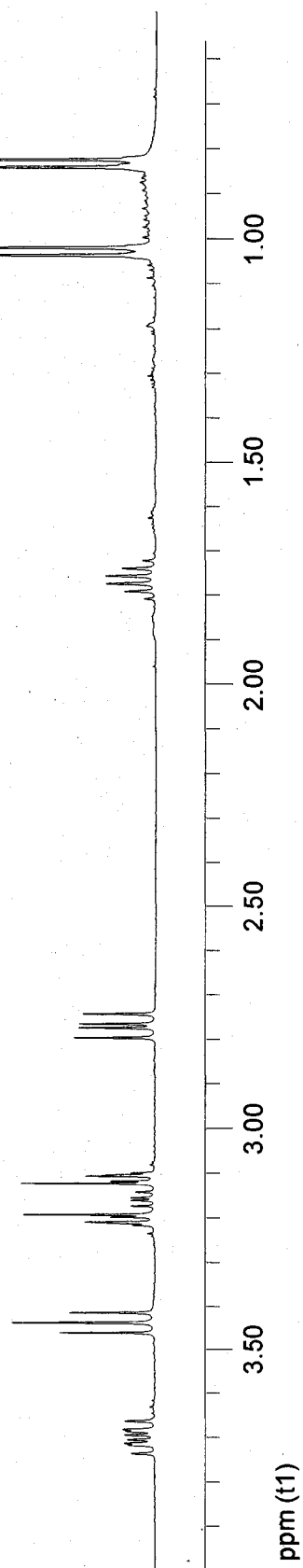


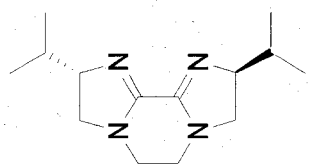




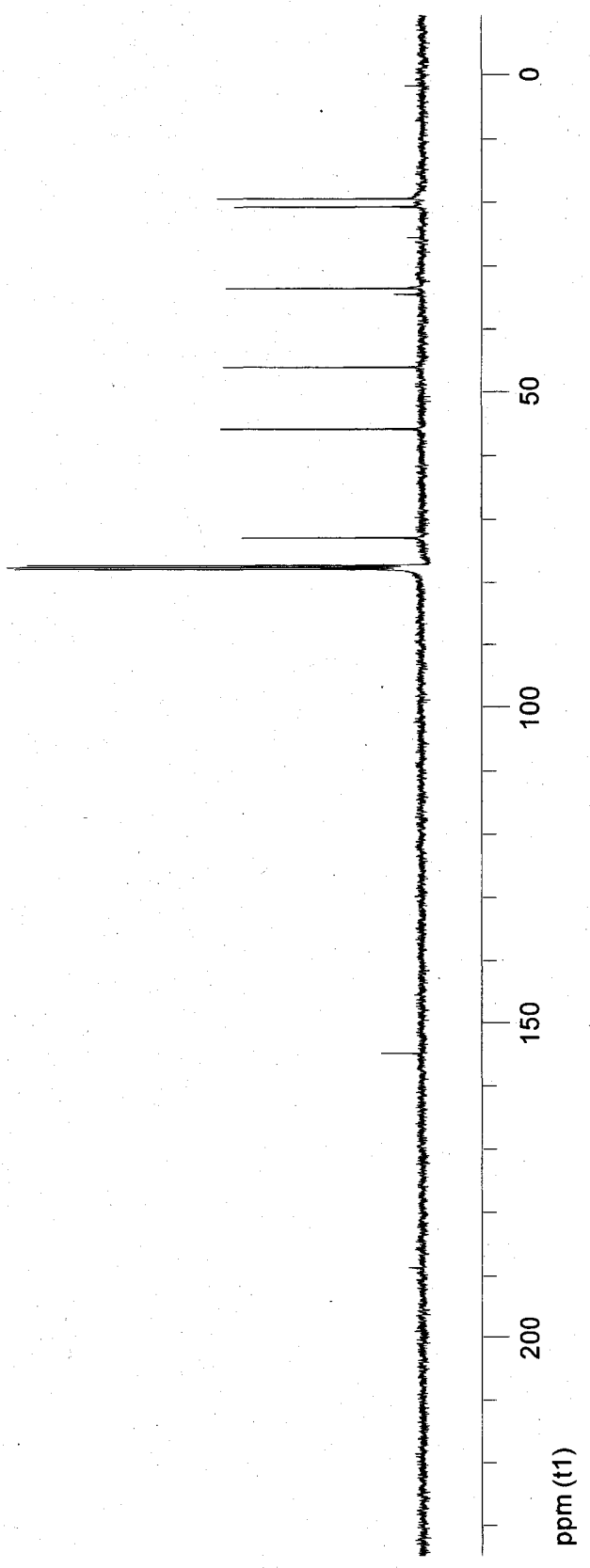
71

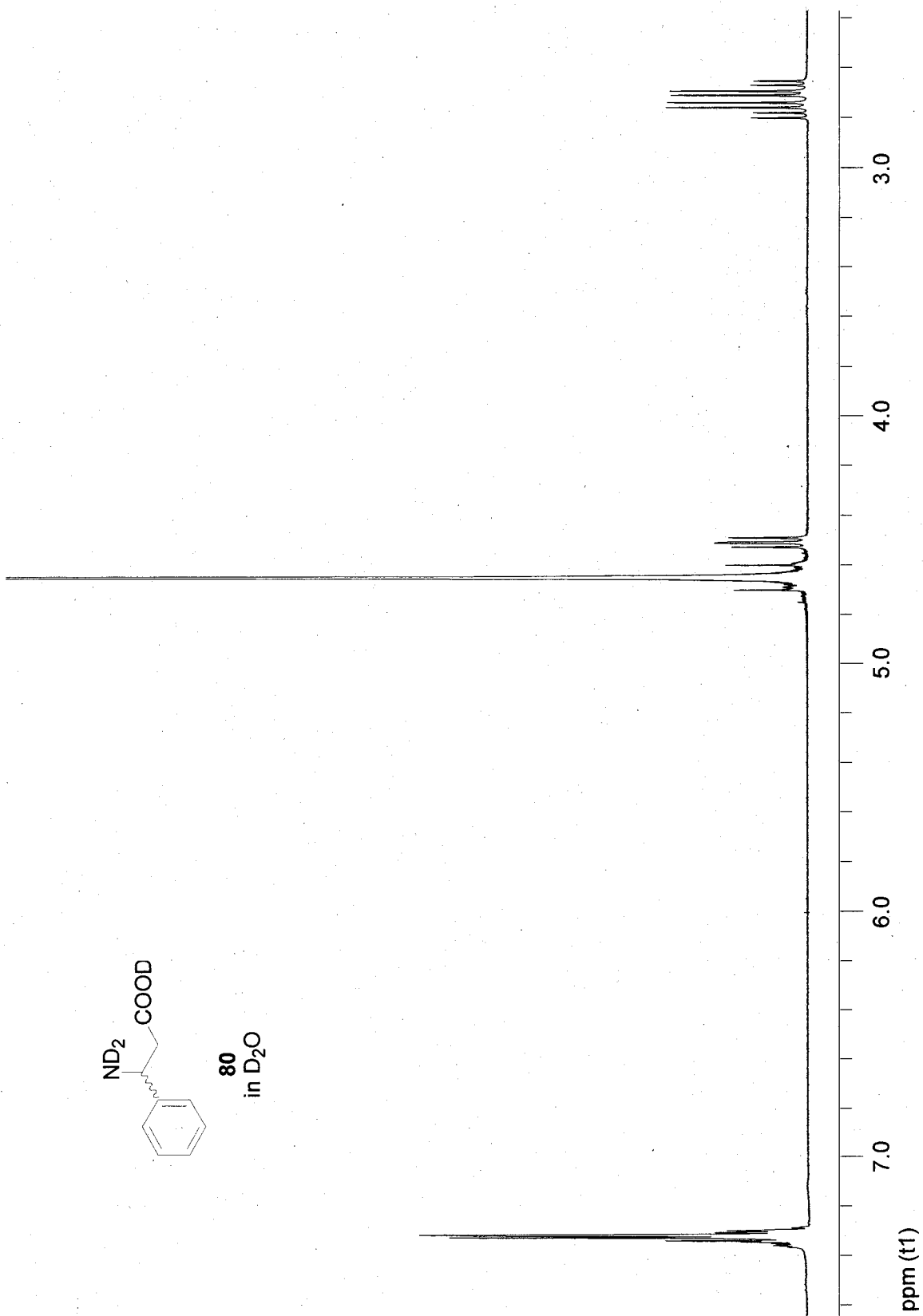
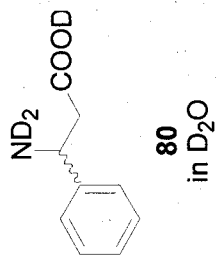
in CDCl<sub>3</sub>

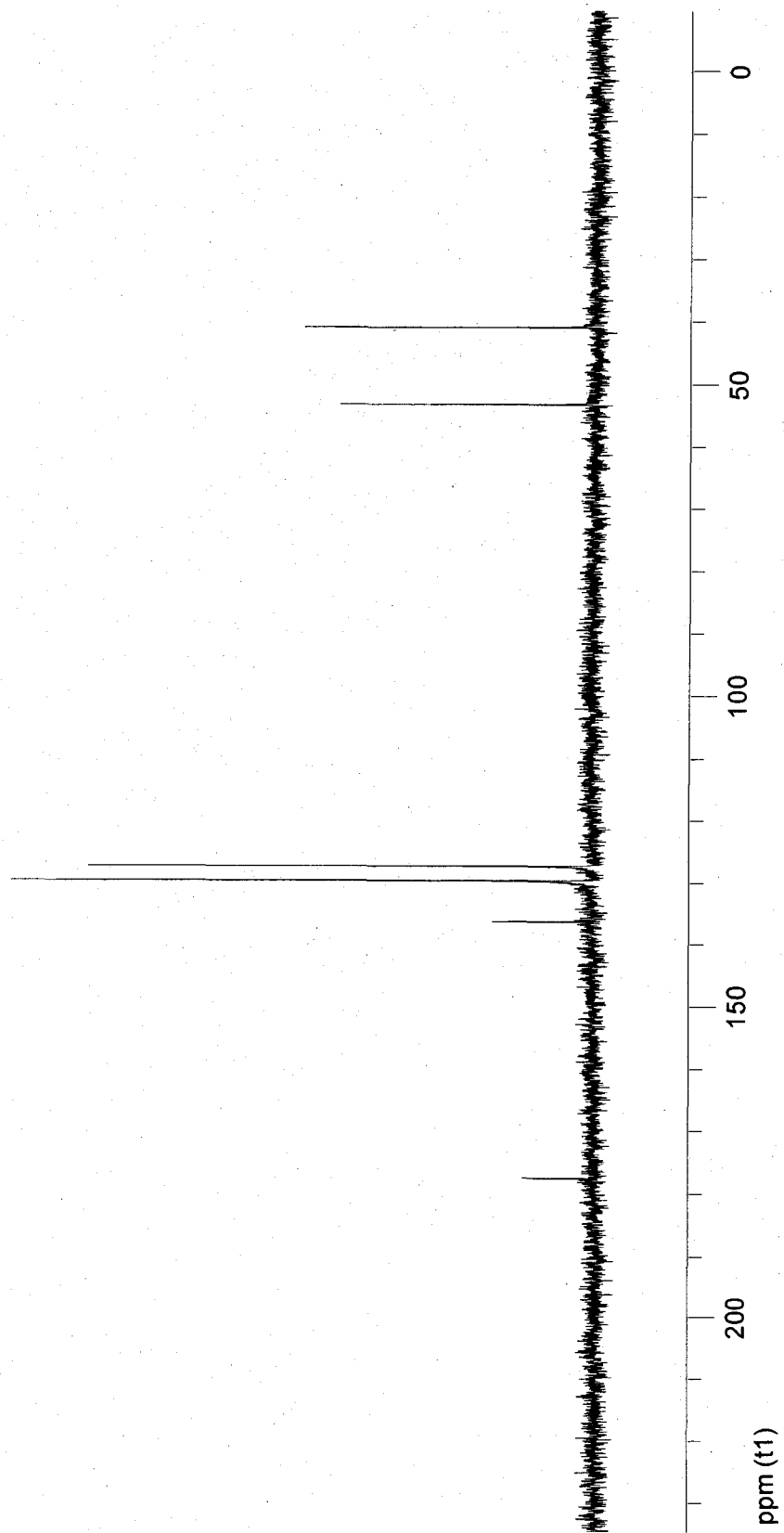
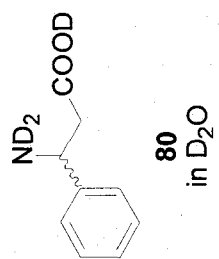


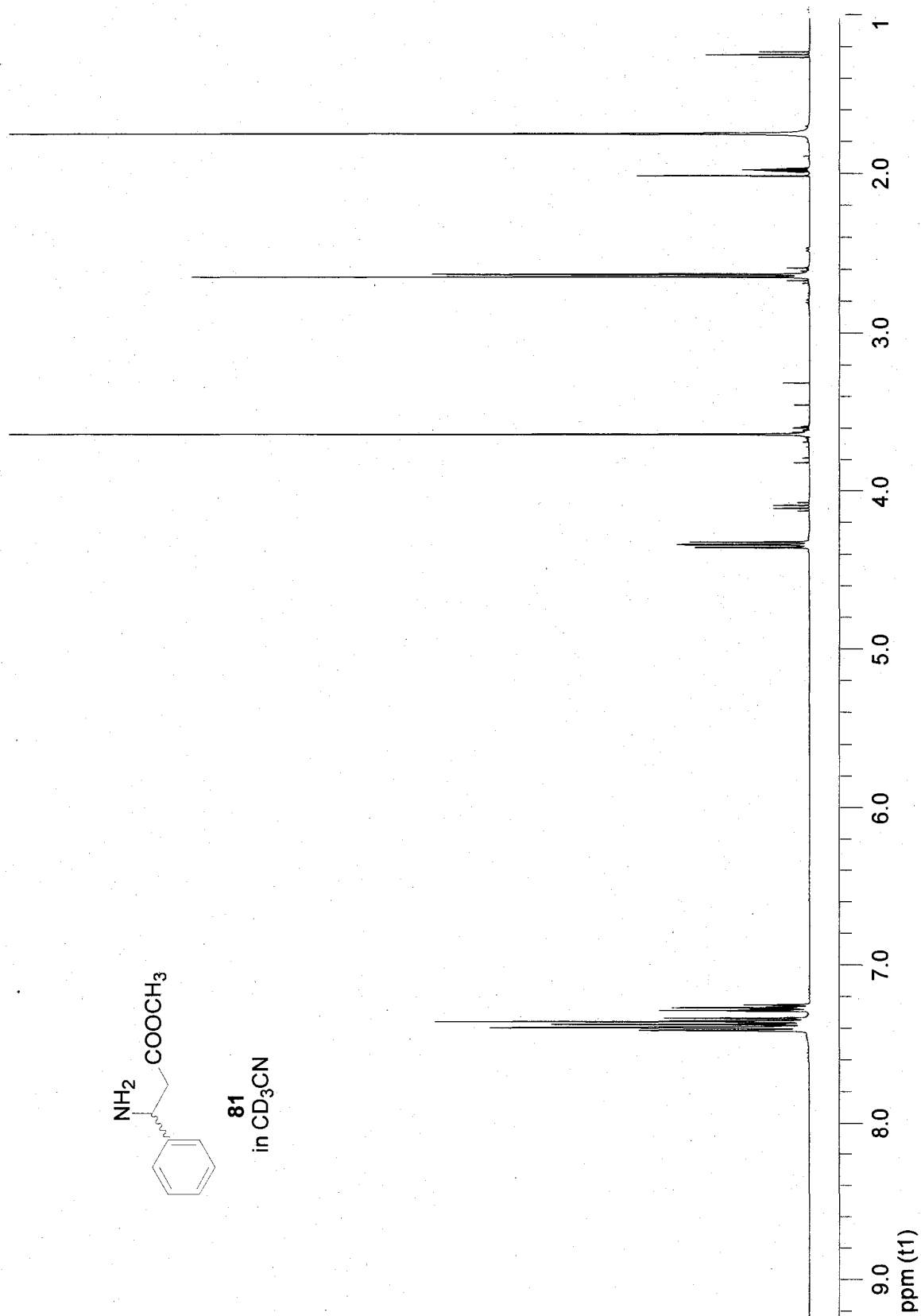
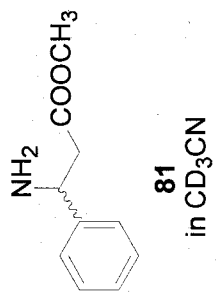


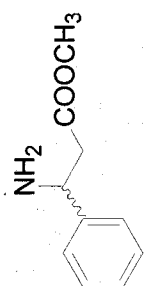
71  
in CDCl<sub>3</sub>



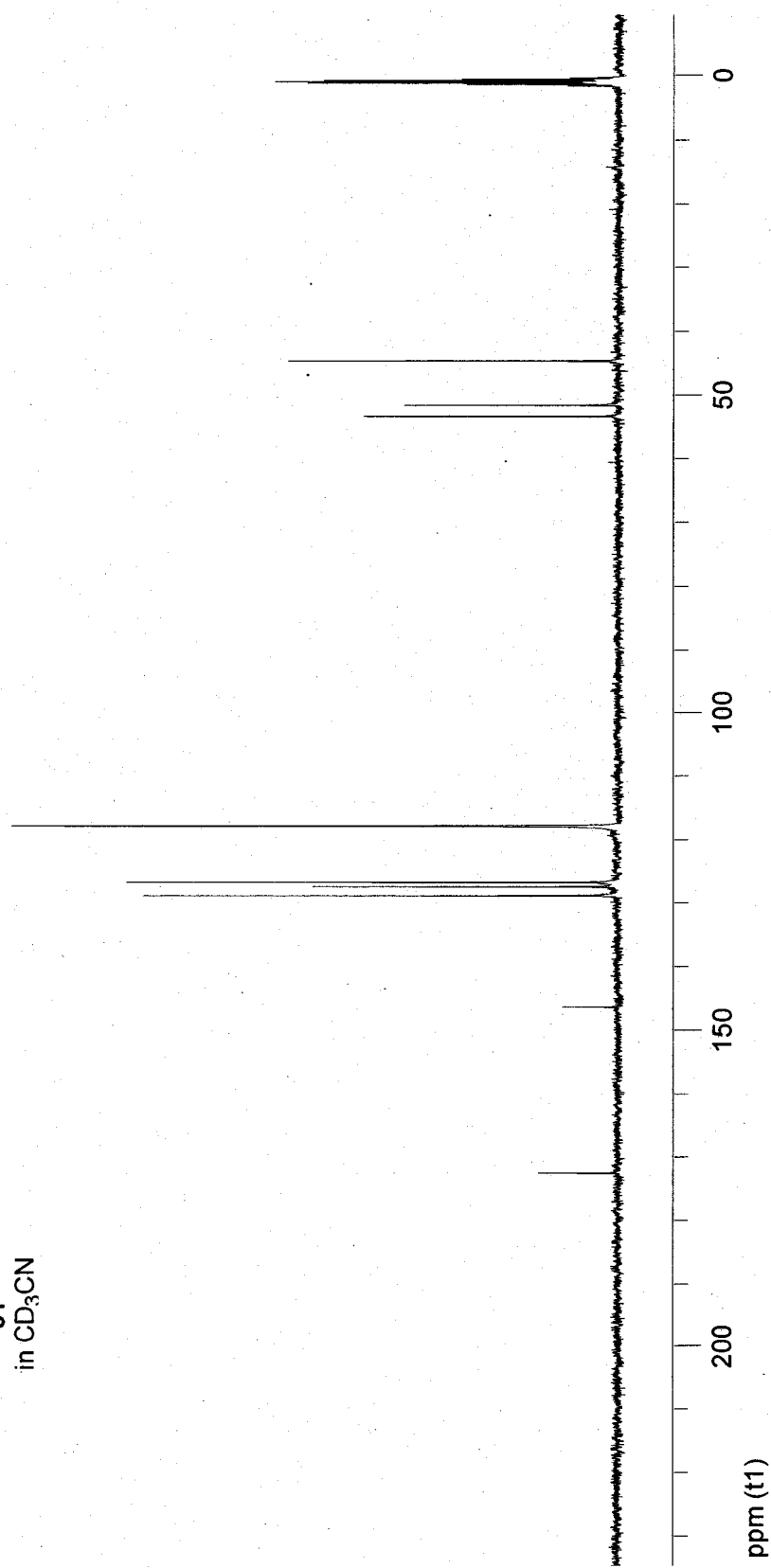


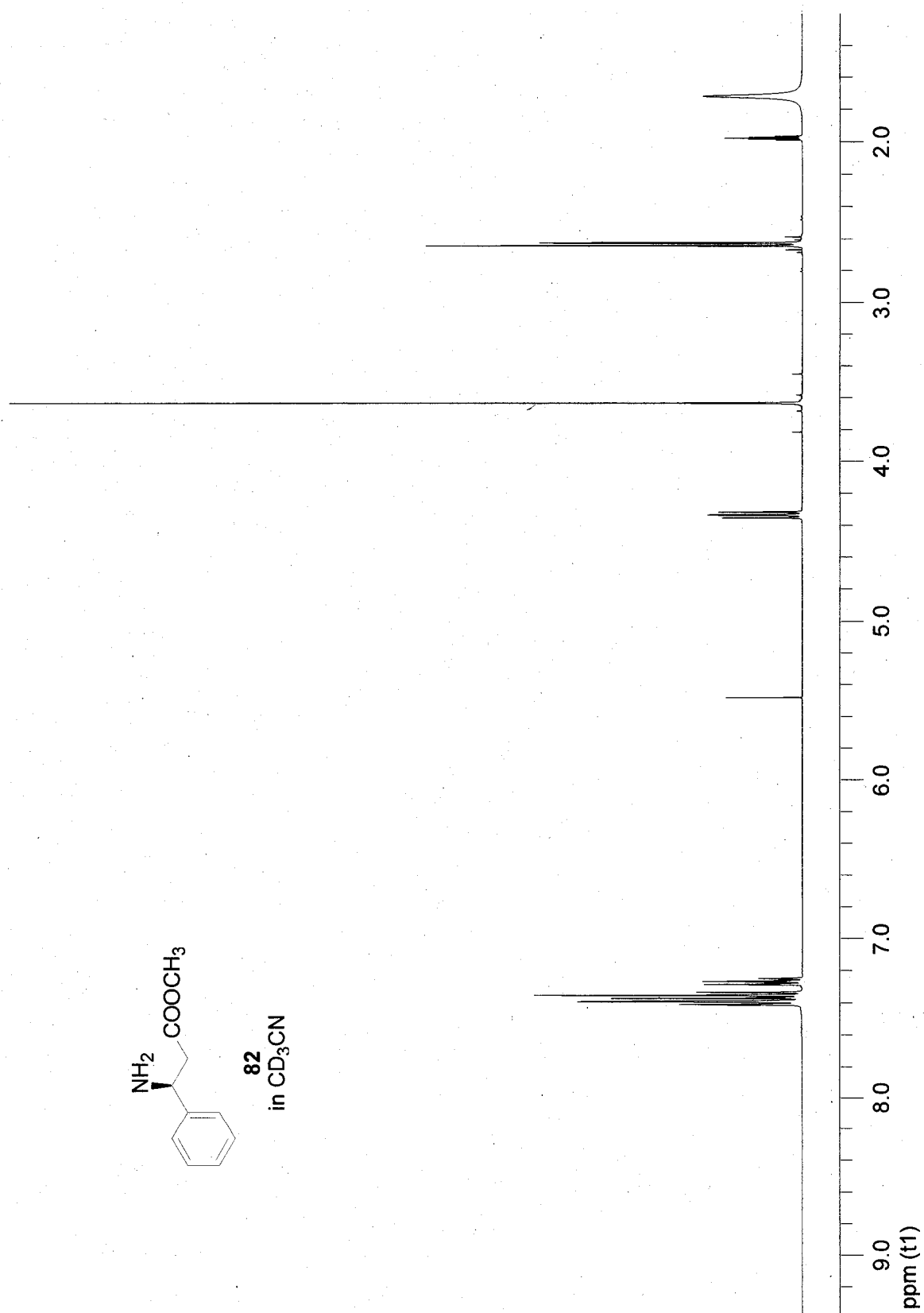
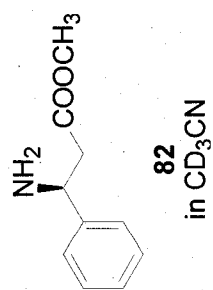


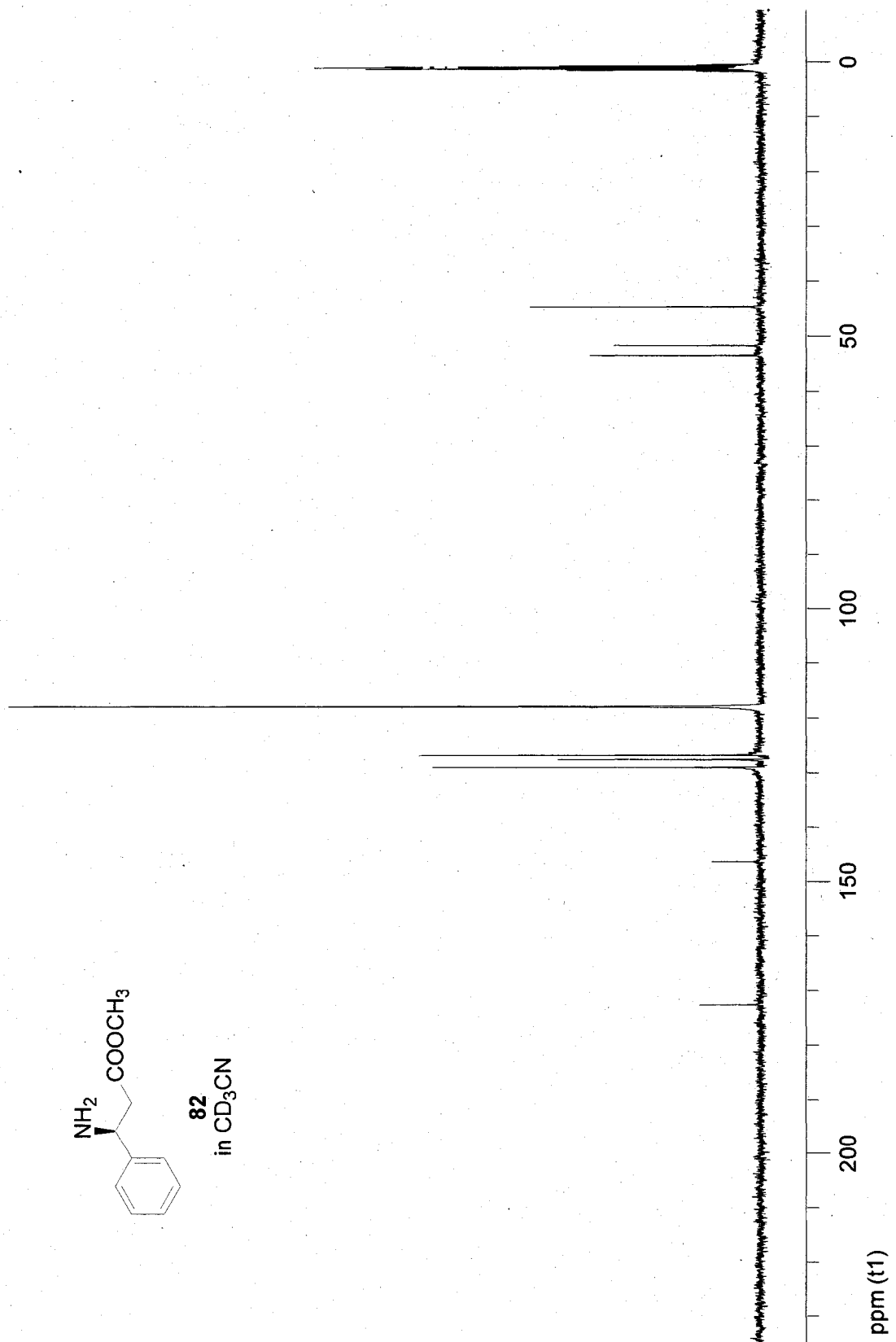
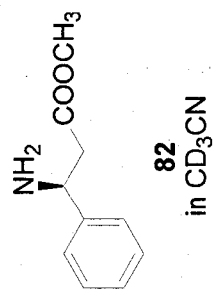




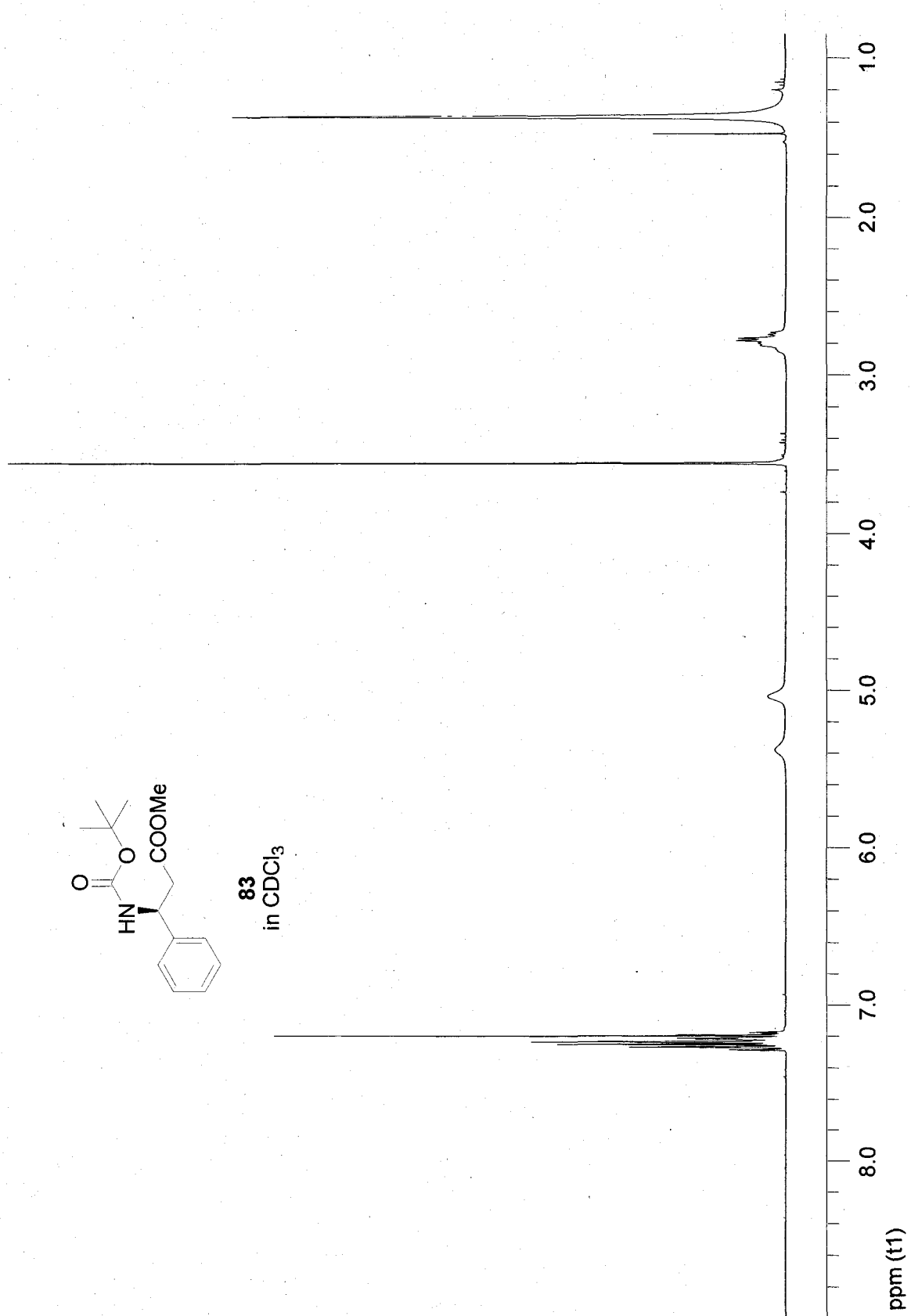
81  
in CD<sub>3</sub>CN

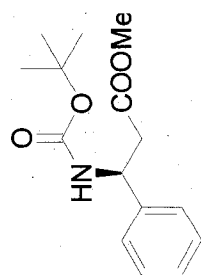






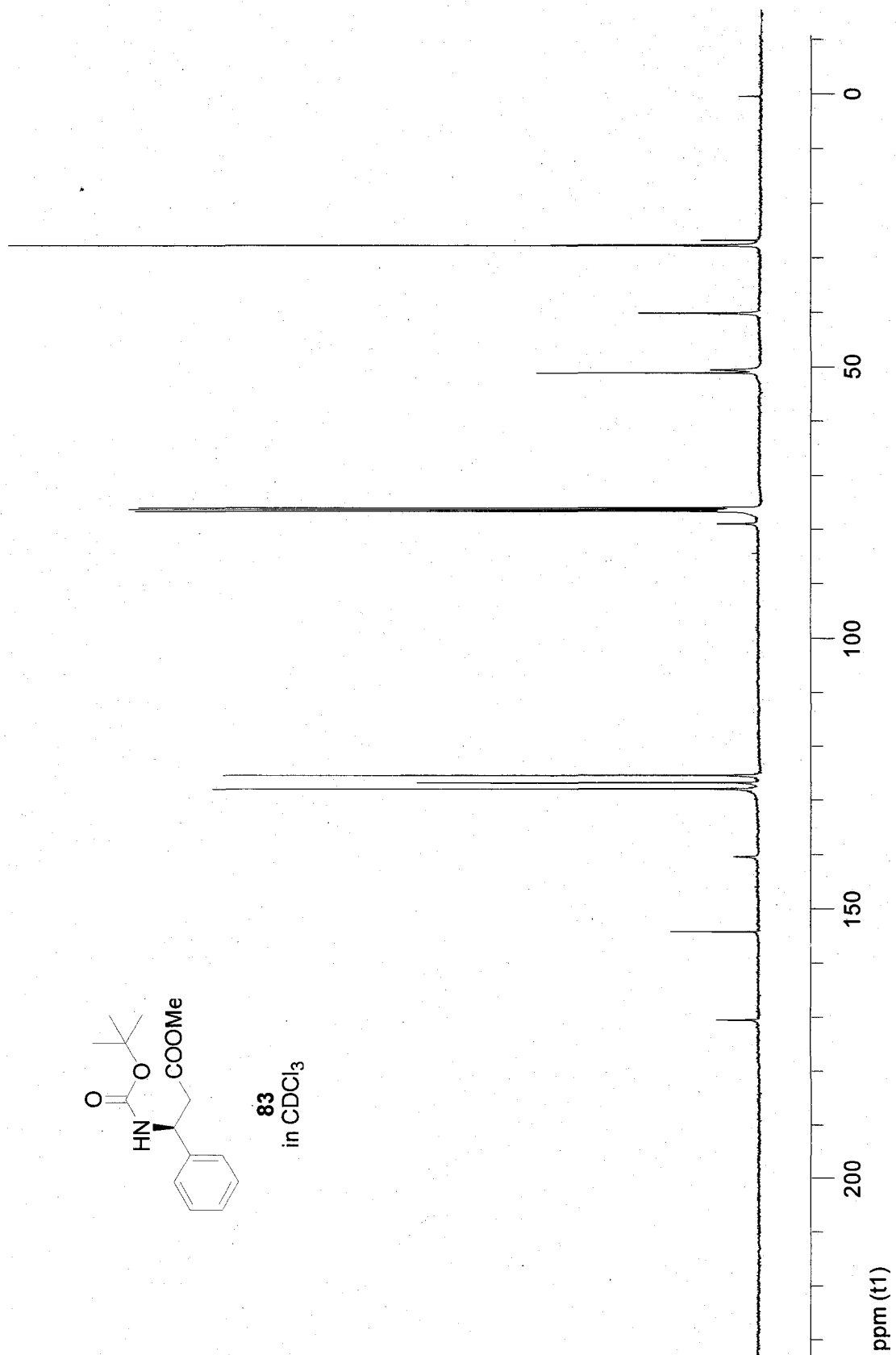


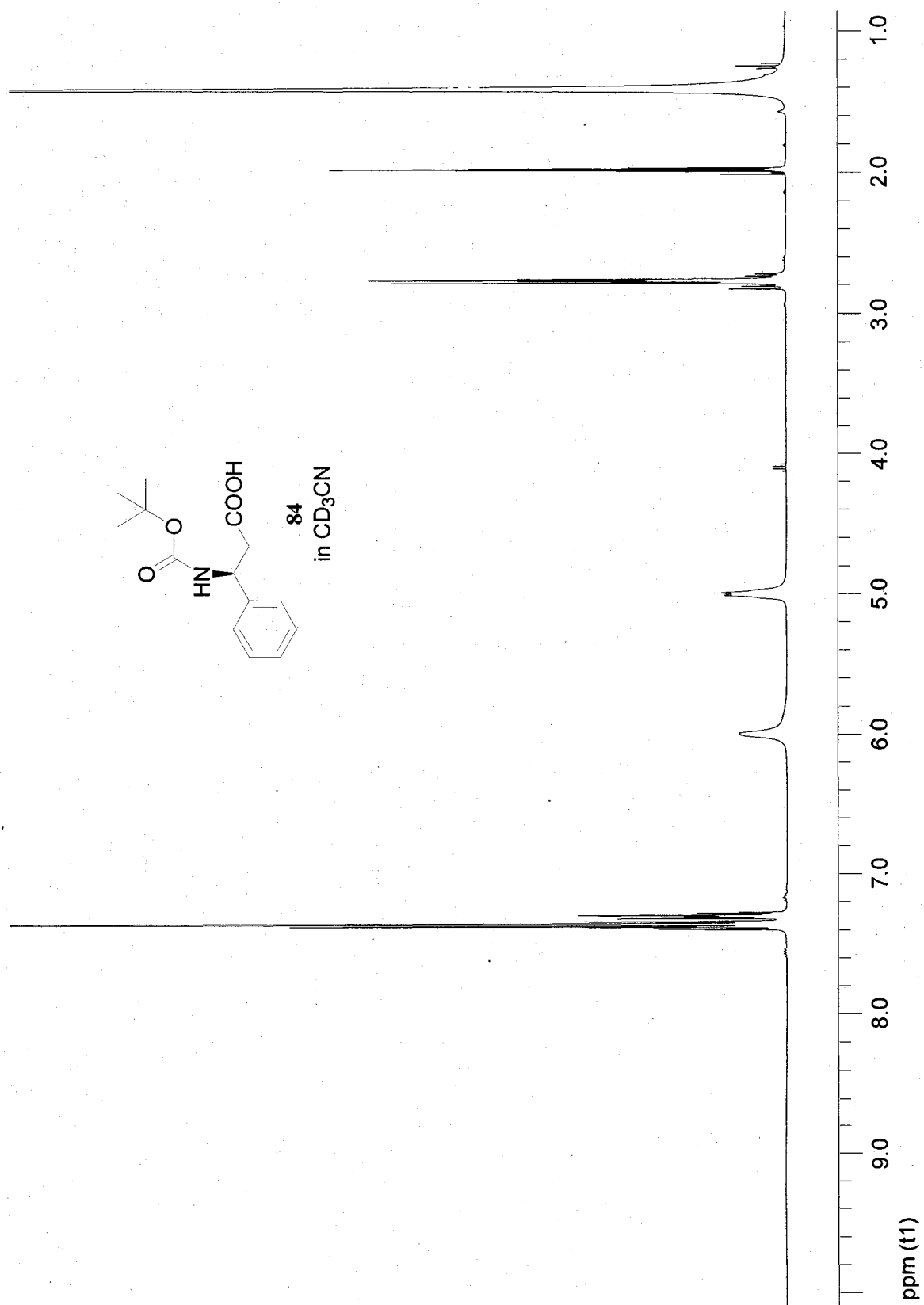


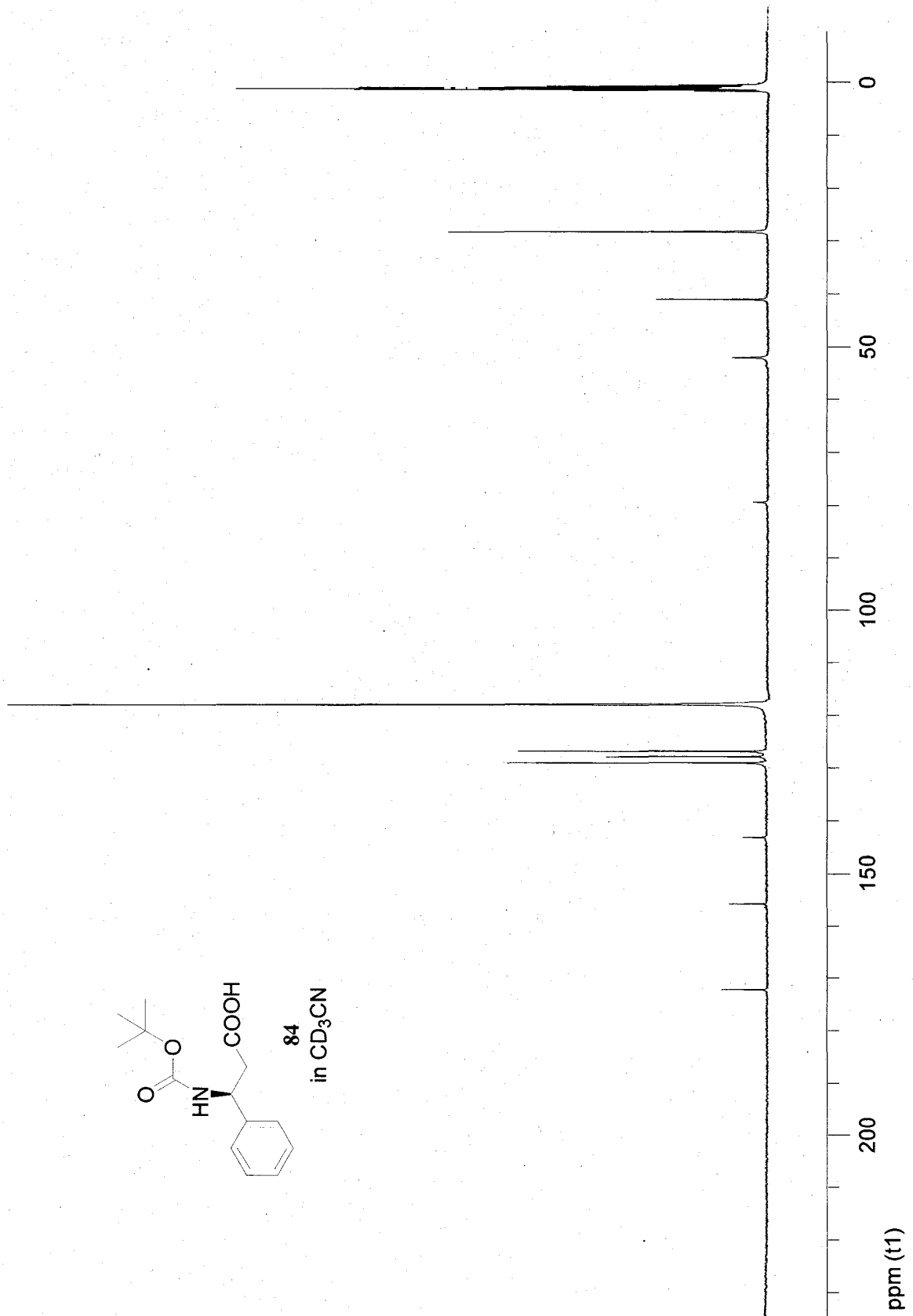
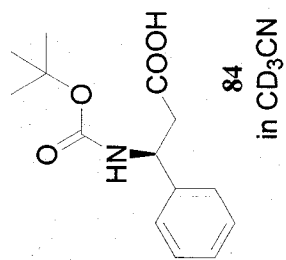


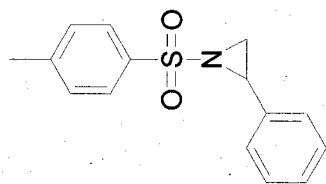
**83**

in CDCl<sub>3</sub>

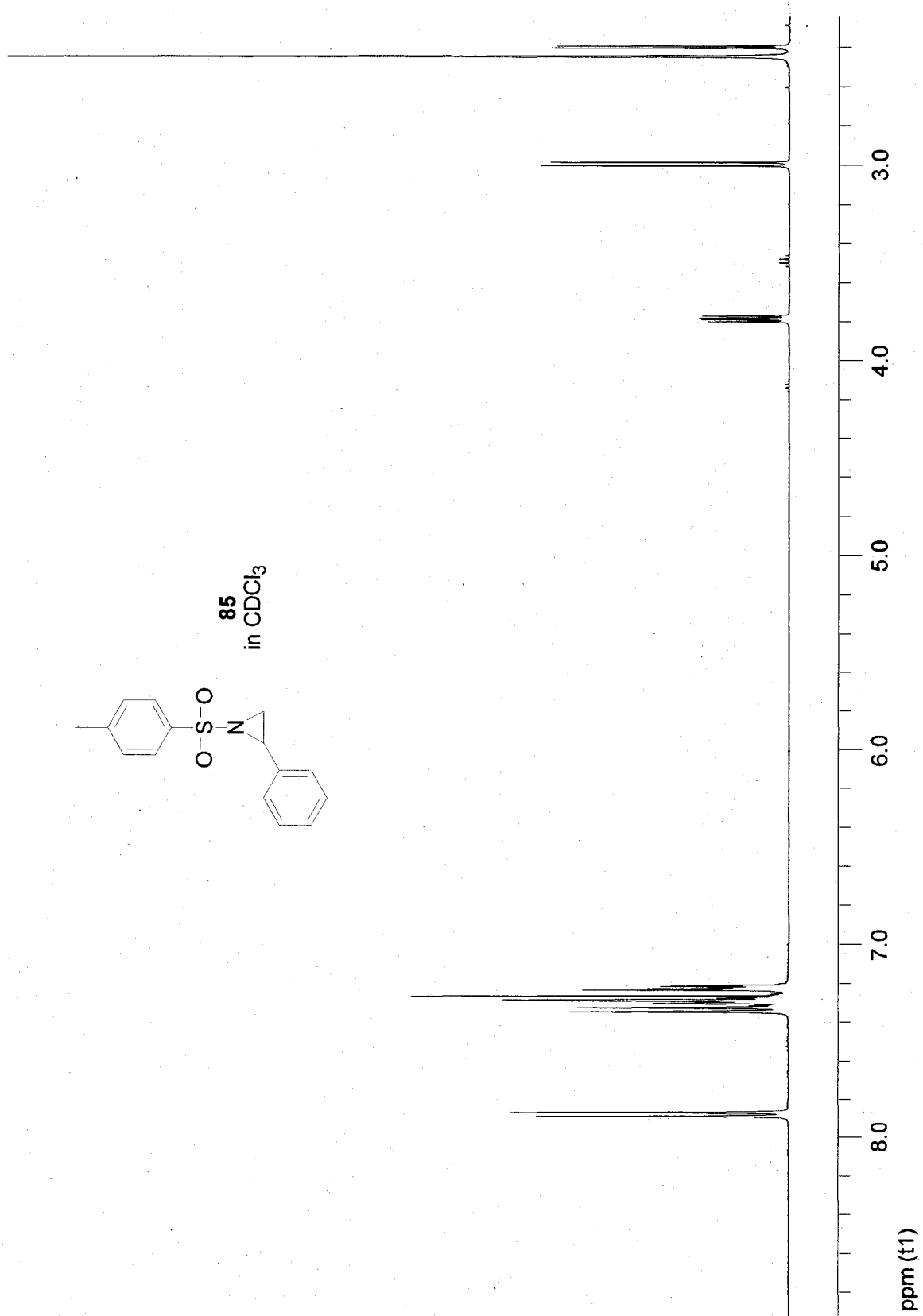


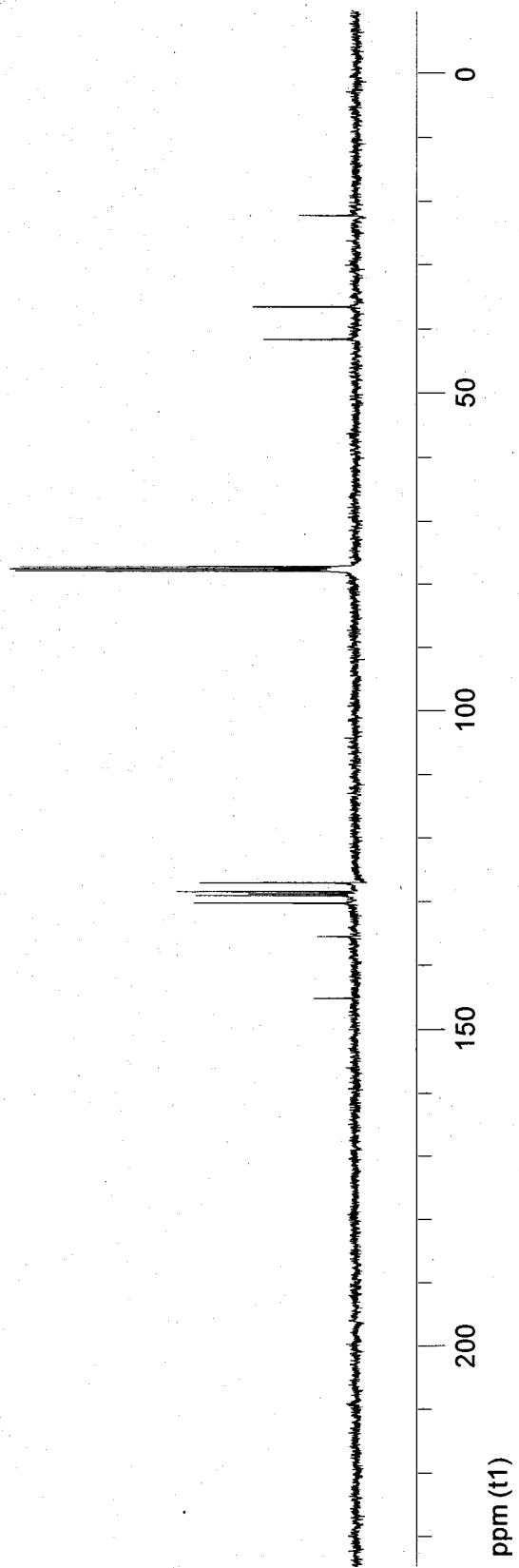
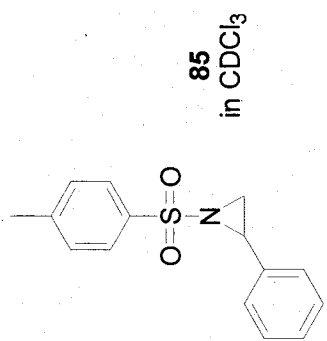






85  
in CDCl<sub>3</sub>





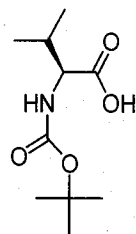
**APPENDIX B**  
**COMPOUND INDEX**

### Compound Index

Compound	Formula or structure	Spectra page
9	$C_{10}H_{16}N_4$	116-122
23	$[Pd(C_{10}H_{16}N_4)(CH_3CN)_2](BF_4)_2$	123-125
24	$[Pd(C_{10}H_{16}N_4)_2](BF_4)_2$	126-129
26	$[Pd(C_{10}H_{16}N_4)_2]Cl_2$	130-131
27	$W(C_{10}H_{16}N_4)(CO)_4$	132-134
28	$[Zn(C_{10}H_{16}N_4)_2](ClO_4)_2$	135-137
29	$[Zn(C_{10}H_{16}N_4)_3]Cl_2$	138-140
30	$[Zn(C_{10}H_{16}N_4)_3](ClO_4)_2$	141-143
32	$[Cd(C_{10}H_{16}N_4)_3](ClO_4)_2$	144-146
33	$[Hg(C_{10}H_{16}N_4)_2](HgCl_4)$	147-149
34	$[Hg(C_{10}H_{16}N_4)_3](BPh_4)_2$	150-152
35	$[Ag(C_{10}H_{16}N_4)_2](BF_4)$	153-155
36	$[Ag(C_{10}H_{16}N_4)_2](BPh_4)$	156-158
37	$[Ag_2(C_8H_{12}N_4)_4](BF_4)_2$	159-161
38	$[Ag_2(C_8H_{12}N_4)_3](BPh_4)_2$	162-164
40	$[Cu(C_{10}H_{16}N_4)_3](ClO_4)_2$	165
41	$[Cu(C_{10}H_{16}N_4)_2](ClO_4)_2$	166
44	$[Cu(C_{10}H_{16}N_4)_2](BF_4)_2$	167
45	$[Eu(C_{10}H_{16}N_4)_4](ClO_4)_3$	168-170

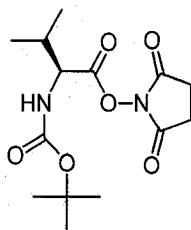


66



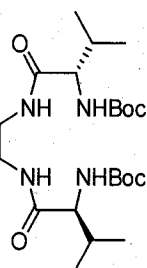
171-172

67



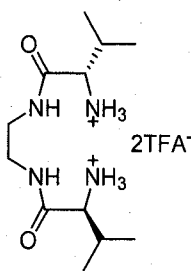
173-174

68



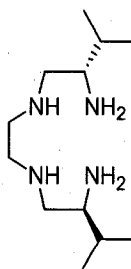
175-176

69

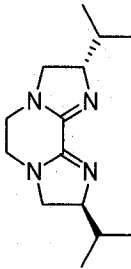
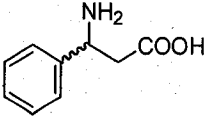
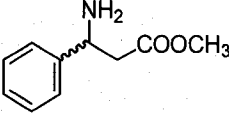
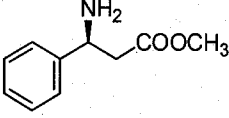
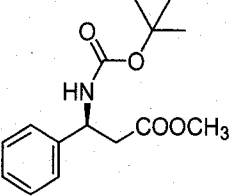
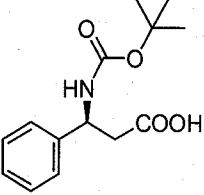
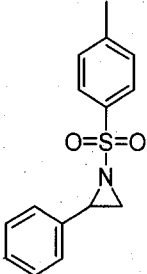


177-178

70



179-182

71		183-184
80		185-186
81		187-188
82a		189-190
83		191-192
84		193-194
85		195-196